PATHWAY APPROACHES TO DISSECTING THE INHERITANCE OF MAIZE SHOOT-BORNE ROOTS

A Dissertation

presented to

the Faculty of the Graduate School

at the University of Missouri-Columbia

In Partial Fulfillment

of the Requirements for the Degree

Doctor of Philosophy

---

by

Michael J. Gerau

Dr. Georgia Davis, Dissertation Supervisor

December 2010

The undersigned, appointed by the dean of the Graduate School, have examined the dissertation entitled

PATHWAY APPROACHES TO DISSECTING THE INHERITANCE

OF MAIZE SHOOT-BORNE ROOTS

Presented by Michael J. Gerau

A candidate for the degree of doctor of philosophy

And hereby certify that in their opinion it is worthy of acceptance.

Professor Georgia Davis

Professor James Birchler

Professor Sherry Flint-Garcia

Professor Michael McMullen

Professor Mary Schaeffer

ACKNOWLEDGEMENTS

First, and foremost, would like to thank my advisor Dr. Georgia Davis for giving me an opportunity to perform undergraduate research in her lab. Without that chance I would not be participating in scientific research today. Her confidence in me has assisted me in completing tasks I was not aware I could achieve. I would also like to thank the numerous undergraduate, graduate and technical help that I have been lucky enough to have over the past years. My success is a testament to their generous contributions.

TABLE OF CONTENTS

LIST OF ILLUSTRATIONS

Figure Page

LIST OF TABLES

LIST OF ABBREVIATIONS

Abbreviation	Full Name
ABA	abscisic acid
aduLf	adult leaf number
AI	average internode
AIear	average internode ear
AItsl	average internode from the tassel to ear
AM	axillary meristem
an1	*anther ear1*
ANOVA	analysis of variance
arl1	*adventitious rootless1*
BL	average tassel branch length
BN	tassel branch number
br2	*brachytic2*
Cg1	*Corngrass1*
Chrom	chromosome
CIM	composite interval mapping
CAN	*CORONA*
cM	centimorgans
CV	coefficient of variance
d1	*dwarf1*
D10	*Dwarf10*

d3 ..... *dwarf3*

d5 ..... *dwarf5*

D8 ..... *Dwarf8*

D9 ..... *Dwarf9*

dfl1 ..... *delayedflowering1*

DNA ..... deoxyribonucleic acid

DTP ..... days to 50% pollen shed

DTS ..... days to 50% ear silk

EarHt ..... ear height

END ..... ear node diameter

elm1 ..... *elongated mesocotyl1*

epc1 ..... *early phase change1*

GA ..... gibberellic acid

GAI ..... gibberellic acid insensitive

GID1 ..... gibberellin insensitive dwarf1

IAA ..... indole acetic acid

ICU *INCURVATA4*

IBM ..... intermated B73 x Mo17

InDel ..... insertion-deletion polymorhism

id1 ..... *indeterminate1*

ids1 ..... *indeterminate spikelet1*

juvLf ..... juvenile leaf number

L1 ..... total tassel length

L2 ..... central spike length of the tassel

LD ..... linkage disequilibrium

Lfarea ..... leaf area

Lfleng ..... leaf length

Lfwidth ..... leaf width

LOB ..... lateral organ boundary

LOD ..... log of odds ratio

LR ..... likelihood ratio

Lsmean ..... least squared mean

MIM ..... multiple interval mapping

miR156 ..... *microRNA156*

miR166 ..... *microRNA166*

miR172 ..... *microRNA172*

MLM ..... multilocus model

MXD ..... mixed

NSS ..... non-stiff stalk

NTE ..... number of nodes to the ear

NTT ..... number of nodes to the tassel

NWSBR ..... number of nodes with shoot-borne roots

NWSBR04 ..... number of nodes with shoot-borne roots in 2004

NWSBR05 ..... number of nodes with shoot-borne roots in 2005

NWSBR08 ..... number of nodes with shoot-borne roots in 2008

PC ..... principal component

PC1 ..... principal componet one

PC2 ..... principal component two

PC3 ..... principal component three

PC4 ..... principal component four

PC9..... principal component nine

PCA..... principal component analysis

PCD..... programmed cell death

PCR..... polymerase chain reaction

PCReg .....principal component regression

PHt ..... plant height

PIF.....phytochrome inactivating factor

PIF3.....phytochrome inactivating factor3

POP .....popcorn

PRINCOMP ..... principal component procedure

PROC CORR .....correlation procedure

PROC GLM .....general linear models procedure

PHB.....*PHABULOSA*

PHV..... *PHAVOLUTA*

phyB ..... phytochrome B

phyB1 .....*phytochrome B1*

phyB2 .....*phytochrome B2*

qnbwsbr1..... QTL for the number of nodes with shoot-borne roots above ground 1

qnbwsbr10..... QTL for the number of nodes with shoot-borne roots above ground 10

qnbwsbr11..... QTL for the number of nodes with shoot-borne roots above ground 11

qnbwsbr12..... QTL for the number of nodes with shoot-borne roots above ground 12

qnbwsbr2..... QTL for the number of nodes with shoot-borne roots above ground 2

qnbwsbr3..... QTL for the number of nodes with shoot-borne roots above ground 3

qnbwsbr4..... QTL for the number of nodes with shoot-borne roots above ground 4

qnbwsbr5..... QTL for the number of nodes with shoot-borne roots above ground 5

qnbwsbr6..... QTL for the number of nodes with shoot-borne roots above ground 6

qnbwsbr7..... QTL for the number of nodes with shoot-borne roots above ground 7

qnbwsbr8..... QTL for the number of nodes with shoot-borne roots above ground 8

qnbwsbr9..... QTL for the number of nodes with shoot-borne roots above ground 9

qsbr1.1 .....QTL for the number of shoot-borne roots at the first node above ground 1

qsbr1.10 .....QTL for the number of shoot-borne roots at the first node above ground 10

qsbr1.2 .....QTL for the number of shoot-borne roots at the first node above ground 2

qsbr1.3 .....QTL for the number of shoot-borne roots at the first node above ground 3

qsbr1.4 .....QTL for the number of shoot-borne roots at the first node above ground 4

qsbr1.5 .....QTL for the number of shoot-borne roots at the first node above ground 5

qsbr1.6 .....QTL for the number of shoot-borne roots at the first node above ground 6

qsbr1.7 .....QTL for the number of shoot-borne roots at the first node above ground 7

qsbr1.8 .....QTL for the number of shoot-borne roots at the first node above ground 8

qsbr1.9 .....QTL for the number of shoot-borne roots at the first node above ground 9

qsbr2.1 ..... QTL for the number of shoot-borne roots at the second node above ground 1

qsbr2.10 ..... QTL for the number of shoot-borne roots at the second node above ground 10

qsbr2.2 ..... QTL for the number of shoot-borne roots at the second node above ground 2

qsbr2.3 ..... QTL for the number of shoot-borne roots at the second node above ground 3

qsbr2.4 ..... QTL for the number of shoot-borne roots at the second node above ground 4

qsbr2.5 ..... QTL for the number of shoot-borne roots at the second node above ground 5

qsbr2.6 ..... QTL for the number of shoot-borne roots at the second node above ground 6

qsbr2.7 ..... QTL for the number of shoot-borne roots at the second node above ground 7

qsbr2.8 ..... QTL for the number of shoot-borne roots at the second node above ground 8

qsbr2.9 ..... QTL for the number of shoot-borne roots at the second node above ground 9

qsbra1 .....QTL for shoot-borne root angle 1

qsbra10 .....QTL for shoot-borne root angle 10

qsbra2 .....QTL for shoot-borne root angle 2

qsbra3 .....QTL for shoot-borne root angle 3

qsbra4 .....QTL for shoot-borne root angle 4

qsbra5 .....QTL for shoot-borne root angle 5

qsbra6 .....QTL for shoot-borne root angle 6

qsbra7 .....QTL for shoot-borne root angle 7

qsbra8 .....QTL for shoot-borne root angle 8

qsbra9 .....QTL for shoot-borne root angle 9

QTL.....quantitative trait locus

R1..... first reproductive stage

RGA.....repressor of gibberellic acid

ra1..... *ramosa1*

ra2..... *ramosa2*

RIL..... recombinant inbred line

RLD1.....*Rolled leaf1*

SAM..... shoot apical meristem

SAR..... shade avoidance response

SBR.....shoot-borne root

SBR1..... number of shoot-borne roots at the first node above ground

SBR104..... number of shoot-borne roots at the first node above ground in 2004

SBR105..... number of shoot-borne roots at the first node above ground in 2005

SBR108..... number of shoot-borne roots at the first node above ground in 2008

SBR2..... number of shoot-borne roots at the second node above ground

SBR204..... number of shoot-borne roots at the second node above ground in 2004

SBR205 ..... number of shoot-borne roots at the second node above ground in 2005

SBR208 ..... number of shoot-borne roots at the second node above ground in 2008

SBRA ..... shoot-borne root angle

SCR ..... *SCARECROW*

SHR ..... *SHORT ROOT*

SND ..... soil node diameter

SNP ..... single nucleotide polymorphism

SPB ..... *squamosa protein binding*

SPL ..... squamosa binding protein like

SS ..... stiff stalk

rtcs ..... *rootless concerning crown and seminal roots*

rtcl ..... *rootless concerning crown and seminal roots-like*

SWT ..... sweet

TND ..... tassel node diameter

totlSBR ..... total number of shoot-borne

totlSBR04 ..... total number of shoot-borne in 2004

totlSBR05 ..... total number of shoot-borne in 2005

totlSBR08 ..... total number of shoot-borne in 2008

totLf ..... total leaf number

Tp1 ..... *Teopod1*

Tp2 ..... *Teopod2*

transLf ..... transition leaf number

ts4 ..... *tasselseed4*

Ts6 ..... *tasselseed6*

TS ..... tropical and semitropical

V1..... first vegetative stage

V3..... third vegetative stage

V6..... sixth vegetative stage

Vgt1..... *Vegetative-to-generative growth1*

wx1..... *waxy1*

PATHWAY APPROACHES TO DISSECTING THE INHERITANCE

OF MAIZE (*ZEA MAYS* L.) SHOOT-BORNE ROOTS

Michael J. Gerau

Dr. Georgia Davis, Dissertation Supervisor

ABSTRACT

Shoot-borne roots are essential plant components. Two pathway-based approaches were pursued to increase our understanding of genetic mechanisms controlling shoot-borne root patterning. The first pathway approach characterized the contribution of gibberellic acid-related genes in shoot-borne root patterning. Quantitative trait loci mapping in the Intermated B73xMo17 linkage mapping population identified chromosome regions controlling shoot-borne root patterning which also contained gibberellic acid biosynthetic and response genes. Phenotyping of mutants with altered gibberellic acid production and response validated these genes as potentially underlying the identified quantitative trait loci. Association analysis was conducted in a set of 260 diverse maize inbred lines. The association analysis identified significant polymorphisms in the catalytic domain of the gibberellic acid biosynthetic gene *dwarf3* and in the promoter region of the gibberellic acid response regulator *Dwarf8*. These results confirmed the previous hypothesis that gibberellic acid production is involved in shoot-borne root patterning and expanded it to include DELLA-mediated gibberellic acid response. In the second pathway-based approach a multivariate phenotypic analysis was conducted on 25 diverse maize inbred lines that were phenotyped for 23 developmental traits along with three shoot-borne root traits to define novel hypotheses about pathways involved in shoot-borne root patterning,. Evidence for a light-signaling component in root development was found. Further support for the involvement of light-signaling was provided by mutant phenotyping and field experiments which confirmed the

predictions of the multivariate analysis. The two pathways were integrated into one model where light-mediated redistribution of gibberellic acid dictates shoot-borne root patterning.

CHAPTER1: Introduction

The Importance of Maize as a Crop

Since its domestication in Central American between 6000 to 9000 years ago (Piperno and Flannery, 2001; Matsuoka et al., 2002) corn (*Zea mays* L. ssp. *mays*), hereafter referred to as maize, has been adapted to grow in diverse conditions worldwide. Maize is among the most important crops used as food, feed, and more recently fuel (Edgerton, 2009). Maize products also include absorbents, adhesives, alcohols, cleaning products, cosmetics, lubricants, packing material, paint, pharmaceuticals, plastics, and solvents (NCGA, 2010). Demand for these products generally increases with global population growth, however other factors can contribute to a sharp increase in demand for individual products. Edgerton (2009) points to rises in biofuel production and meat consumption as major causes for the increase in demand for maize. Global meat consumption is expected to increase to 310 million tonnes/year from 55 million tonnes/year over the next decade (OECD-FAO, 2008). Much of this increase is attributed to increases in expendable income in developing countries (von Braun, 2007). This demand for meat translates into demand for maize as it is a popular and effective feed for livestock. Concurrently, interest in renewable biofuels has increased. Biofuel production from maize is expected to grow from 28 billion liters to 67 billion liters per year (OECD-FAO, 2008). As a result demand for corn is expected to increase by nearly 17 percent over the next decade to 896 million tonnes/year (FAPRI 2008; OECD-FAO, 2008). This increase is apparent since U.S. maize production has increased from 9.4 billion bushels in 1999 to 13.1 billion bushels in 2009 (USDA-NASS, 2010). Meeting these demands for maize will require the discovery and application of new agricultural technologies including the development of superior maize hybrids.

Genetic Enhancement of Maize Roots as an Avenue for Yield Gains

Historically, conventional phenotypic selection in maize breeding programs has been a gradual and reliable method for increasing grain yields of maize. More recently, researchers have recognized the role secondary traits or components of yield play in enhancing yield. Among these secondary traits are tolerance to stresses (Tollenaar and Wu, 1999) including drought stress, nitrogen acquisition and adaptation to increased planting density (Messmer et al., 2009; Gallais and Hirel, 2004; Gonzalo et al. 2006). Enhancing maize root number, and modifying root patterning and functionality are avenues that have the potential to address issues associated with these stresses.

The role of both, biotechnology traits and molecular markers, in plant improvement is increasing (Edgerton, 2009). Before molecular breeding projects can use existing variation in these traits, the genes controlling them must be detected and characterized. Therefore, initial detection and characterization of genes involved in root patterning is required.

The root system of maize secures the plant to the ground and provides the plant with structural support to stay upright. Maize roots also provide the plant with water and nutrients to promote growth and respiration. The maize root system is comprised of two parts, the embryonic root system and the shoot-borne root (SBR) system (Kiesselbach, 1949; McCully, 1999). The embryonic root system is also known as the temporary, or primary root system. This root system emerges from the germinating seed and consists of the primary seminal root (radical) and a variable number of seminal roots and their associated root hairs (Kiesselbach, 1949; McCully, 1999). All of the embryonic roots, with the exception of the primary seminal root, emerge from above the scutellar node (Kiesselbach, 1949). While the embryonic root system is invaluable for the early establishment and success of maize seedlings, in many inbred lines it will senesce and the SBR system will take over as the main root system (Ritchie et al., 1993).

SBR roots emerge from the vasculature of the shoot at the nodes (Martin and Harris, 1976). The SBR system consists of above and below ground components. The below ground class is made up of the SBRs which emerge from six subterranean nodes while the above ground portion contains SBRs formed from a variable number of above ground nodes. The first whorl of SBRs begins to elongate at the V1 stage. At the V3 stage the embryonic root system stops growing and the SBRs begin to grow root hairs (Ritchie et al., 1993). At the V6 stage the embryonic root system is superseded by the SBR system. The SBR system will continue to grow until the R1 phase of development (onset of the reproductive phase).

Agronomically important traits are associated with SBR-patterning and function. Vertical root-pulling resistance, a measure of SBR complexity and prolificacy, has been correlated with lodging resistance (Holbert and Koehler, 1924; Guingo and Hébert, 1997), drought stress paramaters (Lebreton et al., 1995), and nitrogen uptake and low nitrogen stress tolerance (Kamara et al., 2001, 2002). These observations suggest that genotypic differences in SBR-patterning between maize inbred lines could be exploited to improve performance under adverse conditions and hence increase maize productivity.

The Genetics of Maize Root Systems

Genotypic differences in SBR formation occur along two axes. Along the basal-to-apical plane is the vertical axis of SBR variation. This axis of variation is described by the number of nodes that have SBRs starting at the base of the stem and moving apically. The second axis of SBR variation is the radial axis which lies perpendicular to the vertical axis. This axis is described by the number of SBRs at each individual node. While genotypic effects have been observed contributing to SBR variation (Tuberosa et al., 2002; Hébert et al., 2001; Flint-Garcia et al., 2005), less is known about the genes controlling their development.

The pathway recognized as controlling the vertical axis of SBR-patterning also dictates the duration of the juvenile-vegetative phase. The maize plant is comprised of a repeating

segments known as the phytomers which contain a node, a leaf or related structure and a variable number of axillary meristems (AM) (Poethig, 1993). The oldest phytomers contain juvenile tissue and are located at the basal region of the plant. Moving apically along the plant, the phytomers become chronologically younger and become phenotypically adult. The juvenile and adult vegetative phases are distinguished from one another based on the physical characteristics of the phytomers formed during each phase (Poethig, 1993). The basal, juvenile phytomers possess bluish juvenile leaf wax, SBRs, and cell wall crenulations which can be stained with toluidine blue (Poethig, 1993). The phytomers formed during the adult-vegetative phase have adult leaf wax and do not form SBRs. This developmental dichotomy where certain characteristics are associated with a developmental stage is called heterochrony. Consequently, genes controlling heterochrony establish the vertical axis of SBR variation by controlling the final manifestation of the AMs at the node.

Research in both maize and *Arabidopsis thaliana* has shed light on genes involved in the transition from juvenile-to-adult vegetative phase. In maize, Evans and Poethig (1995) linked the expression of juvenile-vegetative phase to gibberellic acid (GA). They observed that mutants deficient in GA biosynthesis displayed a longer juvenile-vegetative phase and increased formation of SBRs along the vertical axis. Additional support for the involvement of phase change in the vertical patterning of SBRs is provided by studies performed on the heterochronic maize mutants *earlyphasechange1* (*epc1*), *Teopod1* (*Tp1*), and *Teopod2* (*Tp2*). The heterochronic maize mutant *epc1* has a loss-of-function allele for a nuclear exportin orthologous to the *hasty* gene in *Arabidopsis* (Vega et al., 2002). Loss-of-function of *epc1* results in a precocious transition to adult-vegetative phase resulting in a reduction in the number of nodes with SBRs. In *Arabidopsis*, loss-of-function has been connected to the changes in *microRNA* accumulation (Park et al., 2005). Coincidently, *Tp1* and *Tp2* have been informally reported as over-expressers of

microRNA156 (*miR156*), resulting in prolonged vegetative phase and an increase in the number of nodes with shoot-borne roots.

Further evidence in *Arabidopsis* implicates *miR156* in vegetative-phase transition. Wu et al. (2006, 2009) provide evidence that *miR156* targeting of *SPL* transcription factors dictate the extent of juvenile-vegetative phase and *miR156* repression of SPLs determines the time of the phase transition. Wu and Poethig (2009) established *microRNA172*(*miR172*) as a factor counteracting *miR156* activity thus providing a balance of signals controlling heterochrony. Therefore the genes involved in juvenile-to-adult phase change, as well as those regulating this pathway, provide potential avenues for the manipulation of the vertical axis of SBR-patterning.

Considerably less is known about the radial patterning of SBRs in maize. With the exception of *rootless concerning crown and seminal roots* (*rtcs*), no other genes have been linked to radial SBR-patterning (Taramino et al., 2007). Extensive research in *Arabidopsis* has identified a myriad of genes contributing to the development of roots. However, there are many anatomical differences between the root systems of maize, a monocot, and *Arabidopsis*, a dicot. Therefore, extrapolating results from *Arabidopsis* to maize root systems should be approached with a healthy degree of skepticism.

Maize Diversity as a Genetic Resource

Maize has a multitude of genetic tools for the identification and characterization of genes involved in SBR-patterning. Many resources have been developed for reverse genetic screens in maize. In addition to a extensive library of classical maize mutants (Neuffer et al., 1996) three transposon-tagging systems have been exploited for gene-tagging in maize (Candela and Hake, 2008). Recently, forward genetic tools which take advantage of the abundant molecular diversity found in maize have gained popularity (Flint-Garcia et al., 2005; Canaran et al., 2008; Yu et al., 2008; Gore et al., 2009; Yan et al., 2009; Yang et al., 2010).

The dissection of quantitative trait variation in maize has relied for years on bi-parental linkage mapping populations (family-based analysis). Typically, parents which differ for the trait of interest are mated with one another to produce F_1 progeny which are selfed to produce F_2 progeny. At the F_2 stage plants are either genotyped and phenotyped, mated to siblings to produce immortalized $F_{2:3}$, or selfed to produce recombinant inbred lines (RILs). Studies using these materials have relatively high power, assuming adequate sample size, to link chromosome regions to the inheritance of complex traits. However, one major drawback to conventional quantitative trait locus (QTL) analysis is low map resolution (Flint-Garcia et al., 2005; Buckler and Thornsberry, 2002). Family-based linkage mapping results in QTL intervals ranging from 10 to 30 cM (map units) in size, containing hundreds to a thousand genes. To overcome this problem in maize, the Intermated B73 x Mo17 (IBM) mapping population was developed (Lee et al., 2002). By means of randomly intermating the F_2 progeny for four generations prior to selfing down to RILs, mapping resolution was improved three to four fold (Lee et al., 2002). The effectiveness of this resource is enhanced by the availability of the genome sequence of the population parents, B73 (Schnable et al., 2009; Zhou et al., 2009), as well as through tools linking it to other experimental linkage maps, QTL, and the placement of maize mutants (Lawrence et al., 2008).

Use of association mapping, a population-based mapping method has gained wide acceptace in the last decade. Association mapping tests if an allele is frequently inherited with a phenotype of interest (Balding, 2006). It uses the full spectrum of allelic diversity in a species and the ancient recombination accumulated over generations of meioses (Buckler and Thornbserry, 2002; Rafalski, 2002). As a population-based mapping method, association mapping does not require custom populations. This feature facilitates quick genotype-to-phenotype associations (Flint-Garcia et al., 2005). Deployment of association mapping methods in maize has resulted in the dissection of quantitative variation in physiological (Zhang et al., 2010), metabolic (Szalma et al., 2005), and developmental (Krill et al., 2010; Thornsberry et al., 2001) processes in maize. As

mapping populations continue to be assembled and new mapping methodologies are explored, association mapping will continue to provide valuable insight to quantitative inheritance of complex traits.

Family-based linkage mapping and population-based association mapping use natural allelic variation to explain the origins of phenotypic variation. Each method has advantages and disadvantages rooted in the fundamental differences between natural and experimental populations. The extent of linkage disequilibrium (LD) within each type of population is one variable which differs between the two mapping methods.

LD is a term used to describe the co-inheritance of alleles in a population (Flint-Garcia, et al., 2003). It is influenced by most population genetic forces such as selection, migration, mutation, recombination, and population expansion. When linkage disequilibrium is high, the physical distance between polymorphic sites which are inherited together (a unit known a haplotype) is large. LD is reduced by mutation, recombination, and the migration of new alleles into an existing population. The difference in map resolution between family-based linkage and population-based association mapping can be attributed to differences in LD arising primarily from mutation and recombination.

Conventional family-based QTL mapping studies rely on recombination events that occur after the F_1 generation between polymorphic sites of only two parents. As such, this type of mapping is limited by the polymorphic sites between the parents and the number of recombination events generated during population development. This scenario produces large haplotype blocks containing tens to thousands of genes physically linked to quantitative variation. Alternatively, association mapping can be made to include species level variation, maximizing the number of mutational sites. Since association mapping uses natural populations, it capitalizes on historic recombination re-assorting these mutations, minimizing the extent of LD and providing high resolution mapping (Buckler et al., 2006).

Although LD is smaller around a given gene in an association compared to a family-based mapping population, LD can also occur between alleles at unlinked loci. This can arise through intentional selection and complex breeding histories. Alleles co-inherited with underlying causative polymorphisms can be falsely identified as contributing to phenotypic variation of a given trait using association mapping. Population stratification and relative kinship enhance this type of inter-locus LD. As a result, association mapping methods have incorporated different estimates of population structure and kinship (Yu et al., 2006; Price et al., 2006). However, a negative impact of population structure on statistical power has been observed using these methods (Zhao et al., 2007).

Population structure is not the only factor limiting the statistical power of association mapping. Low frequency of a minor allele greatly reduces the power of an association test at a given locus (Myles et al., 2009; Zhao et al., 2007). Where an F_2 or RIL linkage mapping population is expected to have a minor allele frequency of approximately 0.5 the minor allele frequencies in association studies may range from nearly zero to rarely 0.5. This issue becomes increasingly prohibitive in association studies attempting to catalog species level variation in finite population sizes.

While family-based linkage mapping and population-based association mapping differ in power, resolution, and genetic properties, they can complement each other when used concurrently. Studies which exploit the advantages of both approaches have been effective in isolating genes controlling quantitative variation (Butrón et al., 2009; Pressoir et al., 2009; Salvi et al., 2007). Future studies will likely combine these methods to understand quantitative variation.

Experimental Objectives

Despite the important roles SBRs play in the survival and commercial success of maize, few studies have focused on identifying pathways contributing to their development and variation. The aim of this study was to identify pathways controlling SBR development using natural variation in maize.

Objective One: Identify pathways contributing to SBR variation by family-based linkage mapping using the IBM mapping population.

Objective Two: Validate the pathway(s) identified in Objective One using maize mutant phenotyping and population-based association analysis.

Objective Three: Identify additional pathway(s) affecting SBR-patterning by performing a systems analysis of phenotypic data collected in a diverse set of germplasm.

Objective Four: Attempt to validate the light-signaling pathway observed in Objective Three using mutant phenotyping, field treatments, and population-based association analysis.

REFERENCES

BALDING, D.J., 2006 A tutorial on statistical methods for population association studies. Nat. Rev. Genet. **7(10):** 781-791.

BUCKLER, E. S., B. S. GAUT, and M. D. MCMULLEN, 2006 Molecular and functional diversity of maize. Curr. Opin. Plant Biol. **9(2):** 172-176.

BUCKLER, E.S. 4TH and J. M. THORNSBERRY, 2002 Plant molecular diversity and applications to genomics. Curr. Opin. Plant Biol. **5(2):** 107-111.

BUTRÓN, A., Y. C. CHEN, G. E. ROTTINGHAUS, and M. D. MCMULLEN, 2009 Genetic variation at *bx1* controls DIMBOA content in maize. Theor. Appl. Genet. **120(4):** 721-734.

CANARAN, P., E. S. BUCKLER, J. C. GLAUBITZ, L. STEIN, Q. SUN, W. ZHAO, and D. WARE, 2008 Panzea: an update on new content and features. Nucl. Acids Res. **36:** D1041-1043.

CANDELA, H. and S. HAKE, 2008 The art and design of genetic screens: maize. Nat. Rev. Genet. **9(3):**192-203.

EDGERTON, M. D., 2009 Increasing crop productivity to meet global needs for feed, food, and fuel. Plant Physiol. **149(1):** 7-13.

EVANS, M. M. and R. S. POETHIG, 1995 Gibberellins promote vegetative phase change and reproduction in maize. Plant Physiol. **108(2)**: 475-487.

FAPRI, 2008 U.S. and world agriculture outlook. FAPRI, Ames, IA.

FLINT-GARCIA, S. A., A. C. THUILLET, J. YU, G. PRESSOIR, S. M. ROMERO, S. E. MITCHELL, J. DOEBLEY, S. KRESOVICH, M. M. GOODMAN, and E. S. BUCKLER, 2005 Maize association population: a high-resolution platform for quantitative trait locus dissection. Plant J. **44(6):** 1054-1064.

FLINT-GARCIA, S. A., J. M. THORNSBERRY, and E. S. BUCKLER 4TH, 2003 Structure of linkage disequilibrium in plants. Annu. Rev. Plant Biol. **54:** 357-374.

GALLAIS, A. and B. HIREL, 2004 An approach to the genetics of nitrogen use efficiency in maize. J. Exp. Bot. **55(396):** 295-306.

GONZALO, M., T. J. VYN, J. B. HOLLAND, and L. M. MCINTYRE, 2006 Mapping density response in maize: a direct approach for testing genotype and treatment interactions. Genetics **173(1):** 331-348.

GORE, M. A., J. M. CHIA, R. J. ELSHIRE, Q. SUN, E. S. ERSOZ, B. L. HURWITZ, J. A. PEIFFER, M. D. MCMULLEN, G. S. GRILLS, J. ROSS-IBARRA, D. H. WARE, and E. S. BUCKLER, 2009 A first-generation haplotype map of maize. Science **326(5956):** 1115-1117.

GUINGO, E. and Y. HEBERT, 1997 Relationships between mechanical resistance of the maize root system and root morphology, and their genotypic and environmental variation. Maydica **42**: 265-274.

HÉBERT, Y., E. GUINGO, and O. LOUDET, 2001 The response of root/shoot partitioning and root morphology to light reduction in maize genotypes. Crop Sci. **41:** 363-371.

HOLBERT, J. R. and B. KOEHLER, 1924 Anchorage and extent of corn root system. J. Agric. Res. **27**: 71–78.

KAMARA, A. Y., J. G. KLING, S. O. AJALA, and A. MENKIR, 2002 The relationship between vertical root-pulling resistance and nitrogen uptake and utilization in maize breeding lines. Maydica **47**: 135-141.

KAMARA, A. Y., J. G. KLING, S. O. AJALA, and A. MENKIR, 2001 Vertical root-pulling resistance in maize is related to nitrogen uptake and yield. Seventh Eastern and Southern Africa Regional Maize Conference. 11th-15th Febuary, 2001. P. 228-232.

KIESSELBACH, T.A., 1949. *The Structure and Reproduction of Corn*. CSHL Press. Cold Spring Harbor, NY. 101p.

KRILL, A. M., M. KIRST, L. V. KOCHIAN, E. S. BUCKLER, and O. A. HOEKENGA, 2010 Association and linkage analysis of aluminum tolerance genes in maize. PLoS One **5(4):** e9958.

LAWRENCE, C. J., L. C. HARPER, M. L. SCHAEFFER, T. Z. SEN, T. E. SEIGFRIED, and D. A. CAMPBELL, 2008 MaizeGDB: The maize model organism database for basic, translational, and applied research. Int. J. Plant Genomics **2008**: 496957.

LEBRETON, C., V. LAZIC-JANCIC, A. STEED, S. PEKIC and S. A. QUARRIE, 1995 Identification of QTL for drought responses in maize and their use in testing causal relationships between traits. J. Exp. Bot. **46(7)**: 853–865.

LEE, M., N. SHAROPOVA, W. D. BEAVIS, D. GRANT, M. KATT, D. BLAIR, and A. HALLAUER, 2002 Expanding the genetic map of maize with the intermated B73 x Mo17 (IBM) population. Plant Mol. Biol. **48(5-6):** 453-461.

MARTIN, E.M., AND W.M. HARRIS, 1976 Adventitious root development from the coleoptilar node in *Zea mays* L. Amer. J. Bot. **63(6):** 890-897.

MATSUOKA, Y., Y. VIGOUROUX, M. M. GOODMAN, G. J. SANCHEZ, E. BUCKLER, and J. DOEBLEY, 2002 A single domestication for maize shown by multilocus microsatellite genotyping. Proc. Natl. Acad. Sci. U. S. A. **99(9):** 6080-6084.

MCCULLY, M. E., 1999 Roots in soil: Unearthing the complexities of roots and their rhizospheres. Annu. Rev. Plant Physiol. Plant Mol. Biol. **50**: 695-718.

MESSMER, R., Y. FRACHEBOUD, M. BÄNZIGER, M. VARGAS, P. STAMP, and J. M. RIBAUT, 2009 Drought stress and tropical maize: QTL-by-environment interactions and stability of QTLs across environments for yield components and secondary traits. Theor. Appl. Genet. **119(5):** 913-930.

MYLES, S., J. PEIFFER, P. J. BROWN, E. S. ERSOZ, Z. ZHANG, D. E. COSTICH, and E. S. BUCKLER, 2009 Association mapping: critical considerations shift from genotyping to experimental design. Plant Cell **21(8):** 2194-2202.

NCGA, 2010 Corn based products guide. Available at http://www.ncga.com/corn-based-products-guide.

NEUFFER, M. G., E. H. COE and S. R. WESSLER, 1996 *Mutants of Maize*. CSHL Press. Cold Spring Harbor, NY. 469p.

OECD-FAO, 2008 Agriculture Outlook 2008-2017. OECD Publications, Paris.

PARK, M. Y., G. WU, A. GONZALEZ-SULSER, H. VAUCHERET, and R. S. POETHIG, 2005 Nuclear processing and export of microRNAs in *Arabidopsis*. Proc. Natl. Acad. Sci. U. S. A. **102(10):** 3691-3696.

PIPERNO, D. R. and K. V. FLANNERY, 2001 The earliest archaeological maize (*Zea mays* L.) from highland Mexico: new accelerator mass spectrometry dates and their implications. Proc. Natl. Acad. Sci. U. S. A. **98(4):**2101-2103.

POETHIG, R. S., 1993 The maize shoot, p. 11-16 in *The Maize Handbook*, edited by M. Freeling and V. Walbot. Springer-Verlag, New York. 759p.

PRESSOIR, G., P. J. BROWN, W. ZHU, N. UPADYAYULA, T. ROCHEFORD, E. S. BUCKLER, AND S. KRESOVICH, 2009 Natural variation in maize architecture is mediated by allelic differences at the PINOID co-ortholog *barren inflorescence2*. Plant J. **58(4):** 618-628.

PRICE, A. L., N. J. PATTERSON, R. M. PLENGE, M. E. WEINBLATT, N. A. SHADICK, and D. REICH, 2006 Principal components analysis corrects for stratification in genome-wide association studies. Nat. Genet. **38(8):** 904-909.

RAFALSKI, A., 2002 Applications of single nucleotide polymorphisms in crop genetics. Curr. Opin. Plant Biol. **5(2):** 94-100.

RITCHIE, S.W., J. J. HANAWAY and G. O. BENSON, 1993 How a corn plant develops. Special Report No. 48, Iowa State University of Science and Technology, Cooperative Extension Service, Ames, IA.

SALVI, S., G. SPONZA, M. MORGANTE, D. TOMES, X. NIU, K. A. FENGLER, R. MEELEY, E. V. ANANIEV, S. SVITASHEV, E. BRUGGEMANN, B. LI, C. F. HAINEY, S.

RADOVIC, G. ZAINA, J. A. RAFALSKI, S. V. TINGEY, G. H. MIAO, R. L. PHILLIPS, AND R. TUBEROSA, 2007 Conserved noncoding genomic sequences associated with a flowering-time quantitative trait locus in maize. Proc. Natl. Acad. Sci. U. S. A. **104(27):** 11376-11381.

SCHNABLE, P. S., D. WARE, R. S. FULTON, J. C. STEIN, F. WEI, S. PASTERNAK, C. LIANG, J. ZHANG, L. FULTON, T. A. GRAVES, P. MINX, A. D. REILY, L. COURTNEY, S. S. KRUCHOWSKI, C. TOMLINSON, C. STRONG, K. DELEHAUNTY, C. FRONICK, B. COURTNEY, S. M. ROCK, E. BELTER, F. DU, K. KIM, R. M. ABBOTT, M. COTTON, A. LEVY, P. MARCHETTO, K. OCHOA, S. M. JACKSON, B. GILLAM, W. CHEN, L. YAN, J. HIGGINBOTHAM, M. CARDENAS, J. WALIGORSKI, E. APPLEBAUM, L. PHELPS, J. FALCONE, K. KANCHI, T. THANE, A. SCIMONE, N. THANE, J. HENKE, T. WANG, J. RUPPERT, N. SHAH, K. ROTTER, J. HODGES, E. INGENTHRON, M. CORDES, S. KOHLBERG, J. SGRO, B. DELGADO, K. MEAD, A. CHINWALLA, S. LEONARD, K. CROUSE, K. COLLURA, D. KUDRNA, J. CURRIE, R. HE, A. ANGELOVA, S. RAJASEKAR, T. MUELLER, R. LOMELI, G. SCARA, A. KO, K. DELANEY, M. WISSOTSKI, G. LOPEZ, D. CAMPOS, M. BRAIDOTTI, E. ASHLEY, W. GOLSER, H. KIM, S. LEE, J. LIN, Z. DUJMIC, W. KIM, J. TALAG, A. ZUCCOLO, C. FAN, A. SEBASTIAN, M. KRAMER, L. SPIEGEL, L. NASCIMENTO, T. ZUTAVERN, B. MILLER, C. AMBROISE, S. MULLER, W. SPOONER, A. NARECHANIA, L. REN, S. WEI, S. KUMARI, B. FAGA, M. J. LEVY, L. MCMAHAN, P. VAN BUREN, M. W. VAUGHN, K. YING, C. T. YEH, S. J. EMRICH, Y. JIA, A. KALYANARAMAN, A. P. HSIA, W. B. BARBAZUK, R. S. BAUCOM, T. P. BRUTNELL, N. C. CARPITA, C. CHAPARRO, J. M. CHIA, J. M. DERAGON, J. C. ESTILL, Y. FU, J. A. JEDDELOH, Y. HAN, H. LEE, P. LI, D. R. LISCH, S. LIU, Z. LIU, D. H. NAGEL, M. C. MCCANN, P. SANMIGUEL, A. M. MYERS, D. NETTLETON, J. NGUYEN, B. W. PENNING, L. PONNALA, K. L. SCHNEIDER, D. C. SCHWARTZ, A. SHARMA, C.

SODERLUND, N. M. SPRINGER, Q. SUN, H. WANG, M. WATERMAN, R. WESTERMAN, T. K. WOLFGRUBER, L. YANG, Y. YU, L. ZHANG, S. ZHOU, Q. ZHU, J. L. BENNETZEN, R. K. DAWE, J. JIANG, N. JIANG, G. G. PRESTING, S. R. WESSLER, S. ALURU, R. A. MARTIENSSEN, S. W. CLIFTON, W. R. MCCOMBIE, R. A. WING, and R. K. WILSON, 2009 The B73 maize genome: complexity, diversity, and dynamics. Science **326(5956):** 1112-1115.

SZALMA, S. J., E. S. BUCKLER 4TH, M. E. SNOOK, and M. D. MCMULLEN, 2005 Association analysis of candidate genes for maysin and chlorogenic acid accumulation in maize silks. Theor. Appl. Genet. **110(7):** 1324-1333.

TARAMINO, G., M. SAUER, J. L. STAUFFER, D. MULTANI, X. NIU, H. SAKAI, and F. HOCHHOLDINGER, 2007 The maize (*Zea mays* L.) *RTCS* gene encodes a LOB domain protein that is a key regulator of embryonic seminal and post-embryonic shoot-borne root initiation. Plant J. **50(4):** 649-659.

THORNSBERRY, J. M., M. M. GOODMAN, J. DOEBLEY, S. KRESOVICH, D. NIELSEN, and E. S. BUCKLER 4TH, 2001 *Dwarf8* polymorphisms associate with variation in flowering time. Nat. Genet. **28(3):** 286-289.

TOLLENAAR, M. and J. WU, 1999 Yield improvement in temperate maize is attributable to greater stress tolerance, Crop Sci. **39:** 1597-1604.

TUBEROSA, R., S. SALVI, M. C. SANGUINETI, P. LANDI, M. MACCAFERRI and S. CONTI, 2002 Mapping QTLs regulating morpho-physiological traits and yield: case studies, shortcomings, and perspectives in drought-stressed maize. Ann. Bot. **89**: 941-963.

USDA-NASS. 2010 Corn statistics. Available at http://www.nass.usda.gov/QuickStats/index2.jsp.

VEGA, S. H., M. SAUER, J. A. ORKWISZEWSKI, and R. S. POETHIG, 2002 The early phase change gene in maize. Plant Cell **14(1):** 133-147.

VON BRAUN, J., 2007 The world food situation: new driving forces and the required actions. Food Policy Report 18. International Food Policy Research Institute. http://www.ifpri.org.

WU, G., M. Y. PARK, S. R. CONWAY, J. W. WANG, D. WEIGEL, and R. S. POETHIG, 2009 The sequential action of *miR156* and *miR172* regulates developmental timing in *Arabidopsis*. Cell **138(4):** 750-759.

WU, G. and S. POETHIG, 2006 Temporal regulation of shoot development in *Arabidopsis thaliana* by *miR156* and its target *SPL3*. Development **133(18):** 3539-3547.

YAN, J., T. SHAH, M. L. WARBURTON, E. S. BUCKLER, M. D. MCMULLEN, and J. CROUCH, 2009 Genetic characterization and linkage disequilibrium estimation of a global maize collection using SNP markers. PLoS One **4(12):** e8451.

YANG, X, J. YAN, T. SHAH, M. L. WARBURTON, Q. LI, L. LI, Y. GAO, Y. CHAI, Z. FU, Y. ZHOU, S. XU, G. BAI, Y. MENG, Y. ZHENG, and J. LI, 2010 Genetic analysis and

characterization of a new maize association mapping panel for quantitative trait loci dissection. Theor. Appl. Genet. Mar 27. [Epub ahead of print]

YU, J., J. B. HOLLAND, M. D. MCMULLEN, and E. S. BUCKLER, 2008 Genetic design and statistical power of nested association mapping in maize. Genetics **178(1):** 539-551.

ZHANG, N., A. GUR, Y. GIBON, R. SULPICE, S. FLINT-GARCIA, M. D. MCMULLEN, M. STITT, and E. S. BUCKLER, 2010 Genetic analysis of central carbon metabolism unveils an amino acid substitution that alters maize NAD-dependent isocitrate dehydrogenase activity. PLoS One **5(4):** e9991.

ZHAO, K., M. J. ARANZANA, S. KIM, C. LISTER, C. SHINDO, C. TANG, C. TOOMAJIAN, H. ZHENG, C. DEAN, P. MARJORAM, and M. NORDBORG, 2007 An *Arabidopsis* example of association mapping in structured samples. PLoS Genet. **3(1):** e4.

ZHOU, S., F. WEI, J. NGUYEN, M. BECHNER, K. POTAMOUSIS, S. GOLDSTEIN, L. PAPE, M. R. MEHAN, C. CHURAS, S. PASTERNAK, D. K. FORREST, R. WISE, D. WARE, R. A. WING, M. S. WATERMAN, M. LIVNY, and D. C. SCHWARTZ, 2009 A single molecule scaffold for the maize genome. PLoS Genet. **5(11):** e1000711.

CHAPTER 2: Quantitative trait loci for shoot-borne root patterning identify positional candidates related to hormones and phase change

ABSTRACT

Shoot-borne roots are an essential part of the mature maize (*Zea mays* L.) plant. They provide terrestrial anchorage and facilitate access to water and nutrients found in the soil. Despite their indispensable roles in cereal crops, few studies have attempted to dissect the underlying mechanisms controlling their growth and development. In this study the intermated B73 x Mo17 (IBM) recombinant inbred line mapping population was used to identify chromosomal regions harboring factors controlling maize SBR-patterning. QTL were mapped near loci controlling GA biosynthetic and response genes in addition to genes controlling phase change. These results suggest that these genes should be tested further as candidates for the QTL since polymorphisms between these genes in B73 and Mo17 may lead to differential SBR-patterning.

INTRODUCTION

The root systems of terrestrial plants are essential for nutrient and water acquisition as well as mechanical anchorage. The roots of maize may be subdivided into two different categories, the embryonic root system and the SBR system (Kiesselbach, 1949; McCully, 1999). The embryonic root system, often referred to as the temporary or primary root system, emerges from the germinated seed. It consists of the primary seminal root, a variable number of seminal lateral roots emerging from the scutellar node, and the root hairs (Wiggins, 1916; Kiesselbach, 1949). The SBRs consist of the subterranean SBRs, a set of crown roots positioned at the soil level, and a series of SBRs originating from nodes above the ground, some of which penetrate the soil surface and are referred to as brace roots.

SBR-patterning has been implicated in many agronomically important traits and processes. Vertical root-pulling force has been used to quantify SBR-patterning and has been correlated with lodging resistance (Holbert and Koehler,1924; Guingo and Hebert, 1997), plant stress parameters under drought (Lebreton et al., 1995), and nitrogen uptake, low nitrogen stress tolerance and yield (Kamara et al., 2000, 2001). Kiesselbach (1949) ablated the seminal root systems of three week old Krug variety maize plants leading to only a 9% reduction in grain yield suggesting that the SBRs supply the majority of water and nutrients to the adult plant.

Differences in SBR-patterning between maize genotypes can be observed along two axes. The first is the vertical axis along the basal-to-apical plane. This axis describes the number of nodes, from the base of the stem upward, that possess SBRs. The second axis is a radial axis which is perpendicular to the vertical axes. This radial axis describes the patterning of SBRs that originate at a single node along the vertical axis.

The vertical axis of SBR-patterning is comprised of a repeating shoot segment called the phytomer. The phytomer contains a node, a leaf or similar structure and a variable number of AMs (Poethig 1993). The identity of phytomers changes with time, with the oldest phytomers formed during the juvenile-vegetative phase located basally, and the adult and reproductive phytomers forming acropetally. Ultimately the manifestation of the AMs is determined by the identity of the phytomer from which they originate. In *wild-type* plants, the only AMs which have the potential to form SBRs emerge from juvenile or partially juvenile phytomers (Poethig, 1993), thus the vertical component of SBR-patterning is determined by the number of juvenile phytomers.

Previous research in maize and Arabidopsis has established a role for the phytohormone GA as controlling phytomer identity and hence vertical SBR-patterning. Evans and Poethig (1995) associated production of gibberellins with SBR formation by comparing the number of

nodes with SBRs in mutants deficient in GA and their *wild-type* counterparts. The researchers concluded that GA production promotes the change from juvenile-to-adult vegetative phase, and as a result, controls the number of nodes with AMs from which SBR may initiate.

Additional support for the association between juvenile phytomers and SBR formation is provided by studies involving the heterochronic mutants *Tp1*, *Tp2*, and *epc1*. The semidominant mutants *Tp1*and *Tp2* display a prolonged juvenile state resulting in increased phytomers with juvenile wax, cell wall crenulations and SBRs.

SBR development is a normal and essential event in the development of maize and other agronomically important monocots such as rice (*Oryza sativa* L.), sorghum (*Sorghum bicolor* L.), and wheat (*Trticum aestivum* L.). Arabidpsis, a dicot, has provided a wealth of knowledge on root patterning; however SBR are not observed under usual growth conditions in Arabidopsis. Therefore, caution should be taken in extrapolation of events which occur in Arabidopsis root development to maize and other monocots pending further research into the impact of the anatomical difference on the underlying biology. A study which identified genes involved in SBR-patterning in maize would shed light on the genetic regulation of these important cereal structures and assist in the continued comparative analysis of mechanistic similarities and divergence between monocots and dicots.

Few QTL mapping studies have aimed to identify chromosome regions affecting SBR-patterning (Lebreton, et al., 1995, Tuberosa, et al., 2002, Giuliani et al., 2005). The most in depth study validated a QTL, *Root-ABA1*, as controlling SBR number at the second node above ground and other various root parameters. Although the study has successfully characterized the effects of *Root-ABA1*, it has not provided the identity of the heritable factor at the locus.

Our goal was to use the intermated B73 x Mo17 recombinant inbred line (IBM- RIL) mapping population to identify QTL and candidate genes underlying variation in maize SBR-patterning along the two axes of development. The position of the identified QTL relative to relevant mutants is discussed.

MATERIALS AND METHODS

Plant Material and Experimental Design: The 94 lines used for linkage map construction and QTL analysis are a subset of lines from the IBM mapping population. B73, a Stiff Stalk Synthetic inbred, and Mo17, a Lancaster Sure Crop inbred, represent two important dent heterotic groups used in commercial breeding. The IBM mapping population was derived from a B73 x Mo17 cross. The resulting F_2 lines were randomly intermated with each line contributing only once as a male and once as a female to the next generation for four generations followed by selfing to produce $F_{7:8}$ recombinant inbred lines (Lee et al., 2002). The increased meioses, which result from the random-mating, allow researchers to accurately map larger numbers of molecular markers with relatively fewer individuals.

The 94 lines were sown in the field in Columbia, Missouri during the first week of May in 2003, 2004, and 2005. In 2006, 274 lines of the IBM mapping population were planted. The plants were grown following common agricultural practices in a randomized complete block design with two replications. The traits evaluated were the number of nodes with SBRs above ground (NWSBR), and the number of SBRs at the first and at the second node above ground (SBR1 and SBR2 respectively). SBR angle (SBRA) was evaluated in 2004 and 2005 using digital camera images in the ImageJ software package (Rasband, 1997). Angles were measured from the stem counter-clockwise to the apical root surface.

Trait Analysis: The trait data was initially evaluated using the PROC UNIVARIATE command in SAS/STAT® software version 8.0 (SAS Institute Inc., Raleigh, NC, USA). Normality of the data generated each year was tested using the Shapiro-Wilk test. Homogeneity of variances across years was tested using the Bartlett test. Analysis of variance (ANOVA) was conducted for each trait within each year using PROC GLM in SAS. The fixed effect terms included in the model were Line, Year, and Line x Year.

Genetic Linkage Map and QTL analysis: The 643 markers used in the linkage map were selected based on an average genetic distance of approximately 10 cM between adjacent markers on the IBM 2004 map (Appendix 1). The linkage map was generated in Mapmaker Exp.3.0 (Lander et al., 1987) using the Haldane option with a placement threshold of LOD=3.0. Chromosomal assignment and order for each marker was based on the assembly data provided by MaizeGDB (www.maizegdb.org).

Least squares means were generated for each year with the SAS/STAT® software were used for QTL mapping. Composite interval mapping (CIM) was performed using QTL Cartographer version 2.5, for Windows (Wang et al., 2007). The experiment-wise test statistic for α=0.1 was identified through 1000 permutations of the data in the ZmapQTL function of QTL Cartographer with window size=10, background markers=5, and model=6 as prescribed by Churchill and Doerge (1994). QTL identified as significant using CIM were loaded into the multiple interval mapping (MIM) function, MImapQTL, of QTL Cartographer as the initial model for MIM (Kao et al., 1999). Once the initial model was generated in the MImapqtl module, the QTL were compared to the result files from which they were extracted. The MImapqtl module

was used solely to optimize QTL positions, test QTL significance, to test for epistatic interactions between QTL, and to estimate QTL contribution to phenotypic variance in a multilocus model (MLM).

Identification of candidate genes: The IBM2 map (http://www.maizegdb.org/) was used to identify the bin in which each QTL resided. Subsequently bins were used to identify mutants which mapped coincident with the QTL on the Genetic Map 2005 (http://www.maizegdb.org/). Two regions, bins 1.10 and 10.04, were examined more closely by simultaneously plotting, the likelihood ratio (LR) statistics, and candidate genes onto the linkage map using MapChart 2.2 (Voorrips, 2002).

RESULTS

Trait and QTL Analysis

SBRA: Comparison of the parental lines identified statistical differences for SBRA in 2004 and in 2005 ($P = 0.043$, $P = 0.0003$). The ANOVA performed on the 2005 data indicated highly significant differences between RILs. Although the ranges of phenotypic values were similar across years, the population mean in 2004 more closely approximated the mean performance of the parental line B73 in 2004 than in 2005 (data not shown).

Five QTL were identified for SBRA in 2004, providing a MLM which accounted for 58.4% of the phenotypic variation (Table 1A). Four of the five QTL had B73 as the positive parent collectively controlling 50% of the trait variance from that year. In 2005, five QTL for SBRA were identified resulting in a MLM that explained 66.2% of the phenotypic variance (Table 1B). Two of the four QTL with a positive contribution from B73 had large R^2 values, *qsbra7* (R^2=24.7%) and *qsbra8* (R^2=20.1%). Four QTL had B73 as the positive parent in 2004 (Table 1A).

NWSBR: In 2004 and 2005 B73 had more NWSBR than Mo17 (3.5 and 2.9 respectively, 2.6 and 2.5 respectively), but a significant difference between the two parents was found only in 2005 (*P* = 0.0438). The mean value for NWSBR in the RIL population was approximately the same as Mo17 in 2004 and 2005 (2.4 and 2.7 respectively). A highly significant line effect was identified in the ANOVAs performed on the trait data from each year.

Twelve QTL for NWSBR were found across the four years (Table 2). B73 was the positive parent for seven of the twelve QTL. Three QTL were identified for NWSBR in 2003 including a major QTL, *qnwsbr1*, on chromosome 1 at marker *umc94a*, with an R^2 value of 20.2%. The MLM containing the three QTL identified accounts for 42.4% of the phenotypic variance (Table 2A). Five QTL were found for NWSBR in 2005, explaining 59.5% of the phenotypic variance (Table 2C). *umc94a* was again identified as linked to a QTL for NWSBR in 2005. Three QTL were identified in 2006 controlling 18.5% of the variance.

SBR2: Variances across the years were unequal and the two ANOVAs (one from 2004 and the other for 2005) identified highly significant differences between RILs. No statistical difference was found between the parental lines for SBR2 in 2005, despite finding a significant difference between the parents in 2004 (*P* = 0.0004). In 2004, the mid-parent value for SBR2 (13.4) approximated the RIL population mean (14.3). However, in 2005 the mid-parent value (18.3) was much greater than the RIL population mean (16.2).

A total of 10 QTL were mapped controlling SBR2. Four QTL were identified for SBR2 in 2004, three in 2005, and three in 2006 (Table 3). The four QTL identified in 2004 accounted for 49.1% of the phenotypic variation (Table 3A), with B73 providing the positive contribution for three of the QTL (total R^2 38.6%). Two of the three QTL identified for SBR2 in 2005 had positive contributions from B73 (Table 3B). The MLM explained 25.6% of the phenotypic

variance. In 2006, the three QTL contributed to 17.1% of the phenotypic variance in two of which Mo17 was the positive parent (Table 3C).

SBR1: Differences between parental lines were tested in 2004 and 2005 for SBR1. In 2004, the parental lines were significantly different ($P = 0.0282$), with B73 (15.7) having more brace roots at node one than Mo17 (13.7). No difference was found between the parental lines in 2005 although B73 had a greater number of brace roots (15.5). The mean number of SBR1 for the RIL population approximated the mid-parent value in each year. SBR1 variances between the 2004 and 2005 seasons were unequal, so separate ANOVAs were performed for each year. The inbred line effect was highly significant.

A total of ten QTL were identified for SBR1: two in 2003, two in 2004, three in 2005, and three in 2006 (Table 4). The amount of phenotypic variance explained by the MLMs was 22.7, 21.8, 40.3, and 16.7 percent. Two chromosome arms, 9L and 10L, had multiple QTL. Each year the trait was measured, a QTL was detected on 10L. For each QTL located on 10L, B73 was identified as the positive parent. Alternatively, the two QTL identified on 9L had positive effects from both parents, *qsbr1.3* from Mo17 and *qsbr1.6* from B73.

DISCUSSION

QTL controlling both axes of SBR-patterning map near GA mutants: Evans and Poethig (1995) established a link between GA production and SBR-patterning by evaluating NWSBR in GA-deficient dwarf mutants. The mutants examined in that study, *dwarf1* (*d1*), *dwarf3* (*d3*), *dwarf5* (*d5*), and *anther ear1* (*an1*), all possessed more NWSBR than the *wild-type* controls. From this they concluded that the underlying structural genes involved in GA biosynthesis regulate NWSBR by controlling phase change through their regulation of GA levels.

Each of the four mutants map to a bin containing QTL for SBR-patterning (Figure 1). *d1* maps near *qsbr2.2* on chromosome three. *d3* maps on the border of bins 9.02 and 9.03 near *qsbr2.4*, and *d5* maps near a QTL for SBR2 and NWSBR on chromosome two between bins 2.02 and 2.03 (*qsbr2.1* and *qnwsbr12*). This region on chromosome two has also been identified as controlling root traits in hydroponics in the Lo964xLo1016 and Ac7643xAc7729 mapping populations, in addition to SBR in the field in the F2xIo mapping population (Tuberosa et al., 2002). *an1* maps coincident with a QTL for SBRA but not for NWSBR. Taken together these results suggest that allelic variation at these loci controlling GA production may contribute to the phenotypic variation observed in the IBM and various other mapping populations previously described.

Evidence that GA response may regulate SBR-patterning: Three dominant GA-nonresponsive dwarf mutants have been assigned to bins on the Maize Genetic 2005 map. *Dwarf8* (*D8*) and *Dwarf9* (*D9*) are orthologous to the negative-gibberellin-response regulators RGA/GAI found in Arabidopsis (Ikeda et al., 2001). In contrast to the previous group of mutations in structural genes responsible for GA biosynthesis, the *D8* and *D9* loci encode genes affecting GA response. The mutation responsible for the *D8/D9* phenotype occurs in the DELLA domain (Peng et al. 1999), which is required for ubiquination of the protein and its subsequent degradation by the 26S proteasome in response to GA accumulation (Itoh et al., 2003). The locus determining the *Dwarf10* (*D10*) phenotype is still unknown, but the short stature phenotype is not restored by the application of GA leading to speculation that it may also be a response regulator. Mapping of QTL for SBR-patterning near these loci, along with the phenotypic changes in SBR-patterning which accompany mutations in structural genes for GA biosynthesis, further implicate GA as a potential regulator of SBR-patterning.

D8 maps to bin 1.09-1.10 near four SBR-patterning QTL in the IBM mapping population, *qnwsbr3, qnwsbr6, qnwsbr11,* and *qsbr2.9* (Figure 2). Upon closer inspection, only *qnwsbr11* overlaps with *D8* (Figure 2). In addition, *qnwsbr11,* was the only QTL in bin 1.10 that has B73 as a positive parent suggesting that the other QTL are controlled by another locus. *D9,* a duplicate locus of *D8,* maps to bin 5.02-5.03 near *qnwsbr8* in the IBM and two other QTL for root traits in the Ac7643xAc7729 mapping population (Tuberosa et al., 2002). *D10* is located in bin 2.08. Two QTL for root traits in hydroponics are located near *D10* in the Lo964xLo1016 population as well as two QTL for root traits in the field for Ac7643xAc7729 mapping (Tuberosa et al., 2002).

Considering the evidence that GA biosynthetic genes affect SBR-patterning, loci regulating GA response represent genetic factors potentially contributing to SBR variation. Mutant evaluations have revealed that GA suppresses SBR-patterning through the regulation of phase change, but it is less obvious how DELLA restraint promotes SBR emergence and growth. Evaluation of the SBR phenotypes of GA response mutants will shed further light on how GA acts to shape SBR development.

Phase Change and SBR-patterning: Evans and Poethig (1995) examined GA-deficient mutants and found that they produced more NWSBR than their *wild-type* counterparts. This discovery led to the conclusion that GA suppresses the juvenile-vegetative phase and as a result influences SBR-patterning. Another mutant from that study, *Tp2* located in bin 10.05, also exhibits prolonged expression of the juvenile-vegetative phase. Recently, *Corngrass1* (*Cg1*), a mutant with a phenotypesimilar to *Tp2,* including increased NWSBR and leaves with juvenile wax was cloned and identified as two tandem copies of *miR156* whose expression led to the extended production of juvenile traits (Chuck et al., 2007). *Tp2* not only shares a similar, albeit weaker, phenotype with *Cg1,* but is also located near another *miR156* family member, *miR156h,* recently mapped by Zhang et al. (2009a). This suggests that the *Tp2* phenotype may be the result of the

ectopic expression of *miR156h*. Five QTL for SBR-patterning mapped near *Tp2*: *qsbr1.2, qsbr1.7, qsbr1.10, qsbr2.7,* and *qsbr2.10* (all with B73 as a positive parent, Figure 3). This implies that variation at the *Tp2* locus may contribute to the phenotypic variability for SBR-patterning in the IBM mapping population and that *miR156h* is a candidate gene for SBR-patterning.

miR156 family members regulate phase change by targeting SQUAMOSA PROMOTER BINDING (SPB) proteins (Wu and Poethig, 2006). Recently, prolonged expression of *miR156* was discovered in GA-deficient mutants (Zhang et al., 2009b, S. Moose, personal communication). The temporal modification of *miR156* cleavage of SPB transcripts via GA activity provides a basic framework for control of NWSBR. Consequently, further investigation into the role of GA and *miR156* activity in SBR-patterning should be pursued. Particular attention should be given not just to their roles in NWSBR production, but also to their role in SBR1 and SBR2 emergence.

REFERENCES

CHUCK, G., A. M. CIGAN, and S. HAKE, 2007 The heterochronic maize mutant *Corngrass1* results from overexpression of a tandem microRNA. Nat. Genet. **39(4):** 544-549.

CHURCHILL, G. A. and R. W. DOERGE, 1994 Empirical threshold values for quantitative trait mapping. Genetics **138:** 963–971.

EVANS, M. M. and R. S. POETHIG, 1995 Gibberellins promote vegetative phase change and reproduction in maize. Plant Physiol. **108**: 475-487.

GIULIANI, S., M. C. SANGUINETI, R. TUBEROSA, M. BELLOTTI, S. SALVI, and P. LANDI, 2005 *Root-ABA1*, a major constitutive QTL, affects maize root architecture and leaf ABA concentration at different water regimes. J. Exp. Bot. **56(422):** 3061-3070.

GUINGO, E. and Y. HEBERT, 1997 Relationships between mechanical resistance of the maize root system and root morphology, and their genotypic and environmental variation. Maydica **42**: 265-274.

HOLBERT, J. R. and B. KOEHLER, 1924 Anchorage and extent of corn root system. J. Agric. Res. **27:** 71–78.

IKEDA A., M. UEGUCHI-TANAKA , Y. SONODA , H. KITANO , M. KOSHIOKA , Y. FUTSUHARA, M. MATSUOKA, and J. YAMAGUCHI, 2001 *slender rice*, a constitutive gibberellin response mutant, is caused by a null mutation of the *SLR1* gene, an ortholog of the height-regulating gene *GAI/RGA/RHT/D8*. Plant Cell **13**: 999-1010.

ITOH, H., M. MATSUOKA and C. M. STEBER, 2003 A role for the ubiquitin–26S-proteasome pathway in gibberellin signaling. Trends Plant Sci. **8**: 495-497.

KAMARA, A. Y., J. G. KLING, S. O. AJALA and A. MENKIR, 2001 Vertical root-pulling resistance in maize is related to nitrogen uptake and yield. Seventh Eastern and Southern Africa Regional Maize Conference. 11^{th}-15^{th} Febuary, 2001. 228-232.

KAMARA, A. Y., J.G. KLING, S .O. AJALA and A. MENKIR, 2000 The relationship between vertical root-pulling resistance and nitrogen uptake and utilization in maize breeding lines. Maydica **47**: 135-141.

KAO, C. H., Z-B. ZENG and R. D. TEASDALE, 1999 Multiple interval mapping for quantitative trait loci. Genetics **152:** 1203–1216.

KIESSELBACH, T. A., 1949. *The Structure and Reproduction of Corn*. CSHL Press. Cold Spring Harbor, NY.

LANDER, E. S. and D. BOTSTEIN, 1989 Mapping mendelian factors underlying quantitative traits using RFLP linkage maps. Genetics **121**: 185-199.

LEBRETON, C., V. LAZIC-JANCIC, A. STEED, S. PEKIC and S. A. QUARRIE, 1995 Identification of QTL for drought responses in maize and their use in testing causal relationships between traits. J. Exp. Bot. **46**: 853–865.

LEE, M., N. SHAROPOVA, W. D. BEAVIS, D. GRANT, M. KATT, D. BLAIR, and A. HALLAUER., 2002 Expanding the genetic map of maize with the intermated B73 x Mo17 (IBM) population. Plant Mol. Biol. **48**: 453-61.

MCCULLY, M.E., 1999 Roots in soil: Unearthing the complexities of roots and their rhizospheres. Annu. Rev. Plant Physiol. Plant Mol. Biol. **50**: 695-718.

PENG, J., D. E. RICHARDS, N. M. HARTLEY, G. P. MURPHY, K. M. DEVOS, J. E. FLINTHAM, J. BEALES, L. J. FISH, A. J. WORLAND, F. PELICA, D. SUDHAKAR, P. CHRISTOU, J. W. SNAPE, M. D. GALE, and N. P. HARBERD, 1999 'Green revolution' genes encode mutant gibberellin response modulators. Nature **400**: 256-261.

POETHIG, R. S., 1993 The maize shoot, 11-16 in *The Maize Handbook*, edited by M. Freeling and V. Walbot. Springer-Verlag, New York.

RASBAND, W. S., 1997-2007 *ImageJ*, U. S. National Institutes of Health, Bethesda, Maryland, USA, http://rsb.info.nih.gov/ij.

SAS INSTITUTE, 2004 SAS Version 9.1. SAS Institute, Cary, NC.

TUBEROSA, R., S. SALVI, M. C. SANGUINETI, P. LANDI, M. MACCAFERRI and S. CONTI, 2002 Mapping QTLs regulating morpho-physiological traits and yield: Case studies, shortcomings, and perspectives in drought stressed maize. Ann. Bot. **89**: 941-963.

VOORRIPS, R. E., 2002 MapChart: Software for the graphical presentation of linkage maps and QTLs. J. Hered. **93 (1):** 77-78.

WANG S., C. J. BASTEN, and Z.-B. ZENG, 2007 *Windows QTL Cartographer 2.5*. Department of Statistics, North Carolina State University, Raleigh, NC. (http://statgen.ncsu.edu/qtlcart/WQTLCart.htm).

WIGGINS, R. G., 1916 The number of temporary roots in the cereals. Jour. Amer. Soc. Agron. **8**: 31-37.

WU, G., and S. POETHIG, 2006 Temporal regulation of shoot development in Arabidopsis thaliana by *miR156* and its target *SPL3*. Development **133(18):** 3539-3547.

ZHANG, L., J. M. CHIA, S. KUMARI, J. C. STEIN, Z. LIU, A. NARECHANIA, C. A. MAHER, K. GUILL, M. D. MCMULLEN, and D. WARE, 2009a A genome-wide characterization of microRNA genes in maize. PLoS Genet. **5(11):** e1000716.

ZHANG, W., N. LAUTER, R. PULAM, and S. P. MOOSE, 2009b Molecular interactions among regulatory factors influencing shoot maturation in maize. 2009 Maize Genetics Conference Abstract **51:P103**.

TABLES

Table 1. QTL detected for SBRA. Position and effects of QTL were estimated in the MIM module of QTL cartographer using the initial model identified in CIM for the 0.10 (α=0.10) quantile of 1000 permutations in Zmapqtl of the phenotypic data.

QTL	Chrom	Bin[a]	Marker	Position	LOD[b]	Effect[c]	Effect (%)[d]
A. QTL detected in 2004 for SBRA							
qsbra1	1	1.01	*umc76a*	186	1.54	-2.671	6.6
qsbra2	2	2.04	*php10012*	257	2.32	-3.592	14.7
qsbra3	2	2.09	*umc36a*	522	1.59	-2.977	12
qsbra4	4	4.08	*ufg23*	443	1.99	-3.853	16.7
qsbra5	7	7.02	*bnlg1808*	281	1.79	2.937	8.4
							58.4
B. QTL detected in 2005 for SBRA							
qsbra6	1	1.06	*umc1925*	528	0.95	2.243	4.5
qsbra7	1	1.08	*an1*	698	2.61	-4.380	24.7
qsbra8	2	2.09	*AY110389*	526	2.48	-3.938	20.1
qsbra9	3	3.06	*lim486*	361	1.95	-2.984	12.1
qsbra10	3	3.09	*bnlg1754*	653	0.76	-1.792	4.8
							66.2

[a] Bin assignments were based upon the IBM2 map located at maizegdb.org.
[b] The LOD score presented is based on the value given in the MIM module of WinQTL Cartographer 2.5.
[c] Magnitude of the effect is based on the substitution of a Mo17 allele in the B73 parent at the reported locus.
[d] The value at the end of the empty row is the estimated effect for the MLM.

Table 2. QTL detected for number of NWSBR. Position and effects of QTL were estimated in the MIM module of QTL cartographer using the initial model identified in CIM for the 0.10 (α=0.10) quantile of 1000 permutations in Zmapqtl of the phenotypic data.

QTL	Chrom	Bin[a]	Marker	Position	LOD[b]	Effect[c]	Effect (%)[d]
A. QTL detected for NWSBR in 2003							
qnwsbr1	1	1.01	*umc94a*	28	2.14	-0.238	15.8
qnwsbr2	1	1.06	*ntrf1*	511	1.17	-0.183	6.4
qnwsbr3	1	1.09	*AY110452*	761	2.71	0.268	20.2
							42.4
B. QTL detected for NWSBR in 2004							
qnwsbr4	5	5.07	*bnlg118*	495	1.15	0.184	10.8
							10.8
C. QTL detected for NWSBR in 2005							
qnwsbr5	1	1.01	*umc94a*	33	3.51	-0.247	16.7
qnwsbr6	1	1.10	*adh1*	799	2.56	0.222	11.8
qnwsbr7	3	3.08	*mmc0251*	524	1.58	-0.168	6.9
qnwsbr8	5	5.03	*bnlg1879*	162	1.92	-0.177	9.7
qnwsbr9	6	6.02	*csu923(sec61)*	124	3.95	0.273	14.4
							59.5
D. QTL detected for NWSBR in 2006							
qnwsbr10	1	1.02	*umc1166*	167	3.48	0.302	5.9
qnwsbr11	1	1.10	*nfa103a*	1011	3.50	-0.301	5.5
qnwsbr12	2	2.03	*umc44b*	242	3.83	-0.325	7.1
							18.5

[a] Bin assignments were based upon the IBM2 map located at maizegdb.org.
[b] The LOD score presented is based on the value given in the MIM module of WinQTL Cartographer 2.5.
[c] Magnitude of the effect is based on the substitution of a Mo17 allele in the B73 parent at the reported locus.
[d] The value at the end of the empty row is the estimated effect for the MLM.

Table 3. QTL detected for SBR2. Position and effects of QTL were estimated in the MIM module of QTL cartographer using the initial model identified in CIM for the 0.10 (α=0.10) quantile of 1000 permutations in Zmapqtl of the phenotypic data.

QTL	Chrom	Bin[a]	Marker	Position	LOD[b]	Effect[c]	Effect (%)[d]
A. QTL detected for SBR2 in 2004							
qsbr2.1	2	2.03	*phi109642*	214	2.48	-1.763	15.6
qsbr2.2	3	3.01	*umc2049*	26	1.64	1.529	10.5
qsbr2.3	3	3.08	*bnlg1108*	526	2.04	-1.535	12.7
qsbr2.4	9	9.03	*wx1*	173	1.81	-1.393	10.3
							49.1
B. QTL detected for SBR2 in 2005							
qsbr2.5	2	2.00	*isu53a*	1	1.33	1.000	10.3
qsbr2.6	10	10.00	*mmp48b*	24	1.09	-1.058	9.6
qsbr2.7	10	10.05	*umc259a*	256	0.73	-0.790	5.7
							25.6
C. QTL detected for SBR2 in 2006							
qsbr2.8	1	1.02	*umc1166*	167	3.21	2.72	5.0
qsbr2.9	1	1.09	*AY110452*	974	3.97	-3.01	7.0
qsbr2.10	10	10.05	*umc1477*	393	2.85	2.59	5.1
							17.1

[a] Bin assignments were based upon the IBM2 map located at maizegdb.org.
[b] The LOD score presented is based on the value given in the MIM module of WinQTL Cartographer 2.5.
[c] Magnitude of the effect is based on the substitution of a Mo17 allele in the B73 parent at the reported locus.
[d] The value at the end of the empty row is the estimated effect for the MLM.

Table 4. QTL detected for SBR1 Position and effects of QTL were estimated in the MIM module of QTL cartographer using the initial model identified in CIM for the 0.10 (α=0.10) quantile of 1000 permutations in Zmapqtl of the phenotypic data.

QTL name	Chrom	Bin[a]	Marker	Position	LOD[b]	Effect[c]	Effect (%)[d]
			A. QTL detected for SBR1 in 2003				
qsbr1.1	4	4.08	*umc1775*	387	1.10	0.878	10.0
qsbr1.2	10	10.05	*umc259a*	256	1.29	-0.978	12.7
							22.7
			B. QTL detected for SBR1 in 2004				
qsbr1.3	9	9.06	*ufg75c*	388	1.02	0.699	7.1
qsbr1.4	10	10.05	*bnlg1250*	284	1.56	-0.929	14.7
							21.8
			C. QTL detected for SBR1 in 2005				
qsbr1.5	3	3.05	*umc1539*	340	2.09	0.700	16.4
qsbr1.6	9	9.06	*npi439b*	329	1.85	-0.623	12.1
qsbr1.7	10	10.05	*umc1272*	223	1.53	-0.601	11.8
							40.3
			D. QTL detected for SBR1 in 2006				
qsbr1.8	1	1.06	*asg58*	603	3.46	-1.247	5.4
qsbr1.9	10	10.02	*umc2069*	210	3.24	1.282	6.1
qsbr1.10	10	10.05	*ufg37*	371	2.60	-1.156	5.2
							16.7

[a] Bin assignments were based upon the IBM2 map located at maizegdb.org.
[b] The LOD score presented is based on the value given in the MIM module of WinQTL Cartographer 2.5.
[c] Magnitude of the effect is based on the substitution of a Mo17 allele in the B73 parent at the reported locus.
[d] The value at the end of the empty row is the estimated effect for the MLM.

FIGURES

Figure 1. QTL controlling SBR-patterning and their positional candidate genes.

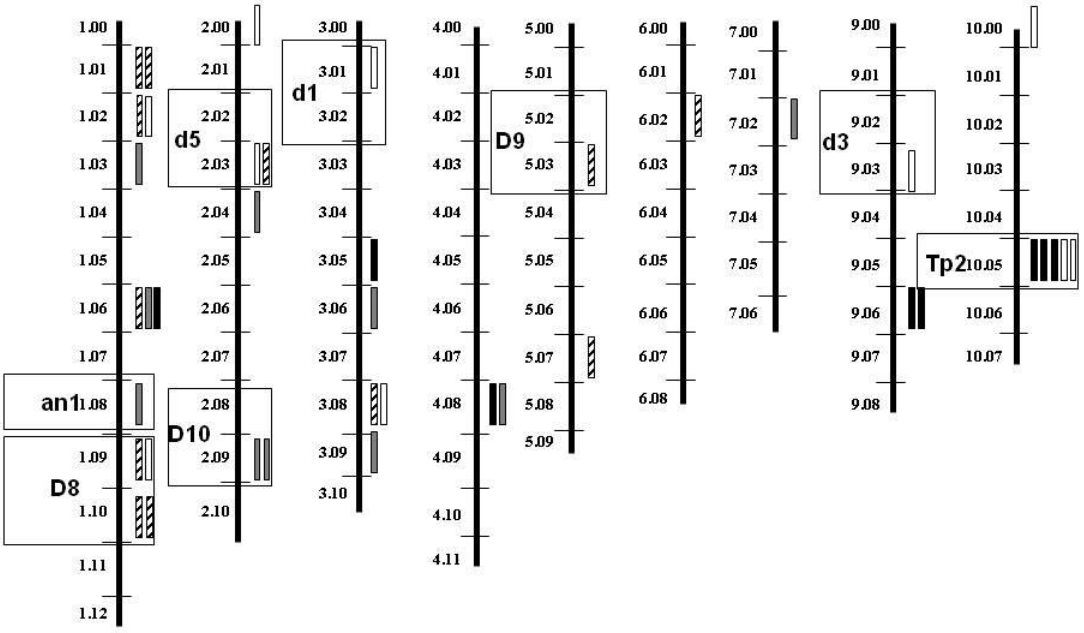

QTL for NWSBR are indicated by a cross hatched box, SBR2 by a white box, SBR1 by a black box, and SBRA by a grey box.

Figure 2. QTL intervals in bins 1.09 and 1.10 for the QTL *qnwsbr3* (green), *qnwsbr5*, (red), *qsbr2.9* (blue) and *qnwsbr11* (black).

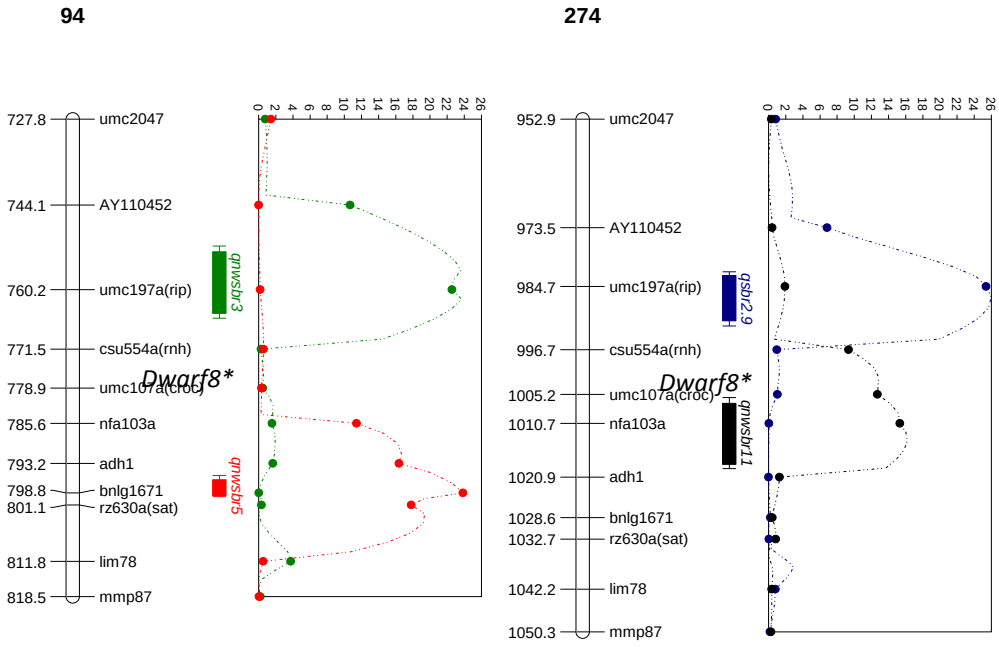

The linkage group with *qnwsbr3* and *qnwsbr5* on the left are from the experiment using the core 94 subset of IBM lines. The linkage group on the right with *qsbr2.9* and *qnwsbr11* was constructed using 274 IBM lines and therefore has different map distances between markers. The horizontal scale to the right of each linkage group depicts the likelihood ratio (LR) statistic for each QTL as determined by composite interval mapping. The LR thresholds for the QTL were 15.7, (*qnwsbr3*), 14.5 (*qnwsbr5*), 13.7 (*qsbr2.9*) and 14.5 (*qnwsbr11*). *The position of the *D8* locus is between *csu554a* and *umc107a*.

Figure 3. QTL intervals in bins 10.04 and 10.05 for the QTL *qsbr1.2* (red), *qsbr1.4*(dark green), *qsbr1.7*(blue), *qsbr1.10* (purple), *qsbr2.7* (black), and *qsbr2.10* (bright green).

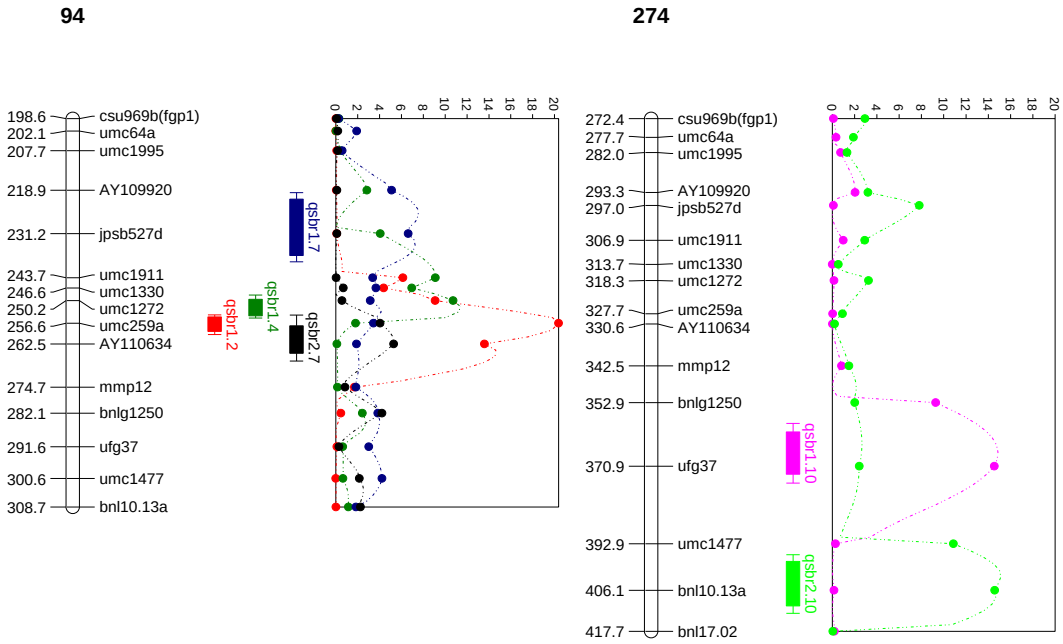

The linkage group with *qsbr1.2*, *qsbr1.4*, *qsbr1.7*, and *qsbr2.7* on the left are from the experiment using the core 94 subset of IBM lines. The linkage group on the right with *qsbr1.10* and *qsbr2.10* was constructed using 274IBM lines and therefore has different map distances between markers. The horizontal scale to the right of each linkage group depicts the likelihood ratio (LR) statistic for each QTL as determined by composite interval mapping. The LR thresholds were 14.5, (*qsbr1.2*), 12.9 (*qsbr1.4*), 14.8, (*qsbr1.7*), 14.4 (*qsbr2.7*), 13.8 (*qsbr1.10*), and 13.7 (*qsbr2.10*). The *Tp2* locus maps 1.25cM distal to *umc259a* on the Genetic 2008 map. The Genetic 2008 map is based on phenotypic markers and may not directly translate the actual position in the IBM.

CHAPTER 3: Contributions of GA-related genes to SBR-patterning in *Zea mays* L.

ABSTRACT

SBRs supply the mature maize plant with water and nutrients and maintain an upright plant growth habit. A previous QTL study chromosome detected regions linked to SBR-patterning and identified positional candidates in the GA biosynthetic and response pathways. The aim of the current study was to assess the roles GA production and signaling play in SBR-patterning using both mutant phenotypes and association mapping in a diverse set of maize germplasm. Comparison of mutant and *wild-type* plants confirmed the role of GA production in vertical SBR-patterning and identified a separate, novel role for GA in radial SBR-patterning. Using association analysis, sequence polymorphisms within the P450 domain of the GA biosynthetic enzyme, *d3,* and the promoter region of the GA negative response regulator, *D8,* were linked to small changes in SBR-patterning (three to seven percent). The correlation of population structure with SBR-patterning (in combination with small QTL effects) may have limited our ability of make strong associations between polymorphism in these genes and SBR traits using association mapping. Models are presented describing how allelic variation in *d3* and *D8* shapes SBR-patterning.

INTRODUCTION

The mature maize plant relies on the SBR system to provide support to maintain its upright growth habit and to access and transport water and nutrients for survival. A previous QTL mapping study identified chromosome regions controlling SBR-patterning, which also contained genes involved in GA biosynthesis and response (Chapter 2, Figure 1). GA is a growth hormone that stimulates stem growth, regulates the transition from juvenile-to-adult vegetative phase, acts as a signaling molecule to determine floral sex determination, and triggers germination (Taiz and Zeiger, 2006). GA was first linked to SBR-patterning by Evans and Poethig (1995) in their seminal paper on genetic factors influencing maize phase-change. Studies in the model crop rice (*Oryza sativa* L.) support the role of GA in root patterning, initiation and growth (Steffens et al.,

2006). While these experiments are an excellent starting point towards understanding the role of GA in SBR-patterning, recent findings highlight the complexity of GA activity in the area of GA response signaling. GA response is induced by the degradation of DELLA proteins, which are GA-negative-response regulators (Ikeda et al., 2001). GA binds to GID1, a soluble GA receptor which then binds to the DELLA protein (Ueguchi-Tanaka et al., 2005). Then SCF^{SLY1} E3 ligase ubiquinates the DELLA transcriptional-repressor complex, targeting it for degradation via the 26S proteosome (Dill et al., 2004; Itoh et al., 2003). The degradation of the DELLA transcriptional-repressor results in expression of GA-response genes (Figure 4). Some of these GA-response genes are implicated in cell growth and cell wall modification, specify products such as expansins, cellulose synthase, tubulins and pectin esterases (Cao et al., 2006). Genes related to abscisic acid (ABA), GA, auxin and ethylene are also regulated by DELLAs (Cao et al., 2006).

Maize has a wide collection of GA-deficient and GA-non-responsive mutants affecting different steps along the GA biosynthetic and response pathways (Figure 5). GA-deficient mutants include *an1, d1, d,3* and *d5* (Fujioka et al., 1988). *d1* catalyzes the production of GA_1 from GA_{20}, *d3* catalyzes the production of GA_{53} from GA_{12}-aldehyde, and *d5* generates *ent*-kaurene from copalylpyrophosphate (Figure 5). *D8*, *D9*, and *D10* are GA-non-responsive mutants. *D8* mutant alleles encode a GA-non-responsive DELLA protein (Ikeda et al., 2001). *D9* is a suspected homologous duplicate gene of *D8* (Winkler and Freeling, 1994). *D10* is a mutant whose underlying mutation is unknown. It is the goal of this study to further investigate the role of GA in SBR-patterning. The specific objectives of the study are two-fold. First, to survey maize mutants with alterations in GA production or response for their SBR phenotypes. Second, to evaluate the impact of natural allelic variation within GA biosynthetic and response genes on the variation in SBR-patterning among maize breeding lines using association analysis.

MATERIALS AND METHODS

Means comparison between GA mutants and *wild-type* SBR-patterning: All mutant strains were obtained from the Maize Genetics Cooperation Stock Center at the University of Illinois Urbana-Champagne. The following mutants were acquired; *dwarf1-R, dwarf3-Coop, dwarf5-R, Dwarf8-R, Dwarf8-N1452, Dwarf8-N1591, Dwarf8-N2031, Dwarf9-R* and *Dwarf10-R.* Families segregating for the mutant alleles were grown at either the South Farm Research Center, University of Missouri-Columbia in the summer of 2006 or in winter of 2008 in Juana Diaz, Puerto Rico. The SBR traits collected were NWSBR, SBR1, SBR2, and total number of SBR (totlSBR). Details regarding measurement of these traits were given in Chapter 2. The number of individual plants phenotyped in each genotypic class varied from seven to 23. In addition to the two growing seasons, *d1* was also grown in the summer of 2007 at the South Farm Research Center, Columbia, MO. Despite this there were not enough *d1* mutant individuals in any of the growing seasons to perform a means comparison due to poor emergence. Normality and summary statistics were examined for all SBR traits using the UNIVARIATE procedure with the "normal" and "plot" commands in SAS (SAS Institute Inc, Cary, North Carolina). Equality of variances between genotypic treatments was compared using the Bartlett test in the GLM procedure of SAS. Due to deviations from normality and unequal variances across phenotypic classes, a non-parametric procedure called the NPAR1WAY procedure was used to perform a Wilcoxon-rank-sum test.

Phenotyping of maize association panel: A subset of 100 lines (Appendix 2) from the maize association panel (Flint-Garcia et al., 2005) was grown in 2004 and 2005 at the Genetics Farm, Columbia, Missouri. Ten kernels of each genotype were sown in 10 foot rows in a randomized complete block design with two replications. Between three and five individuals were phenotyped in each row. In 2008, 275 (Appendix 2) lines were grown at the Genetics Farm, Columbia,

Missouri. Twenty kernels were sown in ten foot rows and were subsequently thinned to ten plants per ten foot row. The experimental design was a randomized complete block with two replications. Only inbred lines that had three observations in both replications in a given year were used for statistical and association analyses.

SBR1 was normally distributed and required no transformations. NWSBR and totlSBR required a log(x+1) transformation where x represents the raw trait value. For each year outliers were identified and removed by plotting the studentized residuals against the observed phenotypes. Equal variance across years for each trait was tested using Bartlett's test. Due to unequal variances between years, each year was analyzed separately. Least squares means (LSmeans) were calculated for SBR1, NWSBR and totlSBR using Line, Replication and Line*Replication as terms in the model. Grand means were calculated for each year for SBR2. Heritability estimates were calculated for each year on an entry means basis; $h = \sigma_G / \sigma_G + \sigma_E$ where σ_G equals mean squared genotypes minus mean squared error divided by two and σ_E equals mean squared error.

To examine the confounding of population structure and SBR phenotypes, single factor regression was performed for SBR traits using the STRUCTURE group coefficient as determined by Liu et al., (2003). A weighted Welch's ANOVA was conducted using group membership (Liu et al., 2003) as the treatment class. Additionally, descriptive statistics for each trait were calculated for the entire population and for each STRUCTURE group using the LSMeans transformed back to resemble their original raw values by a $y=1+10^{(LSmean)}$ transformation.

Preliminary association analysis of *d3* and *D8*: Whole gene sequences for *d3* (n=53) and *D8* (n=92) were obtained from the Panzea website (www.panzea.org; Canaran et al., 2008). Mixed model association analysis (Yu et al., 2006) was performed in Tassel 2.1 (Zhang et al., 2010; Bradbury et al., 2007) for all root traits described. The kinship and population structure estimates

used in the analysis have been previously described (Yu et al., 2006; Liu et al., 2003). Polymorphic sites with allele frequencies lower than 0.01 were removed from the analysis. The STRUCTURE coefficients used as covariates in the mixed model were Q1 and Q2 and represent nonstiff stalk (NSS) and stiff stalk (SS) membership. The expectation maximization (EM) analysis method was selected along with the P3D heritability option (Zhang et al., 2010). Spidey (Wheelan et al., 2001) was used to predict intron-exon structures of both *d3* and *D8* using the gene sequence from the Panzea database. CDART (Geer et al., 2002) was used to identify conserved regions in the *D3* protein. Significant results were plotted onto the gene model prediction.

Re-sequencing of candidate gene regions: To validate the preliminary association analysis results selected regions within the two genes (*d3* and *D8*) were chosen for further sequencing and analysis in 260 maize lines. The regions were selected based on the observed p-values for multiple root traits repeated across multiple field seasons. The phenotypes of the mutants used in the means comparison study were also considered when identifying the functional region within the gene to investigate. DNA was produced by planting 20 kernels per genotype into flats grown in a growth chamber under standard conditions (16/8 hours light/dark and 28° C/20° C day/night temperature). Seedlings were bulk harvested and frozen in liquid nitrogen. The frozen tissue was pulverized in a mortar and pestle. DNA was extracted from the tissue according to the manufacturer's protocol using the Plant DNAzol Reagent (Invitrogen Life Sciences, Carlsbad CA). Primers for each gene were developed using PrimerQuest™ (Integrated DNA Technologies, Coralville, IA). The polymerase chain reaction (PCR) mixture contained 50 ng each of forward and reverse primer, 50 ng total DNA, and 15 µl of JumpStart™ RED Taq® Ready Mix™ (Sigma-Aldrich, St. Louis, MO) in a total reaction volume of 30 µl. A touchdown amplification protocol was used for PCR. PCR primers used were 5'-AAA CAT GCT CCA TGG CCT GAC AGA-3' (*d3* forward primer), 5'-ACG GGT CGA ACT TGG TGG G-3' (*d3* reverse primer), 5'-

CAC TTT CCA AAG TTG TTC TGA TAT GCT-3' (*d8* forward primer) and 5'- GAG TAA AGG GAA GGC TGG ATC CTT-3' (*d8* reverse primer). Purification of PCR products was performed using E-Gel® (Invitrogen Life Sciences, Carlsbad CA). PCR products were sequenced at the DNA Core Facility at the University of Columbia-Missouri. Sequence output was aligned to the previous alignment provided at www.panzea.org. Association analysis was performed as described above utilizing the new sequence combined with the sequence from Panzea in the same region.

RESULTS

Means comparison between GA mutants and *wild-type* sibling SBR-patterning: To assess the role of GA-related genes in SBR-patterning GA deficient and GA non-responsive mutants were phenotyped along with their *wild-type* siblings for SBR trait comparisons. The GA-deficient mutants, *d3* and *d5*, formed a greater number of NWSBR than their *wild-type* counterparts (Table 5A, Figure 6) and produced fewer SBR2 and SBR1 than their *wild-type* siblings (Table 5B and Table 5C). The GA non-responsive mutants *D8, D9,* and *D10* were also analyzed (Figure 7). *D10* mutants produced no SBRs and *D8* mutants formed almost no SBRs (Table 6). While *D9* mutants produced some SBRs, they too had significantly fewer SBRs than their *wild-type* siblings (Table 6). Three other *D8* mutant alleles were phenotyped. With the exception of *D8-N1591,* all of them produced fewer SBRs at a node (SBR1, SBR2), fewer NWSBR, and fewer totlSBR than their *wild-type* siblings (Tables 6 and 7).

SBR phenotypes of maize association panel: The phenotypic performance of the maize association panel was analyzed to better dissect SBR-patterning. Means for 2004 and 2005 were generally similar and markedly different from those observed in 2008. Plants in 2008 generally produced fewer SBRs (Table 8). Coefficients of variation (CV) values were high for totlSBR and SBR2, while SBR1 had the smallest CV (Table 8). Despite the large CVs broad sense heritabilities for the traits ranged from 0.50 to 0.86.

The influence of population structure on SBR-patterning was explored by performing single factor regression on the SBR phenotypes using the STRUCTURE coefficients from Liu et al. (2003). The data indicate that there is a negative relationship between the percentage of NSS background and NWSBR, SBR2, and totlSBR number (Table 9A). The R^2 values for the regressions range from 0.09 to 0.24 for the significant traits. While some SBR traits had a significant relationship with SS percentage (Table 9B), the amount of variation explained by these models was small relative to the other models. The regression models for tropical/semitropical (TS) point to a positive relationship between the percentage of TS background and values for NWSBR, SBR2 and totlSBR (Table 9C). A Welch' s weighted ANOVA indicated that STRUCTURE group designation as determined by Liu et al. (2003) was a highly significant source of variation in NWSBR, SBR2 and totlSBR (Table 9D). R^2 values ranged from 0.12 to 0.37 for these traits.

Summary statistics were also calculated for each trait by STRUCTURE group. TS and SS lines consistently produced the most NWSBR while NSS and Sweet corn (SWT) lines produced the fewest (Table 10). Mixed (MXD) and TS lines had simultaneously larger standard deviations and CVs for NWSBR, 2008 performance being the exception (Table 10C). SBR1 trait performance, subdivided by STRUCTURE group are relatively stable across STRUCTURE groups and years with greater variation found in 2008 (Table 11). Examining SBR2 among STRUCTURE groups revealed differences consistent with those observed for NWSBR (Tables 10 and 12). TS and SS consistently rank as the top two groups for SBR2 production while SWT lines remain the lowest producers of SBR2 (Table 12). The largest values for totlSBR were for the TS and SS groups (Table 13).

Preliminary association analysis of *d3* and *D8*: Preliminary association mapping of *d3* (N=38) and *D8* (N=92) utilized sequence from Remington et al. (2001) retrieved from www.panzea.org. The *d3* locus was selected for association mapping for two reasons. First, the genetic location of

the *d3* locus and *qsbr2.4* (a QTL for SBR2 described in Chapter 2) is precise (Figure 8). The marker on the genetic linkage map used for QTL analysis (which was linked to *qsbr2.4*) was *waxy1* (*wx1)* (Chapter 2, Table 3). The *d3* locus maps nearly 9 cM from the *wx1* locus placing it within the QTL interval peak (Figure 8). Second, sequence of *d3* was available for 38 lines in the association panel. The preliminary mapping results for *d3* revealed many polymorphisms segregating in the population that significantly control SBR traits, however only one region was stable across years and traits. The Insersion/Deletion (InDels) at site 2888 and 2918 and sincle nucleotide polymorphisms (SNPs) at 2905, 2907, 2909, and 2916 were frequently associated with SBR-patterning (Table 14). According to the intron-exon modeling performed with the Spidey program, these polymorphisms are located within the fifth exon (Figure 9). Protein analysis using CDART indicated that the region contained sequence similarity to cytochrome P450s domains (data not shown). Cytochrome P450s participate in enzymatic reactions involving oxygenation or hydroxylation of metabolites (Mitzutani and Ohta, 2010). This suggests that this *D3* protein domain is directly involved in the enzymatic reaction turning GA_{12} to GA_{53} (Figure 5). As a result of this region's consistent influence on multiple SBR traits across years and the regions potential functionality, it was targeted for further genotyping.

Initial analysis of *D8* haplotypes found significant associations throughout the gene. Consistent associations were found for sites at 677, 699, 702, 710, 1518, 1690, 3104 and 3210 (Table 15). The sites at 677, 699, 702 and 710 are located in the promoter region of the gene and were previously associated with changes in days to flowering (Thornsberry et al., 2001; Andersen et al., 2005) (Figure 10). Since variation at these sites affected days to flowering and the *D8* mutant alleles could be considered over-expressers that shape SBR-patterning, the promoter region was targeted for further analysis.

Targeted association analysis: The fifth exon of the *d3* gene was targeted for genotyping in 260 lines from the maize association panel (sequence polymorphisms presented in Appendix 3). The

d3 locus is within the confidence interval for *qsbr2.4* (Figure 8). Of the 12 association tests (three years by four traits), only two polymorphisms had a p-value greater than 0.05 (SBR2 in 2008 and SBR1 in 2005 at site 2888, Figure 11, Table 14). Examination of *d3* from site 2888 to 2918 reveals a potential haplotype block extending the entire region including the polymorphisms at 2888, 2893, 2894, 2898, 2900, 2905, 2907, 2909 and 2916 (Figure 11). A Bonferroni adjustment was performed to correct for multiple comparisons. The Bonferroni adjustment assumes that the outcomes for the multiple tests are not correlated (Zar, 1999). Because of the close physical linkage of the five sites tested, they should not be considered independent statistical tests. Conversely, each year is considered an independent trial and the Bonferroni adjustment then considers the p-value for significance to be 0.0167 (equals 0.05/3) for the single trait of SBR2. As a result of the correction, the only significant associations were between SBR2 in 2005 at sites 2905 and 2909. The number of independent trials is 12 when all four traits and three years are included. An adjusted p-value of 0.0042, applied to the mapping results from the 12 trait by year combinations reveals eleven associations below 0.0042 (Table 14).

The promoter region of the *D8* gene was also selected for further genotyping and analysis (sequence polymorphisms presented in Appendix 4). Four QTL mapped near *D8*: three for NWSBR, and one for SBR2 (Chapter 2, Figure 3). Eleven significant (p-value less than 0.05) associations were found for SBR2 and NWSBR across the three years, and a total of 14 associations within the *D8* promoter region were significantly associated with at least one of the traits collected (Table 15, Figure 12). Significant associations accounted for three to four percent of the variation in the respective traits (Table 15). None of these associations remained significant after the Bonferroni adjustments were applied.

DISCUSSION

Altering GA activity affects SBR-patterning: Evans and Poethig (1995) previously linked GA to NWSBR in their pioneering study on phase-change in maize and provided the basis for focusing on the contribution of the GA pathway to SBR-patterning. In the previous QTL mapping study, loci controlling SBR-patterning mapped to chromosome regions containing GA biosynthetic and response genes (Chapter 2, Figure 1). QTL identified in the study also controlled the root traits SBR1 and SBR2 (Chapter 2). Evans and Poethig (1995) examined NWSBR in GA-deficient mutants but not in GA non-responsive mutants. In addition, they did not evaluate SBR1 or SBR2. We expanded on this work by examining NWSBR, SBR1 and SBR2 in GA-deficient and non-responsive mutants in order to assess the role of GA production and signaling on multiple SBR phenotypes.

The GA-deficient mutants had different magnitudes of effects on radial and vertical axes of SBR-patterning. GA-deficiency resulted in a prolonged juvenile phase leading to greater NWSBR and also reduced SBR1 and SBR2 (Table 5, Figure 6) pointing to a previously undocumented role for GA synthesis in the patterning of SBRs: while GA suppresses the production of NWSBR by controlling phase change, it can also stimulate SBR1 and SBR2 via an independent mechanism.

The GA-non-responsive mutants *D8-R*, *D8-N1452*, *D8-N1591*, and *D8-N2031*, encode negative-GA-response regulators known as DELLAs. Positional evidence suggests that *D9* encodes a DELLA protein (Winkler and Freeling, 1994). These mutants produce markedly reduced SBR1, SBR2, NWSBR, and totlSBR relative to their *wild-type* counterparts (Tables 6 and 7, Figure 7). This suggests that GA-mediated patterning of SBR occurs through de-repression of DELLA transcriptional suppression of GA response genes. These results also suggest that GA biosynthetic and response genes are potential candidates underlying the QTL mapped near them.

Allelic variation in GA related genes contributes to SBR-patterning: To validate the role of GA-related genes on SBR-patterning, association analysis was conducted on *d3*, a GA biosynthetic enzyme, and *D8*, a GA-response regulator. Five polymorphisms were significant within exon five of *d3*, $p<0.05$ (Table 13). The protein structure from this genomic region contains elements that have similarity to cytochrome P450s indicating this region is likely to be involved in an oxygenation/hydroxylation step in the conversion of GA_{12} to GA_{15} (Figure 5). This suggests that the significant polymorphisms may control SBR-patterning by affecting the ability of the D3 protein to catalyze the formation of GA_{53} from its substrate GA_{12} (Figure 5).

The *D8* promoter region was also targeted for association analysis. This region was previously linked to flowering time in maize (Thornsberry et al., 2001; Andersen et al., 2005). We identified association between SBR phenotypes and this region ($p< 0.05$, Table 15). However, after adjusting for multiple comparisons the polymorphisms were no longer significant. This suggests that at best *D8* expression plays a minor role in determining SBR-patterning.

SBR-patterning in the maize association panel: Four major factors contribute to the power to detect QTL in association studies; heritability, population structure, minor allele frequency and magnitude of QTL affect (Zhao et al., 2007; Yu et al., 2006).

Effect of heritability. Broad sense heritabilities were estimated from the genotypic variance on an entry means basis (Table 8). Despite high CVs, heritability estimates were high, ranging from 0.52 to 0.86, suggesting that inbred lines perform similarly across replicates but that there is tremendous variation for SBR-patterning among inbred lines in the association panel. Broad sense heritabilities are the ratio of the genetic variance divided by the total phenotypic variance. The higher the heritability, the more precisely the phenotype represents the genotype. Although broad sense estimates of heritability for the SBR traits were generally high (0.5 to 0.86; Table 8), they are most likely over-estimates considering the limitations of performing a heritability estimate using entry means for a location with only two replications. Most of the R^2

for full model association analyses were between 45 and 62 percent. Like the MLM for QTL analyses Chapter 2, Tables 1-4), the R^2 explained a maximum of 60 percent of the phenotypic variation in SBR traits. These results imply that the true genetic component of our phenotype may be more accurate at the low end of our estimates, around 50 percent. Despite the over-estimation bias of our calculation method, the heritabilities are high enough to facilitate QTL detection.

Impact of population structure. Correlation of population structure to quantitative traits results in a significant reduction in power to detect QTL in association studies. Single factor regression onto STRUCTURE sub-population coefficients identified a significant relationship between population stratification and SBR-patterning (Table 9A-C). The data indicate that the percentage of TS and NSS significantly affects NWSBR, SBR2 and totlSBR with R^2 ranging from approximately 10 to 20 percent of the variation for a single factor (Table 9 A and C). A Welch's weighted ANOVA determined that STRUCTURE population membership explained 12 to 37 percent of the variation in NWSBR, SBR2 and totlSBR (Table 9D).

Another method of quantifying population stratification is to determine how much of the heritable variation is confounded with the population structure. A quick but simplistic estimate would be to divide the percentage of the phenotypic variation explained by structure by the heritability. Dividing conservative estimates of heritabilities ranging from 45 to 60 percent by effect of population structure ranging from 12 to 37 percent for NWSBR, SBR1, and SBR2 we obtain estimates of 20 to 82 percent of the heritable variation sub-divided between STRUCTURE groups. This suggests that allelic differences at loci controlling SBR-patterning are most likely nested within the STRUCTURE groups. Through computer simulations Zhao et al. (2007) displayed the negative impact that population structure has on the power of mixed-model analysis, especially in the event that the genetic effect of the QTL tested is less than 10 percent. These results predict that our ability to detect allelic differences at loci for SBR-patterning will be severely limited after adjusting for population structure.

Effect of allele frequency. Allele frequencies must also be taken into consideration when evaluating association results. Zhao et al. (2007) studied the impact that minor allele frequencies had on the power to detect associations at QTL with different levels of genetic affect. Large affect QTL (20 to 30 percent) are easily detectable when minor allele frequencies are five and ten percent. However, at the same allele frequency, power to detect QTL becomes very small for QTL which explain less than ten percent of the phenotypic variation. Minor allele frequencies ranged from six to seven percent for SNPs and 30 to 36 percent for InDels at the *d3* locus (cumulative for all non-major alleles when more than two alleles are observed). Minor allele frequencies for *D8* were 30% for SNPs and 10% for InDels. Assuming allele frequencies in the range we observed and small QTL effects of five percent our power to detect associations would be less than 0.20 according to the simulation models by Zhao et al. (2007).

Impact of QTL magnitude. Previously discussed simulation models indicated that small affect QTL have a low likelihood of discovery (Zhao et al., 2007). The SBR-patterning QTL coincident to *D8* had estimated effects of six to 20 percent and *sbr2.4*, the QTL near d3, had an effect of ten percent (Chapter 2). These estimates of QTL effects are unique to the IBM mapping population and cannot be directly extended to a diverse set of germplasm such as those which make up the association panel used in this study. Due to the impacts of population structure and potential epistatic interactions, significant reductions in QTL affects should be expected. When jointly using QTL and association mapping, the genetic diversity of the estimated QTL effects will not be the same in both populations. By using phenotypically/genotypically diverse parents in the QTL study, association results are more likely to mirror the QTL findings. When the parents of the QTL study are phenotypically and genotypically similar, then the QTL estimates in the linkage study will be over-estimated relative to the findings in the association study. Taken together, the heritability, population structure, allele frequencies, and magnitude of QTL effects suggest two potential interpretations of the association analysis results. The first is that correlation

of SBR phenotypes with population structure leads to false associations at the *d3* and *D8* loci. This conclusion does not take into account that although NWSBR, SBR2 and totlSBR are moderately to highly related to population structure, SBR1 is not (Table 9). SBR1 is not closely linked to maize sub-population membership and statistical associations are still found suggesting a biological origin for the association results not a statistical origin. A second interpretation is that our study suffers from low power, due to confounding of the SBR traits with population structure and the small magnitude of QTL affects. Elevated minor allele frequencies at some of the loci do not improve the association, ruling out allele frequency *per se* as a contributing factor in our analysis. The simulation results of Zhao et al. (2007) indicate the power to detect QTL with 5 percent effects at the 0.001 level is nearly zero, thus setting an upper limit on significance values in our study. As a result relying solely on the association mapping p-values to determine the involvement of a gene in SBR-patterning may be misleading and instead evidence from multiple genetic and/or molecular studies to determine the role of GA-activity in SBR-patterning should be considered.

Mechanisms for GA-regulated SBR-patterning: SBR-patterning varies across two planes, a vertical- and radial-axis of variation. GA activity impacts these axes in different ways. GA activity suppresses NWSBR while it promotes SBR1, SBR2, and totlSBR (Table 5, 6, and 7, Figure 6 and 7). This requires GA activity to play different roles along each axis of variation in SBRs.

The vertical axis of variation is described by NWSBR. This trait was first studied by Evans and Poethig (1995). They observed that GA-deficient mutants, along with the *Tp1* and *Tp2* mutants, produced more NWSBR than their *wild-type* counterparts and that GA application could suppress the *Tp1* and *Tp2* phenotypes. Chuck et al. (2007) found that the origin of a phenotypically similar mutant, *Cg1*, was the result of the over-expression of two tandem *miR156* genes. Recently Zhang et al. (2009a) electronically mapped *miR156* family members near *Tp1*

and *Tp2* suggesting they too may result from *miR156* over-expression. Quantification of *miR156* and *miR172* in shoot apical meristems (SAMs) of plants treated with exogenous GA indicate that GA simultaneously suppresses *miR156* expression while promoting *miR172* expression (Zhang et al., 2009b). This is in agreement with studies in *Arabidopsis* that indicates that *miR156* regulates *miR172* through targeted suppression of *SQUAMOSA PROMOTER BINDING PROTEIN LIKE* (*SPL*) proteins (Wu et al., 2009). We suggest that the pleiotropic effects of GA-deficiency on leaf wax and number in addition to NWSBR, is the outcome of GA suppression of the juvenile phase and NWSBR by suppressing *miR156* early on in the SAM. Via this model the vertical axis of SBR-patterning is dictated by the vegetative identity of a phytomer through *miR156* activity during phytomer development, and the trigger for phase change is the production of biologically active GAs. Allelic variation at *d3*, a cytochrome P450 catalyzing the step GA_{53} to GA_{12}, may regulate the onset of adult-vegetative phase by influencing the kinetics of the enzymatic step and hence altering biologically active GAs.

The radial axis of SBR variation is described by SBR1 and SBR2. While vertical patterning is regulated through GA-mediated control of phase change via *miR156* some evidence points to radial patterning being governed independently. GA-deficiency promotes NWSBR but suppresses SBR1 and SBR2 as evidenced by the phenotypes observed for *d3* and *d5* (Table 5). The phenotypes of the GA-deficient and non-responsive mutants indicate that GA stimulates SBR1 and SBR2 production. GA-deficient mutants and non-responsive mutants produce fewer SBR1 and SBR2 (Tables 5 and 6). This suggests that GA regulates SBR1 and SBR2 numbers through its control of DELLA (*D8*) accumulation. DELLA activity may shape radial patterning by controlling programmed cell death (PCD) and cell wall modifying factors. Steffens et al. (2006) describes a developmental model for SBR development in rice (*Oryza sativa* L.) consisting of GA-ethylene mediated PCD followed by root emergence and elongation. Additionally expression analysis of DELLA-independent and -dependent transcriptomes revealed

DELLA-mediated down regulation of 21 cell-wall-modifying proteins required for seed germination in *Arabidopsis* (Cao et al., 2006). These cell-wall-modifying proteins assist in weakening of the embryonic cell wall and promote emergence of the embryonic root or radicle (Bewley et al., 1997; Chen and Bradford, 2000). GA regulated DELLA-de-repression leading to cell wall modifications and PCD is one example of how allelic variation in *d3* and *D8* contributes to radial patterning (Figure 13).

DELLA-de-repression also contributes to SBR radial patterning through control of anisotropic growth (polar-cell growth). Ubeda-Tomás et al. (2008) observed this phenomenon when they ectopically expressed a GA-non-responsive allele of the *gai* locus in the root endodermis. Inhibition of cell expansion in the endodermis altered the expansion of neighboring cortical and epidermal cell layers, prohibiting root growth. Ubeda-Tomás et al. (2009) subsequently expressed *gai* in the primary root meristem and observed that it resulted in diminished meristem size due to reduced cell division. Since plant cells are bound to one another via their cell walls, development of lateral organs like SBRs requires that certain cell types expand and contract in a coordinated manner. This coordinated cell patterning in the root is dictated by GA-mediated DELLA activity (Ubeda-Tomás et al., 2008; Ubeda-Tomás et al., 2009). Differences in *D8* expression (driven by polymorphisms within the promoter) can alter the spatio-temporal activity of DELLA proteins and thus radial patterning of SBRs. In the *D8* and *D9* mutants, ectopic activity results in no SBRs. This is in agreement with both of the preceding models describing the requirement of DELLA de-repression for SBR emergence and growth (Figure 13).

We evaluated mutant alleles of genes with varying functions in the GA biosynthetic and response pathway for their effects on SBR-patterning. Our results support the role of GA in NWSBR formation initially described by Evans and Poethig (1995). We expanded on their findings by linking radial root patterning to GA biosynthesis and response genes. The mutant and

QTL analyses together imply that natural allelic variation in GA biosynthetic and response genes contribute to variation found in the IBM mapping population for SBR-patterning. This theory was tested through association mapping in the putative enzymatic domain of *d3* and the promoter region of *D8*. The results from the mapping study indicate that allelic variations in these regions have relatively small contributions to SBR variation in a genetically and phenotypically diverse set of maize germplasm. These findings could be confirmed by QTL cloning, development of near isogenic lines or mapping in the nested association mapping population (Yu et al., 2008).

REFERENCES

ANDERSEN, J. R., T. SCHRAG, A. E. MELCHINGER, I. ZEIN, and T. LÜBBERSTED, 2005 Validation of *Dwarf8* polymorphisms associated with flowering time in elite European inbred lines of maize (*Zea mays* L.). Theor. Appl. Genet. **111(2):** 206-217.

BRADBURY, P. J., Z. ZHANG, D. E. KROON, T. M. CASSTEVENS, Y. RAMDOSS, and E. S. BUCKLER, 2007 TASSEL: software for association mapping of complex traits in diverse samples. Bioinformatics **23(19):** 2633-2635.

BEWLEY, J. D., 1997 Seed germination and dormancy. Plant Cell **9:** 1055–1066.

CANARAN, P., E. S. BUCKLER, J. C. GLAUBITZ, L. STEIN, Q. SUN, W. ZHAO, and D. WARE, 2008 Panzea: an update on new content and features. Nucl. Acids Res. **36:** D1041-D1043.

CAO, D., H. CHENG, W. WU, H. M. SOO and J. PENG, 2006 Gibberellin mobilizes distinct DELLA-dependent transcriptomes to regulate seed germination and floral development in *Arabidopsis*. Plant Physiol. **142 (2)**: 509-525.

CHEN, F. and K. J. BRADFORD, 2000 Expression of an expansin is associated with endosperm weakening during tomato seed germination. Plant Physiol. **124 (3)**: 1265-1274.

CHUCK, G., A. M. CIGAN, K. SAETEURN, and S. HAKE, 2007 The heterochronic maize mutant *Corngrass1* results from overexpression of a tandem microRNA. Nat. Genet. **39(4):** 544-549.

DILL, A., S. G. THOMAS, J. HU, C. M. STEBER, and T. P. SUN, 2004 The *Arabidopsis* F-box protein SLEEPY1 targets gibberellin signaling repressors for gibberellin-induced degradation. Plant Cell **16(6):** 1392-1405.

EVANS, M. M. and R. S. POETHIG, 1995 Gibberellins promote vegetative phase change and reproduction in maize. Plant Physiol. **108(2)**: 475-487.

FLINT-GARCIA, S. A., A. C. THUILLET, J. YU, G. PRESSOIR, S. M. ROMERO, S. E. MITCHELL, J. DOEBLEY, S. KRESOVICH, M. M. GOODMAN, and E. S. BUCKLER, 2005 Maize association population: a high-resolution platform for quantitative trait locus dissection. Plant J. **44(6):**1054-1064.

FUJIOKA, S., H. YAMANE, C. R. SPRAY, P. GASKIN, J. MACMILLAN, B. O. PHINNEY, and N. TAKAHASHI, 1988 Qualitative and quantitative analyses of gibberellins in vegetative

shoots of normal, *dwarf-1*, *dwarf-2*, *dwarf-3*, and *dwarf-5* seedlings of *Zea mays* L. Plant Physiol. 88: 1367-1372.

GEER, L. Y., M. DOMRACHEV, D. J. LIPMAN, and S. H. BRYANT, 2002 CDART: protein homology by domain architecture. Genome Res. **12(10):** 1619-1623.

IKEDA A., M. UEGUCHI-TANAKA , Y. SONODA , H. KITANO , M. KOSHIOKA, Y. FUTSUHARA, M. MATSUOKA AND J. YAMAGUCHI, 2001 *slender rice*, a constitutive gibberellin response mutant, is caused by a null mutation of the *SLR1* gene, an ortholog of the height-regulating gene *GAI/RGA/RHT/D8*. Plant Cell **13(5)**: 999-1010.

ITOH, H., M. MATSUOKA and C. M. STEBER, 2003 A role for the ubiquitin–26S-proteasome pathway in gibberellin signaling. Trends Plant Sci. **8(10)**: 492-497.

LIU, K., M. GOODMAN, S. MUSE, J. S. SMITH, E. BUCKLER, and J. DOEBLEY, 2003 Genetic structure and diversity among maize inbred lines as inferred from DNA microsatellites. Genetics **165(4):** 2117-2128.

MITZUTANI, M. and D. OHTA, 2010 Diversification of P450 genes during land plant evolution. Annu. Rev. Plant Biol. **61:** 291-315.

REMINGTON, D. L., J. M. THORNSBERRY, Y. MATSUOKA, L. M. WILSON, S. R. WHITT, J. DOEBLEY, S. KRESOVICH, M. M. GOODMAN, and E. S. BUCKLER ES 4TH, 2001 Structure of linkage disequilibrium and phenotypic associations in the maize genome. Proc. Natl. Acad. Sci. U. S. A. **98(20):** 11479-11484.

SAS INSTITUTE, 2009 SAS Version 9.1. SAS Institute Inc, Cary, NC.

SCHWECHHEIMER, C., 2008 Understanding gibberellic acid signaling--are we there yet? Curr. Opin. Plant Biol. **11(1):**9-15.

STEFFENS, B., J. WANG and M. SAUTER, 2006 Interactions between ethylene, gibberellin, and abscisic acid regulate emergence and growth rate of adventitious roots in deepwater rice. Planta **223(3)**: 604-612.

TAIZ, L. and E. ZEIGER, 2006 *Plant Physiology* 4th Edition. Sinauer Associates Inc, Sunderland, M.A. 764p.

THORNSBERRY, J. M., M. M. GOODMANN, J. DOEBLEY, S. KRESOVICH, D. NIELSEN and E. S. BUCKLER 4th, 2001 *Dwarf8* polymorphisms associate with variation in flowering time. Nat. Genet. **28(3)**: 286-289.

UBEDA-TOMÁS, S., F. FEDERICI, I. CASIMIRO, G. T. BEEMSTER, R. BHALERAO, R. SWARUP, P. DOERNER, J. HASELOFF, and M. J. BENNETT, 2009 Gibberellin signaling in the endodermis controls *Arabidopsis* root meristem size. Curr. Biol. **19(14):** 1194-1199.

UBEDA-TOMÁS, S., R. SWARUP, J. COATES, K. SWARUP, L. LAPLAZE, G. T. S. BEEMSTER, P. HEDDEN, R. BHALERAO, and M. J. BENNETT, 2008 Root growth in *Arabidopsis* requires gibberellin/DELLA signalling in the endodermis. Nat. Cell. Biol. **10(5):** 625-628.

UEGUCHI-TANAKA, M., M. ASHIKARI, M. NAKAJIMA, H. ITOH, E. KATOH, M. KOBAYASHI, T. Y. CHOW, Y. I. HSING, H. KITANO, I. YAMAGUCHI, and M. MATSUOKA, 2005 *GIBBERELLIN NON-RESPONSIVE DWARF1* encodes a soluble receptor for gibberellin. Nature **437(7059):** 693-698.

WHEELAN, S. J., D. M. CHURCH, and J. M. OSTELL, 2001 Spidey: a tool for mRNA-to-genomic alignments. Genome Res. **11(11):** 1952-1957.

WINKLER, R.G. and M. FREELING, 1994 Physiological genetics of the dominant gibberellin-nonresponsive maize dwarfs, *Dwarf8* and *Dwarf9*. Planta **193:** 341-348.

WU, G., M. Y. PARK, S. R. CONWAY, J. W. WANG, D. WEIGEL, and R. S. POETHIG, 2009 The sequential action of miR156 and miR172 regulates developmental timing in *Arabidopsis*. Cell **138(4):**750-759.

YU, J., J. B. HOLLAND, M. D. MCMULLEN, and E. S. BUCKLER, 2008 Genetic design and statistical power of nested association mapping in maize. Genetics **178(1):** 539-551.

YU, J., G. PRESSOIR, W. H. BRIGGS, I. VROH BI, M. YAMASAKI, J. F. DOEBLEY, M. D. MCMULLEN, B. S. GAUT, D. M. NIELSEN, J. B. HOLLAND, S. KRESOVICH, and E. S. BUCKLER, 2006 A unified mixed-model method for association mapping that accounts for multiple levels of relatedness. Nat. Genet. **38(2):** 203-208.

ZHAO, K., M. J. ARANZANA, S. KIM, C. LISTER, C. SHINDO, C. TANG, C. TOOMAJIAN, H. ZHENG, C. DEAN, P. MARJORAM, and M. NORDBORG, 2007 An *Arabidopsis* example of association mapping in structured samples. PLoS Genet. **3(1):** e4.

ZHANG, L., J. M. CHIA, S. KUMARI, J. C. STEIN, Z. LIU, A. NARECHANIA, C. A. MAHER, K. GUILL, M. D. MCMULLEN, and D. WARE, 2009a A genome-wide characterization of microRNA genes in maize. PLoS Genet. **5(11):** e1000716.

ZHANG, W., N. LAUTER, R. PULAM, and S. P. MOOSE, 2009b Molecular interactions among regulatory factors influencing shoot maturation in maize. 2009 Maize Genetics Conference Abstract **51:P103**.

ZHANG, Z., E. ERSOZ, C. Q. LAI, R. J. TODHUNTER, H. K. TIWARI, M. A. GORE, P. J. BRADBURY, J. YU, D. K. ARNETT, J. M. ORDOVAS, and E. S. BUCKLER, 2010 Mixed linear model approach adapted for genome-wide association studies. Nat. Genet. **42(4):**355-360.

ZAR, J., 1999 *Biostatistical Analysis* 4th Edition. Prentice Hall Inc., Upper Saddle River, N. J. 929p.

TABLES

Table 5. Means comparisons among the recessive GA-deficient mutants and their *wild-type* siblings for SBR traits.

N[a]	*D3/-*	*d3/d3*[b]	N[a]	*D5/-*	*d5/d5*[b]
	A. Number of nodes with shoot-borne roots (NWSBR)				
18	2.2±0.8	4.6±0.51***	14	2.2±0.6	3.3±1.1**
	B. Number of shoot-borne roots at node two (SBR2)				
17	13.7±2.4	8.6±2.9***	13	17.9±2.0	12.3±3.3***
	C. Number of shoot-borne roots at node one (SBR1)				
13	13.6±3.0	7.9±3.2***	12	16.8±1.5	16.8±1.5***

[a] the number of individual plants measured for each phenotype.
[b] significance level of means comparison *,**,***, represent *P*-values of <0.05, <0.01 and <0.001 respectively.

Table 6. Mean comparisons among the dominant GA non-responsive mutants and their *wild-type* siblings for SBR traits.

N[a]	*d8/d8*	*D8/d8*	N[a]	*d9/d9*	*D9/d9*	N[a]	*d10/d10*	*D10/d10*
				A. Number of nodes with shoot-borne roots (NWSBR)				
8	1.6±0.5	0.1±0.3***	23	1.3±0.7	0.5±0.59***	30	1.5±0.57	0***
				B. Number of shoot-borne roots at node two (SBR2)				
7	1.4±1.4	0*	23	4.1±6.5	0.09±0.42**	30	6.1±8.1	0***
				C. Number of shoot-borne roots at node one (SBR1)				
8	17.7±3.5	0.13±0.35***	23	14.6±5.3	4.5±6.8***	30	17.3±5.4	0***
				D. Total number of shoot-borne roots (totlSBR)				
8	21.6±5.3	0.13±0.35***	23	18.8±9.6	4.6±6.9***	30	24±11.7	0***

[a] the number of individual plants measured for each phenotype.
[b] significance level of means comparison *,**,***, represent *P*-values of <0.05, <0.01 and <0.001 respectively.

Table 7. Mean comparisons among *D8* mutant alleles and *wild-type* siblings for SBR traits.

N[a]	d8/*d8*	*D8-N1452/d8*[b]	N[a]	d8/*d8*	*D8-N1591/d8*[b]	N[a]	d8/*d8*	*D8-N2031/d8*[b]
				A. Number of nodes with brace roots (NWSBR)				
10	1.9±0.7	0.9±0.7*	9	1.3±0.7	0.7±0.7[ns]	7	1.9±0.5	0.4±0.8**
				B. Number of brace roots at node two (SBR2)				
10	9.6±7	0.6±1**	9	3.9±7.1	0.2±0.7[ns]	7	8.1±6.5	0±0**
				C. Number of brace roots at node one (SBR1)				
10	15.1±2.9	8.2±5.8**	9	13.5±5.7	5.4±3.8*	5	14.8±1.3	2.3±3.6**
				D. Total number of brace roots (totlSBR)				
10	26.1±11.6	8.8±6.4**	9	17.4±10.2	5.7±7.1*	5	20.2±5.1	2.3±3.6**

[a] the number of individual plants measured for each phenotype.
[b] significance level of means comparison*,**,***, represent *P*-values of <0.05, <0.01 and <0.001 respectively.

Table 8. Summary statistics for SBR traits measured in maize association panel members across three growing seasons.

Trait[a]	Mean	High	Low	StDev[b]	CV[c]	N[d]	*h*[e]
NWSBR04	2.1	6.1	1.0	0.85	39.58	90	0.77
NWSBR05	2.8	6.5	1.1	1.04	37.62	91	0.82
NWSBR08	2.2	2.9	1.0	0.35	15.74	260	0.57
SBR104	13.9	20.5	5.4	3.21	23.10	90	0.65
SBR105	15.3	23.2	9.0	2.90	18.94	91	0.50
SBR108	14.0	22.8	0.1	3.90	27.96	260	0.52
SBR204	12.2	24.6	0.0	6.97	57.22	90	0.82
SBR205	15.2	28.0	0.0	6.44	42.41	91	0.74
SBR208	7.3	22.2	0.0	6.34	86.92	260	0.63
totlSBR04	30.6	139.5	7.4	18.84	61.57	90	0.86
totlSBR05	44.5	161.4	12.0	24.23	54.50	91	0.75
totlSBR08	22.9	70.3	1.1	12.85	56.20	260	0.62

[a] The last two digits of the trait abbreviation indicate the year the trait data was collected (2004, 2005 or 2008).
[b] Standard deviation.
[c] Coefficient of variation.
[d] The number of inbred lines from the maize association panel.
[e] Broad sense heritability.

Table 9. The contributions of population structure to SBR-patterning traits among maize association panel members.

Trait[a]	Slope	R^2	p-value	Trait[a]	Slope	R^2	p-value
	A. NSS				B. SS		
NWSBR04	-0.41	0.23	6.03E-06	NWSBR04	0.02	0.00	NS
NWSBR05	-0.11	0.16	0.000265	NWSBR05	0.02	0.00	NS
NWSBR08	-0.05	0.09	2.56E-06	NWSBR08	0.05	0.06	0.000152
SBR104	-0.48	0.00	NS	SBR104	0.19	0.00	NS
SBR105	-0.26	0.00	NS	SBR105	0.65	0.01	NS
SBR108	-1.65	0.03	0.003847	SBR108	1.87	0.03	0.007034
SBR204	-6.22	0.15	0.000418	SBR204	-0.36	0.00	NS
SBR205	-4.95	0.10	0.002144	SBR205	1.97	0.01	NS
SBR208	-5.37	0.13	8.71E-09	SBR208	5.42	0.09	2.18E-06
totlSBR04	-0.55	0.15	0.000349	totlSBR04	-0.03	0.00	NS
totlSBR05	-0.18	0.12	0.001823	totlSBR05	0.04	0.00	NS
totlSBR08	-0.24	0.10	2.99E-07	totlSBR08	0.24	0.07	2.68E-05
	C. TS				D. Group[b]		
NWSBR04	0.38	0.21	1.87E-05	NWSBR04	NA	0.37	2.36E-07
NWSBR05	0.09	0.11	0.002413	NWSBR05	NA	0.22	0.000765
NWSBR08	0.02	0.01	NS	NWSBR08	NA	0.12	8.19E-06
SBR104	0.35	0.00	NS	SBR104	NA	0.02	NS
SBR105	-0.13	0.00	NS	SBR105	NA	0.06	NS
SBR108	0.44	0.00	NS	SBR108	NA	0.07	0.003971
SBR204	6.16	0.15	0.000344	SBR204	NA	0.29	2.16E-05
SBR205	3.56	0.06	0.026020	SBR205	NA	0.24	0.000285
SBR208	1.94	0.01	0.059960	SBR208	NA	0.16	3.98E-08
totlSBR04	0.55	0.16	0.000291	totlSBR04	NA	0.25	0.000214
totlSBR05	0.15	0.08	0.008717	totlSBR05	NA	0.21	0.000855
totlSBR08	0.09	0.01	NS	totlSBR08	NA	0.13	1.22E-06

[a] The last two digits of the trait abbreviation indicate the year the trait data was collected (2004, 2005, or 2008).
[b] Group analysis used results from a Welch's weighted ANOVA, not from a regression.
NS = not significant. NA = not applicable.

Table 10. Descriptive statistics for NWSBR categorized by structure group membership.

Group[a]	Mean	High	Low	StDev[b]	CV[c]	N
A. NWSBR in 2004 (NWSBR04)						
MXD	2.0	3.6	1.0	0.71	35.71	19
NSS	1.8	2.7	1.0	0.47	25.93	26
Popcorn	1.6	2.2	1.1	0.42	27.34	5
SS	2.2	3.3	1.4	0.59	26.98	10
Sweet	1.3	1.5	1.0	0.20	15.25	5
TS	2.9	6.1	1.6	0.99	34.39	25
B. NWSBR in 2005 (NWSBR05)						
MXD	2.8	5.5	1.2	1.23	44.45	20
NSS	2.4	3.7	1.1	0.73	30.48	26
Popcorn	2.4	3.8	2.0	0.79	32.53	5
SS	3.0	4.2	1.9	0.65	21.90	10
Sweet	1.6	1.7	1.4	0.17	10.60	5
TS	3.3	6.5	1.3	1.09	32.73	25
C. NWSBR in 2008 (NWSBR08)						
MXD	2.3	2.7	1.3	0.33	14.73	58
NSS	2.2	2.7	1.0	0.36	16.81	102
Popcorn	2.0	2.8	1.1	0.55	27.83	7
SS	2.5	2.8	1.8	0.21	8.36	35
Sweet	1.9	2.3	1.2	0.50	26.32	5
TS	2.3	2.9	1.5	0.29	12.50	51

[a] Subpopulation membership as per Liu et al., 2003.
[b] Standard deviation.
[c] Coefficient of variation.

Table 11. Descriptive statistics for SBR1 categorized by structure group membership.

Group[a]	Mean	High	Low	StDev[b]	CV[c]	N
			A. SBR1 in 2004 (SBR104)			
MXD	14.3	20.5	5.9	3.83	26.76	19
NSS	13.6	18.9	5.4	3.36	24.80	26
Popcorn	14.3	19.1	8.0	4.08	28.59	5
SS	13.9	16.8	10.5	1.82	13.08	10
Sweet	12.4	17.4	8.8	3.26	26.31	5
TS	14.1	20.1	8.6	2.96	20.96	25
			B. SBR1 in 2005 (SBR105)			
MXD	15.4	23.2	10.5	3.40	22.16	20
NSS	15.4	19.4	11.8	2.14	13.94	26
Popcorn	17.0	21.1	10.4	4.07	23.95	5
SS	15.4	18.5	11.8	2.15	13.91	10
Sweet	12.9	15.0	10.0	1.91	14.82	5
TS	15.4	22.0	9.0	3.27	21.28	25
			C. SBR1 in 2008 (SBR108)			
MXD	14.2	22.6	3.1	3.68	25.94	58
NSS	13.4	22.8	0.1	4.46	33.26	102
Popcorn	12.1	16.8	1.8	5.20	43.00	7
SS	15.5	18.8	11.2	1.77	11.38	35
Sweet	9.3	16.4	2.9	5.52	59.22	5
TS	14.4	20.6	3.4	3.17	21.99	51

[a] Subpopulation membership as per Liu et al., 2003.
[b] Standard deviation.
[c] Coefficient of variation.

Table 12. Descriptive statistics for SBR2 categorized by structure group membership.

Group[a]	Mean	High	Low	StDev[b]	CV[c]	N
A. SBR2 in 2004 (SBR204)						
MXD	12.4	23.4	0.0	7.83	63.31	19
NSS	10.0	20.3	0.0	6.48	64.64	26
Popcorn	7.5	11.9	1.6	3.91	52.37	5
SS	12.4	19.0	4.0	5.60	45.31	10
Sweet	2.9	7.0	0.0	2.59	90.16	5
TS	17.0	24.6	6.4	4.79	28.15	25
B. SBR2 in 2005 (SBR205)						
MXD	15.0	28.0	0.7	7.59	50.50	20
NSS	13.5	22.2	0.0	6.16	45.55	26
Popcorn	14.8	20.0	11.1	4.37	29.49	5
SS	17.1	21.3	5.1	4.69	27.43	10
Sweet	5.0	8.5	0.5	2.90	58.20	5
TS	18.4	25.5	10.8	4.54	24.70	25
C. SBR2 in 2008 (SBR208)						
MXD	7.7	22.2	0.0	5.78	75.04	58
NSS	5.1	21.5	0.0	5.74	112.65	102
Popcorn	2.7	12.0	0.0	4.20	157.81	7
SS	11.8	21.4	0.4	5.80	49.02	35
Sweet	2.9	10.7	0.0	4.52	153.51	5
TS	8.9	21.8	0.0	6.51	73.35	51

[a] Subpopulation membership as per Liu et al., 2003.
[b] Standard deviation.
[c] Coefficient of variation.

Table 13. Descriptive statistics for totlSBR categorized by structure group membership.

Group[a]	Mean	High	Low	StDev[b]	CV[c]	N
A. totlSBR in 2004 (totlSBR04)						
MXD	30.5	62.5	5.9	15.8	51.8	19
NSS	23.6	45.9	4.1	10.7	45.3	26
Popcorn	21.8	26.8	9.5	7.1	32.7	5
SS	27.8	50.9	14.1	10.3	37.1	10
Sweet	14.9	16.7	11.1	2.3	15.3	5
TS	43.9	139.5	19.7	25.5	58.0	25
B. totlSBR in 2005 (totlSBR05)						
MXD	46.3	104.2	12.2	27.4	59.3	20
NSS	37.1	65.0	12.0	14.5	39.2	26
Popcorn	39.3	79.6	22.1	23.0	58.5	5
SS	45.9	69.2	20.9	14.6	31.7	10
Sweet	17.6	20.7	15.6	2.5	14.3	5
TS	56.5	161.4	14.5	29.1	51.6	25
C. totlSBR in 2008 (totlSBR08)						
MXD	22.6	53.1	2.3	11.4	50.3	58
NSS	18.9	47.2	1.1	10.8	57.3	102
Popcorn	17.5	56.8	1.6	18.7	106.6	7
SS	32.2	64.1	7.5	12.1	37.7	35
Sweet	11.5	18.6	1.7	8.0	69.5	5
TS	25.7	70.3	3.5	13.0	50.8	51

[a] Subpopulation membership as per Liu et al., 2003.
[b] Standard deviation.
[c] Coefficient of variation.

Table 14. Association mapping results for the six targeted polymorphisms in *d3*.

Trait[a]	Position[b]	p-value[c]	Model[d]	Marker[e]
NWSBR04	2888	0.0364	0.61	0.02
NWSBR05	2888	0.0197	0.57	0.03
NWSBR08	2888	0.0086	0.51	0.02
SBR104	2888	0.0292	0.51	0.03
SBR105	2888	0.5694	0.44	0.00
SBR108	2888	0.0124	0.50	0.01
SBR204	2888	0.0243	0.57	0.03
SBR205	2888	0.0225	0.55	0.03
SBR208	2888	0.0605	0.51	0.01
totlSBR04	2888	0.0056	0.60	0.05
totlSBR05	2888	0.0281	0.55	0.03
totlSBR08	2888	0.0070	0.52	0.02
NWSBR04	2894	0.0872	0.62	0.04
NWSBR05	2894	0.0268	0.60	0.06
NWSBR08	2894	0.0750	0.51	0.02
SBR104	2894	0.0376	0.53	0.06
SBR105	2894	0.1279	0.48	0.04
SBR106	2894	0.0386	0.50	0.02
SBR204	2894	0.0221	0.60	0.06
SBR205	2894	0.0184	0.58	0.06
SBR206	2894	0.1243	0.51	0.01
totlSBR04	2894	0.0138	0.62	0.06
totlSBR05	2894	0.0066	0.60	0.08
totlSBR08	2894	0.0446	0.52	0.02

[a] The last two digits of the trait abbreviation indicate the year the trait data was collected (2004, 2005, or 2008).
[b] Position of polymorphism along gene.
[c] p-value of the marker trait association.
[d] Amount of the variation explained by the mixed model.
[e] Amount of the variation explained by the polymorphism at the indicated position.

Table 14. Association mapping results for the six targeted polymorphisms in *d3* (continued).

Trait[a]	Position[b]	p-value[c]	Model[d]	Marker[e]
NWSBR04	2905	0.1204	0.60	0.01
NWSBR05	2905	0.0029	0.59	0.05
NWSBR08	2905	0.0059	0.51	0.02
SBR104	2905	0.3851	0.48	0.01
SBR105	2905	0.6504	0.44	0.00
SBR108	2905	0.0053	0.50	0.02
SBR204	2905	0.0177	0.57	0.04
SBR205	2905	0.0082	0.56	0.04
SBR208	2905	0.0399	0.51	0.01
totlSBR04	2905	0.0475	0.58	0.02
totlSBR05	2905	0.0010	0.59	0.07
totlSBR08	2905	0.0038	0.52	0.02
NWSBR04	2907	0.1204	0.60	0.01
NWSBR05	2907	0.0029	0.59	0.05
NWSBR08	2907	0.0060	0.51	0.02
SBR104	2907	0.3851	0.48	0.01
SBR105	2907	0.6504	0.44	0.00
SBR108	2907	0.0044	0.50	0.02
SBR204	2907	0.0177	0.57	0.04
SBR205	2907	0.0082	0.56	0.04
SBR208	2907	0.0210	0.51	0.01
totlSBR04	2907	0.0475	0.58	0.02
totlSBR05	2907	0.0010	0.59	0.07
totlSBR08	2907	0.0033	0.52	0.02

[a] The last two digits of the abbreviation indicate the year the trait data was collected (2004, 2005, or 2008).
[b] Position of polymorphism along gene.
[c] p-value of the marker trait association.
[d] Amount of the variation explained by the mixed model.
[e] Amount of the variation explained by the polymorphism at the indicated position.

Table 14. Association mapping results for the six targeted polymorphisms in *d3* (continued).

Trait[a]	Position[b]	p-value[c]	Model[d]	Marker[e]
NWSBR04	2909	0.1204	0.60	0.01
NWSBR05	2909	0.0029	0.59	0.05
NWSBR08	2909	0.0216	0.51	0.02
SBR104	2909	0.3851	0.48	0.01
SBR105	2909	0.6504	0.44	0.00
SBR108	2909	0.0193	0.50	0.02
SBR204	2909	0.0177	0.57	0.04
SBR205	2909	0.0082	0.56	0.04
SBR208	2909	0.0494	0.51	0.01
totlSBR04	2909	0.0475	0.58	0.02
totlSBR05	2909	0.0010	0.59	0.07
totlSBR08	2909	0.0133	0.52	0.02
NWSBR04	2916	0.1204	0.60	0.01
NWSBR05	2916	0.0029	0.59	0.05
NWSBR08	2916	0.0055	0.50	0.02
SBR104	2916	0.3851	0.48	0.01
SBR105	2916	0.6504	0.44	0.00
SBR108	2916	0.0047	0.50	0.02
SBR204	2916	0.0177	0.57	0.04
SBR205	2916	0.0082	0.56	0.04
SBR208	2916	0.0425	0.51	0.01
totlSBR04	2916	0.0475	0.58	0.02
totlSBR05	2916	0.0010	0.59	0.07
totlSBR08	2916	0.0036	0.52	0.02

[a] The last two digits of the trait abbreviation indicate the year the trait data was collected (2004, 2005, or 2008).
[b] Position of polymorphism along gene.
[c] p-value of the marker trait association.
[d] Amount of the variation explained by the mixed model.
[e] Amount of the variation explained by the polymorphism at the indicated position.

Table 14. Association mapping results for the six targeted polymorphisms in *d3* (continued).

Trait[a]	Position[b]	p-value[c]	Model[d]	Marker[e]
NWSBR04	2918	0.1111	0.60	0.01
NWSBR05	2918	0.3489	0.55	0.01
NWSBR08	2918	0.3387	0.49	0.00
SBR104	2918	0.0997	0.49	0.02
SBR105	2918	0.0613	0.46	0.03
SBR108	2918	0.3078	0.48	0.00
SBR204	2918	0.0414	0.57	0.03
SBR205	2918	0.0889	0.54	0.02
SBR208	2918	0.8296	0.50	0.00
totlSBR04	2918	0.0661	0.58	0.02
totlSBR05	2918	0.1131	0.54	0.02
totlSBR08	2918	0.3244	0.50	0.00

[a] The last two digits of the trait abbreviation indicate the year the trait data was collected (2004, 2005, or 2008).
[b] Position of polymorphism along gene.
[c] p-value of the marker trait association.
[d] Amount of the variation explained by the mixed model.
[e] Amount of the variation explained by the polymorphism at the indicated position.

Table 15. Association mapping results for the four targeted polymorphisms in *D8*.

Trait[a]	Position	p-value	Model[b]	Marker[c]
NWSBR04	677	0.0428	0.61	0.03
NWSBR05	677	0.0729	0.57	0.02
NWSBR08	677	0.5045	0.49	0.00
SBR104	677	0.3349	0.48	0.01
SBR105	677	0.2872	0.45	0.01
SBR108	677	0.4915	0.47	0.00
SBR204	677	0.0193	0.57	0.04
SBR205	677	0.1299	0.53	0.02
SBR208	677	0.1264	0.51	0.01
totlSBR04	677	0.0995	0.57	0.02
totlSBR05	677	0.0294	0.55	0.03
totlSBR08	677	0.3888	0.51	0.00
NWSBR04	699	0.0326	0.61	0.03
NWSBR05	699	0.0505	0.57	0.03
NWSBR08	699	0.5189	0.49	0.00
SBR104	699	0.3626	0.48	0.01
SBR105	699	0.3102	0.45	0.01
SBR108	699	0.5399	0.47	0.00
SBR204	699	0.0240	0.56	0.04
SBR205	699	0.1183	0.53	0.02
SBR208	699	0.1292	0.51	0.01
totlSBR04	699	0.0823	0.57	0.02
totlSBR05	699	0.0250	0.55	0.04
totlSBR08	699	0.3982	0.50	0.00

[a] The last two digits of the trait abbreviation indicate the year the trait data was collected (2004, 2005, or 2008).
[b] Amount of the variation explained by the mixed model.
[c] Amount of the variation explained by the polymorphism at the indicated position.

Table 15. Association mapping results for the four targeted polymorphisms in *D8* (continued).

Trait[a]	Position	p-value	Model[b]	Marker[c]
NWSBR04	702	0.0271	0.62	0.03
NWSBR05	702	0.0364	0.59	0.03
NWSBR08	702	0.2894	0.49	0.00
SBR104	702	0.3313	0.49	0.01
SBR105	702	0.3128	0.45	0.01
SBR108	702	0.3513	0.47	0.00
SBR204	702	0.0189	0.58	0.04
SBR205	702	0.0721	0.55	0.02
SBR208	702	0.0759	0.51	0.01
totlSBR04	702	0.0748	0.58	0.02
totlSBR05	702	0.0167	0.57	0.04
totlSBR08	702	0.2141	0.51	0.00
NWSBR04	710	0.0271	0.62	0.03
NWSBR05	710	0.0364	0.59	0.03
NWSBR08	710	0.2880	0.49	0.00
SBR104	710	0.3313	0.49	0.01
SBR105	710	0.3128	0.45	0.01
SBR108	710	0.3490	0.47	0.00
SBR204	710	0.0189	0.58	0.04
SBR205	710	0.0721	0.55	0.02
SBR208	710	0.0824	0.51	0.01
totlSBR04	710	0.0748	0.58	0.02
totlSBR05	710	0.0167	0.57	0.04
totlSBR08	710	0.2152	0.51	0.00

[a] The last two digits of the trait abbreviation indicate the year the trait data was collected (2004, 2005, or 2008).
[b] Amount of the variation explained by the mixed model.
[c] Amount of the variation explained by the polymorphism at the indicated position.

FIGURES

Figure 4. Mechanism of GA-mediated de-repression of GA response genes through the degradation of DELLA transcriptional repressors. Modified from Schwechheimer, 2008.

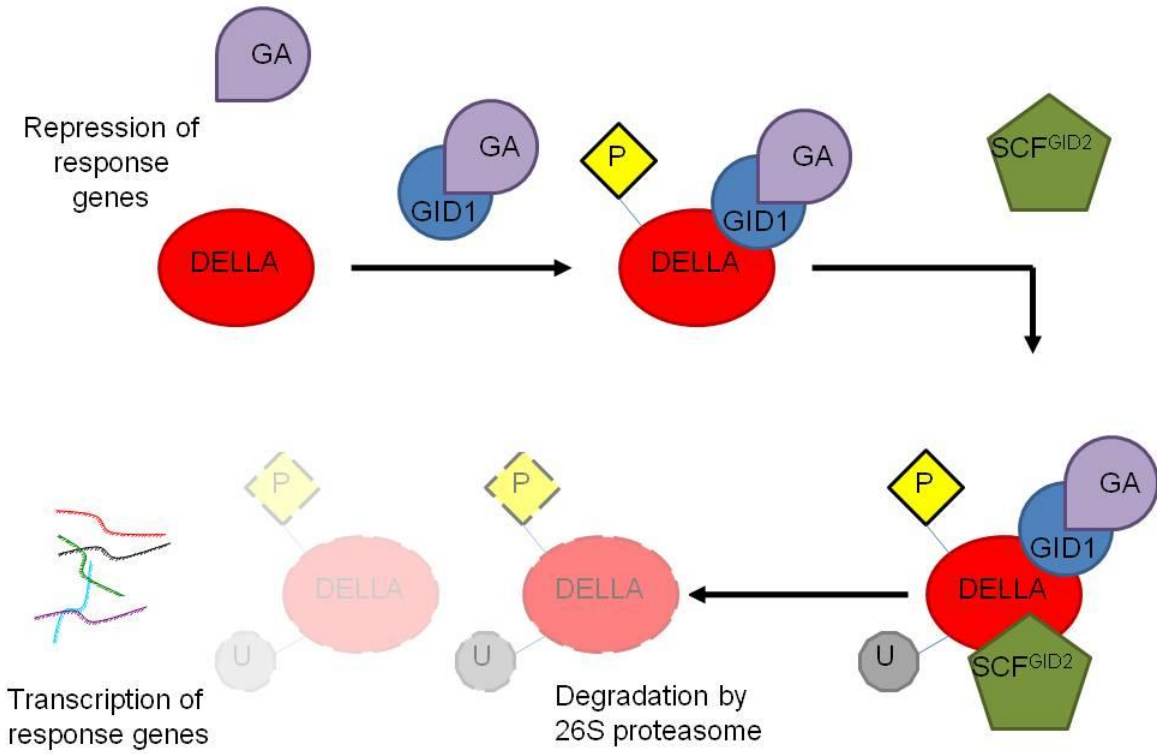

DELLA transcription factor in red.
GA molecule show in purple.
GID1 soluble GA receptor in blue.
Phosphate molecule in yellow.
SCF complex in green.
Ubiquitin molecule in grey.

Figure 5. Placement of GA-deficient and non-responsive mutants along the GA biosynthetic and response pathway.

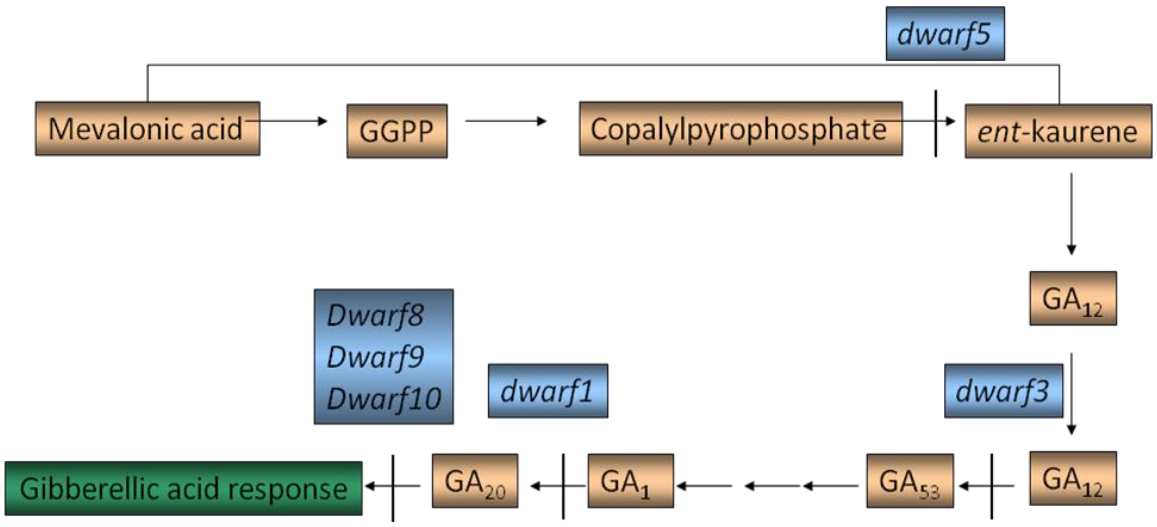

Salmon colored boxes include the names of GA biosynthetic intermediates.
Light blue boxes include the locus names for genes involved in the GA biosynthetic and response pathway.
Green box indicates the final action of GA response in the pathway.
Arrows indicate progression through the pathway.
Lines perpendicular to the arrows indicate a step that is blocked by mutations at the locus in the light blue box above the step.

Figure 6. Whole plant and root phenotypes of recessive GA-deficient dwarfs and their *wild-type* siblings. (A, B) *wild-type* sibling (*D3*/-) of *dwarf3* mutant plants, (C, D) *dwarf3* (*d3*/*d3*) mutant, (E, F) *wild-type* sibling (*D5*/-) of *dwarf5* mutant plants, (G, H) *dwarf5* (*d5*/*d5*) mutant plants. Red arrows indicate the soil line in panels D and H.

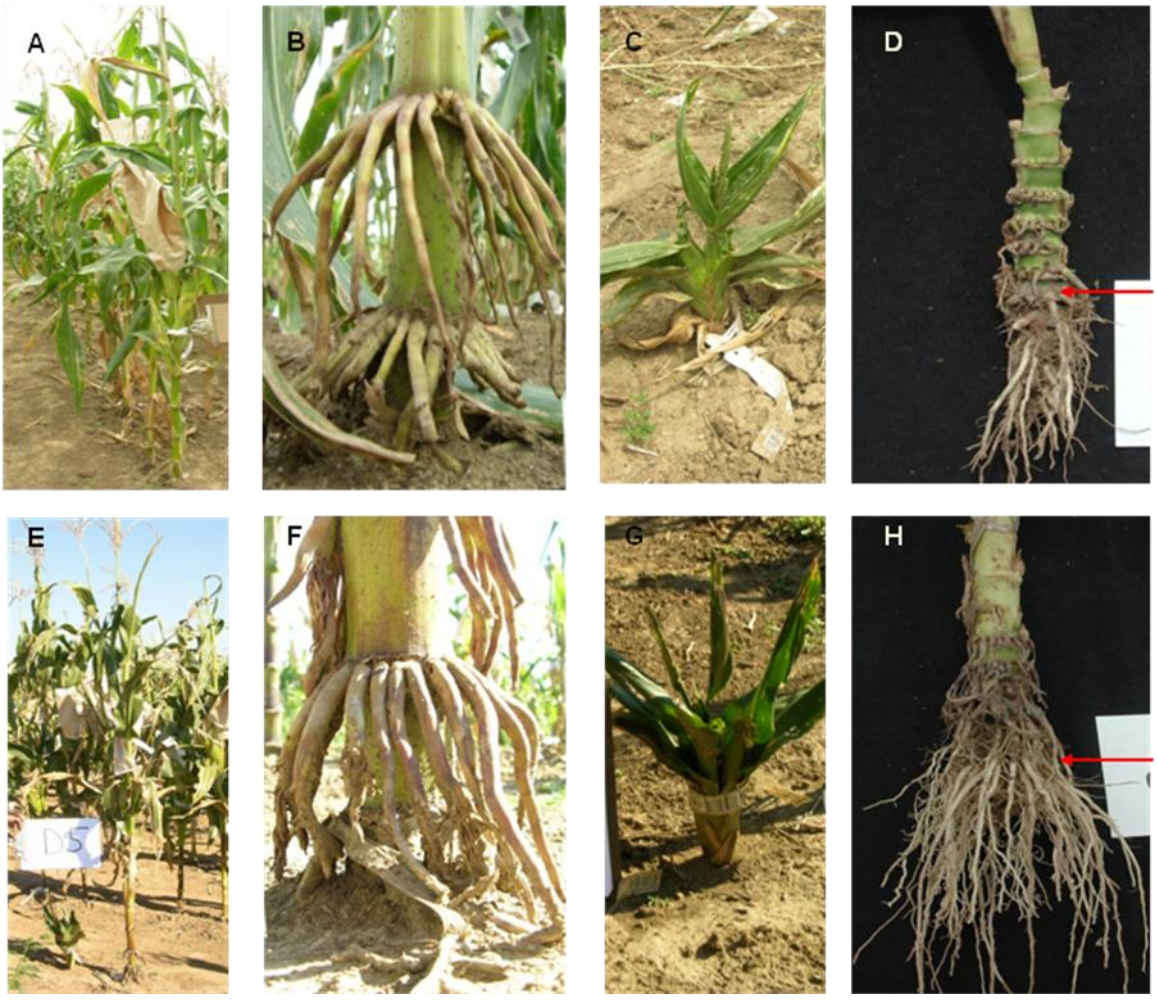

Figure 7. Whole plant and root phenotypes of dominant gibberellin non-responsive dwarfs and their *wild-type* siblings. (A, B) *wild-type* sibling (*d8/d8*) of *D8* mutant plants, (C, D) *D8* (*D8/-*) mutant, (E, F) *wild-type* sibling (*d9/d9*) of *D9* mutant plants, (G, H) *D9* (*D9/-*) mutant, (I, J) *wild-type* (*d10/d10*) sibling of *D10* mutant plants, (K, L) *D10* mutant (*D10/-*).

Figure 8. Map position of the *d3* locus relative to the *qsbr2.4* QTL.

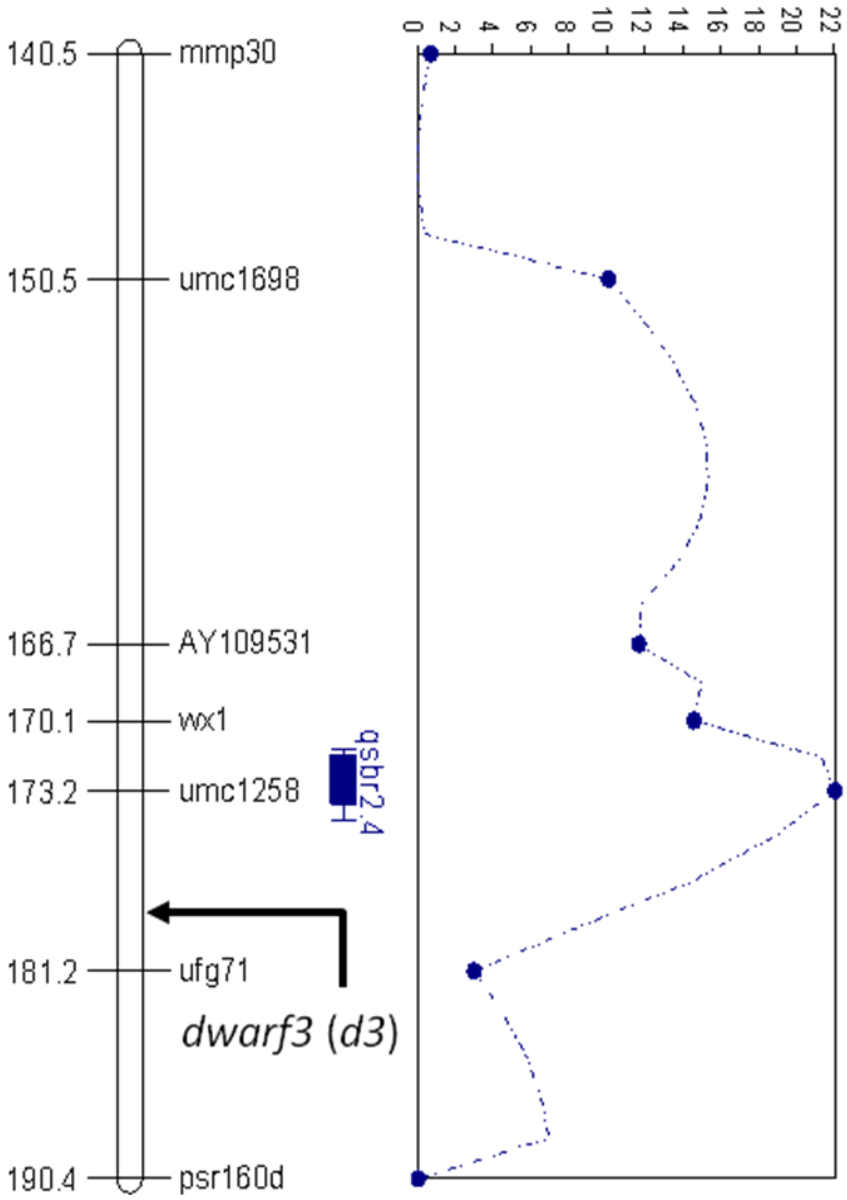

Genetic map of the chromosome region containing *qsbr2.4* is based on 274 individuals from the IBM mapping population. The likelihood ratio statistic from the QTL analysis is plotted on the right in blue. The LR threshold for *qsbr2.4* is 14.6.

Figure 9. Gene model for *d3* and relevant preliminary association mapping results.

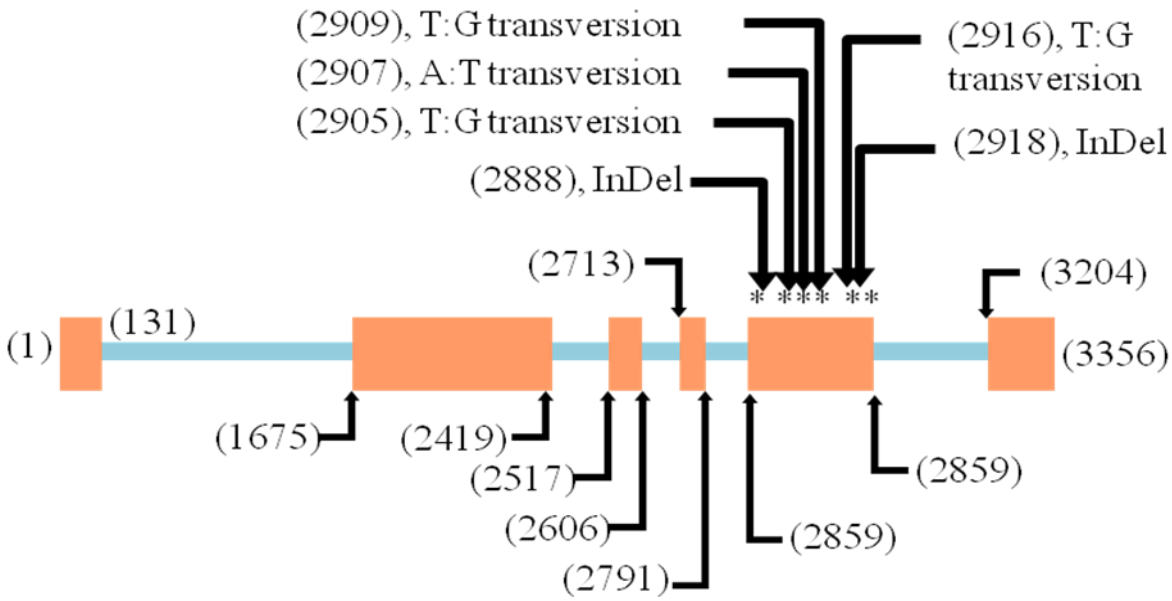

Salmon boxed represent exons while the blue boxed represent introns.
Numbers inside parentheses denote position of intron-exon junctions or important polymorphisms in exon five in base pairs.
*denote polymorphisms within the fifth exon targeted for further analysis.

Figure 10. Gene model for *D8* and relevant preliminary association mapping results.

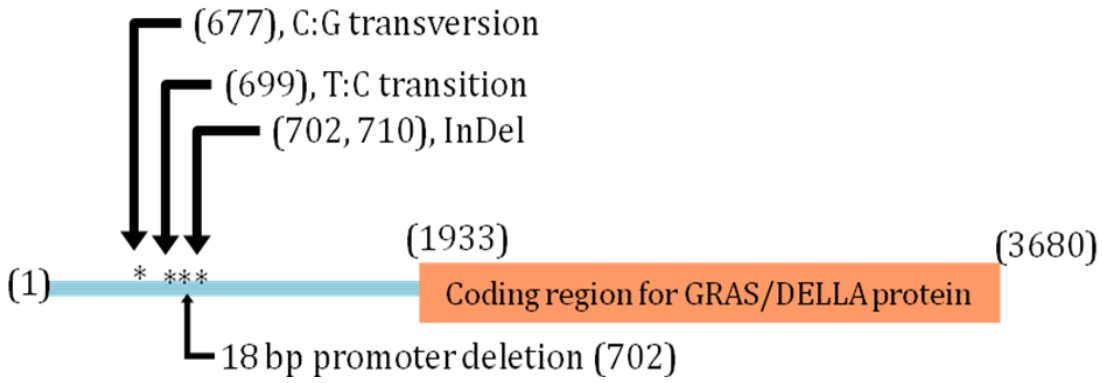

Salmon box represent the exon while the blue box represents the intron.
Numbers inside parentheses denote position of intron-exon junctions or important polymorphisms in the promoter region in base pairs.
*denote polymorphisms within the fifth exon targeted for further analysis.

Figure 11. Graphical display of sequence polymorphisms in *d3* and their associated p-values for SBR2 across three field seasons.

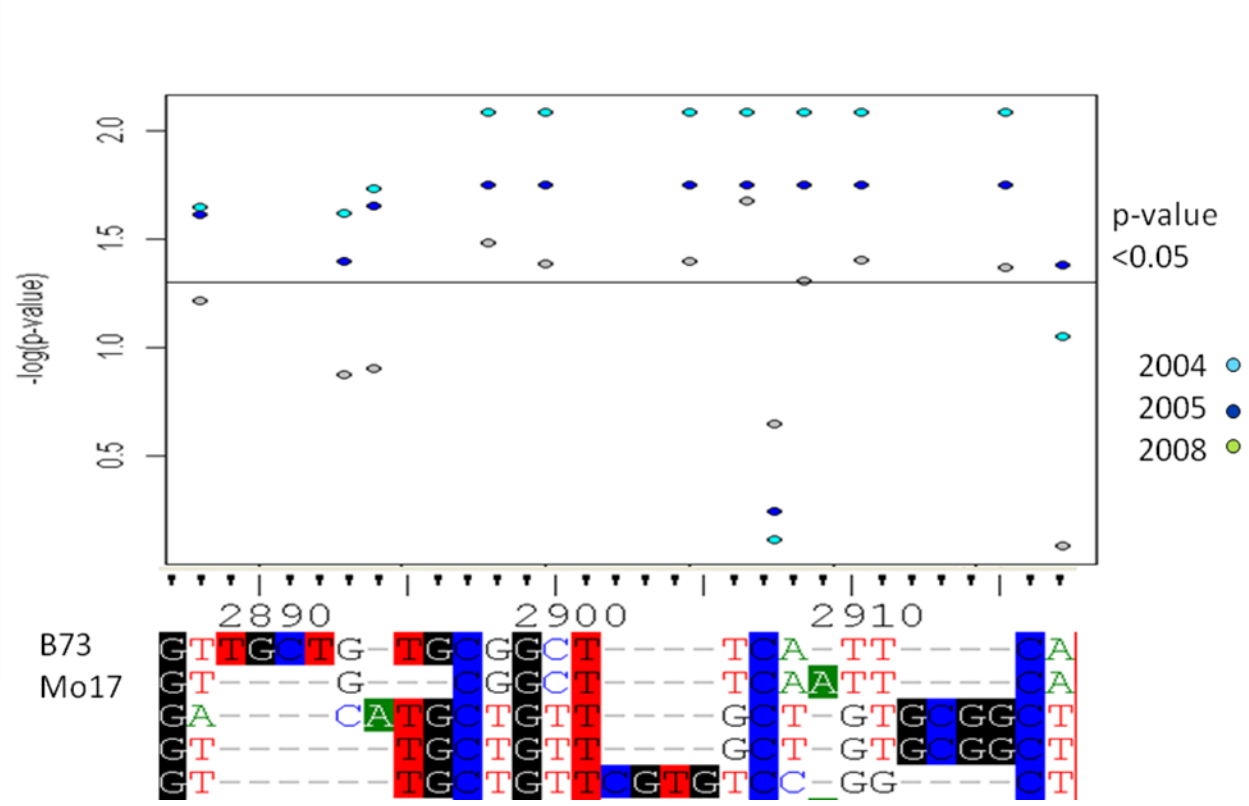

The horizontal line at 1.3 represents a p-value of 0.05. Results from 2004, 2005 and 2008 are colored light blue, royal blue and gray. Nucleic acids on colored boxes are either conserved or insertion/deletions. SNP polymorphisms are not in colored boxes. The first two sequences are from B73 and Mo17.

Figure 12. Graphical display of sequence polymorphisms in *D8* and their associated p-values for NWSBR and SBR2 across three field seasons.

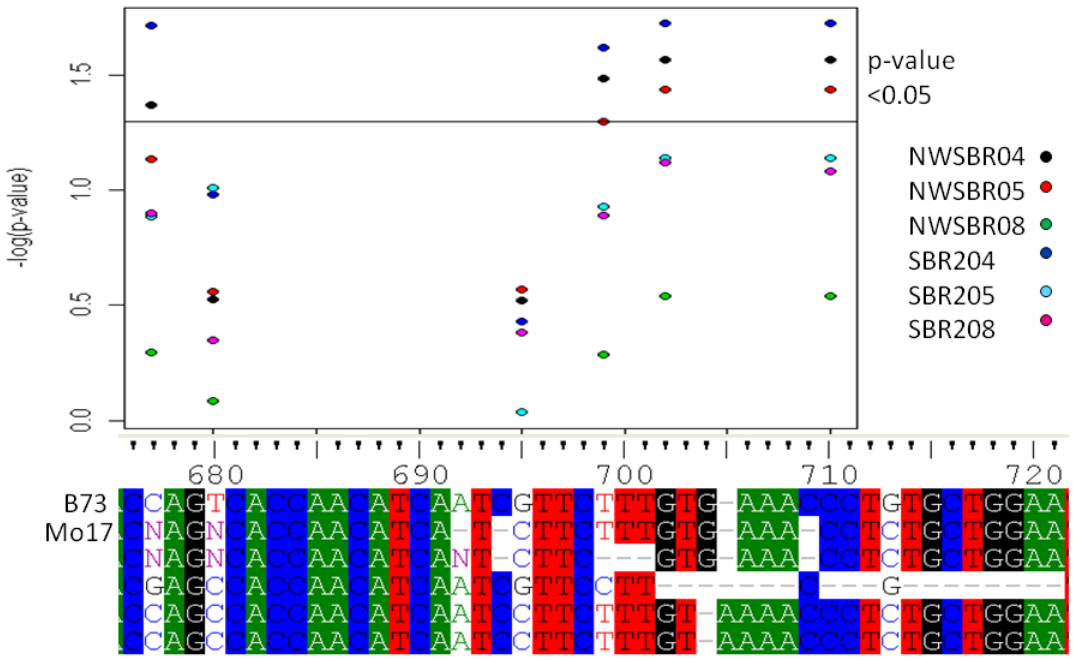

The horizontal line at 1.3 represents a p-value of 0.05. Results from 2004, 2005, and 2008 for NWSBR are black, red and green. Results from 2004, 2005, and 2008 for SBR2 are colored royal blue, light blue and violet. Nucleic acids on colored boxes are either conserved or insertion/deletions. SNP polymorphisms are not in colored boxes. The first two sequences are from B73 and Mo17

Figure 13. Mechanisms for *D8*-mediated radial SBR-patterning. (A) The promotion of cell-wall-modifying factors and PCD via GA-mediated degradation of DELLA transcription factors. (B) Inhibition of SBR as a result of reduced GA or GA-non-responsive alleles of DELLA transcription factors.

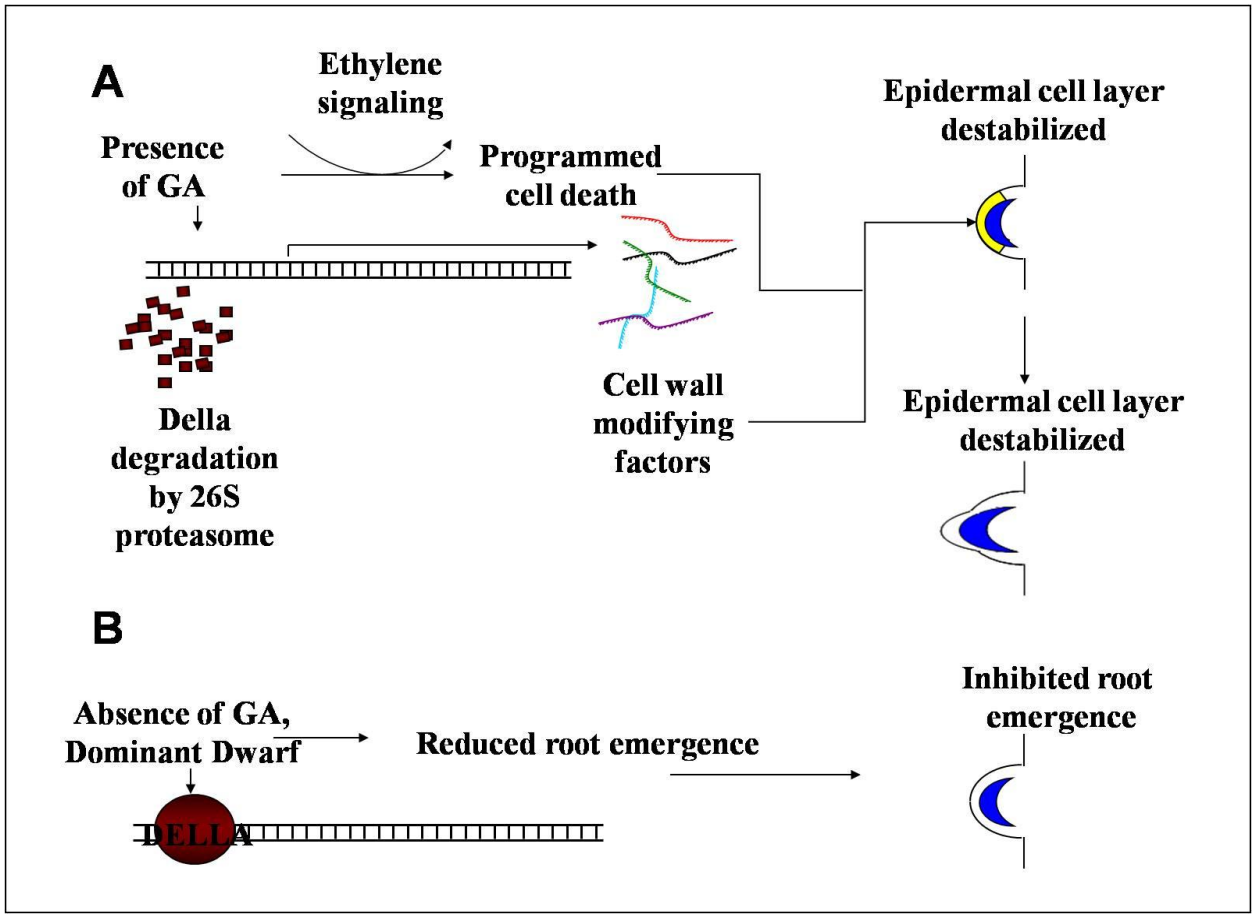

CHAPTER 4: Multivariate data analysis of *Zea mays* L. SBRs and correlated traits reveals candidate pathways and genes affecting root patterning.

ABSTRACT

Water and nutrient absorption are vital activities carried out by the SBR system in maize. Few studies to date have targeted pathways and genes controlling SBR-patterning. To form hypotheses about processes underlying their development, we evaluated SBR-patterning and twenty-three developmental and morphological traits in a diverse set of 25 maize inbred lines. Multivariate data analysis consisted of correlation analysis of all twenty-six traits, principal component analysis of the twenty three morphological traits, and a multiple regression of the principle components onto the SBR traits. Correlation analysis revealed high complexity in relationships among the traits. Principal component regression results suggest that genetic networks controlling vegetative growth, light-signaling, juvenile-phase duration and tassel architecture also affect SBR-patterning. Previous studies performed on the mutants *Vegetative-to-generative growth1* (*Vgt1*) and *epc1* validate the role of vegetative growth and juvenile-phase length as factors contributing to SBR-patterning. Additional phenotyping of SBR-patterning in lines which possess mutations in genes that control light-signaling and tassel architecture may identify additional targets for maize SBR improvement.

INTRODUCTION

The genomics era has fostered interest in systems biology as a way to understand the voluminous data created by high-throughput technologies. Systems biology seeks to identify dynamic networks dictating the observed variation in large biological data sets (Kitano, 2002). In plants, these studies include integrating structural genomic variation with the molecular phenotypes

provided by transcriptomics (Kliebenstein et al., 2006; Shi et al., 2007), proteomics (Stylianou et al., 2008) and metabolomics (Wentzell et al., 2007; McMullen et al., 1998). While these studies have effectively linked structural genomic variation to variation in molecular phenotypes, they have not addressed variation on the organismal level. Kliebenstein (2010) suggests this is representative of the increase in complexity of the network composition underlying phenotypic variation on the organismal level relative to variation found in molecular phenotypes.

The goal of this study is to identify networks which contribute to SBR-patterning by assessing phenotypic variation on a systems level. Data was collected for a set of predictor traits, representing an assortment of developmental pathways and mechanisms to link the pathways to SBR-patterning through a multiple regression analysis. Mutants affecting traits linked to SBR-patterning will assist in discovery of developmental networks which shape SBR variation. Network identification will also generate positional candidates underlying SBR QTL for validation through association analysis.

MATERIALS AND METHODS

Germplasm: The twenty-five maize inbred lines used in the present study represent a significant amount of genetic diversity from the NSS, TS, Popcorn (POP) and Sweet (SWT) corn germplasm pools as well as lines of mixed origin (MXD). These lines are also founders of the maize nested association mapping population (McMullen et al., 2009; Yu et al., 2008). They are as follows: B97 (NSS), CML52 (TS), CML69 (TS), CML103 (TS), CML228 (TS), CML247 (TS), CML277 (TS), CML322 (TS), CML333 (TS), Hp301 (POP), Il14H (SWT), Ki3 (TS), Ki11 (TS), Ky21 (NSS), M37W (MXD), M162W (NSS), Mo18W (MXD), MS71 (NSS), NC350 (TS), NC358 (TS), Oh43 (NSS), Oh7B (MXD), P39 (SWT), Tx303 (MXD), and Tzi8 (TS).

Growth conditions: Maize inbred lines were grown at the South Farm Research Center, Columbia, Missouri, in the summer of 2007 and 2008. Each year a randomized complete block design with two replicates was used for the experimental layout. In 2007, twenty kernels were planted per twenty foot row, and all plants were phenotyped. In 2008 twenty kernels were planted in ten foot rows and were subsequently thinned to ten plants per row. Five plants per row were phenotyped, excluding the two plants on either end of the row. In 2008, seed was sown on June 23rd, three weeks later than the planting date in 2007 on June 2nd.

Phenotypic measurements and data preparation: SBR traits were collected as previously described (Chapter 2, Materials and Methods). Twenty-three traits were phenotyped for use as predictor variables in a multiple regression. Descriptions of their measurements are given in Table 16. Data was visually inspected for outliers using histograms and boxplots in SAS version 9.0 (The SAS Institute, Cary, North Carolina). Once individual outliers were removed, row (inbred line) means were calculated for each replication in each year.

Correlation analysis: The PROC UNIVARIATE procedure with the "normal" and "plot" commands was used to examine summary statistics and distributions. All traits were normally distributed with the exceptions of tassel branch number, ear node diameter, leaf area, leaf length, leaf width, NWSBR, soil node diameter, totlSBR, the total leaf number, transition leaf number, and the tassel node diameter. Square root transformations were applied to tassel branch number, NWSBR, totlSBR, and tassel node diameter, while logarithmic transformations were used for leaf area and soil node diameter to achieve normal distributions. The PROC CORR procedure was used in SAS version 9.0 for correlation analysis. The SPEARMAN command was used to perform the nonparametric, Spearman rank correlation analysis for the untransformed values for ear node diameter, leaf length and leaf width, total leaf number and transition leaf number and all other normally distributed traits. Correlations were considered significant at the $P<0.05$ level.

Principal component analysis (PCA): A parameter reduction procedure, PCA, was conducted with the initial aim of modeling root patterning relative to developmental pathways. PCA creates a new set of uncorrelated variables, eigenvectors (principle components, PCs), which represent linear combinations of the initially correlated predictor variables, *p* (Jackson, 1991). The linear combinations defining the PCs are weighted to explain the greatest amount of variation in the correlation matrix. Fitting the eigenvectors to sequentially explain a maximal amount of variation results in the eigenvectors being orthogonal, meaning each PC is uncorrelated. In doing so, the PCs summarize correlated variables in a data set while utilizing less than *p* eigenvectors. The relationship between the variables which defines the linear combination of the PC, is determined by the loading coefficient of each variable.

The motivation behind using PCA is two-fold: First, PCA is necessary because the complex pattern of correlation among the predictor variables would result in dubious regression coefficients and their associated standard errors if a multiple regression were performed (Jackson, 1991). Since the PCs are not correlated (are orthogonal), an accurate slope between the PCs and the response variable, SBR-patterning, can be obtained. Second, the linear combinations of traits, the trait loadings, can lend themselves to biological interpretation.

The PCA was conducted as follows: For each predictor trait, an experimental mean was calculated. Since missing values are not tolerated in PCA analysis, the missing data points for each trait were replaced by that trait mean. Although imputing the missing data points with the mean results in a less robust PCA, it guards against biasing the data toward exaggerated correlations. In other words, replacing missing trait values with the trait mean results in a dataset biased towards the null hypothesis of no relationship within the correlation matrix. After the missing data was imputed, it was normalized using the standard Z-score (Zar, 1999). This standardization results in a trait mean of zero and a standard deviation of 1. Without this step, the

initial PC will consist of the trait with the largest variance and the traits correlated with it, and the second PC with the trait with the second largest variance and the traits correlated with it, and so on. By calculating the z-score, all traits are equally weighted in the subsequent reduction of the data matrix into PCs. A singular value decomposition of the correlation matrix, excluding the SBR traits, was performed using the PRINCOMP command in SAS/STAT version 9.0 (SAS/STAT Inc., Cary, North Carolina). A three dimensional heatmap displaying variable loading of each PC was constructed using the *levelplot()* command in the Lattice package (Sarkar, 2008) in R (Ihaka and Gentleman, 1996). The "Broken stick" method was used to select PCs which effectively summarize the data (Jackson, 1991). The "Broken stick" method asks if the information content of each PC (eigenvalue) explains enough of the variation in the data set to be considered nonrandom. When dividing a line into *n* (n=23) spaces by *n-1* random points the expected size of the i^{th} largest space is $\frac{\sum_{j=0}^{n-i}\frac{1}{n-j}}{n}$. A PC is considered relevant if the observed eigenvalue for the ith PC is larger than the i^{th} largest space.

Principal component regression (PCReg) analyses: Regression analysis was performed in R (Ihaka and Gentleman, 1996) using the three PCs which surpassed the "Broken stick" threshold. To test for PCs which contribute little to the experiment-wise variation, yet are relevant to the modeling of SBR-patterning, simple, single factor regressions of each PC onto the SBR variables was conducted (Jolliffe, 1982; Jackson, 1991). A stepwise regression analysis using all the PCs was also conducted. The parameter selection rules were a p-value of 0.05 for entry into the model and a retention p-value of 0.01. ANOVA for the regression models were calculated using the *summary ()* command in R (Ihaka and Gentleman, 1996). Diagnostic plots of the regression models were constructed using the *plot(lm)* command where *lm* represents the regression model object name. Horizontal bar plots were created in Microsoft Excel to visualize the trait loadings for the PCs relevant to the interpretation of the regression models.

RESULTS

Correlation analysis: Significant correlations were observed between a majority of the predictor variables, in addition to the SBR variables (60.6% with p-values of less than 0.0001 (Figure 14). The only two traits not significantly correlated to at least one root trait were juvenile leaf number and transition leaf number. In cases where all three SBR traits were significantly associated with a developmental trait the direction of their relationship (sign) was the same. Adult leaf number, average internode length, and leaf width were not significantly correlated to SBR1, yet were correlated to totlSBR and NWSBR. SBR1 was significantly correlated to all four of the tassel related traits, while only tassel branch length was significantly correlated to NWSBR.

PCA results: Twenty-three predictor variables were used from which 23 PCs were calculated. Table 17 summarizes the characteristics of the PCs and provides the "Broken stick" test statistics for each. The first three PCs were identified as useful descriptors of the multivariate data. These PCs summarize 61% of the observed multivariate data (33.8%, 17.1% and 10.1% respectively).

Joliffe (1982) recommended performing a single factor regression of response variable onto the PCs to identify relevant predictors that may not explain a large amount of the data. Significance of the single factor regression of each PC onto the three root response variables are summarized in Table 18. In summary, PCs one (PC1), two (PC2), three (PC3), four (PC4) and nine (PC) were found to be significant predictors of at least one root response variable at the $P<0.05$ level (Table 18). Statistical significance for PC4 and PC9 indicates that although they

may not be essential for summarizing the multivariate nature of the data they may be useful in modeling SBR-patterning.

Principal Component Regressions

NWSBR: The initial principal component regression utilized only the first three PCs, which exceeded the broken stick statistic. The initial regression model for NWSBR was highly significant (Table 19). The adjusted model R^2 was 0.3982 (Table 19). All three of the PCs were significantly associated with NWSBR at the $P<0.01$ level (Table 20). PC1 and PC3 had positive regression coefficients, while PC2 possessed a negative regression coefficient (Table 20).

The full regression model for NWSBR included PC1, PC2, PC3, PC4, and PC9 (Table 20). The direction and magnitude of the regression coefficients for the first three PCs were unchanged in the full model (Table 20). The regression coefficients for PC4 and PC9 were positive (Table 20). These two predictor variables contributed nearly 9% of the model adjusted R^2 (Table 20), increasing it to 0.47 (Table 19). The model p-value was also slightly more significant (Table 19). An F-test comparing the initial and the full model indicates that the full model is statistically better at predicting NWSBR at the 0.01 level (Faraway, 2005; Sen and Srivastava, 1990).

totlSBR: The initial regression model for totlSBR including the first three PCs as predictors yielded similar results as the NWSBR model. The adjusted R^2 was 0.4571 and the model p-value was 9.61E-14 (Table 21). PC1 and PC3 both had significant, positive regression coefficients while PC2 was significant and had a negative regression coefficient (Table 22). The full model once again retained all the predictor variables from the initial model. PC1, PC2, PC3, PC4, and PC9 were significant predictors of totlSBR in the full model (Table 22). The direction

and magnitude of the first three principle components were unchanged, and the two added predictors both had positive regression coefficients (Table 22). The F-test comparing the two models indicated that the explanatory power were not significantly different (Faraway, 2005; Sen and Svrivastava, 1990).

SBR1: An R^2 of 0.3982 was obtained for the SBR1 initial model (Table 23). PCs one and three were significant at the $P<0.01$ level in the initial regression model for SBR1 (Table 24). Similar to the previous models, PC1 and PC3 had positive regression coefficients (Table 24). To the contrary, PC2 was not significant and was left out of the full model (as was PC9) however PC4 was included in the full model (Table 24). Both models were highly significant with the subsequent "full" model explaining 6% more of the SBR1 performance than the initial model (Table 23).

DISCUSSION

Interpretation of PCs: The transformation of predictor variables into PCs has two advantages. First, the PCs are orthogonal (not correlated) and as a result will have unbiased regression coefficients. Second, the PCs represent nonrandom trait correlation which may allow them to be biologically interpreted. It is our aim to propose biological context to the PCs by examining the linear combinations from which they are constructed.

The linear combinations of predictor variables that each PC describes should be interpreted in terms of pleiotropy, where a single gene influences many phenotypes. Pleiotropy is most recognizable in mutant strains where a single polymorphism results in large coordinated organismal variation in many phenotypic traits. The pleiotropic impact of the mutations can be thought of as a phenotypic fingerprint that is unique to the pathways in which the mutated gene participates. We can extend the aforementioned phenotypic fingerprinting of a mutated gene to

include the pleiotropic effects of that gene in the context of natural diversity. Using the natural diversity approach, mutant alleles are replaced with functional structural variants and the subtle coordinated phenotypes described by the PCs substitute for the severe pleiotropic affects of mutant alleles. By aligning the linear combinations of the PCs with the phenotypic fingerprints of single gene mutations we can identify the genetic origins of each PC and predict the genes (or role of the gene) and its associated pathway in SBR-patterning.

PC1: PC1 accounted for 33.8% of the variability in the predictor variable data set (Table 17). Examining the trait loadings in Figures 15 and 16 indicates that all the traits, except average internode length, the average internode length from tassel to the ear, juvenile leaf, and transition leaf number have positive loadings in PC1. PC1 is positively associated with traits that control vegetative growth as indicated by positive loadings for plant height, leaf area, and soil node diameter. Days to pollen shed and days to silk are also positively correlated to PC1, indicating its role in determining flowering time. Regulation of phytomer number also appears to be related to PC1 as indicated by positive loadings of nodes to tassel, total leaf number, and tassel branch number. Consulting previous morphological studies on maize varieties by Brown and Anderson (1947, 1948), a relationship between geographic origins of maize inbred lines and PC1 was identified. In their survey of northern flint and southern dent varieties, Brown and Anderson observed that southern dent varieties were taller, had a greater number of nodes, shorter internodes above the ear, and were later maturing than their northern flint counterparts. The combination of these phenotypes accurately describes the linear combination of traits contained in PC1 (Figure 16).

Different geographic origins can lead to systematic differences in allele frequencies emerging from shared coancestry, referred to as population structure. This phenomenon has been observed in maize (Yan et al., 2009; Liu et al., 2003). In both of these studies, germplasm

collections were genotyped and a program called STRUCTURE was used to evaluate population structure (Pritchard et al., 2000). STRUCTURE uses a Bayesian, model-based clustering method to assign individuals to a population. In both cases maize inbred lines formed (among others) a distinct tropical subpopulation based on allele sharing (Yan et al., 2009; Liu et al., 2003). The inbred lines used in the current study are a subset of the panel analyzed by Liu et al., (2003) and have subpopulation membership values determined by STRUCTURE. Utilizing the subpopulation membership of the 25 inbred lines, we were able to explore the link between geographic origin, population structure, and PC1.

To further examine the relationship between PC1 and population structure, a plot relating the percentage of TS contained within each inbred line as determined by STRUCTURE (Liu et al., 2003) was made against PC1 (Figure 17). The plot indicates a positive correlation between percent TS and PC1 (n=48). By substituting the trait loadings for PC1 this translates to increases in TS genetic material resulting in increases in vegetative growth, phytomer number, and increased time to flowering. A single factor ANOVA indicates the subpopulation membership as determined by Liu et al., (2003), accounts for nearly 41% of the variation in PC1 (p-value=4.89E-11).

The data suggests that nonrandom allele frequency patterns at loci controlling adaptation and flowering time are nested within these subpopulations. *D8*, a locus which affects flowering time (Thornsberry et al., 2001; Andersen et al., 2005), exhibits diversifying selection at a 6 base pair InDel polymorphism, with the deletion allele present in 80% of northern flint lines and present in less than 5% of tropical lines (Camus-Kulandaivelu et al., 2006). The locus *Vgt1* controls both nodes to tassel and flowering time (days to pollen shed) in maize (Salvi et al., 2002). Analysis of the allele frequencies at the *Vgt1* locus suggests it has been subjected to selection to improve altalatitudinal performance (Ducrocq et al., 2008). An adaptive genetic

complex, represented by loci such as *Vgt1* and *D8* (which are both confounded in population structure), control vegetative growth, and time to flowering. The data indicate PC1 represents the phenotypic manifestation of the pleiotropic effects of this adaptive genetic complex on multiple morphological traits.

PC2: PC2 accounted for 17% of the variance in the predictor data set (Table 17). In summary, PC2 had positive trait loadings for average internode length, the average internode length from the soil to the ear, average internode length from the tassel to the ear, total tassel length and plant height. The flowering time traits, days to pollen shed and days to silk, along with ear node diameter, and soil node diameter had negative loadings for PC2 (Figures 15 and 18). This trait network can be explained by a light-induced hormone signaling pathway underlying the SAR. In *Arabidopsis* the SAR affects internode elongation and plant height through phytochrome inactivation and subsequent GA response (Peng and Harberd, 1997). Sheehan et al. (2007) recorded the phenotypic effects of loss-of-function *phytochrome B, phyB* alleles in maize. Their study revealed the role PHYB activity played in controlling flowering time, stem diameter, plant height, tassel stem length and average internode length. PHYB inactivation resulted in reduced flowering time, stem diameter, ear height, plant height, and increases in tassel stem length and average internode length. The loadings of these traits in PC2 are in general agreement with PHYB inactivity (resulting in SAR) with the exceptions of plant height and ear height. Thus PC2 might represent the coordinated phenotypic affects of the SAR. Reduction in flowering time and stem diameter relative to increases in internode lengths are experienced in maize *phyB* double mutants. As PC2 values increase, flowering time and stem diameter are reduced and average internode length increases (Figure 18).

PC3: PC3 represents nearly 11% of the variation in the predictor variable data set (Table 17). Positive loadings for ear node diameter, soil node diameter, and average internodes to the ear

suggest that cell number and size play a role in explaining this component (Figure 19). However, negative loadings for leaf area, leaf length, leaf width, and plant height suggest otherwise. One conclusion is that the underlying mechanism controlling cell expansion is tissue specific. This would explain the disparity between leaf cell expansion traits (leaf area, leaf length and leaf width) with radial expansion of the stem (ear node diameter, soil node diameter). Class III HD-ZIP (HD-ZIP III) family members play multiple roles in shoot development such as meristem initiation, establishment of organ polarity and vascular development. This gene family includes *PHABULOSA* (*PHB*), *PHAVOLUTA* (*PHV*), and *CORONA*/*INCURVATA4* (*CNA*/*ICU4*). Mutations in *ICU4* reduced the number of shoot vascular bundles and altered leaf shape making them more circular (Ochando et al., 2008). A mutant paralog of *ICU4*, *CAN* develops larger meristems and fewer leaves than its *wild-type* counterpart (Green et al., 2005). The activity of these HD-ZIP III genes mirror PC3, with their control of radial and vascular patterning in the shoot, their alterations in leaf shape, and regulation of leaf number. Thus PC3 may represent genes involved in radial and vascular patterning.

PC4: Ten percent of the variation in the predictor variable data set was explained by PC4 (Table 17). The largest trait loading is leaf width. Leaf area, and to a lesser extent leaf length are positively associated with PC4 (Figure 20). Other major loadings include a negative loading for adult leaf number and positive loadings for juvenile leaf number and transition leaf number (Figure 20). Together these traits comprise a phytomer identity PC. The heterochronic regulation of leaf identity has been well recorded in maize (Evans and Poethig, 1995, Moose and Sisco, 1994). Wu and Poethig (2006) and Willmann and Poethig (2005) also observed heterochronic changes in leaf geometry in *Arabidopsis*. In *Arabidopsis*, the juvenile leaves start out round and increasingly become longer and more oval shaped. This change in leaf geometry can be observed in PC4 through the increased loading on leaf width. An increase in PC4 indicates a longer expression of juvenile leaf traits, such as juvenile leaf wax, along with wider leaves.

PC9: PC9 represents 3% of the variation in the predictor variable data set (Table 17). The standout trait loading for this PC is tassel branch number (Figure 21). Tassel branch number is unique among the set of predictor variables in that it directly describes tassel branch formation (which requires meristem initiation). Conceptually PC9 may be involved in meristem initiation or regulation.

Interpretation of principal component regression analysis: Two models were examined for each of the three root traits, SBR1, NWSBR, and totlSBR. The initial models contained the three PCs identified by the Broken Stick method. Interpretations of the first three PCs are that they represent an adaptive genetic complex which regulates vegetative growth and flowering time (PC1), the genetic regulatory network controlling SAR (PC2), and a mechanism controlling radial stem growth and expansion (PC3). The full models incorporated other PCs which were identified through single factor regression analysis as associated with root development. Together these models along with their PCs will provide insight into the mechanisms influencing SBR development.

NWSBR regression models: The initial model for NWSBR found the first three PCs as significant. PC1 was highly significant with a positive regression coefficient. This indicates that as TS specific or related alleles increase (in the genetic background of an inbred line) the inbred line is more likely to possess a greater number of NWSBR. PC2 was representative of the SAR, was significant, and had a negative regression coefficient. This relationship predicts SAR-mediated inhibition of the formation of NWSBR. PC3 also exhibited a positive regression coefficient indicating that radial growth is associated with increases in NWSBR.

The full model for NWSBR included two additional terms, PC4 and PC9. These two components describe phase change and tassel meristem initiation (tassel branch number) related traits respectively. The positive relationship between NWSBR and juvenile leaf traits is well

documented in maize (Evans and Poethig, 1995; Moose and Sisco, 1994). These previous studies linked prolonged expression of juvenile traits (leaf identity and NWSBR) with GA and *miR156* activity (Poethig, Personal communication; Zhang et al., 2009). Tassel branch number, the singular trait represented by PC9, has a positive regression coefficient.

totlSBR regression models: The initial model and full model include the same significant factors as the initial and full models for NWSBR. The regression coefficients are also of the same direction (negative or positive) as the models for NWSBR and their magnitudes are larger due to the inherent differences in trait values. This indicates that totlSBR is altered mainly through the same mechanisms that determine NWSBR as is evident from their equivalent regression models and their highly significant and positive correlations (Figure 14).

SBR1 regression models: The initial model for SBR1 had two significant factors PC1 and PC3. PC1 represents the percent of TS related or associated alleles contained in the inbred line. The positive regression coefficient for this term indicates that as the number of TS alleles increase in a genetic background, SBR1 increases along with other vegetative growth traits. PC3, representing radial stem growth, was also significant. A positive regression coefficient was identified for PC3, describing the relationship between radial stem growth and the potential for root meristem initiation. PC2 describing SAR was not significant in either model for SBR1. A lack of significance for PC2 suggests that the SAR plays little if any role in determining SBR1. Perhaps the SAR effect on root patterning may occur after the SBR1 meristem initiation and growth have already occurred. The full model for SBR1 includes PC4 which describes leaf geometry and vegetative identity. Increases in PC4 translate into longer expression of juvenile leaf wax, wider leaves, and greater SBR1.

A systems approach to identifying networks controlling SBR-patterning: The aim of this study was to link SBR-patterning to developmental networks represented by a series of predictor

traits. To simultaneously relate correlated predictor variables and their corresponding root response values, a variable reduction procedure was implemented. PCA transformed correlated predictor variables into non-correlated linear combinations which then served as the new predictor variables. These components were then assessed as predictor variables and were subsequently designated as representatives of developmental pathways. Mutants known to affect the developmental networks described by the PCs are potential candidate genes for controlling SBR-patterning.

PC1 had the largest explanatory value among the PCs. It represents an adaptive genetic complex controlling vegetative growth, had positive loadings for most traits, and a link to population structur, (most notably percent TS background). Genes related to vegetative growth represent plausible candidates for controlling SBR-patterning. Considering their relationship to population structure, *Vgt1* and the 6 bp indel of *D8* represent potential loci controlling SBR-patterning through the regulation of vegetative growth. Other potential candidate genes for this pathway are *indeterminate1* (*id1*) (Colasanti et al., 1998) and *delayedflowering1* (*dfl1*) (Muszynski, 2006). The *id1* gene encodes a nuclear localized zinc-finger protein that controls vegetative growth (Wong and Colasanti, 2007). Loss-of-function *id1* has increased node number and number of days to flowering. Expression of *id1* is limited to immature leaves and appears not to be influenced by light or sink-source transitions, suggesting it is involved in the nonautonomous flowering pathway (Wong and Colasanti, 2007). *dfl1* encodes a putative leucine-zipper transcription factor required to transition from adult-vegetative phase to the reproductive phase. Loss-of-function mutations also produce a greater number of nodes and are delayed in flowering time. The *dfl1* mutant phenotypes, however, are less severe suggesting that *id1* act supstream of *dfl1* (Muszynski et al., 2006).

PC2 represents a genetic network of genes which control the SAR. Constitutive SAR in maize, originating from inactive PHYB, results in increased average internode length, reductions in flowering time, and smaller stem diameter (Sheehan et al., 2007). These coordinated phenotypic effects are similar to the pattern of trait loadings in PC2. A survey of genes involved in SAR may lead to genes influencing SBR-patterning. These genes include but are not limited to the phytochrome family of genes, and *elongated mesocotyl1* (*eml1*). *elm1* is a phytochrome-deficient mutant of maize (Sawers et al., 2002). A mutation in *elm1,* affecting the splicing of the phytochrome 3*E*-phytochromobilin (PΦB) synthase gene Zm*Hy2,* results in decreased production of functional PΦB-an essential component of for spectrally active phytochromes (Sawers et al., 2004). The distinguishing phenotypes of *elm1* are reduced flowering time, increased plant height and internode length, and frequent lodging (Sawers et al., 2002). The coordinated phenotypes of *elm1* make it an attractive candidate for underlying PC2.

PC3 represents the genes involved in vascular patterning. Studies in *Arabidopsis* have begun to elucidate the genetic regulation of radial patterning (Green et al., 2005; Ochando et al., 2008). HD-ZIP III genes regulate vascular development, stem cell specification, and organogenesis. The activity of this class of genes in the roots of *Arabidopsis* is determined by *SHORT ROOT* (*SHR*) and *SCARECROW* (*SCR*), two well known regulators of shoot and root development (Carlsbecker, 2010). Activity of these transcription factors results in the expression of *miRNA165a (miR165a)* and *miRNA166b (miR166b),* which in turn determines the accumulation of HD-ZIP III and hence cylindrical vascular organization (Carlsbecker, 2010). SBRs form opposite the collateral vascular bundles within the vascular cylinder (Martin and Harris, 1976) hence alterations in cell number, type, and patterning (which influence vascular bundle number and organization) may determine the radial organization of SBRs. *SCR* expression was observed in crown roots (SBRs) in maize (Lim et al., 2000) suggesting a conservation of function in maize SBRs. To validate the role of HD-ZIP III activity in SBR-patterning,

examination of SBR phenotypes of *Rolled leaf1 (Rld1)* should be conducted. The mutant allele *Rld1* encodes a *miR166*-insensitive HD-ZIP III (Jaurez et al., 2004). Testing the effects of constitutive HD-ZIP III activity should clarify the effect of radial patterning on SBR-patterning.

The well characterized heterochronic regulation of root patterning is displayed in PC4. Genes which function in this pathway are *epc1* (Vega et al., 2002), *Cg1* (Chuck et al., 2007), *Tp1*, and *Tp2* (Poethig, 1988). The phenotypes of these mutants consist of altered juvenile leaf number, cell crenulations, and NWSBR. The origin of these phenotypes is the altered expression of *miR156*. *Cg1, Tp1*, and *Tp2* over-express *miR156* while the mutant *epc1* exhibits reduce accumulation of *miR156*. The statistical association of PC4 to SBR1 and totlSBR is further evidence that the juvenile-to-adult phase transition influences global root patterning-not just NWSBR. A related finding is the QTL for SBR1 and SBR2 at the *Tp2* locus described in the previous chapter. The positive regression coefficient between all SBR traits and PC4 suggests that an underlying mechanism which controls leaf identity also functions to determine SBR-patterning. Examination of SBR-patterning in additional heterochronic mutants that affect leaf identity may lead to discovery of their root-specific roles.

PC9 had one major trait loading for tassel branch number. Specifically, tassel branch number had a negative loading in PC9, suggesting a negative relationship between NWSBR and tassel branch number. This is distinctly different from the simple correlation analysis where the relationship between the two traits is non-significant (Figure 14). This could be the result of adjusting for the first four PCs, leading to identification of a mechanism independent of their effects. The best known pathway relating to tassel development is the *ramosa* pathway (Vollbrecht et al., 2005). Tassel development is controlled through the activity of *ramosa1* (*ra1*) and *ramosa2* (*ra2*). The transcription factor *ra1* is regulated by *ra2* and shapes tassel architecture by controlling cell fate. Another gene, *tasselseed4* (*ts4*), a *miR172* family member, determines

tassel architecture by targeting the APETELA floral transcription factor *indeterminate spikelet1* (*ids1*)/*Tasselseed6* (*Ts6*). Interestingly, QTL for both SBR-patterning and tassel architecture (Upadyayula et al., 2006b) map near *ts4* and *Ts6* in the intermated B73 x Mo17 mapping population, suggesting that polymorphisms in these genes have pleiotropic affects. It is possible that the *ramosa* genes and *ts4-Ts6* pathway could also alter root development by dictating cell fate.

Caveats and considerations for candidate genes: The phenomic approach to identify candidate genes that control SBR-patterning is useful for quantitative trait dissection but there are limitations. One caveat is that the nature of the analysis targets genes with pleiotropic effects. The genetic basis of pleiotropy takes two forms. First, physically linked polymorphisms may exert independent effects on multiple traits resulting in significant trait correlations in our analysis. This form of pleiotropy can be addressed through the selection of appropriate haplotypes or the generation of new haplotypes through conventional breeding provided the polymorphisms are spaced far enough apart. The second, more problematic form of pleiotropy is where a single polymorphism results in the correlated relationship between the traits. This pleiotropy is especially problematic for plant breeders, because the effect of selection on a locus to improve a trait may have a negative impact on other agronomically important traits. For example, selection at the *Tp2* locus may increase SBR initiation and have negative impacts on flowering time or harvest index by extending juvenile-vegetative growth. To address this situation, a fundamental property of genetic network evolution can be exploited.

The structural evolution of a genome can be described in terms of whole genome and segmental duplication events, followed by condensation - the selective elimination of genetic material. The functional consequence of these duplication events is the sub-functionalization or neo-functionalization of duplicate genes (Kliebenstein, 2008). Sub-functionalization refers to

mutation resulting in altered spatial and or temporal activity of a gene, while neo-functionalization refers to mutation leading to novel activity (separate from the ancestral gene function). Gene duplicates of pleiotropic loci which have undergone neo- and sub-functionalization provide potential targets to enhance an individual trait while maintaining the performance of another. This approach has been successfully used to find genes via sequence homology and to locate QTL which uniquely influence the structural outcome of glucosinolate production. Sønderby et al. (2007) first identified *MYB28* as a locus controlling aliphatic glucosinolate accumulation in *Arabidopsis*. Using sequence for all the MYB transcription factors from *Arabidopsis*, rice (*Oryza sativa* L.) and poplar (*Populus balsamifera* L. ssp. trichocarpa), a phylogenetic tree identified 2 Arabidopsis genes *MYB29* and *MYB7,* with similarity to *MYB28.* Joint transposon-tagging and transgenic overexpression of *MYB28*, *MYB29,* and *MYB76* resulted in glucosinolate profiles unique to each gene. This study provides a framework for a systems approach to manipulate quantitative phenotypes.

This approach can be extended to our data by finding genes with sequence homology to loci with pleiotropic effects on SBR-patterning and correlated predictor traits. For example PC9 was associated with tassel branch number. The ramosa pathway was noted as a network that potentially shapes SBR variation. Means comparison between *ra1* and *wild-type* counterparts revealed reductions in SBR initiation in the mutants. This suggests that *ra1* activity simultaneously suppresses tassel branching and promotes SBR initiation. The PCReg analysis associated increases in PC9 with both reductions in tassel branch number and increases in totlSBR and NWSBR, suggesting *ra1* as a genetic component underlying the PC9 network. *ra2,* a gene with a lateral organ boundary (LOB) protein domain (Bortiri et al., 2006), controls tassel branch number by regulating *ra1*. Querying the maize non-redundant protein database at Genbank with the RA2 protein located the SBR related genes *rtcs* and *rootless concerning crown and seminal roots-like* (*rtcl*). The *rtcs* and *rtcl* genes are expressed in newly initiated seminal

and crown roots (Tamarino et al., 2007). Mutations in the *rtcs* gene result in the absence of any seminal and crown roots (Hetz et al., 2002). Synteny with rice suggests that *rtcs* is a homologue of *adventitious rootless1 (arl1)*, also a LOB gene, that mediates SBR formation (Liu et al., 2005). Five SBR QTL map near *rtcs* (bins 1.01 and 1.02) in the IBM mapping population (Chapter 2, Figure1), and one in the Lo964 x Lo1016 population (Tuberosa et al., 2002). *rtcl* shares 44% nucleotide identity to the *rtcs* gene and 72% protein identity within the LOB domain (Taramino et al., 2007). Two SBR QTL in the IBM (Chapter 2 Figure 1), and two in the Lo964 x Lo1016 population map near *rtcl* on chromosome 9 (Tuberosa et al., 2002). By combining the network identification from the principal component regression analysis with the systems approach from Sønderby et al. (2007) we were able to find positional candidates which may influence SBR-patterning.

Previous system approaches to understanding quantitative variation have primarily focused on connecting changes in DNA structure to differential gene expression, protein accumulation or metabolite production. Here we examined variation on an organismal level by simultaneously quantifying the effect of phenotypic variation for twenty-six traits in a diverse set of maize inbred lines. PCA analysis was conducted on 23 predictor traits to identify linear combinations (PCs) of traits summarizing the covariation in the trait correlation matrix. PCs were then linked to SBR-patterning using multiple regression analysis. The linear combination of predictor traits for significant PCs provided unique phenotypic signatures used to identify pathways linked together through the pleiotropic action of regulator genes. Both pathways previously associated with SBR development and novel networks were identified. The well established relationship between adult (PC1) and juvenile (PC4) vegetative pathways were linked to SBR-patterning, supporting the utility of the systems approach. Novel pathways were proposed such as light-signaling (PC2), vascular development (PC3), and cell determinacy (PC9). Further evidence for the involvement of cell fate (PC9) was provided by the co-localization of tassel

branching QTL and mutants. Structural information from the *ramosa2* protein was used to predict potential targets exclusively involved in SBR-patterning. Further validation of candidate genes will require generating a full phenotypic fingerprint of mutant strains consisting of the 26 traits used in the principal component regression analysis. By aligning the PCs with the phenotypic fingerprints of the mutants we will further relate pleiotropic affects of mutant alleles with coordinated phenotypes which result from an array of naturally-occurring allelic variation. This will simultaneously provide insight into the genetic control of SBR-patterning and begin the investigation into major regulators of variation in the maize phenome.

Despite our effort to identify and link developmental pathways to SBR-patterning, multiple regression analysis only explained roughly 35 to 50 % of the variation in root response variables. This suggested that the regression model is missing some important variables concerning SBR-patterning. Our goal was to focus on organismal level phenotypic variation. With respect to organismal variation we may increase our power to explain SBR-patterning in two ways. First, some organismal variation was observed at only one time point. Organismal variation catalogued temporally could provide valuable clues into the activity of the identified pathways and how they interact. Second, to enhance our understanding of SBR-patterning, more phenotypes could be evaluated while reducing the number of redundant phenotypes. This may more efficiently link additional pathways to SBR-patterning.

Finally, strict adherence to use of organismal level variation alone may itself be a disadvantage. Fluctuations in transcript level, protein accumulation, and metabolite production may contribute to SBR-patterning. These fluctuations may not be readily detectible or interpretable from our PCs. While previous systems level investigations have effectively recorded the genetic origins of this molecular variation, in many cases they fall short of translating their findings to the phenotypic level. One laudable example of research linking structural genomic,

metabolomic and phenotypic variation connected structural variation in flavones synthesis to resistance to corn earworm in maize (Lee et al., 1998; McMullen et al., 1998). Following the example of these studies, integrating molecular phenotypes may enhance not only our understanding of SBR-patterning but help us shape their performance through selection.

REFERENCES

ANDERSEN, J. R., T. SCHRAG, A. E. MELCHINGER, I. ZEIN, and T. LÜBBERSTEDT, 2005 Validation of *Dwarf8* polymorphisms associated with flowering time in elite European inbred lines of maize (*Zea mays* L.). Theor. Appl. Genet. **111(2):** 206-17.

BORTIRI E., G. CHUCK, E. VOLLBRECHT, T. ROCHEFORD, R. MARTIENSSEN, and S. HAKE, 2006 *ramosa2* encodes a LATERAL ORGAN BOUNDARY domain protein that determines the fate of stem cells in branch meristems of maize. Plant Cell **18(3):** 574-85.

BROWN, W. L. and E. ANDERSON, 1947 The Northern Flint Corns. Ann. Missouri Bot. Garden **34(1):** 1-29.

BROWN, W. L. and E. ANDERSON, 1948 The Southern Dent Corns. Ann. Missouri Bot. Garden **35(3):** 255-268.

CAMUS-KULANDAIVELU, L., J. B. VEYRIERAS , D. MADUR , V. COMBES , M. FOURMANN, S. BARRAUD , P. DUBREUIL, B. GOUESNARD, D. MANICACCI, and A. CHARCOSSET, 2006 Maize adaptation to temperate climate: relationship between population structure and polymorphism in the *Dwarf8* gene. Genetics **172(4):** 2449-2463.

CARLSBECKER, A., J. Y. LEE, C. J. ROBERTS, J. DETTMER, S. LEHESRANTA, J. ZHOU, O. LINDGREN, M. A. MORENO-RISUENO, A. VATÉN, S. THITAMADEE, A. CAMPILHO, J. SEBASTIAN, J. L. BOWMAN, Y. HELARIUTTA, and P. N. BENFEY, 2010 Cell signaling by *microRNA165/6* directs gene dose-dependent root cell fate. Nature April 21 Epub ahead of print.

CHUCK, G., A. M. CIGAN, K. SAETEURN, and S. HAKE, 2007 The heterochronic maize mutant *Corngrass1* results from overexpression of a tandem microRNA. Nat. Genet. **39(4):** 544-549.

COLASANTI, J., Z. YUAN, and V. SUNDARESAN, 1998 The indeterminate gene encodes a zinc finger protein and regulates a leaf-generated signal required for the transition to flowering in maize. Cell **93(4):** 593-603.

DUCROCQ, S., D. MADUR, J. B. VEYRIERAS, L. CAMUS-KULANDAIVELU, M. KLOIBER-MAITZ, T. PRESTERL, M. OUZUNOVA, D. MANICACCI, and A. CHARCOSSET, 2008 Key impact of *Vgt1* on flowering time adaptation in maize: evidence from association mapping and ecogeographical information. Genetics **178(4):** 2433-2437.

EVANS, M. M. and R. S. POETHIG, 1995 Gibberellins promote vegetative phase change and reproductive maturity in maize. Plant Physiol. **108**: 475-487.

FARAWAY, J. J., 2005 *Linear Models with R.* Chapman and Hall/CRC, Boca Raton, FL. 240p.

GREEN, K. A., M. J. PRIGGE, R. B. KATZMAN, and S. E. CLARK, 2005 *CORONA*, a member of the class III homeodomain leucine zipper gene family in Arabidopsis, regulates stem cell specification and organogenesis. Plant Cell **17(3):** 691-704.

HETZ, W., F. HOCHHOLDINGER, M. SCHWALL, and G. FEIX, 2002 Isolation and characterization of *rtcs*, a maize mutant deficient in the formation of nodal roots. Plant J. **10(5):** 845-857.

IHAKA, R. and R. GENTLEMAN, 1996 R: a language for data analysis and graphics. J. Comput. Graph. Stat. **5:** 299-314.

JACKSON, J. E., 1991 *A User's Guide to Principle Components*. Wiley and Sons, New York, NY. 592p.

JOLLIFFE, I. T, 1982 A note on the use of principle components in regression. Appl. Statist. **31:** 300-303.

JUAREZ, M. T., J. S. KUI, J. THOMAS, B. A. HELLER, and M. C. P. TIMMERMANS, 2004 microRNA-mediated repression of *rolled leaf1* specifies maize leaf polarity. Nature **428:** 84-88.

KITANO, H., 2002 Systems biology: a brief overview. Science **295:**1662-1664.

KLIEBENSTEIN, D. J., 2010 Systems biology uncovers the foundation of natural genetic diversity. Plant Physiol. **152(2):** 480-486.

KLIEBENSTEIN, D. J., 2008 A role for gene duplication and natural variation of gene expression in the evolution of metabolism. PLoS One **3(3):** e1838.

KLIEBENSTEIN, D. J., M. A. WEST, H. VAN LEEUWEN, O. LOUDET, R. W. DOERGE, and D. A. ST. CLAIR, 2006 Identification of QTLs controlling gene expression networks defined *a priori*. BMC Bioinformatics **7:** 308.

LEE, E. A, P. F. BYRNE, M. D. MCMULLEN, M. E. SNOOK, B. R. WISEMAN, N. W. WIDSTROM, and E. H. COE, 1998 Genetic mechanisms underlying apimaysin and maysin synthesis and corn earworm antibiosis in maize (*Zea mays* L.) Genetics **149(4):** 1997-2006.

LIM, J., Y. HELARIUTTA, C. D. SPECHT, J. JUNG, L. SIMS, W. B. BRUCE, S. DIEHN, and P. N. BENFEY, 2000 Molecular analysis of the *SCARECROW* gene in maize reveals a common basis for radial patterning in diverse meristems. Plant Cell **12:** 1307-1318.

LIU, H., S. WANG, X. YU, J. YU, X. HE, S. ZHANG, H. SHOU, and P. WU, 2005 ARL1, a LOB-domain protein required for adventitious root formation in rice. Plant J. **43(1):** 47-56.

LIU, K., M. GOODMAN, S. MUSE, J. S. SMITH, E. BUCKLER, and J. DOEBLEY, 2003 Genetic structure and diversity among maize inbred lines as inferred from DNA microsatellites. Genetics **165:** 2117-2128.

MARTIN, E.M. AND W.M. HARRIS, 1976 Adventitious root development from the coleoptilar node in *Zea mays* L. Amer. J. Bot. **63(6):** 890-897.

MCMULLEN, M.D., S. KRESOVICH, H. S. VILLEDA, P. BRADBURY, H. LI, Q. SUN, S. FLINT-GARCIA, J. THORNSBERRY, C. ACHARYA, C. BOTTOMS, P. BROWN, C. BROWNE, M. ELLER, K. GUILL, C. HARJES, D. KROON, N. LEPAK, S. E. MITCHELL, B. PETERSON, G. PRESSOIR, S. ROMERO, M. OROPEZA ROSAS, S. SALVO, H. YATES, M. HANSON, E. JONES, S. SMITH, J. C. GLAUBITZ, M. GOODMAN, D. WARE, J. B. HOLLAND, and E. S. BUCKLER, 2009 Genetic properties of the maize nested association mapping population. Science **325(5941):** 737-740.

MCMULLEN, M. D., P. F. BYRNE, M. E. SNOOK, B. R. WISEMAN, E. A. LEE, N. W. WIDSTROM, and E. H. COE, 1998 Quantitative trait loci and metabolic pathways. Proc. Nat. Acad. Sci. U. S. A. **95:** 1996-2000.

MOOSE, S. P. and P. H. SISCO, 1994 *Glossy15* controls the epidermal juvenile-to-adult phase transition in maize. Plant Cell **6(10):** 1343-1355.

MONTGOMERY, E. G., 1911 Correlation studies in corn. Neb. Agric. Exp. Stn. Annu. Rep. **24:** 108-159.

MUSZYNSKI, M. G., T. DAM, B. LI, D. M. SHIRBROUN, Z. HOU, E. BRUGGEMANN, R. ARCHIBALD, E. V. ANANIEV, and O. N. DANILEVSKAYA, 2006 *delayed flowering1* encodes a basic leucine zipper protein that mediates floral inductive signals at the shoot apex in maize. Plant Physiol. **142:** 1523-1536.

OCHANDO, I., S. GONZÁLEZ-REIG, J. J. RIPOLL, A. VERA, and A. MARTÍNEZ-LABORDA, 2008 Alteration of the shoot radial pattern in *Arabidopsis thaliana* by a gain-of-function allele of the class III HD-ZIP gene *INCURVATA4*. Int. J. Dev. Biol. **52:** 953-961.

PENG, J. and N. P. HARBERD, 1997 Gibberellin deficiency and response mutations suppress the stem elongation phenotype of phytochrome-deficient mutants of *Arabidopsis*. Plant Physiol. **113(4):** 1051-1058.

POETHIG, R. S., 1988 Heterochronic mutations affecting shoot development in maize. Genetics **119(4):** 959-973.

PRITCHARD, J. K., M. STEPHENS, and P. DONNELLY, 2000 Inference of population structure using multilocus genotype data. Genetics **155:** 945-959.

SALVI, S., R. TUBEROSA, E. CHIAPPARINO, M. MACCAFERRI, S. VEILLET, L. VAN BEUNINGEN, P. ISAAC, K. EDWARDS, and R. L. PHILLIPS, 2002 Toward positional cloning of *Vgt1*, a QTL controlling the transition from the vegetative to the reproductive phase in maize. Plant Mol. Biol. **48(5-6):** 601-613.

SARKAR, D., 2008 *Lattice: Multivariate Data Visualization with R.* Springer, New York, NY. 268p.

SAWERS, R. J., P. J. LINLEY, J. F. GUTIERREZ-MARCOS, T. DELLI-BOVI, P. R. FARMER, T. KOHCHI, M. J. TERRY, and T. P. BRUTNELL, 2004 The *Elm1* (Zm*Hy2*) gene of maize encodes a phytochromobilin synthase. Plant Physiol. **136(1):** 2771-2781.

SAWERS, R. J., P. J. LINLEY, P. R. FARMER, N. P. HANLEY, D. E. COSTICH, M. J. TERRY, and T. P. BRUTNELL, 2002 *elongated mesocotyl1*, a phytochrome-deficient mutant of maize. Plant Physiol. **130(1):** 155-163.

SEN, A. and M. SRIVASTAVA, 1990 *Regression Analysis: Theory, Methods, and Applications.* Springer, New York, NY. 347p.

SHEEHAN, M.J., L. M. KENNEDY, D. E. COSTICH, and T. P. BRUTNELL, 2007 Subfunctionalization of *PhyB1* and *PhyB2* in the control of seedling and mature plant traits in maize. Plant J. **49**: 338-353.

SHI, C., A. UZAROWSKA, M. OUZUNOVA, M. LANDBECK, G. WENZEL, and T. LÜBBERSTEDT, 2007 Identification of candidate genes associated with cell wall digestibility and eQTL (expression quantitative trait loci) analysis in a Flint x Flint maize recombinant inbred line population. BMC Genomics **8:** 22.

SØNDERBY, I. E., B. G. HANSEN, N. BJARNHOLT, C. TICCONI, B. A. HALKIER, and D. J. KLIEBENSTEIN, 2007 A systems biology approach identifies a R3R2 MYB gene subfamily with distinct and overlapping functions in regulation of aliphatic glucosinolates. PLoS One **12:** e1322.

STYLIANOU, I. M., J. P. AFFOURTIT, K. R. SHOCKLEY, R. Y. WILPAN, F. A. ABDI, S. BHARDWAJ, J. ROLLINS, G. A. CHURCHILL, and B. PAIGEN, 2008 Applying gene expression, proteomics and single-nucleotide polymorphism analysis for complex trait gene identification. Genetics **178:** 1795-1805.

TARAMINO, G., M. SAUER, J. L. STAUFFER, D. MULTANI, X. NIU, H. SAKAI, and F. HOCHHOLDINGER, 2007 The maize (*Zea* mays L.) *RTCS* gene encodes a LOB domain protein that is a key regulator of embryonic seminal and post-embryonic shoot-borne root initiation. Plant J. **50(4):** 649-659.

THORNSBERRY, J. M., M. M. GOODMANN, J. DOEBLEY, S. KRESOVICH, D. NIELSEN, and E. S. BUCKLER 4th, 2001 *Dwarf8* polymorphisms associate with variation in flowering time. Nat. Genet. **28**: 286-289.

TUBEROSA, R., S. SALVI, M. C. SANGUINETI, P. LANDI, M. MACCAFERRI, and S. CONTI, 2002 Mapping QTLs regulating morpho-physiological traits and yield: case studies, shortcomings, and perspectives in drought-stressed maize. Ann. Bot. **89**: 941-963.

UPADYAYULA, N., H. S. DA SILVA, M. O. BOHN, and T. R. ROCHEFORD, 2006a Genetic and QTL analysis of maize tassel and ear inflorescence architecture. Theor. Appl. Genet. **112(4):** 592-606.

UPADYAYULA, N., M. BOHN, and T. ROCHEFORD. 2006b Enhanced detection of inflorescence architecture QTL in the Intermated B73 x Mo17 (IBM) RIL population. Maize Genetics Conference Abstracts. **48:** T28.

VEGA, S. H., M. SAUER, J. A. ORKWISZEWSKI, and R. S. POETHIG, 2002 The early phase change gene in maize. Plant Cell **14(1):** 133-147.

VOLLBRECHT, E., P. S. SPRINGER, L. GOH, E. S. BUCKLER 4TH, and R. MARTIENSSEN, 2005 Architecture of floral branch systems in maize and related grasses. Nature **436(7054):** 1119-1126.

WENTZELL, A. M., H. C. ROWE, B. G. HANSEN, C. TICCONI, B. A. HALKIER, and D. J. KLIEBENSTEIN, 2007 Linking metabolic QTLs with network and *cis*-eQTLs controlling biosynthetic pathways. PLoS Genet. **3:** 1687-1701.

WILLMANN, M. R. and R. S. POETHIG, 2005 Time to grow up: the temporal role of small RNAs in plants. Curr. Opin. Plant Biol. **8(5):** 548-552.

WONG, A. Y. M. and J. COLOSANTI, 2007 Maize floral regulator protein *INDETERMINATE1* is localized to developing leaves and is not altered by light or sink/source transition. J. Exp. Bot. **58(3):** 403-414.

WU, G. and R. S. POETHIG, 2006 Temporal regulation of shoot development in *Arabidopsis thaliana* by *miR156* and its target *SPL3*. Development **133(18):** 3539-3547.

YAN, J., T. SHAH, M. L. WARBURTON, E. S. BUCKLER, M. D. MCMULLEN, and J. CROUCH, 2009 Genetic characterization and linkage disequilibrium estimation of a global maize collection using SNP markers. PLoS One **4(12):** e8451.

YU, J., J. B. HOLLAND, M. D. MCMULLEN, and E. S. BUCKLER, 2008 Genetic design and statistical power of nested association mapping in maize. Genetics **178(1):** 539-551.

ZAR, J., 1999 *Biostatistical Analysis* 4th Edition. Prentice Hall Inc., Upper Saddle River, N. J. 929p.

ZHANG, W., N. LAUTER, R. PULAM, and S. P. MOOSE, 2009 Molecular interactions among regulatory factors influencing shoot maturation in maize. Maize Genetics Conference Abstract **51:**P103.

TABLES

Table 16. Names of the traits measured for the multivariate trait analysis, their abbreviations, and descriptions.

Trait name	Abbreviations	Description
adult leaf number	aduLf	The number of fully adult leaves. Calculated as total leaf number minus juvenile leaf number minus transition leaf number.
average tassel branch length	BL	The average branch length from three randomly chosen tassel branches (branch lengths 1, 2 and 3) in mm (Upadyayula et al., 2006a).
average internode length to ear	AIear	The average internode length beneath the ear was calculated by taking the average ear height for a row and dividing it by the row average for number of nodes to ear (mm/node).
average internode length from the tassel to ear	AItsl	This value was calculated using row means. The formula was (tassel height minus ear height)/(nodes to tassel minus nodes to ear) in mm/node.
average internode	AI	This is calculated as the height to tassel divided by the number of nodes. These values were calculated using the row means for height to tassel and number of nodes (mm/node).
tassel branch number	BN	The number of primary tassel branches emerging from the branching zone (Upadyayula et al., 2006a).
central spike length of the tassel	L2	The length from the last secondary tassel branch to the tip of the primary tassel branch (in mm, Upadyayula et al., 2006a).
days to 50% pollen shed	DTP	The number of days after sowing when 50 percent of the plants of the row exhibit pollen shed on one third of the primary tassel branch.
days to 50% silk	DTS	The number of days after sowing when 50 percent of the plants of the row exhibit silks.
ear height	EarHt	The height, in mm, of the top most ear (ie. the ear furthest from the ground).
ear node diameter	END	The diameter of the node positioned above the top ear of the plant in mm using a caliper.
juvenile leaf number	juvLf	The number of completely juvenile leaves on a plant, where glossy wax is absent.
leaf area	Lfarea	Leaf area was calculated as length*width*0.75 as described by Montgomery (1911).
leaf length	Lfleng	The distance, in mm, from the tip of the leaf to the leaf sheath on the ear leaf.
leaf width	Lfwidth	The length in mm of the widest portion of the ear leaf.
SBR number, node1	SBR1	Number of SBRs at the first node above the soil line. This node can be distinguished from the node containing the crown roots by looking at the angle of root projection.
number of nodes to the ear	NTE	The number of nodes starting at the soil line to the topmost ear.
number of node to the tassel	NTT	The number of nodes starting at the soil line to the tassel node.
number of nodes with SBR	NWSBR	Number of nodes with SBRs defined as roots which have broken the epidermal cell layer.
plant height	PHt	Distance from the soil to the tip of top most point of the tassel.
soil node diameter	SND	The diameter of the node closest to the soil line, in mm, which is measurable (maybe obstructed by roots).
total number of SBR	totlSBR	The sum of the above ground SBRs on all nodes.
total leaf number	totLf	The total number of leaves on a plant.
transition leaf number	transLf	The number of leaves that simultaneously possesses pale juvenile leaf wax and glossy adult leaf wax.
total tassel length	L1	The length from the point of flag leaf emergence to the tip of the primary tassel branch in mm (Upadyayula et al., 2006).
tassel node diameter	TND	The diameter of the base of the tassel sample (near the point of flag leaf emergence).

Table 17. Descriptive statistics for the PCA.

PC	Eigenvalue[a]	Difference[b]	Proportion of Variance[c]	Cumulative Variance[d]	Broken Stick[e]
1	7.76599141	3.83598141	0.3377	0.3377	0.162360500
2	3.93001001	1.50095797	0.1709	0.5085	0.118882240
3	2.42905204	0.63605093	0.1056	0.6141	0.097143109
4	1.79300111	0.17904569	0.0780	0.6921	0.082650356
5	1.61395542	0.55026979	0.0702	0.7623	0.071780790
6	1.06368563	0.18543092	0.0462	0.8085	0.063085138
7	0.87825471	0.05596789	0.0382	0.8467	0.055838761
8	0.82228682	0.12307238	0.0358	0.8824	0.049627581
9	0.69921444	0.11321977	0.0304	0.9128	0.044192799
10	0.58599467	0.21954618	0.0255	0.9383	0.039361881
11	0.36644849	0.10068637	0.0159	0.9543	0.035014055
12	0.26576212	0.02453156	0.0116	0.9658	0.031061485
13	0.24123056	0.08081253	0.0105	0.9763	0.027438297
14	0.16041804	0.06713726	0.0070	0.9833	0.024093815
15	0.09328078	0.00775934	0.0041	0.9873	0.020988225
16	0.08552144	0.01798633	0.0037	0.9910	0.018089675
17	0.06753511	0.01798193	0.0029	0.9940	0.015372283
18	0.04955319	0.00864531	0.0022	0.9961	0.012814739
19	0.04090787	0.01677014	0.0018	0.9979	0.010399280
20	0.02413773	0.01421099	0.0010	0.9990	0.008110950
21	0.00992674	0.00202074	0.0004	0.9994	0.005937037
22	0.007906	0.00198032	0.0003	0.9997	0.003866644
23	0.00592569	NA	0.0003	1.0000	0.001890359

[a] Eigenvalue describes how many variables the PC "explains".
[b] Difference in eigenvalue between two neighboring principle components.
[c] Proportion of the variance in the multivariate predictor data set each PC explains
[d] Cumulative proportion of the variance is the sum of the variance of all preceding principal components.
[e] Broken stick test statistic. The proportion of the variance explained by the individual PC must exceed this value to be selected as "relevant".

Table 18. Results of the single factor regression of PCs onto SBR traits.

PC[a]	SBR1	NWSBR	totlSBR
1	***	***	***
2	NS	*	*
3	***	*	**
4	*	*	0.0811
5	NS	NS	NS
6	NS	NS	NS
7	NS	NS	NS
8	NS	NS	NS
9	NS	*	NS
10	NS	NS	NS
11	NS	NS	NS
12	NS	NS	NS
13	NS	NS	NS
14	NS	NS	NS
15	NS	NS	NS
16	NS	NS	NS
17	NS	NS	NS
18	NS	NS	NS
19	NS	NS	NS
20	NS	NS	NS
21	NS	NS	NS
22	NS	NS	NS
23	NS	NS	NS

*, **, and *** indicate significance at the P<0.05, <0.01 and <0.001 levels.
NS indicated a non-significant P-value.

Table 19. ANOVA tables for regression models for NWSBR.

Source	DF	SS	MS	F-value	p-value	model R^2	Adjusted R^2
A. ANOVA of the initial regression model for NWSBR							
Model	3	7	2.0	22	3.05E-11	0.4152	0.3982
Error	95	10	0.1				
Total	98	17					
B. ANOVA of the full regression model for NWSBR							
Model	5	9	1.70	19	5.51E-13	0.5003	0.4754
Error	93	9	0.09				
Total	98	18					

Table 20. Regression models for NWSBR.

Variable	Slope	SE	Partial	Model	t-value	p-value
A. Initial regression model for NWSBR						
PC1	0.08	0.01	0.2937	0.2937	7	3.83E-10
PC2	-0.05	0.02	0.0622	0.3559	-3	0.001890
PC3	0.07	0.02	0.0593	0.4152	3	0.002570
B. Full regression model for NWSBR						
PC1	0.08	0.01	0.2937	0.2937	7	3.98E-11
PC2	-0.05	0.02	0.0622	0.3559	-3	0.000918
PC3	0.07	0.02	0.0593	0.4152	3	0.001300
PC9	0.10	0.04	0.0426	0.4578	3	0.005234
PC4	0.06	0.02	0.0425	0.5003	3	0.005872

Table 21. ANOVA tables for totlSBR regression models.

Source	DF	SS	MS	F-value	p-value	model R^2	Adjusted R^2
A. ANOVA of the initial regression model for totlSBR							
Model	3	207	69	31	9.61E-14	0.4977	0.4671
Error	95	209	2				
Total	98	416					
B. ANOVA of the full regression model for totlSBR							
Model	5	239	48	22	9.38E-15	0.5444	0.5201
Error	93	200	2				
Total	98	440					

Table 22. Regression models for totlSBR.

Variable	Slope	SE	Partial	Model	t-value	p-value
A. ANOVA of the initial regression model for totlSBR						
PC1	0.46	0.06	0.3714	0.3714	8	6.02E-13
PC2	-0.22	0.08	0.0858	0.4572	-3	0.004180
PC3	0.34	0.10	0.0404	0.4977	3	0.000810
A. ANOVA of the full regression model for totlSBR						
PC1	0.46	0.05	0.3724	0.3724	9	2.01E-13
PC2	-0.23	0.08	0.0644	0.4369	-3	0.003267
PC3	0.34	0.10	0.0463	0.4832	4	0.000585
PC4	0.29	0.11	0.0334	0.5166	3	0.010129
PC9	0.42	0.18	0.0278	0.5444	2	0.018680

Table 23. ANOVA tables for SBR1 regression models.

Source	DF	SS	MS	F-value	p-value	model R^2	Adjusted R^2
A. ANOVA of the initial regression model for SBR1							
Model	3	7	2.0	22	3.05E-11	0.4152	0.3982
Error	95	10	0.1				
Total	98	17					
B. ANOVA of the full regression model for SBR1							
Model	5	9	1.70	19	5.51E-13	0.5003	0.4754
Error	93	9	0.09				
Total	98	18					

Table 24. Regression models for SBR1.

Variable	Slope	SE	Partial	Model	t-value	p-value
A. Initial regression model for SBR1						
PC1	1.09	0.18	0.2609	0.2609	6.0	1.36E-08
PC2	1.28	0.32	0.0007	0.2616	0.3	NS
PC3	0.08	0.25	0.1079	0.3696	4.0	0.000109
B. Full regression model for SBR1						
PC1	1.1	0.17	0.2609	0.2609	6	3.860E-09
PC3	1.3	0.3	0.1079	0.3689	4	0.0000648
PC4	1.01	0.35	0.0505	0.4194	3	0.0049900

NS = not significant.

FIGURES

Figure 14. Correlogram rendering of the trait correlation matrix.

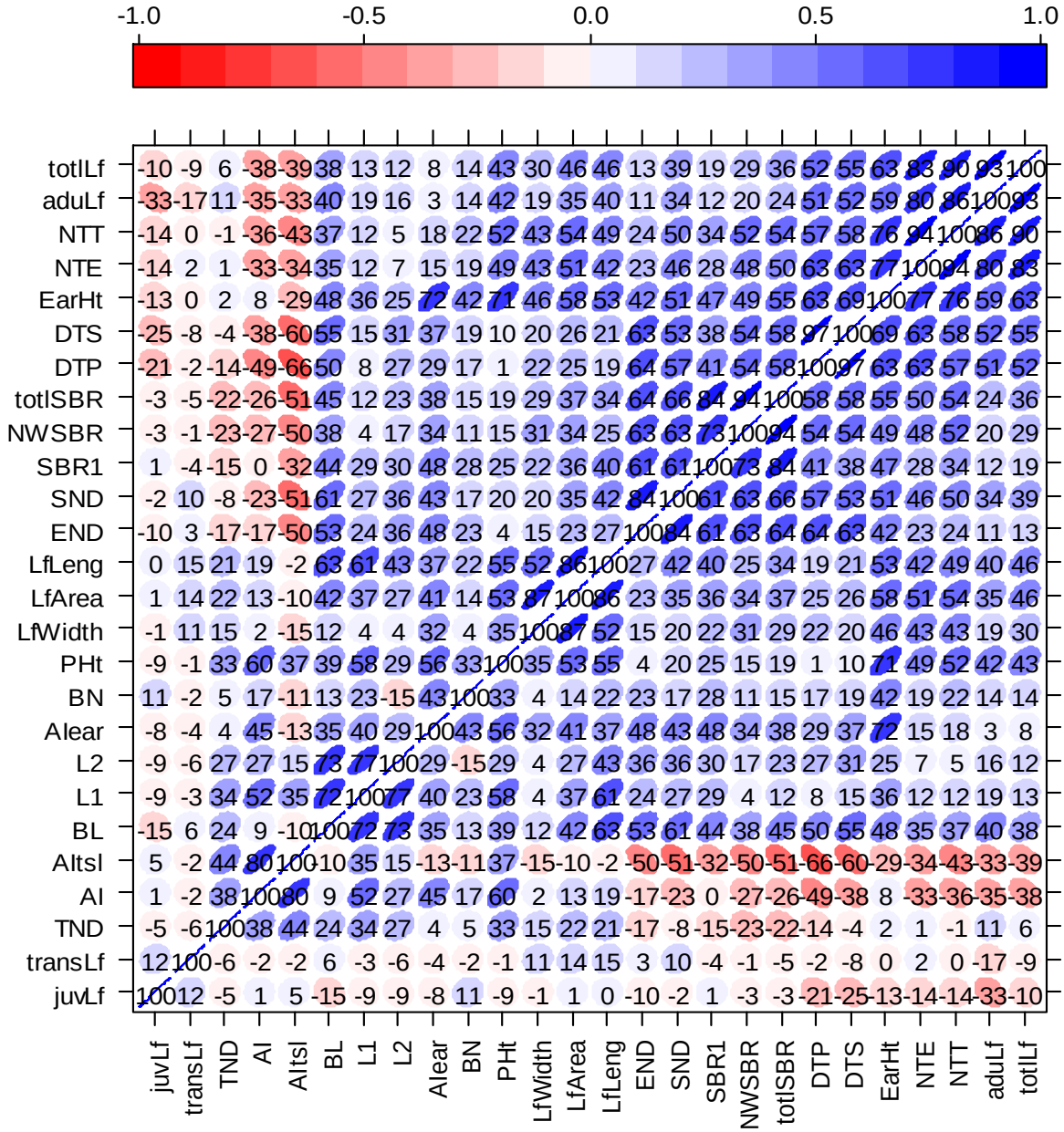

Heat colors indicate magnitude (dark to light, high to low) and direction (red to blue, negative to positive). The numeric labels indicate the correlation coefficient multiplied by 100.

Figure 15. Rendering of the trait loadings (contribution) for each of the 23 PCs.

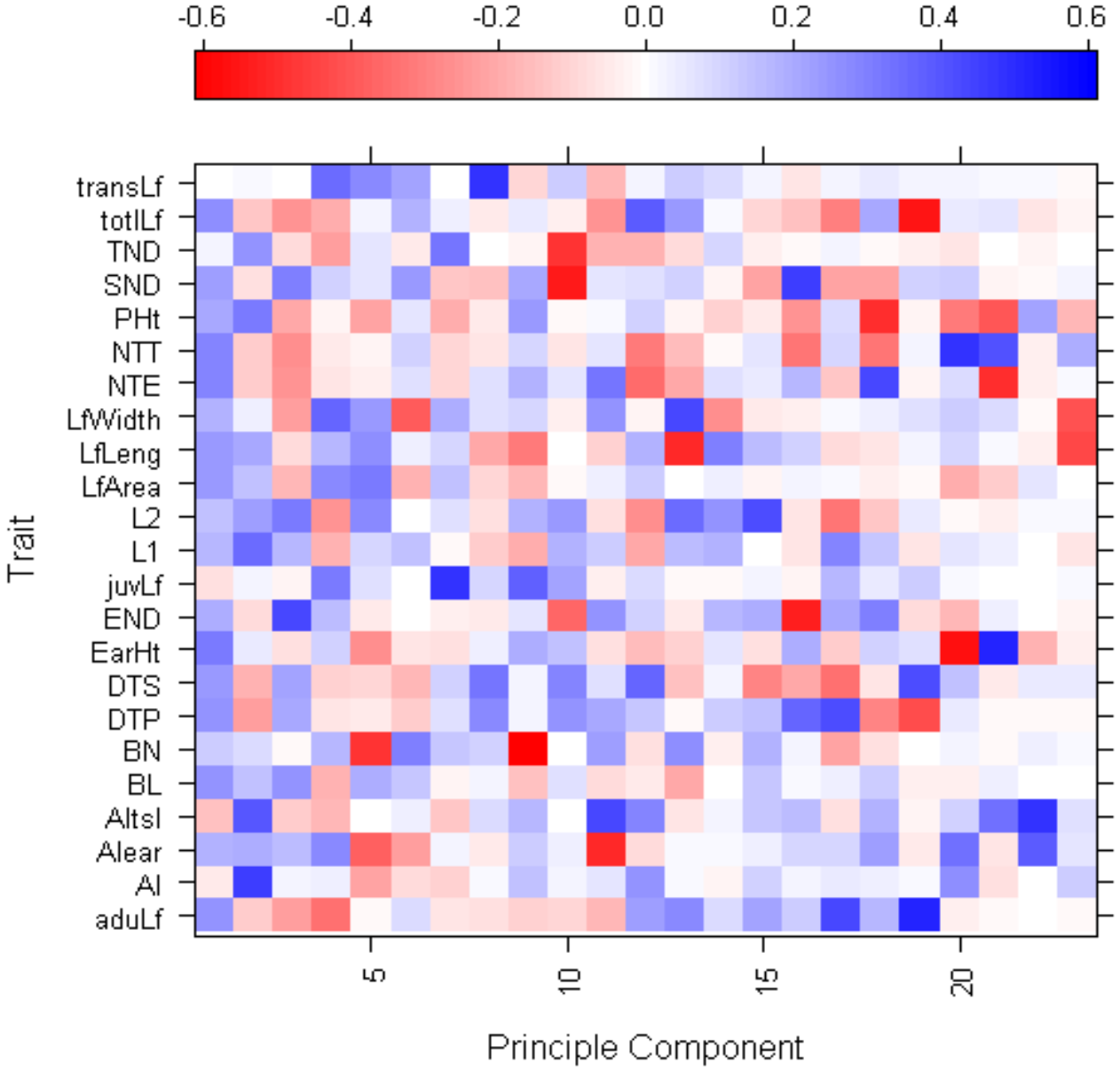

Figure 16. Horizontal bar plot of the traits loadings for Principal Component One

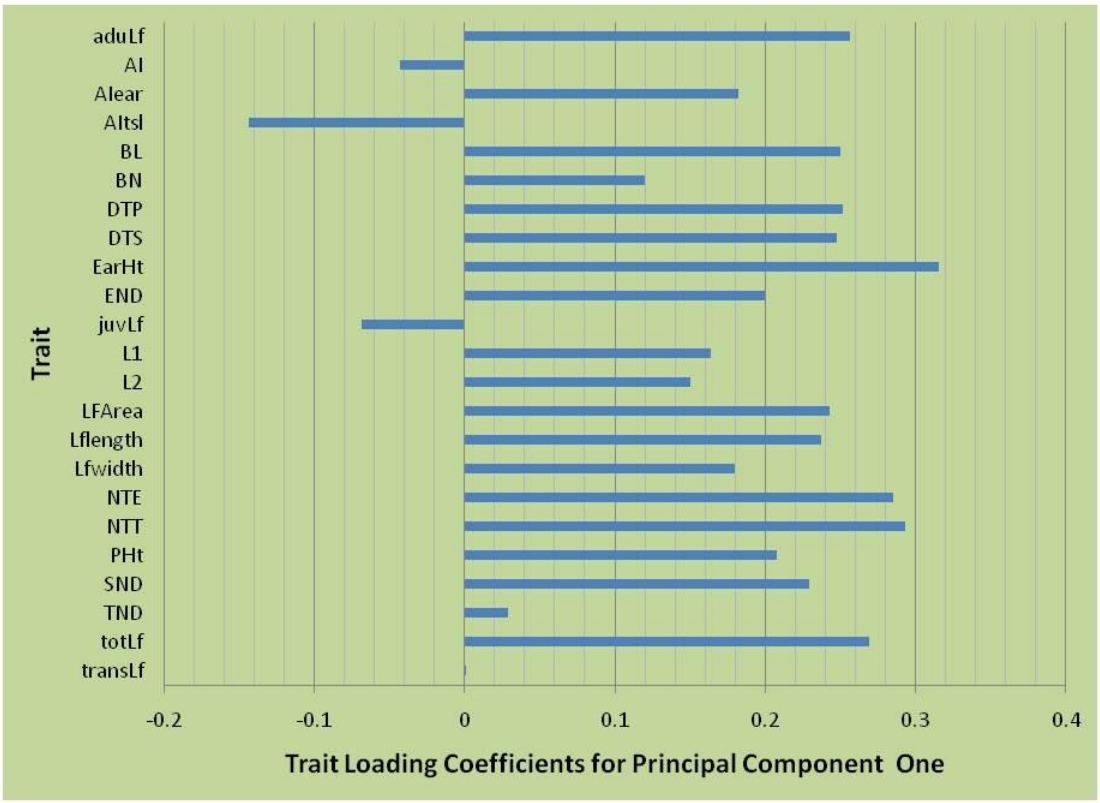

Figure 17. Relationship between the proportion of TS genetic background and PC1.

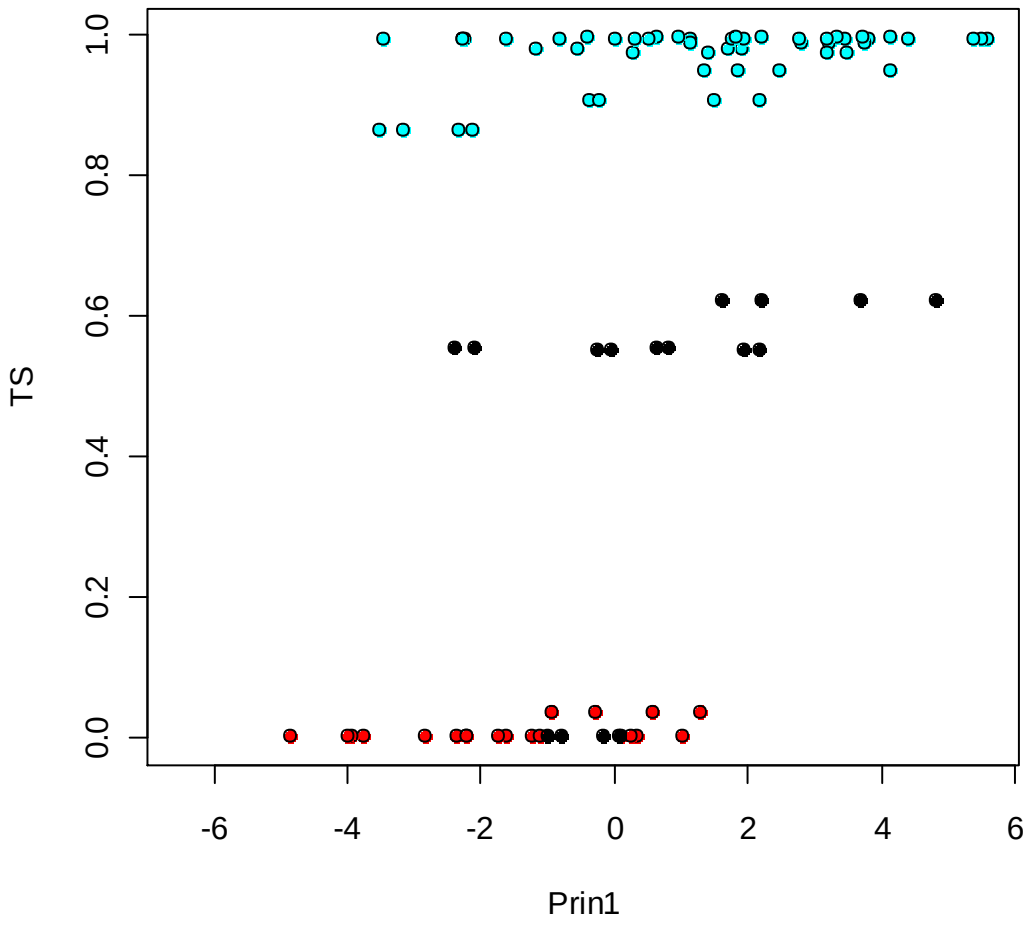

Points are colored according to subpopulation membership red (NSS), black (MXD) and teal (TS).

Figure 18. Horizontal bar plot of the trait loadings for PC2.

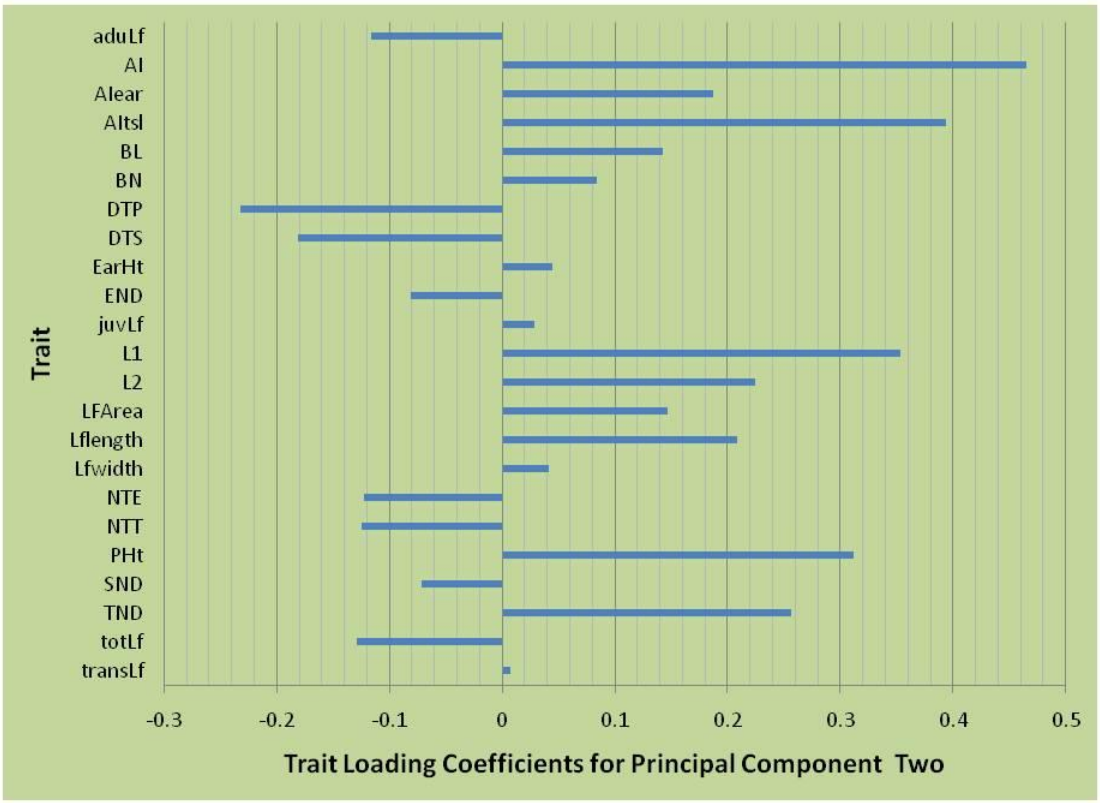

Figure 19. Horizontal bar plot of the trait loadings for PC3.

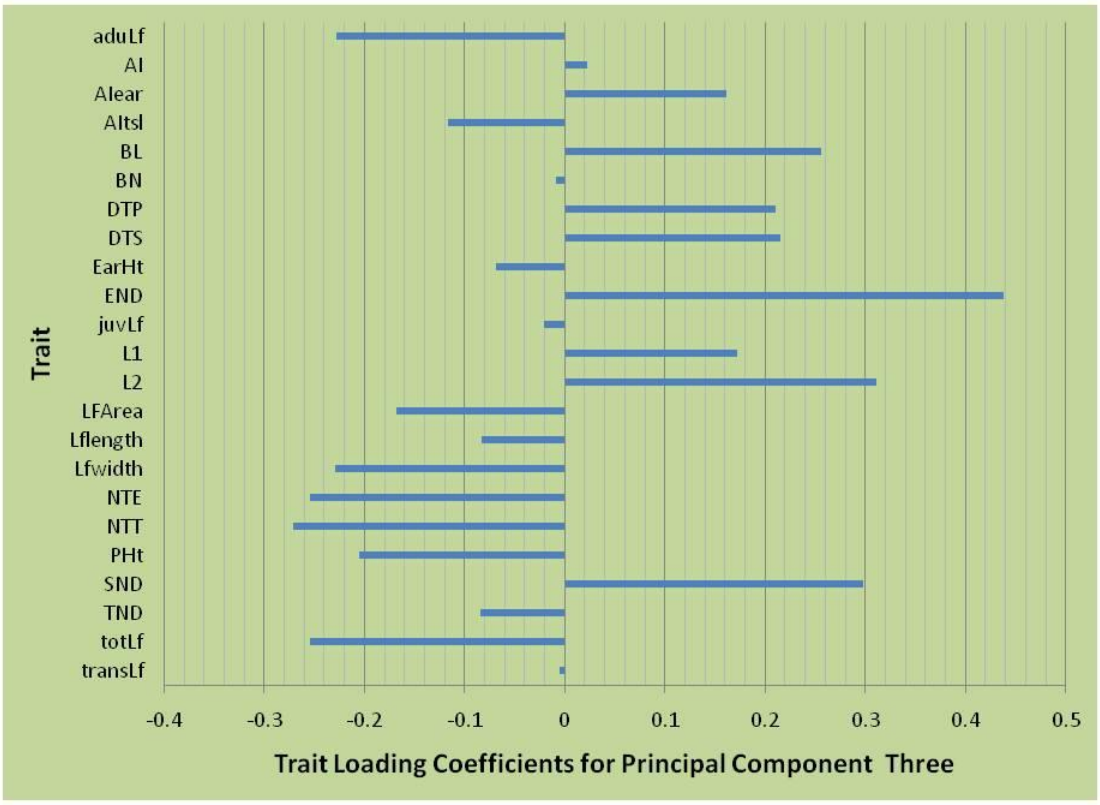

Figure 20. Horizontal bar plot of the trait loadings for PC4.

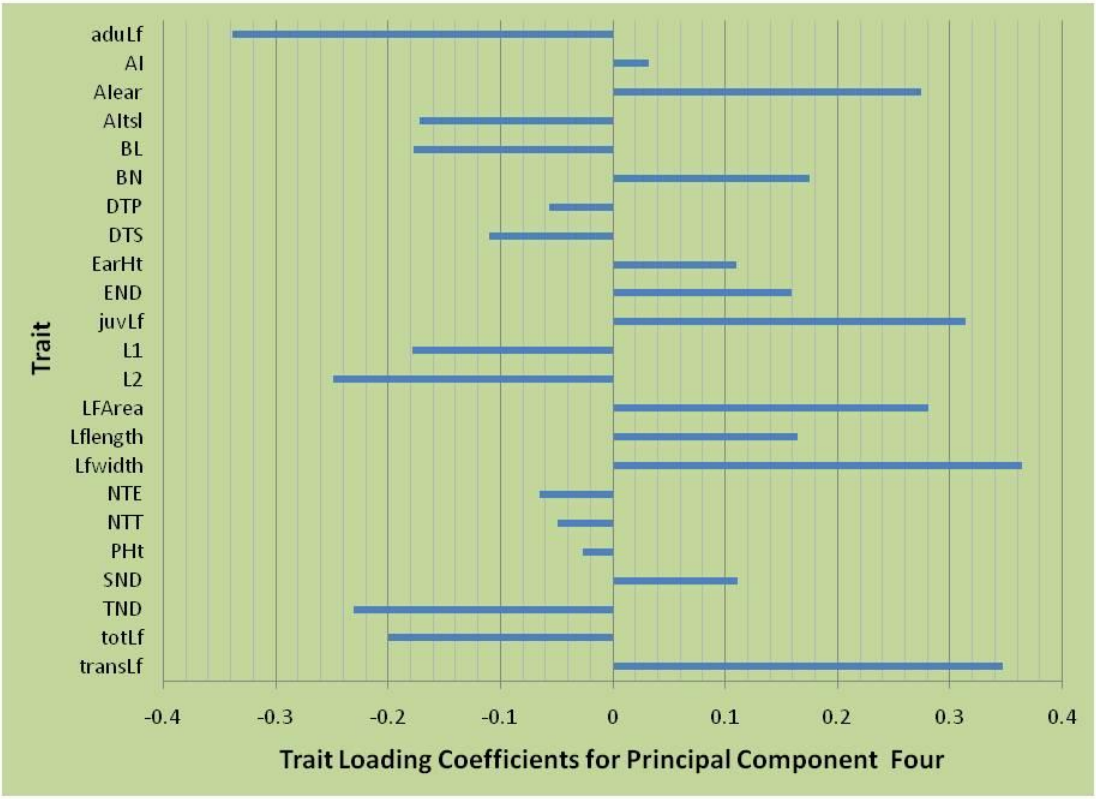

Figure 21. Horizontal bar plot of the trait loadings for PC9.

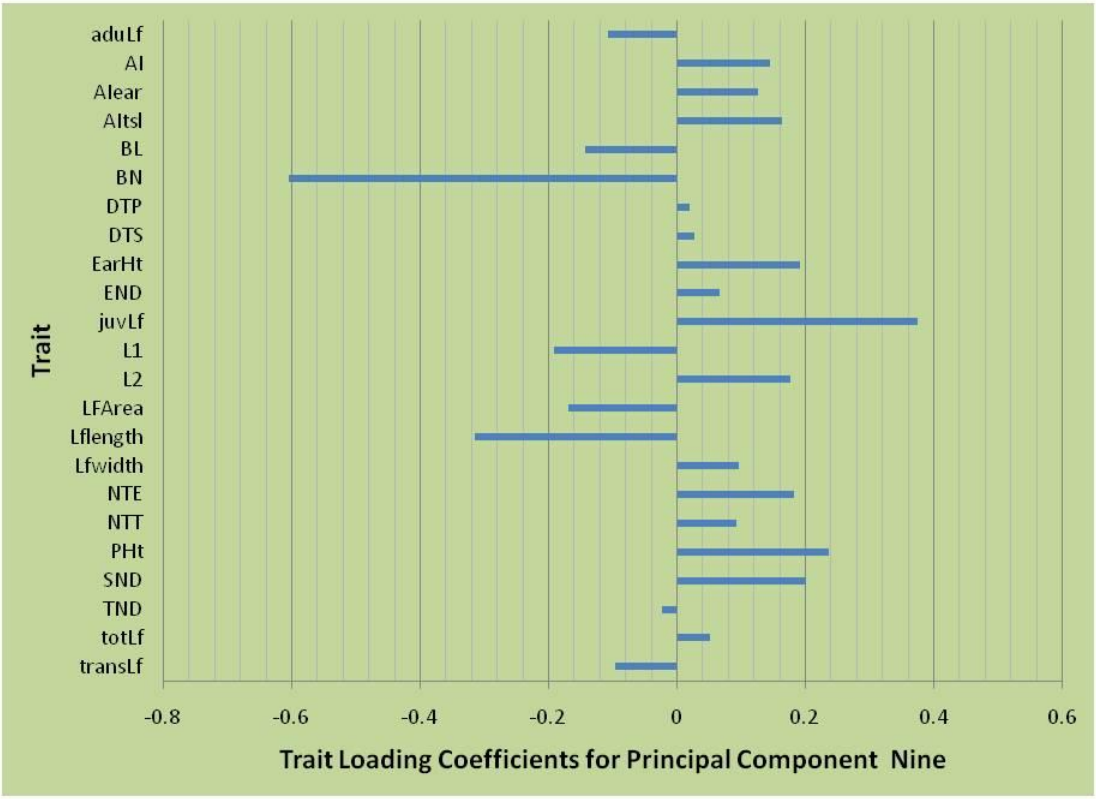

CHAPTER 5: Impact of the shade avoidance response on SBR-patterning in *Zea mays* L.

ABSTRACT

Competition for limited light resources has led to evolution of complex signaling mechanisms. Shade created by neighboring plants alters the quality and quantity of light perceived by plants. Plant perception of altered light quality and quantity is determined through the phytochome activity. Inactivation of phytochromes due to sub-optimal light conditions triggers the SAR. A network-based analysis of a maize phenome dataset predicted the negative impact of SAR on SBR traits. The goal of the study was to validate this prediction using mutant strains, field trials, and association analysis.

phytochromeB double mutants constitutively express the SAR. These mutants produced fewer SBRs than their *wild-type* counterparts. Field experiments exposing maize plants to different planting densities linked increased planting density to significant reductions in SBR production, further supporting the role of the SAR in SBR patterning. Association analysis conducted on the upstream promoter region of *phytochromeB2 (physB2)* in a set of diverse maize germplasm revealed no significant associations, indicating this region of *phyB2* does not contribute to SBR variation. The planting density experiment and *phyB* mutant analysis confirm the involvement of the SAR in SBR-patterning predicted by the network-based phenome analysis presented in Chapter 4.

INTRODUCTION

The fundamental importance of light to proper plant growth and development has led to evolution of highly complex and sensitive mechanisms for response to changes in light quality and quantity (known as the SAR). A series of complicated photo- and hormonal chemistries, redundant and overlapping protein-protein signaling cascades, and global changes in transcription profiles are triggered by the SAR to contend with neighboring plant competition for light. The

outcome of these physiological events is typified by reductions in branching, early flowering, and increased vertical growth (Kebrom et al., 2007).

Much of what is known about the genetic regulation of SAR has been discovered in the model plant *Arabidopsis thaliana.* This research established phytochromes as key regulators of the SAR (Franklin and Quail, 2010). Phytochromes regulate SAR by conversion between active and inactive forms. This conversion is dictated by the ratio of red to far-red light (Taiz and Zeiger, 2006). Biologically inactive phytochromes occupy the cytoplasm and are in the red light absorbing form, a state brought on by elevated incidence of far-red light. Upon exposure to red light the phytochromes convert to their biologically active form, the far-red light absorbing form and are transported to the nucleus. After arriving in the nucleus the phytochromes interact with phytochrome interacting factor 3 (PIF3) (Ni et al., 1998) and other related family members. The negative-regulator model for PIF-activity hypothesizes that after binding to phytochromes, PIFs are phosphorylated and degraded by the 26S proteosome resulting in transcriptional activity (Monte et al., 2007). This repressor of a repressor mechanism is analogous to the relationship between the hormones auxin and GA and their negative response regulators indole acetic acid (IAA) and DELLA proteins (Huq, 2006).

In maize, the SAR is repressed by the activity of the duplicate factors *phyB1* and *phyB2* (Sheehan et al., 2007). Although these duplicate factors share 98 percent sequence identity they also show evidence for subfunctionalization. *phyB1* controls inhibition of mesocotyl growth under red light while *phyB2* triggers the transition to reproductive phase in a photoperiod-mediated fashion (Sheehan et al., 2007). *phyB* double loss-of-function mutants are incapable of actively repressing the SAR. As a result they exhibit alterations in traits linked to the SAR, such as internode length, flowering time, stem diameter, and ear height (Sheehan et al., 2007).

Ecologically the SAR is important for an organism to sustain its niche in an ecosystem where successful acquisition of limited resources is the difference between reproductive failure

and success. Though the SAR is important from an ecological perspective, it also has been targeted for manipulation to enhance performance of crops (reviewed in Sawers et al., 2005; Kebrom et al., 2007), primarily focusing on yield (reviewed in Tokatlidis and Koutroubas, 2004; Tollenaar and Lee, 2002).

A recent network-based analysis of a data set of maize phenotypes in a diverse germplasm set connected SBR-patterning and the SAR (Chapter 4). Linear combinations of traits were constructed using PCA and interpreted as genetic networks controlling organismal level variation. These genetic networks were then coupled to SBR-patterning by way of multiple regressions. Among the networks significantly connected to SBR-patterning, PC2 linked an increase in average internode lengths to reductions in soil node and ear node diameters and days to flowering (Chapter 4), leading to speculation that the genetic origins of PC2 were genes involved in light-signaling. This speculation is based on the observation that maize lines homozygous for loss-of-function alleles at both *phyB* genes have reduced node diameters and flowering times and increased average internode length. As such, the pleiotropic effects of PHYB loss-of-function mirror the linear combinations of traits observed for PC2 suggesting that PHYB-mediated SAR determines SBR-patterning. The principal component regression predicts that SAR brought on by PHYB inactivity should result in a decline in SBR formation (Figure 22). The goal of these experiments is to test the involvement of the SAR in SBR-patterning, specifically whether PHYB inactivity results in fewer SBR. The specific objectives of this study are to: 1) evaluate the SBR phenotype of *phyB* double mutants; 2) measure the effect of planting density on SBR phenotypes in four maize inbreds; and 3) test for associations between SBR phenotypes and sequence variation in an upstream-non-coding region of *phyB2*.

MATERIALS AND METHODS

***phyB* double mutant assessment:** To evaluate the impact of PHYB inactivation on SBR-patterning and light-signaling-related traits, B73 lines homozygous for loss-of-function *phyB1* and *phyB2* alleles were planted along with B73 *wild-type* plants. Individuals were grown in a single replication in the field at the Genetics Farm, Columbia, Missouri in 2009. Using the methods described in Chapter 4, SBR traits were collected along with soil node diameter, number of nodes to ear, number of nodes to tassel, ear height, plant height, average internode length, average internode length between the soil and the ear, average internode length between the ear and the tassel, total leaf number, juvenile leaf number, adult leaf number, and transition leaf number. Distributions and summary statistics were computed using SAS version 9.1 (SAS Institute Inc., Cary N. C.). Homogeneities of variances were tested using Bartlett's test. SBR2, totlSBR, the average internode length between the soil and the ear node, and the average internode length between the ear and the tassel were normally distributed traits and possessed homogeneity of variances. These traits were analyzed using a t-test. The remaining traits were not normally distributed and were analyzed using the Wilcoxon-test, a nonparametric means comparison (Zar, 1999). Response to PHYB inactivity was calculated as M_P-M_C divided by M_C where M_P is the mean for the *phyB* double mutant and M_C is the mean of the *wild-type* control.

Planting density experiment: To confirm the role of light-signaling on SBR-patterning, a field planting density study was conducted. Inbreds B73 (SS), IDS28 (Sweet), Mo17 (NSS) and NC354 (TS) were planted at densities of five, 10, 15 and 20 plants per 10 foot row in three replications. The study employed a split-plot design with inbred as the main plot and planting density as the sub-plot. The split-plot design was chosen to limit the impact of neighboring planting density treatments. In addition, each inbred by density treatment was planted in a block of three rows with the central row (neighbored by rows of the same genotype and planting

density) used for data collection to decrease effects of adjacent treatments. Five plants were evaluated for each inbred-by-density treatment. For the 10, 15, and 20 plants per row treatment, plants on the ends of the row were not used for data collection. Data was collected for SBR2, SBR1, NWSBR, and totlSBR as described in Chapter 4 (Table 16). In addition the SAR related traits of soil node diameter, average internode length from the soil to the ear, and ear height were measured. Pairwise-Wilcoxon tests were conducted to compare the pooled inbred means across density treatments. Kruskal-Wallis tests were performed using density as the single factor. Due to the strong negative response to increased planting density the data were not normally distributed (Figure 23). To analyze the data set, generalized linear models were tested (Nelder and Wedderburn, 1972). Not to be confused with the general linear model, which is based on an assumption of a normally distributed response variable, the generalized linear model can be applied to response variables, which are members of the exponential family of distributions. The link function describes how the response variable is connected to the linear prediction variables. In this case the Poisson distribution, a distribution commonly used for count data, was specified in the generalized linear model with a link function relating the predictor variable to the mean response by the log procedure (Faraway, 2006). NWSBR was re-analyzed using the gamma-distribution with an inverse link function (Faraway, 2006). The Akaike information criteria (Akaike, 1974) indicated the gamma-base generalized linear model fit the response values of NWSBR better. Generalized linear models were computed in R (Ihaka and Gentleman, 1996) using the glm() command. The terms in the generalized linear model were inbred, density, rep and inbred*density. Analysis of deviance tables were retrieved using the anova() command. The deviance is the nonparametric version of the sums of squares reported in parametric tests. Treatment means were tested using a pairwise-Wilcoxon test. Kruskal-Wallis tests were also conducted as a single factor, nonparametric ANOVA.

Association analysis of the *phyB2* upstream noncoding region: The phenotyping component of the maize association panel is described in Chapter 4 (Table 16). Exploratory association analysis was conducted on 17 maize lines available at www.panzea.org. Significant association supported additional sequencing in the upstream non-coding region of the gene. DNA extraction, PCR, and sequencing protocols are the same as those described in Chapter 3, Materials and Methods except for the primers used. Primer sequences were obtained from www.panzea.org. The sequences were 3'- GTA CGG TGC ACG GAT ACC TAA CTA-5' (*phyB2* forward), 3'- TGC ATC GAC AAA ATT GTT TAT TTG-5' (*phyB2* reverse). Sequencing was conducted to bring the final number to 54 sequenced lines and a preliminary association analysis was conducted of *phyB2*. Several polymorphic sites had p-values less than 0.05 and consequently sequencing was performed on the 260 maize lines listed in Appendix 5. The sequence was aligned to previously determined alignments deposited in www.panzea.org. Association analysis was conducted as described in Chapter 3 Materials and Methods.

RESULTS

***phyB* double mutant phenotype comparisons:** To test the impact of PHYB inactivity (which is indicative of SAR) on SBR-patterning, means comparisons of developmental and SBR traits between B73 *wild-type* controls and B73 lines homozygous for loss-of-function alleles at both *phyB* loci were conducted. Results of the means comparisons for the developmental traits are presented in Table 25. Juvenile leaf number and plant height were not significantly different between the *phyB* double mutants and *wild-type* controls. With the exception of ear height (p-value=0.0205), all traits had highly significant differences (p-value less than 0.001). The double mutants possessed higher average internode lengths, fewer nodes and leaves, and had reduced ear heights (Table 25). SBR means comparisons are displayed in Table 26 and the corresponding root phenotypes are shown in Figure 24. The *phyB* double mutants produced fewer SBR2, SBR1,

NWSBR and totlSBR. With the exception of NWSBR (p-value=0.0055) the means comparisons showed highly significant differences (less than 0.0001).

Planting density experiment: Field treatments of increasing planting density were applied to four inbreds in three replications to assess SBR-patterning and light-signaling traits. The means comparisons between treatments for the average internode length between the soil and the ear, average ear height, and soil node diameter are displayed in Figure 25A-C. Increased planting density was accompanied by increases in internode length below the ear and in ear height, with reductions in soil node diameters. The means comparisons for the average internode length beneath the ear identified three distinct groups based on planting density. The five plants per row treatment had the smallest length at 8.8 cm, followed by the ten plants per row treatment at 9.5 cm (Figure 25A). The 15 and 20 plants per row treatments possess significantly longer internode lengths than the five and ten plants per row treatment but were not different from one another (Figure 25A). Two groups were distinguished in the means comparisons for ear height (Figure 25B). The five plant per row treatment produced significantly smaller ear height values than the ten, 15, and 20 plants per row treatments. Four distinct groups were identified in the soil node diameter means comparisons (Figure 25C). Highly significant Kruskal-Wallis p-values indicate that density treatments played a major role in determining the performance of light-signaling related traits (Figure 25A-C).

Increased planting density resulted in reductions in SBR production across multiple SBR traits. Kruskal-Wallis tests indicated that density had a highly significant impact on SBR production (Figure 26 A though D). Means comparisons identified three separate groups for each SBR-patterning trait, with the 15 and 20 planting density treatment not significantly different from one another. The use of generalized linear models described the sources of variation (deviance) in terms of inbred, density, rep and inbred*density effects. All model terms were significant for the models describing SBR2, SBR1 and totlSBR (Tables 27, 28, 29). The Rep term

was not significant in the model for NWSBR (Table 30). Inbred*density interaction terms were significant for all SBR traits. For SBR2 and SBR1 the interaction term explained more deviance than the inbred term. However, density was a greater source of deviance than the inbred term for all SBR traits.

Association analysis of *phyB2* non-coding region: Preliminary association analysis using the 16 available sequences resulted in associations with p-values less than 0.05. Sequencing on additional lines brought the sample size for the preliminary analysis to N=54. Results from this association analysis are contained in Table 31. Significant associations with p-values less than 0.05 were reported for SBR1 at 6 locations in the *phyB2* non-coding region and for 4 locations with SBR2. Additional sequencing of this region in 260 maize inbreds revealed no significant associations (data not shown).

DISCUSSION

PHYB inactivity suppresses SBR formation: Principal component regression analysis suggested a relationship between the SAR and SBR-patterning (Chapter 4) based in the similarities observed between the linear combination of traits comprising PC2 (Figure 18) and the pleiotropic affects PHYB inactivity had on traits evaluated by Sheehan et al. (2007). Complete loss of PHYB activity results in constitutive SAR as PHYB activity is necessary to actively suppress the SAR. According to Sheehan et al. (2007), PHYB inactivity results in reductions in flowering time, plant height, average height of the ear, and stem diameter, and increases in internode length. PC2 displays a positive loading for internode lengths and negative loadings for soil node diameter, and flowering time. The "phenotypic fingerprint" of PC2 paralleled the pleiotropic effects of the SAR as determined in *phyB* double mutants. Our goal was to evaluate *phyB* double mutants for developmental and SBR traits and test the predictive value of the principal component regression results, specifically the loading identified in PC2. Phenotypes of developmental traits in *phyB* double mutants mirrored the PC2 linear combinations (Figure 27).

Adult leaf number, average internode length, average internode length below the ear, average internode length above the ear, number of nodes to ear and to tassel, plant height, soil node diameter and total leaf number showed similar changes in the trait loadings compared to the PHYB inactivity response determined from the mutant phenotypes. Ear height was not in agreement. This may be because the number of nodes to the ear is smaller in *phyB* double mutants than in *wild-types.* The difference between *phyB* double mutant and *wild-type* ear heights is 9 cm and the difference in the number of nodes to ear is 1.4 nodes (Table 25). With internode length beneath the ear ranging from 12 to 14 cm per node, the difference in ear height is mainly due to number of nodes to ear-not differences in internode length. Despite this minor difference PC2 does an excellent job of approximating the SAR response.

Principal component regression analysis predicted that as PC2 values increased (increased SAR or reductions in PHB activity), NWSBR and totlSBR would decrease (Figure 22). Means comparisons between *wild-type* and *phyB* double mutants reveal significant reductions in all SBR traits as the result of PHYB inactivity (Table 26). These findings support the hypothesis that PC2 represents a light-signaling network that influences SBR-patterning, and that the principal component regression accurately predicts the impact of the SAR on SBR-patterning.

Increased planting density limits SBR formation: Taken together, the results of the principal component regression analysis and the finding that PHYB inactivity suppresses SBR formation provide evidence that light-signaling mediated by PHYB activity affects SBR-patterning. Both PHYB inactivity and the SAR are consequences of alterations in light quality and quantity often attributed to shade canopies and planting density. A planting density experiment was conducted to support the finding that the SAR (and by analogy, PHYB-mediated light response) contributes to SBR-patterning. Four inbred lines were planted at four planting density treatments. Evaluations of traits influenced by PHYB inactivity provide phenotypic indicators of the magnitude of

theSAR. The three SAR traits that were investigated were average internode below the ear, ear height, and soil node diameter. Kruskal-Wallis tests indicate that these traits were significantly different among planting density treatments (Figure 25). Increases in planting density increased ear height and internode length beneath the ear, but reduced soil node diameter. Increases in internode length and stem diameters were observed in *phyB* double mutants in this study (Table 25) and in Sheehan et al. (2007). The phenotypic responses to increased planting density are indicative of the SAR and in agreement with PC2 (Figure 27). The inbreds behaved more like *phyB* double mutants as density increased. Assuming that the *phyB* double mutants accurately reflect the SAR in SBR-patterning and other traits, increased planting density should result in diminished SBR formation. The results of the means comparisons and the Kruskal-Wallis test indicate that density treatment significantly affects global SBR-patterning in the manner expected (Figure 26).

A role for genotype in the response of SBR-patterning to planting density: Generalized linear models were constructed and tested for Inbred and Inbred*Density interactions (genotype by treatment) to better understand the sources of variation in planting density. In all cases density treatment was the primary source of variation in the data set. Interestingly the generalized linear models also identified significant inbred*density interactions suggesting that the genetic content of some inbreds caused them to respond differently to increased planting density than other inbreds. Figure 28 displays the planting density data in a manner more conducive to comparisons among inbreds. Closer inspection of Figure 28 reveals two qualitatively different classes of density response: One class that responds acutely to increased plant density and another class that is less sensitive to changes in density. The inbreds IDS28 and Mo17 represent the density-sensitive class. These lines respond acutely to increases in planting density, reaching values of zero for the SBR traits by 15 plants per 10 ft. row treatment. The density-insensitive class is represented by B73 and NC354. These inbred lines experience reductions in SBRs between

treatments but their response is much more muted. Two characteristics distinguish the density-sensitive class from the density-insensitive class. The first is the rate of decrease in SBR formation. SBR numbers decrease more quickly in the density-sensitive group relative to the density-insensitive group. The second characteristic is the asymptotic limit for the rate of decrease curves. The density-sensitive lines reach zero values indicating a complete absence of SBRs due to increased planting density while the density-insensitive lines maintain some degree of SBR formation even under the highest planting density. Whether the insensitive lines have truly reached a biologically meaningful asymptote, or whether further reductions in SBR formation would occur at greater planting densities remains to be seen. However, these findings are promising considering that a genetic component of the SBR formation in response to shade avoidance could be exploited through conventional breeding methods. Further, the differences in genetic response to changes in planting density suggest that mining of allelic variation at genes involved in light-signaling may provide genetic tolerance mechanisms to sustain root function under increased planting density.

Mining allelic variation in the *phyB2* non-coding region: Association analysis was conducted on an upstream non-coding region of the *phyB2* locus in order to capitalize on the previous findings and to potentially isolate favorable alleles which may influence SBR-patterning. Although preliminary results supported the involvement of the non-coding region in SBR-patterning (Table 31), further sequencing rejected this notion. The origin of the early false positives may be partly due to LD of alleles in the non-coding region of the gene and a loss-of-function allele at the transcriptional start site. The loss-of-function allele is found in lines 38-11, F2, CM105, CM174, CMV3, H99, N192 and W153R (population data set NCBI, Figure 29) all of which were present in the preliminary association analysis. Small sample sizes in association studies results in slower rates of LD decay. It is possible that LD extended between the loss of function alleles at the transcription start site and polymorphisms at the non-coding region,

resulting in preliminary false positives, as the sample size increased LD decayed. Further analysis of the contribution of this loss-of-function mutant allele on SBR-patterning should be conducted.

Investigation of the influence of the SAR on SBR-patterning has led to several important findings. First, the mutant analysis confirmed the role of light-signaling in SBR-patterning and validated the principal component regression analysis detailed in Chapter 4. These results provided a proof-of-concept that the genetic networks suggested by the PCA do impact root development as predicted. Second, the planting density study further supported the shade induced SBR suppression model (Figure 30). Together results of the *phyB* mutant analysis and the planting density experiments provide a foundation for a model where PHYB-facilitated light-signaling response determines SBR production. Under adequate light conditions the phytochromes are in their active, far-red light absorbing state and occupy the nucleus, suppressing the SAR. Active suppression of the SAR leads to SBR formation (Figure 30A). Under suboptimal-light conditions (such as those observed under increased planting density), phytochromes are inactivated by the absorption of far-red light. Transport of the phytochromes to the cytoplasm triggers the SAR, ultimately leading to reductions in SBR formation (Figure 30B). Additionally, statistical analyses identified inbred*density interactions and provided an avenue for the genetic enhancement of SBR response to planting density. A more exhaustive survey of elite, diverse, and landrace maize varieties under different planting densities could lead to the identification of inbred lines that sustain SBR development under increased planting density, and provide insight into the evolution of density tolerance under selection. Lastly, although our association results were negative, an alternative target, a mutation at the transcriptional start site of *phyB2*, could prove to be useful for the manipulation of SAR to sustain SBR formation.

REFERENCES

AKAIKE, H., 1974 A new look at the statistical model identification. IEEE Trans. Automat. Contr. **19(6):** 716-723.

FARAWAY, J. J., 2006 *Extending the linear model with R: generalized linear, mixed effects and nonparametric regression models*. Chapman and Hall/CRC. Boca Raton, FL. 301p.

FRANKLIN, K. A. and P. H. QUAIL, 2010 Phytochrome functions in *Arabidopsis* development. J. Exp. Bot. **61(1):** 11-24.

HUQ, E., 2006 Degradation of negative regulators: a common theme in hormone and light signaling networks? Trends Plant Sci. **11(1):** 4-7.

IHAKA, R. and R. GENTLEMAN, 1996 R: a language for data analysis and graphics. J. Comput. Graph. Stat. **5:** 299-314.

KEBROM, T. H. and T. P. BRUTNELL, 2007 The molecular analysis of the shade avoidance syndrome in the grasses has begun. J. Exp. Bot. **58(12):** 3079-3089.

MONTE, E., B. AL-SADY, P. LEIVAR, and P. H. QUAIL, 2007 Out of the dark: how the PIFs are unmasking a dual temporal mechanism of phytochrome signalling. J. Exp. Bot. **58(12):** 3125-3133.

NELDER, J. and R. WEDDERBURN, 1972 Generalized linear models. J. Roy.Stat. Soc., Series A **(132):** 370-384.

NI, M., J. M. TEPPERMAN, and P. H. QUAIL, 1998 PIF3, a phytochrome-interacting factor necessary for normal photoinduced signal transduction, is a novel basic helix-loop-helix protein. Cell **95(5):** 657-667.

SAS INSTITUTE, 2004 SAS Version 9.1. SAS Institute Inc., Cary, NC.

SAWERS, R. J. , M. J. SHEEHAN, and T. P. BRUTNELL, 2005 Cereal phytochromes: targets of selection, targets for manipulation? Trends Plant Sci. **10(3):** 138-143.

SHEEHAN, M. J., L. M. KENNEDY, D. E. COSTICH and T. P. BRUTNELL, 2007 Subfunctionalization of *PhyB1* and *PhyB2* in the control of seedling and mature plant traits in maize. Plant J. **49**: 338-353.

TAIZ, L., and E. ZEIGER, 2006 *Plant Physiology* 4th Edition. Sinauer Associates, Inc. Sunderland, MA. 764p.

TOKATLIDIS, I. S. and S. D. KOUTROUBAS, 2004 A review of maize hybrids' dependence on high plant populations and its implications for crop yield stability. Field Crops Res. **88:** 103-114.

TOLLENAAR, M. and E. A. LEE, 2002 Yield potential, yield stability and stress tolerance in maize. Field Crops Res. **75:** 161-169.

ZAR, J 1999 *Biostatistical Analysis* 4th Edition. Prentice Hall Inc., Upper Saddle River, N. J. 929p.

TABLES

Table 25. Means comparisons of developmental traits for B73 *wild-type* control and *phyB* double mutants.

N[a]	B73	*phyB*	p-value[b]
A. Average internode (cm/node)			
15, 10	17.6±0.8	20.9±0.8	0.0003
B. Average internode below the ear (cm/node)			
15, 10	12.3±0.9	14.2±1.2	0.0001
C. Average internode from the ear to the tassel (cm/node)			
15, 10	25.4±2.2	29.3±2.6	0.0005
D. Ear height (cm)			
15, 15	95.7±7.9	86.7±9.8	0.0205
E. Juvenile leaf number			
15, 15	3.5±0.5	3.7±0.5	*NS*
F. Nodes to ear			
15, 15	7.8±0.4	6.4±0.5	0.0004
G. Nodes to tassel			
15, 15	13.1±0.6	11.4±0.5	0.0004
H. Plant height (cm)			
15, 15	230.3±10.3	236.3±7.7	*NS*
I. Soil node diameter			
15, 15	26.2±3.4	14.2±2.5	<0.0001
J. Total leaf number			
15	17.7±0.6	13.9±0.5	0.0002

[a] Number of observations per genotypic class (B73, *phyB*).
[b] *NS* indicates statistical test was not significant.

Table 26. Means comparisons of SBR traits for B73 *wild-type* control and *phyB* double mutants.

N[a]	B73	*phyB*	p-value[b]
A. Shoot-borne root number node two (SBR2)			
15	18.7±1.9	12.7±1.9	<0.0001
B. Shoot-borne root number node one (SBR1)			
15	16.3±1.4	10.9±1.5	<0.0001
C. Node with shoot-borne roots (NWSBR)			
15	3.3±0.8	2.5±0.5	0.0055
D. Total shoot-borne roots (totlSBR)			
15	55.8±12.9	31.1±8.9	<0.0001

[a] Number of observations per genotypic class (B73, *phyB*).
[b] *NS* indicates statistical test was not significant.

Table 27. Summary table for the generalized linear model for SBR2 in four maize inbreds planted at four densities.

Source	df	Deviance	Residual Dev	z-value	p-value
Null	NA	NA	2402	NA	NA
Inbred	3	326	2076	-6.2	5.50E-10
Density	3	800	1276	6.2	3.66E-10
Rep	2	20	1255	-3.1	0.001700
Inbred*Density	9	327	928	6.0	1.47E-09

NA = not applicable.

Table 28. Summary table for the generalized linear model for SBR1 in four maize inbreds planted at four densities.

Source	df	Deviance	Residual Dev	z-value	p-value
Null	NA	NA	1207	NA	NA
Inbred	3	148	1058	-8.2	< 2.0E-16
Density	3	210	848	6.0	1.2Ee-09
Rep	2	13	834	-2.4	0.014400
Inbred*Density	9	262	572	6.3	3.05e-08

NA = not applicable.

Table 29. Summary table for the generalized linear model for totlSBR in four maize inbreds planted at four densities.

Source	df	Deviance	Residual Dev	z-value	p-value
Null	NA	NA	3026	NA	NA
Inbred	3	399	2628	-11.7	2.00E-16
Density	3	1229	1399	9.5	2.00E-16
Rep	2	50	1349	-4.5	5.42E-06
Inbred*Density	9	373	975	9.9	2.00E-16

NA = not applicable.

Table 30. Summary table for the generalized linear model for NWSBR in four maize inbreds planted at four densities.

Source	df	Deviance	Residual Dev	t-value	p-value
Null	NA	NA	45	NA	NA
Inbred	3	7	38	6.0	9.16e-09
Density	3	16	22	-2.7	0.00693
Rep	2	0.4	21	NS	NS
Inbred*Density	9	6	16	-5.6	5.60e-08

NA = not applicable.

Table 31. Preliminary association mapping results for the *phyB2* gene in maize (N=54).

Trait[a]	Position[b]	p-value[c]	Model[d]	Marker[e]
SBR105	22	0.0040	0.5280	0.0879
SBR105	115	0.0037	0.5295	0.0894
SBR105	145	0.0040	0.5280	0.0879
SBR105	162	0.0037	0.5295	0.0894
SBR105	187	0.0099	0.5135	0.0731
SBR206	221	0.0361	0.5044	0.0441
SBR206	293	0.0361	0.5044	0.0441
SBR105	317	0.0212	0.4981	0.0580
SBR206	352	0.0361	0.5044	0.0441
SBR206	421	0.0361	0.5044	0.0441

[a] Last two digits of the SBR trait abbreviation indicate the year the trait data was collected (2004, 2005 or 2008).
[b] Position of polymorphism along gene.
[c] p-value of the marker-to-trait association.
[d] Amount of the variation explained by the mixed model.
[e] Amount of the variation explained by the polymorphism at the indicated position.

FIGURES

Figure 22. Regression of PC2 onto the square root transformed SBR trait values. (A) number of nodes with shoot-borne roots and (B) total number of shoot-borne roots .

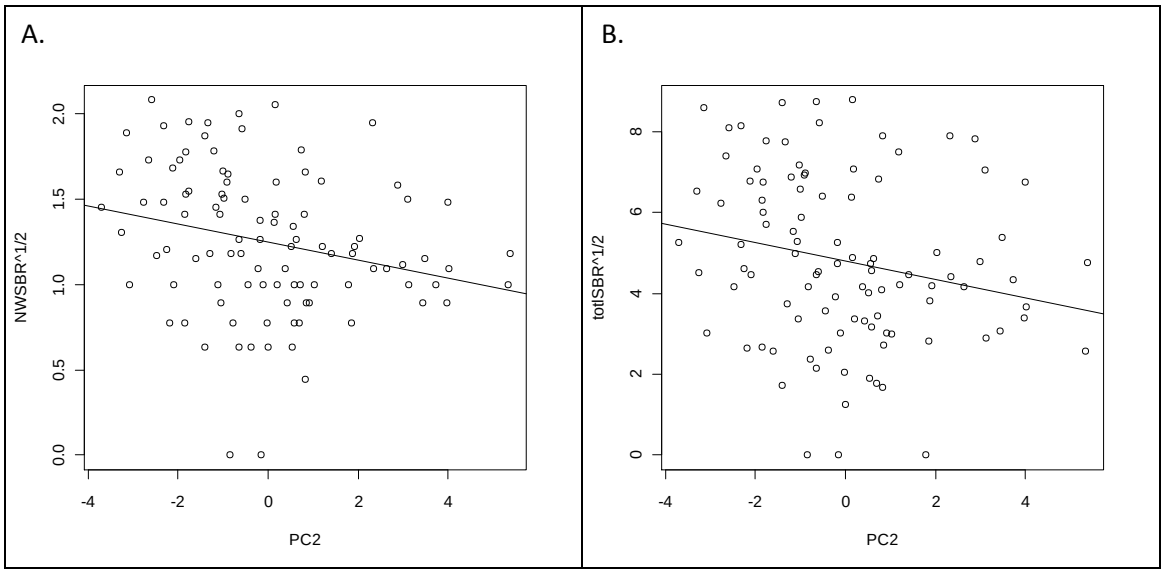

Figure 23. Histograms of raw values for SBR2 (A), SBR1 (B), NWSBR (C), and totlSBR (D) across treatments for all inbred lines included in the planting density experiment.

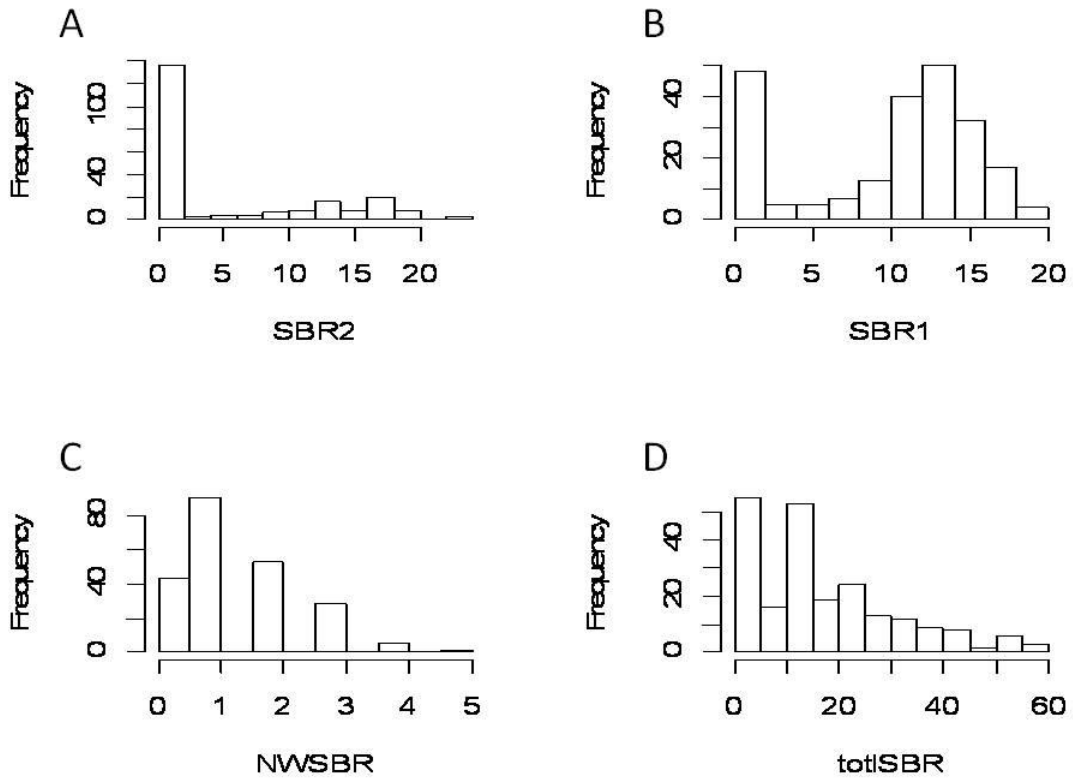

Figure 24. Root phenotypes of the B73, *wild-type* control (A) and *phyB* double mutants (B).

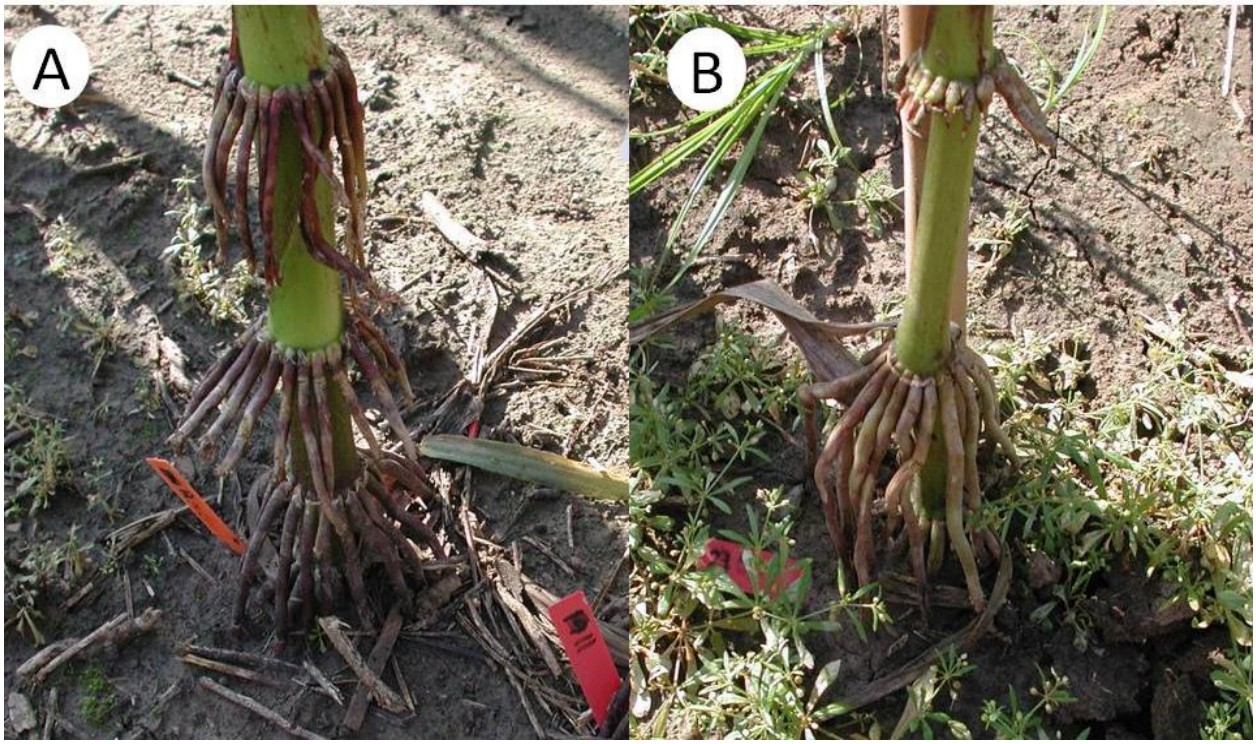

Figure 25. Inbred performance for A) average internode length from the soil to the ear, B) ear height, and C) soil node diameter across density treatments. B73, IDS28, Mo17, and NC354 are in blue, red, green and purple. The grey bar represents the pooled values pooled across inbred lines. Treatment means are presented above the grey bar with the means separation grouping in parentheses. IDS28 is not presented for internode length to the ear and ear height due to lodging.

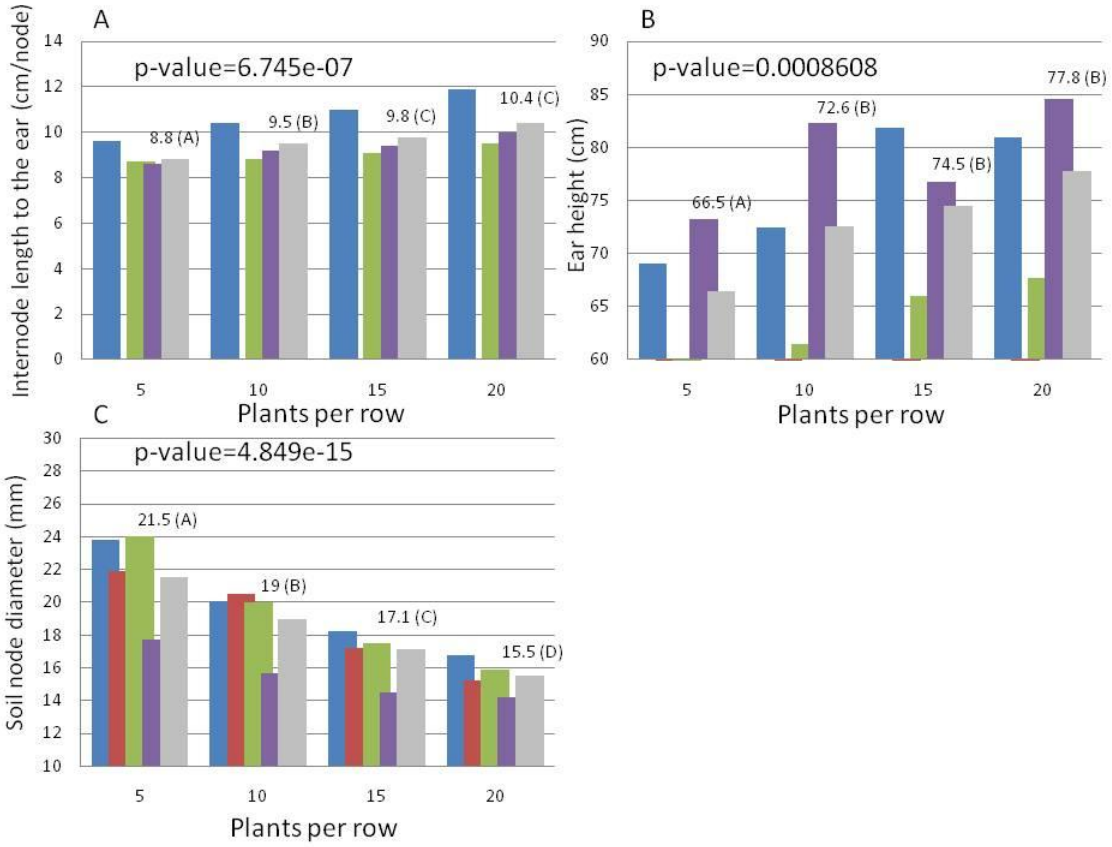

Figure 26. Inbred performance for A) SBR2, B) SBR1, C) NWSBR, and D) totlSBR across density treatments. B73, IDS28, Mo17, and NC354 are in blue, red, green and purple. The grey bar represents the pooled values pooled across inbred lines. Treatment means are presented above the grey bar with the means separation grouping in parentheses.

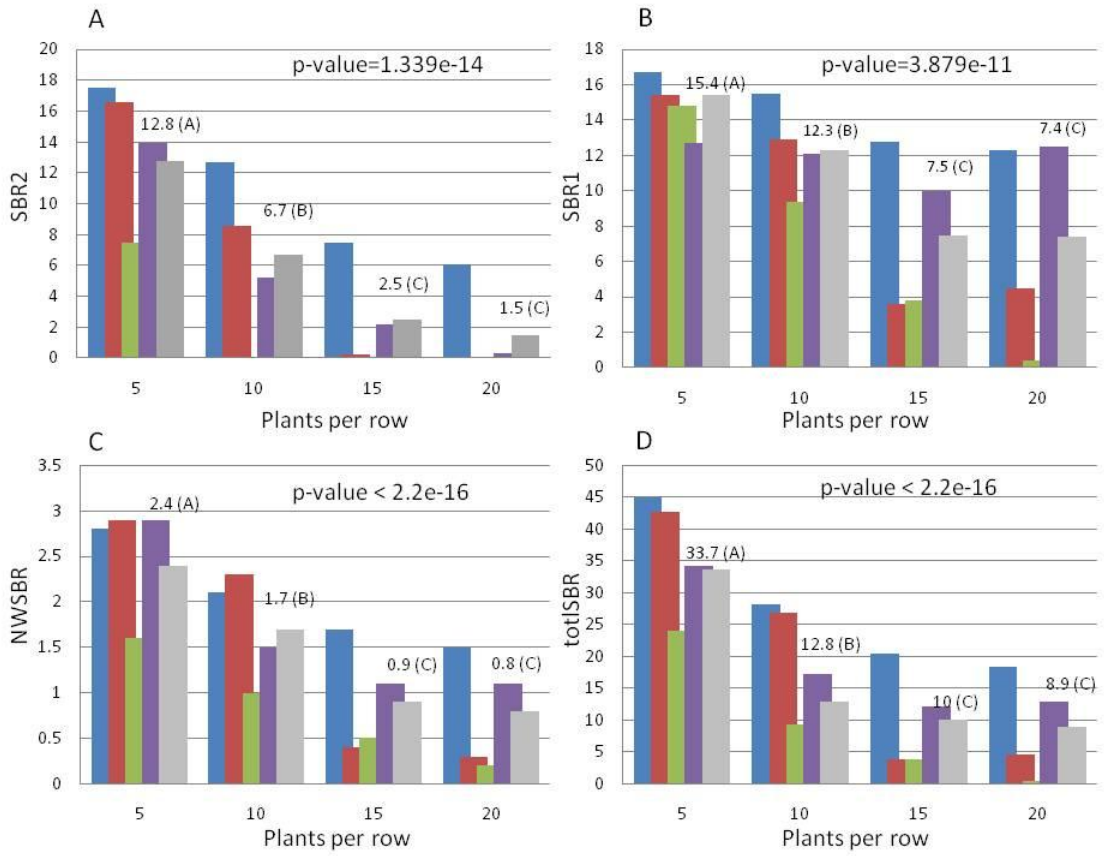

Figure 27. PC2 loadings for a diverse set of maize inbreds (blue) plotted with *phyB* mutant response relative to *wild-type* (green).

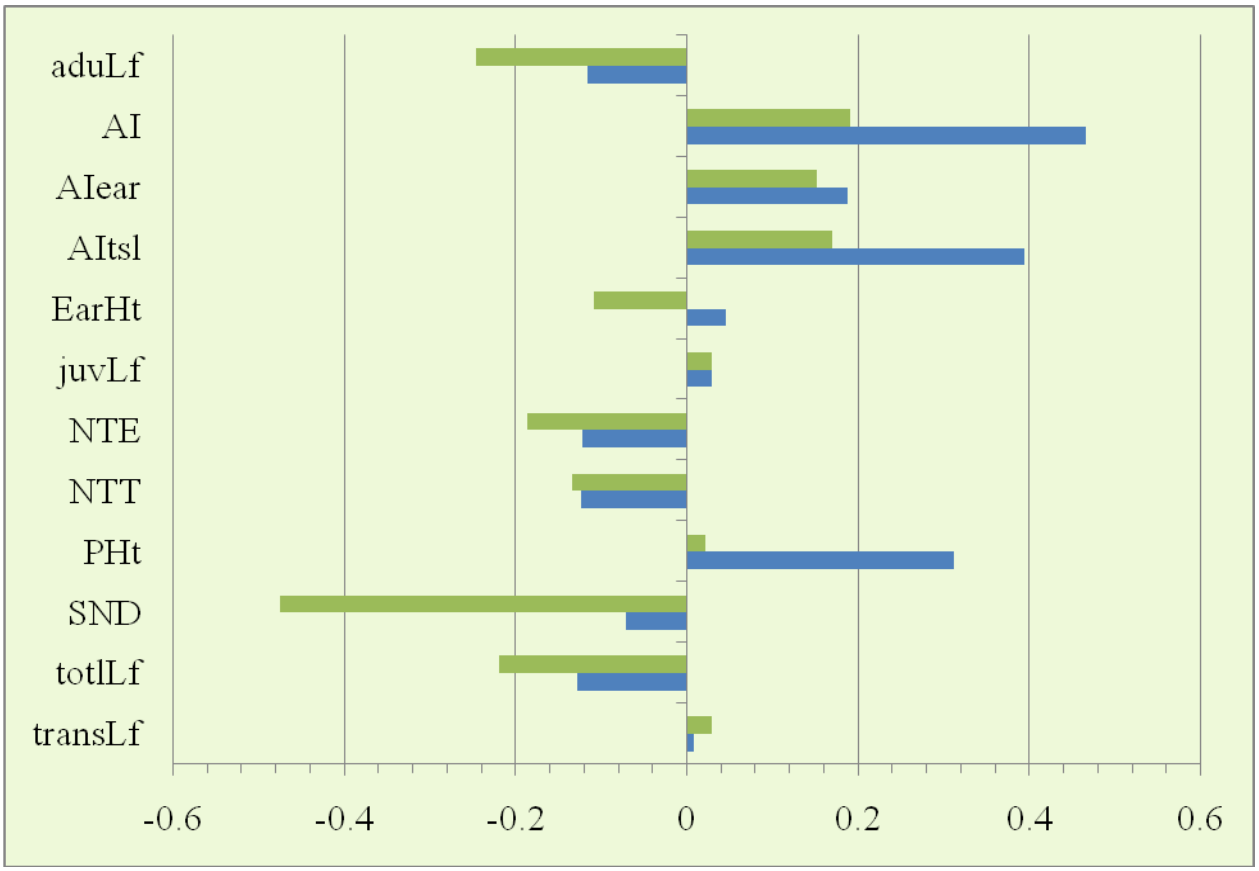

Figure 28. Boxplots of SBR traits by density (5, 10, 15, 20) for four maize inbreds: B73(SS), IDS28 (Sweet), Mo17(NSS), and NC354(TS).

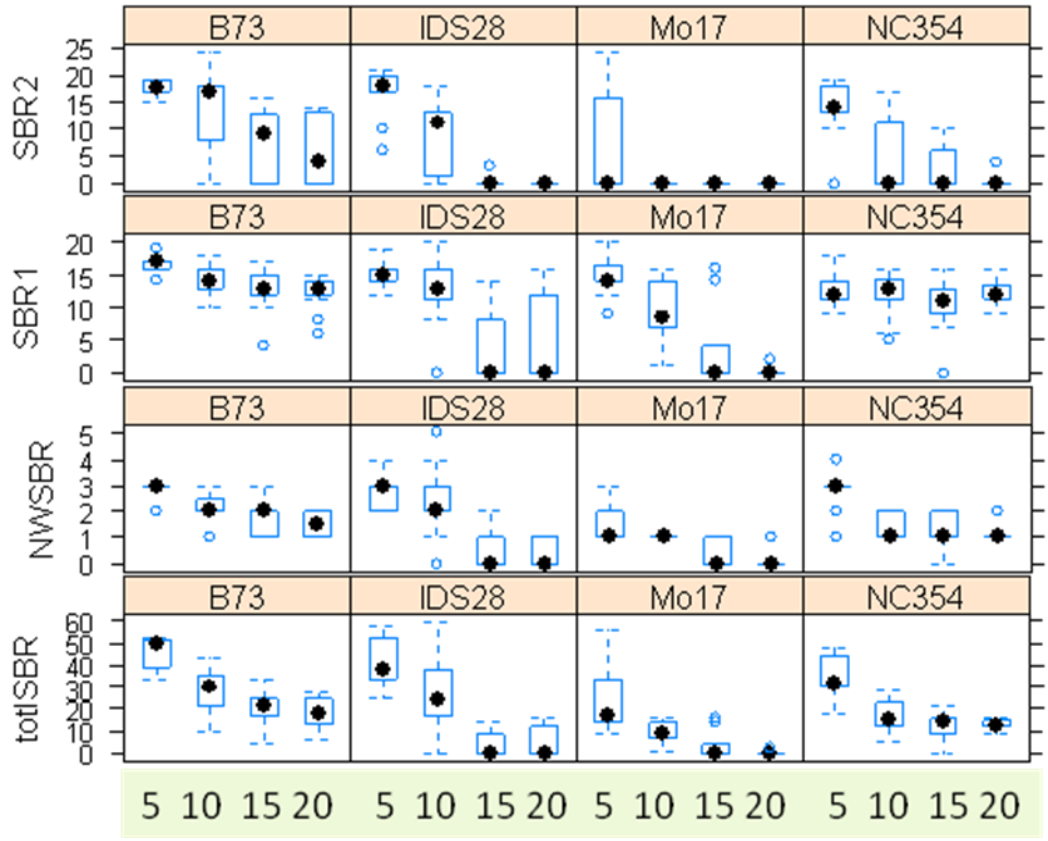

Figure 29. *phytochrome B2* gene model

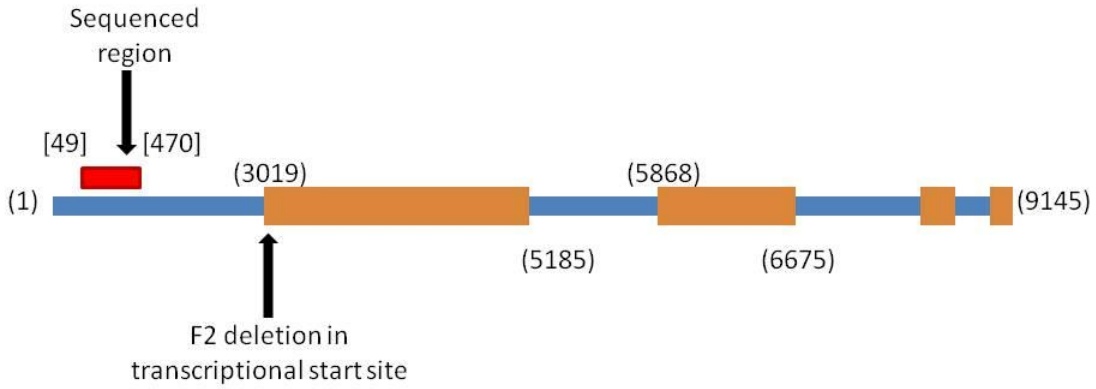

Blue boxes represent introns. Salmon boxes depict exons. Red box indicates the portion of the gene that was sequenced. Numbers in parenthese are the position of intron-exon junctions or the boundaries of the sequenced region.

Figure 30. Model for phytochrome regulation of SBR-patterning.

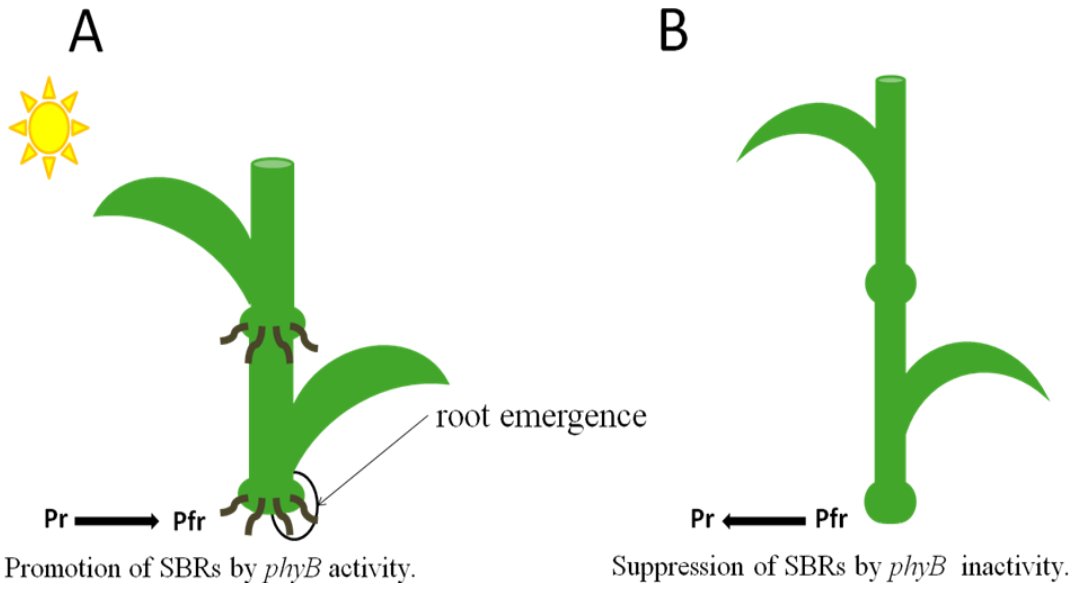

CHAPTER 6: Conclusions and Future Directions

Modeling a GA Pathway with Both Positive and Negative Effects on SBR Formation.

In the preceding chapters, pathways were identified and investigated for their involvement in SBR-patterning. The GA pathway was selected for further investigation due to prior knowledge about the role the hormone played in phase-change transitions and supporting evidence provided by the SBR QTL mapping study in the IBM population. Genes related to GA production and response mapped near QTL linked to variation in vertical- and radial-patterning of SBRs. Together these results encouraged a narrower focus on the involvement of GA genes in SBR-patterning. A survey of GA biosynthetic and response mutants provided novel insight into the role of GA in root patterning. Evans and Poethig (1995) linked GA synthesis to inhibition of NWSBR. The results presented in Chapter 3 demonstrated that GA synthesis not only suppresses NWSBR, but also stimulates the radial formation of SBRs by increasing the number of SBRs present at a node. A second novel finding was the discovery that genes involved in GA response also participate in SBR-patterning. Two such genes, *D8* and *D9*, code for negative GA-response regulators. Altering the function of these genes eliminates SBR formation. This suggests that GA may function to promote SBR formation by eliminating restraint of *D8* and *D9* on GA response genes.

The revelation that GA promotes SBR formation (by triggering the degradation of negative-GA-response regulators) appears at first to be at odds with the findings of Evans and Poethig (1995). How can GA simultaneously suppress NWSBR and promote SBR1 and SBR2? These contradictions can be resolved by placing GA activity in a tissue-specific context. Early in development GA regulates NWSBR by suppressing the juvenile-vegetative phase through SAM-specific activity. This SAM-specific action of GA suppresses *miR156* activity by acting as a molecular switch for vegetative-phase transition. Morphogens, hormones, and microRNAs alike, shape development through concentration-dependent mechanisms (Kutejova et al., 2009). Differences in enzyme kinetics resulting from polymorphisms in functional domains, like the

ones identified in the association analysis of *d3*, could result in altered GA concentration gradients emanating out of the SAM. Consequently *miR156* expression gradients would also be altered in a spatially reciprocal manner. The spatial changes in *miR156* activity subsequently lead to changes in NWSBR and alter the number of SBRs at a node. Validation of this model requires examination of the spatial distribution of *miR156* expression and GA levels in different maize lines. This could be achieved using locked nucleic acid (Song et al., 2010) probes for *miR156* and antibodies for GA. Evaluation of maize lines with different *d3* alleles would allow testing of polymorphisms relative to the spatial distribution of the morphogens (*miR156* and GAs) regulating SBR-patterning.

The role conventional DELLA-controlled GA response activity plays in SBR-patterning is conspicuously absent from the above model. Phenotyping of the GA-non-responsive, DELLA mutants, *D8* and *D9*, revealed the requirement of GA-mediated DELLA de-repression for SBR formation (Chapter 3). Association analysis suggests that polymorphisms in the *D8* promoter control SBR-patterning (Chapter 3). Two scenarios the "early and distal" model and the "late and local" model may explain how expression of *D8* contributes to SBR-patterning. Under the "early and distal" model, *D8* expression could contribute to SBR-patterning through direct regulation of GA biosynthesis. Fujioka et al. (1988) observed elevated GAs in *D8* mutants suggesting that DELLA activity under certain circumstances could promote GA synthesis. In this model, elevated *D8* expression leads to increased GA production. Increased GA production would then lead indiscriminately to the degradation of DELLA transcription factors and influence DELLA-independent GA response genes. One of these DELLA independent mechanisms could be GA-mediated suppression of *miR156.* Two approaches could be used to test this model. First, if elevated DELLA accumulation and activity suppresses SBR-patterning in *D8* and *D9* mutants through increasing GA production, then blocking GA production should restore SBR formation in *D8* and *D9* mutants. This could be tested by blocking the production of GA in *D8* and D9 mutants

through the introduction of mutant alleles of *d1*, *d3,* and *d5*. A second approach would capitalize on the genotypes collected in the association analysis. Association analysis could be used to evaluate the network architecture by linking genotypes to transcript and protein accumulation of *D8* with GA synthesis. Simultaneous measurement of *D8* expression, DELLA-protein accumulation, and GA production in the maize association lines would enable elucidation of the network dynamics between hormone and hormone regulator (Figure 31). This systems approach could be used to identify feedback-regulatory networks that link elevated *D8* accumulation to elevated GA synthesis while providing valuable insight into how structural genomic variation causes molecular (transcriptomic, proteomic, and metabolomic) variation and consequently phenotypic variation.

The previously proposed models define a SAM-specific "early and distal" activity which suppresses SBR formation through transcriptional control of *miR156*. A second model, where GA stimulates SBR formation positions GA activity locally, as well as later in development ("late and local" model). In the "late and local" model the role of GA is to stimulate SBR formation through de-repression of DELLA activity locally (near the SBR meristems post phase change). Local spatial and temporal changes in transcript accumulation and changes in the magnitude of transcript accumulation could impact the ability of SBRs to emerge, by regulating PCD and cell-wall modifying proteins essential for SBR emergence. Variation in *D8* activity would also alter the GA-mediated growth and the three-dimensional patterning of vascular tissue from which SBRs form, paralleling the findings of Ubedás-Tomas (2008, 2009). To confirm this model, expression of GA-insensitive alleles of *D8* could be assessed using different tissue specific promoters to assist in determining the exact role spatial and temporal regulation of *D8* plays locally in radial-patterning.

The experiments presented in Chapter 2 and 3, which document the role of GA in SBR-patterning, illustrate the complexity with which pathways operate to dictate phenotypic variation.

They indicate that both GA biosynthesis and response genes contribute to variation in SBR-patterning. The association analysis presented in Chapter 3 provides evidence that naturally-occurring variation in GA synthesis and response play a role in the phenotypic variation observed in maize breeding germplams. Subsequently, the results of the association analysis were used to identify functional variation in the *d3* enzymatic region and the *D8* promoter region. The potential roles for *d3* and *D8* can be described by the "early and distal" and the "late and local" models. Under the "early and distal" model, GA shapes SBR-patterning by suppressing *miR156* early in development distally in the SAM. In the "late and local" model GA controls SBR-patterning through its influence on the transcriptional activity of DELLA proteins which determine spatial growth. Both models suggest changes in GA influenced SBR-patterning (although these changes are of different magnitude) and both models propose that GA elicits a tissue-specific activity.

Refining the Light-Signaling Model

A second pathway was implicated in SBR-patterning through a systems biology approach to analyze of a large set of developmental/morphological phenotypes in a diverse set of maize germplasm (Chapter 4). The analysis consisted of PCA which identified linear combinations of correlated traits. These linear combinations were interpreted as representing a network of genes which control multiple traits through their pleiotropic effects. The pathways identified included an adaptive complex, SAR, radial/vascular patterning, vegetative-phase change, and tassel branching/meristem initiation. The SAR pathway was targeted for further analysis. Confirmation of SAR as a pathway influencing SBR-patterning utilized mutant analysis, field experiments, and association analysis (Chapter 5). Phenotyping of *phyB* double mutants, which constitutively express the SAR, revealed that the SAR decreases SBR formation, a result also predicted by the principal component regression analysis. To provide evidence SBR depletion was due to a light stimulated response, SBR-patterning was evaluated under four different planting densities in four

inbred lines (Chapter 5). The data indicated that increased planting density led to reductions in SBR formation. Furthermore, statistical analysis revealed a significant genotype-by-treatment component suggesting genetic variation within genes regulating SBR-response to planting density. To take advantage of this discovery, allelic variation at an upstream region of *phyB2* was tested for associations to SBR-patterning (Chapter 5). However, no significant association was identified in this region. Taken together, the PCA, mutant analysis, and planting density experiments suggest that light-signaling genes hold promise for future investigations and molecular manipulation of SBR-patterning.

A previous study conducted in maize identified a redistribution of biomass, observed as a change in the ratio of root: shoot dry weight under control and a neutral shaded treatment consisting of low light quantity (Hébert et al., 2001). In contrast to the data presented in Chapter 5, the light treatment effect in Hébert et al. (2001) was non-significant at nodes two through eight, while genotype was a significant factor affect SBR number at all nodes. Hébert et al. (2001) found that genotype-by-environment interactions were significant for SBR count on node three, six, seven, nine, ten, and 11. The difference between the affect of shading on SBR-patterning in our study vs. that of Hébert et al. (2001) may be due to different experimental designs. First the light treatment is different on two levels. The neutral shade used by Hébert et al. alters only light quantity while the planting density study presented in Chapter 5 impacts both the quantity and quality of light. Additionally, Hébert et al. (2001) grew their plants as isolated individuals in the field while our plants were grown in bordered rows. The impacts of growing isolated plants versus plants in a row are two-fold. First, a greater degree of SAR may be experienced in five or ten plant rows relative to an isolated but neutrally shaded plant, and second, inter-plant competition for water and nutrients is likely to be present in the our study but not in isolated plants. These differences suggest that our treatment, while less controlled, is more similar to conditions observed during production. An appropriate comparison between the two methods

would require data on light quality and quantity on each treatment which is not available. The second design difference is the germplasm used. Hébert et al. (2001) used French hybrids while our study examined diverse inbreds. The hybrid nature of the lines in Hébert et al. (2001) may result in them being more robust in the face of shading. On the other hand if they contain F2 (an inbred line of French origin) or F2-related lines in their pedigree, they may contain loss-of-function *phyB2* alleles impairing their ability to respond to shade.

These results lead to an important question. What are the effects of changes in light quality vs. quantity exemplified by the SAR on SBR formation? The previous studies do not uncouple these effects. Experimentally the effect of these stimuli on SBR-patterning could be investigated by comparing SBR-patterning of maize inbreds grown under a neutral shade canopy, which reduces the light quantity (but not quality) with a control, and also comparing SBR formation in inbred lines subjected to end of day far-red light with controls. Although Hébert et al. (2001) examined SBR-patterning under neutral shade, differences in their methodology impairs our ability to interpret the results directly in the context of uncoupling the effects of light quality from those of light quantity.

Integration of the GA and Light-Signaling models of SBR-Patterning

The notion of interplay between light-signaling and GA activity is not new (Talon et al., 1991; Reed et al., 1996; Peng and Harberd, 1997; Kamiya and Gracía-Martínez, 1999). Although previous research documented the relationship between low light/PHYB activity and GA production, it did not predict how GA may function to suppress SBRs due to SAR. Based on the literature and the studies presented in the previous chapters we have extended the GA "early and distal" and "late and local" models to include predicting the effect of the SAR on SBR-patterning. First the "early and distal" model predicts that the SAR would suppress SBR by increasing GA levels in the SAM and as a result alter the distribution of *miR156* and hence the SBR-patterning. Evidence from the *phyB* double mutant phenotyping study suggests this model is false. If PHYB

regulated SBR-patterning in this way, we would expect to see significant reductions in juvenile leaf number which are not observed in the double mutants (Table 26, Chapter 5). Additionally, significant reductions in juvenile leaf number are not present in the planting density experiment (data not shown). Preliminary data suggests that the SBR phenotypes of *Tp1* mutants are also suppressed by shading (data not shown). The "early and distal" model could be further tested by planting *Tp1* and *Tp2* under different planting densities, by evaluation of *phyB, Teopod* triple mutants, or by quantification of *miR156* in *phyB* double mutant, and control plants.

The "late and local" model is a more likely explanation for the interaction of GA in the light-regulation of SBR-patterning. This model suggests that GA activity is reduced in response to SAR-mediated PHYB inactivation. Morelli and Ruberti (2000) propose a similar mechanism for the role of auxin in the SAR. In their model, auxin initiates SBR-patterning by accumulating in the vasculature and establishing a meristem. The SAR redistributes auxin from the developing vasculature to the epidermal and cortical cells to promote upward growth (Figure 32). Recent transcriptome analysis in *Arabidopsis* suggests that auxin activity regulates GA metabolism and that GA activity mediates a component of auxin response (Frigerio et al., 2006). With GA as a component of auxin response, alterations of the transport of auxin would subsequently impact both GA and DELLA activity. This has been observed by Fu and Harberd (2002) in primary root elongation in Arabidopsis. Further support for this hypothesis comes from studies of root patterning in *brachytic2* (*br2*) which encodes a light-dependent multi-drug resistance P-glycoprotein. Significant differences in SBR-patterning were observed between *br2* and *wild-type* maize plants (data not shown) further implicating light-signaling in SBR-patterning. Additional testing of the "late and local" model could be accomplished by observing SBR-patterning in double mutants between *br2* and *d3* or *d5*. *br2* suppression of SBR formation in GA-deficient mutants would suggest that the light-dependent auxin transport activity dictates GA-stimulated SBR formation, thus linking a SAR-mediated redistribution of auxin-GA activity, resulting in

shoot growth at the expense of SBR growth. Under this model, when sufficient light conditions are present, auxin accumulates in the vasculature, initiating a meristematic region from which a SBR will emerge. Auxin activity stimulates GA production, resulting in DELLA degradation in neighboring tissues which in turn activates growth, PCD, and transcription of cell-wall-modifying proteins (Figure 2A). Alternatively when light is insufficient, the SAR leads to redistribution of auxin out of the vasculature at the expense of SBR formation, prompting internode elongation via GA-directed cell expansion (Figure 2B). This model provides a schematic of the molecular basis for the suppression of SBRs by SAR through control of the spatial activities of auxin and GA.

SBR-patterning is complex. The final SBR phenotype of a plant is determined by both genetic and environmental factors. The previous research provided evidence of genetic networks, more specifically GA and light-signaling, that controls SBR-patterning. Understanding the roles of these networks is both academically engaging and agriculturally important. By partnering high-throughput transcriptome, proteome, and metabolome data with the phenotype and haplotype data presented here, we can further elucidate the individual genes and pathways contributing to SBR-patterning and unravel how these networks work synergistically to define the physiological basis of SBR-patterning.

REFERENCES

CAO, D., H. CHENG, W. WU, H. M. SOO, and J. PENG, 2006 Gibberellin mobilizes distinct DELLA-dependent transcriptomes to regulate seed germination and floral development in *Arabidopsis*. Plant Physiol. **142(2):** 509-525.

EVANS, M. M. and R. S. POETHIG, 1995 Gibberellins promote vegetative phase change and reproduction in maize. Plant Physiol. **108(2)**: 475-487.

FRIGERIO, M., D. ALABADÍ, J. PÉREZ-GÓMEZ, L. GARCÍA-CÁRCEL, A. L. PHILLIPS, P. HEDDEN, and M. A. BLÁZQUEZ, 2006 Transcriptional regulation of gibberellin metabolism genes by auxin signaling in *Arabidopsis*. Plant Physiol. **142(2):** 553-563.

FU, X. and N. P. HARBERD, 2003 Auxin promotes *Arabidopsis* root growth by modulating gibberellin response. Nature **421(6924):** 740-743.

FUJIOKA, S., H. YAMANE, C. R. SPRAY, M. KATSUMI, B. O. PHINNEY, P. GASKIN, J. MACMILLAN, and N. TAKAHASHI, 1988 The dominant non-gibberellin-responding dwarf mutant (*D8*) of maize accumulates native gibberellins. Proc. Natl. Acad. Sci. U. S. A. **85(23):** 9031-9035.

HÉBERT, Y., E. GUINGO, and O. LOUDET, 2001 The response of root/shoot partitioning and root morphology to light reduction in maize genotypes. Crop Sci. **41:** 363-371.

KAMIYA, Y. and J. L. GARCÍA-MARTÍNEZ, 1999 Regulation of gibberellin biosynthesis by light. Curr. Opin. Plant Biol. **2(5):** 398-403.

KUTEJOVA, E., J. BRISCOE, and A. KICHEVA, 2009 Temporal dynamics of patterning by morphogen gradients. Curr. Opin. Genet. Dev. **19(4):** 315-322.

MORELLI, G. and I. RUBERTI, 2000 Shade avoidance responses. Driving auxin along lateral routes. Plant Physiol. **122(3):** 621-626.

MULTANI, D. S., S. P. BRIGGS, M. A. CHAMBERLIN, J. J. BLAKESLEE, A. S. MURPHY, and G. S. JOHAL, 2003 Loss of an MDR transporter in compact stalks of maize *br2* and sorghum *dw3* mutants. Science **302(5642):** 81-84.

PENG, J. and N. P. HARBERD, 1997 Gibberellin deficiency and response mutations suppress the stem elongation phenotype of phytochrome-deficient mutants of *Arabidopsis*. Plant Physiol. **113(4):** 1051-1058.

REED, J. W., K. R. FOSTER, P. W. MORGAN, and J. CHORY, 1996 Phytochrome B affects responsiveness to gibberellins in *Arabidopsis*. Plant Physiol. **112(1):** 337-342.

SONG, R., S. RO, and W. YAN, 2010 *In situ* hybridization detection of microRNAs. Methods Mol. Biol. **629:** 287-294.

TALON, M., J. A. ZEEVAART, and D. A. GAGE, 1991 Identification of gibberellins in spinach and effects of light and darkness on their levels. Plant Physiol. **97(4):** 1521-1526.

UBEDA-TOMÁS, S., R. SWARUP, J. COATES, K. SWARUP, L. LAPLAZE, G. T. BEEMSTER, P. HEDDEN, R. BHALERAO, and M. J. BENNETT, 2008 Root growth in *Arabidopsis* requires gibberellin/DELLA signalling in the endodermis. Nat. Cell. Biol. **10(5):** 625-628.

UBEDA-TOMÁS, S., F. FEDERICI, I. CASIMIRO, G. T. BEEMSTER, R. BHALERAO, R. SWARUP, P. DOERNER, J. HASELOFF, and M. J. BENNETT, 2009 Gibberellin signaling in the endodermis controls *Arabidopsis* root meristem size. Curr. Biol. **19(14):** 1194-1199.

FIGURES

Figure 31. Model describing regulatory feedback of GA production by DELLA activity resulting from natural allelic variation.

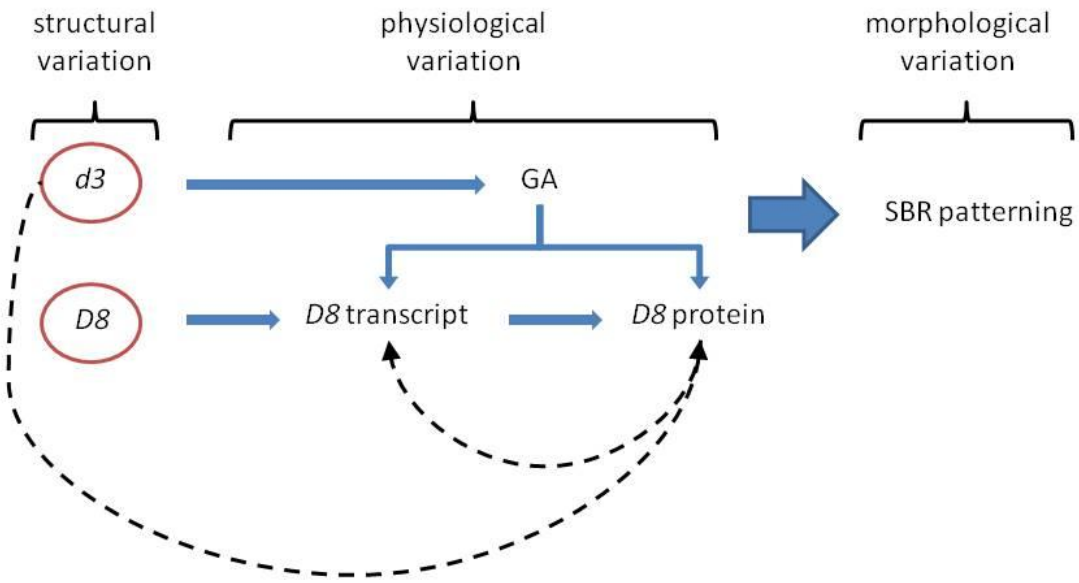

Figure 32. Light-regulated distribution of auxin-GA mediated SBR-patterning.

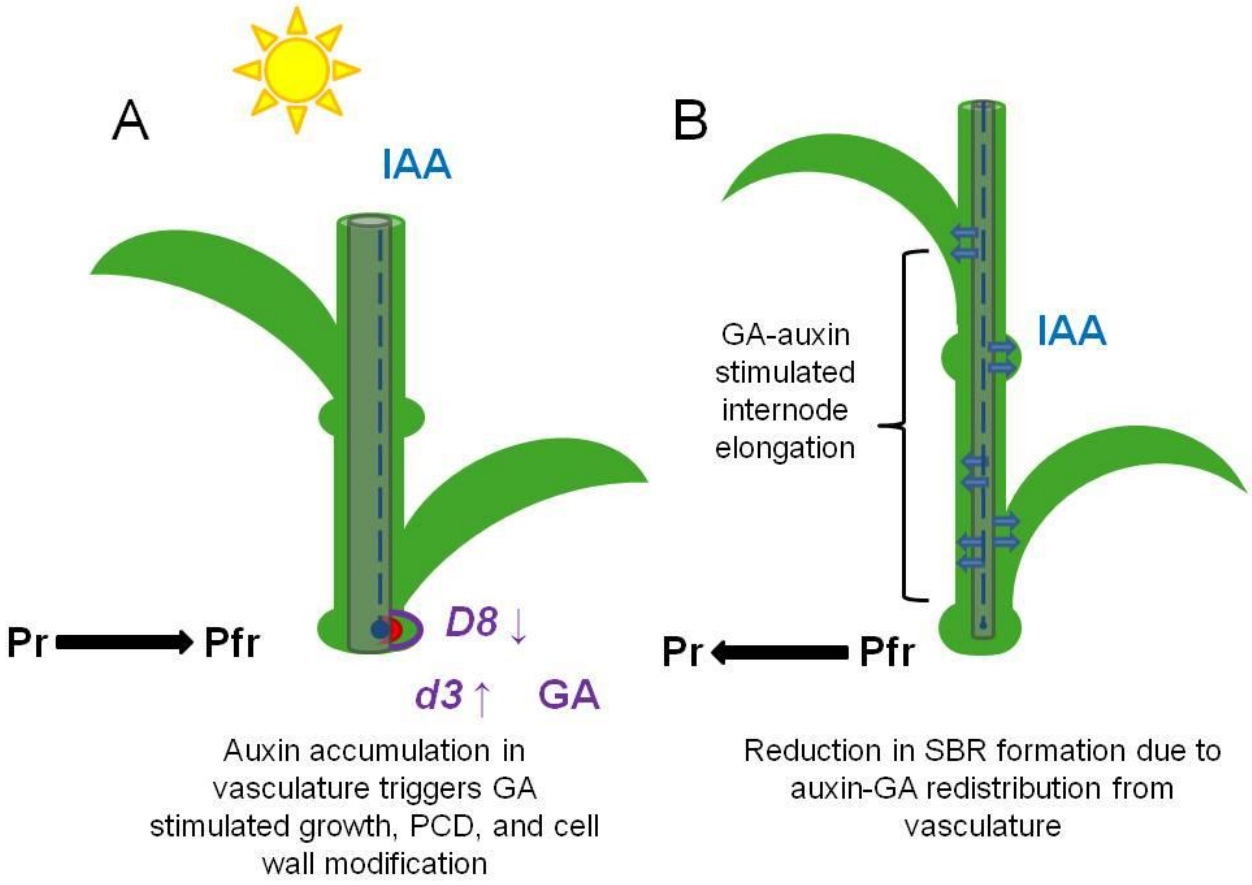

Appendix 1: Linkage map used in the QTL analyses.

Chrom	Marker # Map[a]	Marker # Chrom[b]	Marker Name	Position[c]	Position[d]
1	1	1	*umc1354*	0.0	0.0
1	2	2	*phi056*	2.1	5.6
1	3	3	*umc1177*	6.8	11.4
1	4	4	*umc1566*	10.1	19.5
1	5	5	*mmp102*	19.5	31.9
1	6	6	*umc94a*	25.0	46.4
1	7	7	*lim179*	33.4	57.4
1	8	8	*mmp49*	41.7	71.2
1	9	9	*npi415*	52.5	86.1
1	10	10	*ufg34*	59.9	94.7
1	11	11	*umc1269*	66.1	105.7
1	12	12	*umc1977*	70.6	107.4
1	13	13	*php20689*	82.0	125.9
1	14	14	*umc1160*	87.7	135.8
1	15	15	*umc157a(chn)*	96.3	142.9
1	16	16	*mmp68*	104.4	156.7
1	17	17	*csu1171*	111.1	159.6
1	18	18	*umc1166*	119.5	166.8
1	19	19	*umc1568*	125.5	178.7
1	20	20	*lim504*	132.1	190.5
1	21	21	*umc1976*	141.6	204.2
1	22	22	*bnlg1953*	149.5	216.1
1	23	23	*npi403b*	165.1	237.0
1	24	24	*umc76a*	185.6	259.3
1	25	25	*lim122*	189.5	267.7
1	26	26	*umc1403*	191.4	272.6
1	27	27	*bnlg1484*	200.3	286.2
1	28	28	*AY110052*	213.1	300.3
1	29	29	*AY110028*	231.5	323.3
1	30	30	*umc1479*	241.3	334.8
1	31	31	*AY110640*	250.4	345.6
1	32	32	*asg35b*	258.9	359.0
1	33	33	*ndp2*	267.6	371.5
1	34	34	*umc1598*	272.5	381.1
1	35	35	*mmp151a*	278.5	388.1
1	36	36	*mmp100*	291.1	404.7
1	37	37	*mmp56*	303.6	415.5
1	38	38	*umc2124a*	305.9	420.2

1	39	39	*sod4*	312.5	430.7
1	40	40	*AY110330*	315.5	439.8
1	41	41	*umc2227*	321.6	445.9
1	42	42	*ufg77*	327.7	451.5
1	43	43	*ufg43*	335.8	459.7
1	44	44	*bnl9.11b(lts)*	343.0	471.9
1	45	45	*bnlg2295*	350.1	484.5
1	46	46	*csu3*	357.6	495.4
1	47	47	*umc2025*	371.5	507.4
1	48	48	*umc1515*	378.6	520.9
1	49	49	*umc1076*	387.9	532.1
1	50	50	*umc1676*	389.2	533.7
1	51	51	*cdo344c(rga)*	391.2	537.8
1	52	52	*umc2232*	397.6	546.8
1	53	53	*hac101b*	401.5	554.1
1	54	54	*umc67a*	410.4	563.8
1	55	55	*umc1972*	412.8	570.5
1	56	56	*myb6*	427.7	588.8
1	57	57	*asg58*	434.1	602.6
1	58	58	*umc1123*	439.7	612.9
1	59	59	*mmp156*	448.2	625.9
1	60	60	*umc1919*	457.8	641.2
1	61	61	*umc2151*	472.9	652.5
1	62	62	*ntf1*	482.5	657.9
1	63	63	*mmp123*	502.0	673.8
1	64	64	*umc1924*	515.1	690.4
1	65	65	*umc1925*	523.8	700.4
1	66	66	*asg62*	524.4	700.9
1	67	67	*umc2237*	544.3	718.9
1	68	68	*umc2239*	555.8	733.1
1	69	69	*mdh6*	565.9	747.6
1	70	70	*bcd98a*	573.7	756.6
1	71	71	*bnlg1556*	581.6	770.1
1	72	72	*umc23a*	591.7	788.5
1	73	73	*lim442*	613.4	810.4
1	74	74	*mmp173*	621.1	817.6
1	75	75	*bnlg1025*	625.6	827.4
1	76	76	*umc1128*	630.9	835.5
1	77	77	*umc128*	638.9	847.1
1	78	78	*AY110313*	649.5	853.0
1	79	79	*cdo98b*	659.5	861.3
1	80	80	*bnlg2228*	668.0	872.4

1	81	81	*npi120*	670.4	880.0
1	82	82	*npi255*	675.7	887.6
1	83	83	*an1*	677.8	894.0
1	84	84	*umc1991*	691.6	908.2
1	85	85	*cdj2*	710.8	922.8
1	86	86	*csu696*	714.4	928.4
1	87	87	*chrom7*	725.8	945.7
1	88	88	*umc2047*	727.8	952.9
1	89	89	*AY110452*	744.1	973.5
1	90	90	*umc197a(rip)*	760.2	984.7
1	91	91	*csu554a(rnh)*	771.5	996.7
1	92	92	*umc107a(croc)*	778.9	1005.2
1	93	93	*nfa103a*	785.6	1010.7
1	94	94	*adh1*	793.2	1020.9
1	95	95	*bnlg1671a*	798.8	1028.6
1	96	96	*rz630a(sat)*	801.1	1032.7
1	97	97	*lim78*	811.8	1042.2
1	98	98	*mmp87*	818.5	1050.3
1	99	99	*lim39*	826.5	1062.6
1	100	100	*umc161a*	840.2	1084.0
1	101	101	*phi265454*	847.1	1097.5
1	102	102	*AY110426*	870.7	1117.3
1	103	103	*mmp195g*	886.9	1131.5
1	104	104	*umc1421*	891.4	1140.1
1	105	105	*bnl8.29a*	892.8	1148.9
1	106	106	*umc2241*	897.0	1160.8
1	107	107	*AY110479*	909.9	1172.6
1	108	108	*umc1744*	920.8	1191.6
1	109	109	*umc1630*	922.7	1199.2
1	110	110	*AY110160*	935.7	1211.6
1	111	111	*lim228*	974.4	1254.1
1	112	112	*phi064*	981.8	1263.2
1	113	113	*bnl6.32*	999.9	1280.4
1	114	114	*umc1605*	1001.9	1286.4
1	115	115	*umc2244*	1005.1	1290.1
1	116	116	*AY109916*	1020.6	1292.6
2	117	1	*isu53a*	0.0	0.0
2	118	2	*isu144a*	18.4	32.4
2	119	3	*php20568b*	22.5	39.7
2	120	4	*umc1165*	29.0	55.2
2	121	5	*umc1542*	41.2	72.1
2	122	6	*bnlg1017*	53.2	79.9

2	123	7	*umc1980*	68.5	92.7
2	124	8	*BE640649*	78.0	102.3
2	125	9	*umc1824a*	84.8	110.6
2	126	10	*tps1*	106.9	151.4
2	127	11	*bnlg2277*	119.0	183.7
2	128	12	*umc1262*	128.2	199.0
2	129	13	*umc6a*	134.4	213.6
2	130	14	*lim328*	145.0	223.2
2	131	15	*umc44b*	158.6	242.0
2	132	16	*umc61*	171.9	257.4
2	133	17	*mmp33*	180.2	272.2
2	134	18	*psr901*	190.3	285.7
2	135	19	*AI920398*	204.1	303.6
2	136	20	*AY104214*	212.1	326.2
2	137	21	*phi109642*	213.9	334.0
2	138	22	*umc2247*	215.6	341.0
2	139	23	*sam2*	224.4	355.1
2	140	24	*umc1541*	227.9	366.2
2	141	25	*prp2*	234.3	377.4
2	142	26	*bnlg1018*	237.2	383.3
2	143	27	*mmp91*	247.8	393.9
2	144	28	*umc2030*	253.7	403.8
2	145	29	*php10012*	256.1	410.6
2	146	30	*mmp89*	261.4	426.1
2	147	31	*umc131*	264.2	429.7
2	148	32	*zpu1*	265.5	431.2
2	149	33	*csu1080b*	271.6	439.6
2	150	34	*pbf1*	277.0	450.5
2	151	35	*umc1080*	286.4	467.9
2	152	36	*umc1108*	297.7	500.1
2	153	37	*umc2129*	305.3	511.2
2	154	38	*umc1890*	310.2	525.5
2	155	39	*rz474c(dnaj)*	326.4	552.2
2	156	40	*phi251315*	331.3	558.5
2	157	41	*AY109722*	338.4	566.4
2	158	42	*umc1560*	351.7	580.2
2	159	43	*asg20*	354.6	586.8
2	160	44	*mmp116*	355.7	589.7
2	161	45	*mmp84*	370.3	613.3
2	162	46	*umc137a*	378.3	624.6
2	163	47	*phi435417*	379.8	632.6
2	164	48	*umc1604*	385.6	637.3

2	165	49	*npi210*	394.9	656.6
2	166	50	*npi298*	398.5	663.7
2	167	51	*mmp34*	403.3	675.5
2	168	52	*mmc0381*	410.7	692.3
2	169	53	*psr144c*	421.2	699.5
2	170	54	*umc49a*	427.8	715.3
2	171	55	*umc1252*	437.0	730.4
2	172	56	*mmp195e*	473.2	786.9
2	173	57	*bnlg469b*	487.0	806.3
2	174	58	*umc36a*	498.8	820.5
2	175	59	*AY110389*	523.4	854.5
2	176	60	*mmp183*	538.2	872.4
2	177	61	*lim104*	547.5	886.7
2	178	62	*zap1*	553.2	898.2
3	179	1	*umc1931*	0.0	0.0
3	180	2	*bnl8.15*	4.0	9.0
3	181	3	*umc1394*	15.2	27.2
3	182	4	*mmp158a*	19.9	39.5
3	183	5	*umc2049*	23.3	48.6
3	184	6	*umc121*	39.6	71.2
3	185	7	*csu32a*	40.8	76.5
3	186	8	*umc1458*	51.4	87.5
3	187	9	*umc1886*	62.0	104.3
3	188	10	*eif3*	72.8	127.8
3	189	11	*asg24a(gts)*	88.7	146.6
3	190	12	*lim66*	106.9	173.8
3	191	13	*mmp79*	119.2	195.9
3	192	14	*asg48*	130.5	215.7
3	193	15	*umc1030*	134.3	229.9
3	194	16	*umc1608*	143.3	234.7
3	195	17	*umc1495*	152.2	249.0
3	196	18	*umc1742*	161.5	267.6
3	197	19	*mmp144*	165.5	271.9
3	198	20	*mmc0132*	171.5	289.5
3	199	21	*AY109870*	177.0	293.3
3	200	22	*umc2263*	183.4	298.7
3	201	23	*umc1223*	189.1	303.6
3	202	24	*AY110297*	201.3	316.2
3	203	25	*AY110151*	211.5	325.9
3	204	26	*mmp9*	217.6	331.7
3	205	27	*umc1449*	225.6	336.8
3	206	28	*jpsb527a*	235.4	344.0

3	207	29	*umc102*	246.4	355.6
3	208	30	*phys2*	251.1	361.5
3	209	31	*umc1102*	252.2	366.1
3	210	32	*umc1501*	259.7	382.3
3	211	33	*AY111541*	267.0	383.6
3	212	34	*umc26a*	281.2	402.0
3	213	35	*umc2265*	300.7	424.9
3	214	36	*csu636*	314.9	436.5
3	215	37	*AY106230*	329.1	461.2
3	216	38	*umc1539*	338.5	471.3
3	217	39	*lim486*	352.6	493.3
3	218	40	*asg39*	361.0	508.2
3	219	41	*BE639846*	367.4	517.4
3	220	42	*umc2266*	377.5	531.0
3	221	43	*phi102228*	388.3	554.2
3	222	44	*umc60*	391.4	574.2
3	223	45	*umc2268*	399.4	584.9
3	224	46	*umc1644*	411.6	588.8
3	225	47	*csu1183*	415.3	590.5
3	226	48	*bnlg1160*	422.4	596.8
3	227	49	*lim424*	433.5	614.3
3	228	50	*bnlg197*	436.0	623.9
3	229	51	*asg7b*	436.5	628.5
3	230	52	*bnl6.16a*	438.8	629.6
3	231	53	*umc3b*	443.7	638.9
3	232	54	*umc1135*	451.7	652.2
3	233	55	*AY104511*	472.8	683.1
3	234	56	*umc1404*	479.6	688.7
3	235	57	*umc1825*	491.3	706.2
3	236	58	*umc17a*	497.3	716.1
3	237	59	*AY105849*	508.0	735.2
3	238	60	*mmc0251*	522.3	752.7
3	239	61	*bnlg1108*	526.0	759.3
3	240	62	*umc2081*	535.1	771.0
3	241	63	*umc1273*	540.8	778.5
3	242	64	*umc2276*	559.3	794.5
3	243	65	*umc2174*	590.8	832.0
3	244	66	*umc63a*	594.7	844.6
3	245	67	*csu845*	601.7	851.1
3	246	68	*jpsb107c*	628.5	887.0
3	247	69	*umc2152*	635.6	903.2
3	248	70	*lim182*	640.4	910.6

3	249	71	*bnlg1754*	652.5	926.9
3	250	72	*AY110567*	662.8	939.8
3	251	73	*npi420*	683.7	970.6
3	252	74	*umc1641*	698.2	998.9
3	253	75	*lim96*	707.4	1018.5
3	254	76	*umc1594*	709.2	1026.1
4	255	1	*umc2278*	0.0	0.0
4	256	2	*msf1*	9.4	10.4
4	257	3	*umc123*	15.1	20.7
4	258	4	*bx4*	30.2	38.8
4	259	5	*bx2*	44.6	69.7
4	260	6	*umc1669*	53.7	110.9
4	261	7	*umc1759*	71.0	136.2
4	262	8	*php20725a*	73.5	195.0
4	263	9	*umc1943*	95.3	195.2
4	264	10	*umc31a*	132.6	196.1
4	265	11	*umc1926*	144.7	206.4
4	266	12	*AY110253*	155.4	222.1
4	267	13	*AY110573*	166.7	234.4
4	268	14	*umc2176*	179.8	248.2
4	269	15	*umc1902*	187.1	255.2
4	270	16	*bx7*	195.1	268.8
4	271	17	*wip2*	197.7	279.6
4	272	18	*umc1117*	208.9	296.1
4	273	19	*umc1652*	214.5	304.1
4	274	20	*bnlg490*	221.2	310.7
4	275	21	*umc1969*	228.5	315.7
4	276	22	*gpc1*	235.3	330.4
4	277	23	*bnlg1265*	241.3	345.5
4	278	24	*Nnr1*	247.3	353.0
4	279	25	*umc42a*	253.7	360.0
4	280	26	*umc1511*	255.8	364.0
4	281	27	*umc1346*	260.0	372.7
4	282	28	*mmp78*	267.7	375.6
4	283	29	*AY110562*	282.5	382.6
4	284	30	*umc1945*	297.2	388.8
4	285	31	*umc2027*	315.1	416.1
4	286	32	*AY110310*	323.0	430.4
4	287	33	*rz567b(klc)*	330.6	447.7
4	288	34	*umc66a(lcr)*	353.5	482.8
4	289	35	*umc2038*	359.2	498.6
4	290	36	*mmp115a*	367.9	511.1

4	291	37	*bnl5.24b*	374.7	526.2
4	292	38	*umc1775*	387.3	551.6
4	293	39	*umc1808*	397.9	573.2
4	294	40	*bnlg1444*	401.4	580.7
4	295	41	*umc158*	408.7	593.0
4	296	42	*npi570*	415.4	598.9
4	297	43	*AY112127*	421.2	605.3
4	298	44	*ufg23*	436.9	622.7
4	299	45	*AY110631*	453.6	632.9
4	300	46	*ssu1*	462.3	640.8
4	301	47	*umc1842*	468.3	649.9
4	302	48	*umc2135*	473.7	656.4
4	303	49	*umc52a*	483.9	673.7
4	304	50	*umc2139*	487.0	687.5
4	305	51	*umc1999*	495.7	698.0
4	306	52	*umc1854*	508.4	719.0
4	307	53	*mmp94*	512.1	726.9
4	308	54	*zfp30*	514.3	734.8
4	309	55	*sbp2*	531.6	761.5
4	310	56	*umc1101*	538.8	774.3
4	311	57	*php20608a*	552.2	794.4
4	312	58	*umc124b(chk)*	554.9	798.4
4	313	59	*umc1109*	570.4	824.3
4	314	60	*umc1180*	576.0	828.1
4	315	61	*umc2289*	582.0	849.0
4	316	62	*AY109611*	589.4	855.6
4	317	63	*umc169a*	600.0	870.3
4	318	64	*bip2*	616.5	883.6
4	319	65	*umc1707*	620.2	889.1
5	320	1	*AI676903*	0.0	0.0
5	321	2	*AY110625*	16.0	14.5
5	322	3	*umc1253*	23.1	21.2
5	323	4	*umc1423*	29.8	31.0
5	324	5	*umc1097*	34.7	36.8
5	325	6	*umc1901*	38.8	45.3
5	326	7	*umc1260*	50.5	65.3
5	327	8	*npi409a*	52.3	67.1
5	328	9	*lim407*	60.6	87.6
5	329	10	*AY109733*	63.4	93.6
5	330	11	*umc2036*	94.0	143.6
5	331	12	*rz630f(sat)*	105.2	161.4
5	332	13	*asg73*	116.0	173.8

5	333	14	*umc1587*	126.4	182.8
5	334	15	*cdo122b(nad)*	131.2	192.1
5	335	16	*mmp130*	156.1	217.1
5	336	17	*bnlg1879*	162.5	230.0
5	337	18	*umc2293*	170.4	241.3
5	338	19	*rz474a(dnaj)*	175.1	250.4
5	339	20	*umc1597*	189.2	270.6
5	340	21	*umc2035*	197.4	278.4
5	341	22	*bnl5.02a*	201.2	283.5
5	342	23	*lim175*	207.3	293.6
5	343	24	*ufg49*	214.9	309.9
5	344	25	*umc1609*	222.1	322.9
5	345	26	*dwf1*	225.1	329.6
5	346	27	*bnlg1902*	232.5	342.0
5	347	28	*umc40*	241.7	350.7
5	348	29	*umc1990*	247.9	360.3
5	349	30	*npi449a*	260.0	373.5
5	350	31	*umc1349*	267.8	390.3
5	351	32	*myb3*	276.0	400.8
5	352	33	*csu308*	280.1	408.0
5	353	34	*umc1482*	289.5	422.7
5	354	35	*phi333597*	299.9	435.8
5	355	36	*umc1264*	309.2	447.3
5	356	37	*nbp35*	315.0	456.8
5	357	38	*serk2*	333.5	457.3
5	358	39	*mmp104*	356.1	497.8
5	359	40	*umc126a*	369.5	514.9
5	360	41	*umc54*	376.3	526.0
5	361	42	*umc1524*	391.0	546.8
5	362	43	*bnlg609*	399.9	556.1
5	363	44	*rz567a(klc)*	408.2	572.0
5	364	45	*ant1*	418.3	585.6
5	365	46	*npi442*	427.1	601.1
5	366	47	*umc108*	427.9	610.7
5	367	48	*bnlg1118*	480.1	684.2
5	368	49	*umc1072*	484.8	697.1
5	369	50	*bnlg118*	495.7	713.9
5	370	51	*mmp170*	507.6	731.1
5	371	52	*AY110413*	516.0	745.4
5	372	53	*umc1225*	523.6	760.2
5	373	54	*mmp175*	525.3	765.0
5	374	55	*php10017*	543.8	793.0

6	375	1	*umc49f*	0.0	0.0
6	376	2	*umc1143*	23.3	25.1
6	377	3	*umc2310*	27.4	41.1
6	378	4	*gpc2*	53.5	81.0
6	379	5	*umc85a*	59.3	88.5
6	380	6	*bnlg1867*	66.0	101.0
6	381	7	*php20854*	69.2	110.8
6	382	8	*umc2313*	77.7	111.4
6	383	9	*mmp160*	88.9	114.4
6	384	10	*mmp10*	95.8	117.0
6	385	11	*umc1006*	102.2	122.8
6	386	12	*jpsb108*	111.5	142.6
6	387	13	*csu923(sec61)*	117.1	150.5
6	388	14	*AY104775*	125.2	164.4
6	389	15	*umc65a*	129.9	174.8
6	390	16	*rz476d*	137.1	185.5
6	391	17	*umc1857*	145.9	198.7
6	392	18	*pl1*	155.1	210.9
6	393	19	*umc2006*	173.6	235.9
6	394	20	*isu61f*	180.5	252.0
6	395	21	*isu111a*	181.2	257.5
6	396	22	*uaz280c(ppp)*	191.7	272.7
6	397	23	*csu481*	196.4	282.3
6	398	24	*umc1352a*	198.4	290.9
6	399	25	*umc1114*	207.9	304.2
6	400	26	*AY110542*	218.5	315.7
6	401	27	*umc1388*	227.5	324.3
6	402	28	*jpsb107b*	234.7	333.1
6	403	29	*pmg1*	242.0	340.9
6	404	30	*npi608*	270.8	366.0
6	405	31	*uaz121a*	289.0	395.1
6	406	32	*rz444d*	303.2	410.4
6	407	33	*umc38a*	311.3	421.6
6	408	34	*umc1762*	314.4	429.6
6	409	35	*umc2322*	320.6	440.4
6	410	36	*lim379*	336.8	460.0
6	411	37	*lim151*	342.2	462.5
6	412	38	*umc2170*	350.2	479.1
6	413	39	*umc132a(chk)*	357.7	490.8
6	414	40	*mlg3*	366.2	502.1
6	415	41	*umc1490*	378.4	524.7
6	416	42	*AY110400*	386.8	531.2

6	417	43	*npi419a*	401.6	542.7
6	418	44	*mmp113*	413.3	555.6
6	419	45	*umc1350*	419.3	563.6
6	420	46	*umc62*	425.7	575.1
6	421	47	*npi561*	437.1	591.8
6	422	48	*mmp105*	445.8	602.4
6	423	49	*umc2059*	455.4	617.2
7	424	1	*csu582*	0.0	0.0
7	425	2	*cka4*	18.1	17.6
7	426	3	*umc1378*	32.5	38.8
7	427	4	*umc1672*	53.8	65.1
7	428	5	*bnlg2132*	60.0	79.2
7	429	6	*asg8(myb)*	68.2	91.7
7	430	7	*php20581a(tb)*	79.3	108.7
7	431	8	*AW308691*	91.0	126.1
7	432	9	*umc1159*	99.9	134.0
7	433	10	*mmp18*	123.7	169.2
7	434	11	*o2*	127.6	176.3
7	435	12	*asg34a(msd)*	128.2	183.1
7	436	13	*gta101a*	148.1	209.7
7	437	14	*umc2327*	149.5	214.3
7	438	15	*npi600*	151.7	219.1
7	439	16	*cyp6*	156.9	229.1
7	440	17	*bnlg1380*	160.0	238.1
7	441	18	*lim333*	162.2	243.4
7	442	19	*umc1932*	170.0	255.2
7	443	20	*AY109968*	203.6	286.3
7	444	21	*umc1983*	236.2	308.7
7	445	22	*umc1393*	253.8	326.5
7	446	23	*mmp21*	258.9	333.9
7	447	24	*ufg54*	274.5	361.1
7	448	25	*bnlg1808*	280.9	366.9
7	449	26	*mmp127*	283.2	367.2
7	450	27	*php20569a*	292.9	383.6
7	451	28	*bnl15.21*	301.9	400.4
7	452	29	*bnlg1070*	312.9	413.8
7	453	30	*npi394*	324.0	423.2
7	454	31	*mmp152*	340.7	441.5
7	455	32	*npi389*	346.2	450.3
7	456	33	*umc56*	354.9	459.5
7	457	34	*rz404(ccp)*	360.7	467.3
7	458	35	*bnlg2271*	361.8	473.2

7	459	36	*isu150*	368.4	483.4
7	460	37	*tif1*	376.7	491.5
7	461	38	*umc1710*	387.3	501.9
7	462	39	*asg32*	394.9	510.4
7	463	40	*bnlg1666*	409.0	525.9
7	464	41	*bnl8.29c*	419.6	540.3
7	465	42	*bcd349*	444.7	576.0
7	466	43	*umc1708*	448.2	586.2
7	467	44	*umc1768*	453.6	591.8
7	468	45	*bnlg2259*	460.9	601.4
7	469	46	*ufg57*	467.8	615.7
7	470	47	*umc1412*	502.3	651.3
7	471	48	*umc245*	516.0	672.8
7	472	49	*phi069*	527.1	687.0
7	473	50	*cdo938d*	560.4	738.0
7	474	51	*umc1406*	568.7	751.1
7	475	52	*umc168*	574.7	761.4
7	476	53	*AY109703*	585.8	776.0
8	477	1	*npi220a*	0.0	0.0
8	478	2	*csu319*	8.9	9.0
8	479	3	*npi114a*	13.3	12.4
8	480	4	*umc1139*	39.6	39.0
8	481	5	*umc1592*	48.6	45.3
8	482	6	*bnl13.05a*	62.2	60.8
8	483	7	*umc1327*	73.0	80.4
8	484	8	*umc1483*	106.7	126.2
8	485	9	*mmp85*	131.6	151.8
8	486	10	*umc2352a*	137.1	162.9
8	487	11	*cdo460*	147.4	175.5
8	488	12	*mmp57*	148.6	177.4
8	489	13	*mmp166*	169.2	208.6
8	490	14	*umc1974*	185.2	228.8
8	491	15	*umc1913*	190.4	238.1
8	492	16	*umc124a(chk)*	207.6	262.6
8	493	17	*umc1530*	209.3	264.3
8	494	18	*mmp120*	224.4	280.5
8	495	19	*bnlg2082*	231.1	287.4
8	496	20	*npi260b*	234.5	294.0
8	497	21	*umc1910*	240.7	300.6
8	498	22	*php3818*	246.0	308.5
8	499	23	*umc1984*	250.4	310.3
8	500	24	*umc2075*	259.1	317.2

8	501	25	*AY110032*	274.6	326.6
8	502	26	*AY109740*	303.8	344.0
8	503	27	*umc1735*	327.1	364.4
8	504	28	*umc1457*	329.4	371.2
8	505	29	*rip1*	336.3	385.0
8	506	30	*umc1460*	339.6	397.3
8	507	31	*bnlg2046*	345.2	410.3
8	508	32	*gta101d*	350.1	421.6
8	509	33	*umc1130*	354.3	427.8
8	510	34	*AY104566*	364.5	441.2
8	511	35	*umc1959*	370.4	444.6
8	512	36	*ufg74*	376.5	453.0
8	513	37	*umc1889*	380.3	459.4
8	514	38	*bnl12.30a*	387.9	468.7
8	515	39	*umc1149*	417.1	511.2
8	516	40	*umc1728*	434.7	541.3
8	517	41	*bnlg1031*	452.7	574.0
8	518	42	*umc1607*	460.5	586.4
8	519	43	*bnlg1823*	477.1	611.9
8	520	44	*umc1268*	484.3	622.4
8	521	45	*npi414a*	490.8	634.6
8	522	46	*php20793*	510.9	652.4
8	523	47	*umc1933*	521.3	677.1
8	524	48	*AY110053*	531.0	688.4
8	525	49	*npi107*	545.5	705.8
8	526	50	*gst1*	546.9	715.1
8	527	51	*agrr21*	555.7	731.2
8	528	52	*AY110127*	571.1	752.9
8	529	53	*phi233376*	587.0	769.8
8	530	54	*umc1638*	600.5	789.2
8	531	55	*bnlg1131*	607.6	798.2
9	532	1	*umc109*	0.0	0.0
9	533	2	*npi253a*	11.9	13.2
9	534	3	*umc1867*	20.4	24.1
9	535	4	*php10005*	24.3	30.4
9	536	5	*lim343*	39.2	59.2
9	537	6	*ufg41*	42.6	65.2
9	538	7	*bnlg1583*	52.3	82.6
9	539	8	*umc2335*	58.4	98.4
9	540	9	*umc1967*	67.5	108.2
9	541	10	*bz1*	71.3	111.8
9	542	11	*csu471*	89.7	129.1

9	543	12	*isu111b*	98.2	145.4
9	544	13	*umc2336*	104.2	159.2
9	545	14	*omt2*	108.1	166.4
9	546	15	*bnlg1401*	119.7	191.0
9	547	16	*mmp77*	127.5	195.9
9	548	17	*mmp30*	140.5	207.5
9	549	18	*umc1698*	150.5	217.9
9	550	19	*AY109531*	166.7	234.9
9	551	20	*wx1*	170.1	241.9
9	552	21	*umc1258*	173.2	245.4
9	553	22	*ufg71*	181.2	257.7
9	554	23	*psr160d*	190.4	266.8
9	555	24	*rz953*	192.0	272.0
9	556	25	*asg63a*	196.5	279.0
9	557	26	*umc1271*	200.1	281.3
9	558	27	*umc1921*	203.0	287.7
9	559	28	*rz682*	212.5	297.1
9	560	29	*sbp4*	213.7	301.3
9	561	30	*bnlg1209*	219.3	308.0
9	562	31	*umc1107*	221.8	316.5
9	563	32	*bnlg1012*	228.5	325.7
9	564	33	*umc1120*	233.0	337.3
9	565	34	*umc95*	239.4	348.4
9	566	35	*ufg64*	244.4	351.7
9	567	36	*php20554*	252.4	357.4
9	568	37	*mmp151d*	259.2	367.8
9	569	38	*ufg67*	272.6	388.1
9	570	39	*AY109792*	280.4	395.8
9	571	40	*csu634*	290.5	408.5
9	572	41	*ufg24*	296.5	414.1
9	573	42	*umc2134*	303.4	430.4
9	574	43	*npi443*	310.6	438.1
9	575	44	*mmp142*	317.1	455.7
9	576	45	*npi439b*	329.0	469.6
9	577	46	*asg44*	343.5	483.9
9	578	47	*mmp131*	372.8	506.6
9	579	48	*psk3*	380.2	511.8
9	580	49	*ufg75c*	388.2	527.2
9	581	50	*mmp168*	394.5	537.9
9	582	51	*bnl5.09a*	404.7	549.9
9	583	52	*bnl14.28a*	411.1	565.5
9	584	53	*asg12a*	417.3	573.5

9	585	54	*umc1675*	420.5	579.5
9	586	55	*bnlg619*	432.7	601.9
9	587	56	*umc2131*	442.7	616.4
9	588	57	*mmp171a*	449.3	630.5
9	589	58	*wc1*	458.0	649.8
9	590	59	*umc1137*	470.0	672.5
9	591	60	*umc1505*	500.1	718.0
10	592	1	*mmp48a*	0.0	0.0
10	593	2	*mmp48b*	10.6	13.9
10	594	3	*AY110060*	26.3	25.7
10	595	4	*php20753a*	31.5	31.5
10	596	5	*php20075a(gast)*	35.1	36.7
10	597	6	*AW330564*	54.6	68.5
10	598	7	*AW225120*	63.7	82.0
10	599	8	*umc2053*	75.8	100.4
10	600	9	*umc2018*	80.3	105.2
10	601	10	*npi285a(cac)*	90.0	117.7
10	602	11	*cr4*	101.5	136.6
10	603	12	*umc2034*	116.2	163.2
10	604	13	*AI795367*	132.2	182.4
10	605	14	*isu85b*	142.6	193.1
10	606	15	*umc2069*	150.6	210.4
10	607	16	*umc130*	155.2	216.7
10	608	17	*lim2*	168.2	228.7
10	609	18	*bnlg210*	174.1	235.7
10	610	19	*AY110411*	179.7	238.3
10	611	20	*umc1345*	185.4	244.0
10	612	21	*rps3*	187.7	249.4
10	613	22	*bnlg1712*	194.1	262.0
10	614	23	*AY111178*	196.7	262.9
10	615	24	*csu969b(fap)*	198.6	272.4
10	616	25	*umc64a*	202.1	277.7
10	617	26	*umc1995*	207.7	282.0
10	618	27	*AY109920*	218.9	293.3
10	619	28	*jpsb527d*	231.2	297.0
10	620	29	*umc1911*	243.7	306.9
10	621	30	*umc1330*	246.6	313.7
10	622	31	*umc1272*	250.2	318.3
10	623	32	*umc259a*	256.6	327.7
10	624	33	*AY110634*	262.5	330.6
10	625	34	*mmp12*	274.7	342.5
10	626	35	*bnlg1250*	282.1	352.9

10	627	36	*ufg37*	291.6	370.9
10	628	37	*umc1477*	300.6	392.9
10	629	38	*bnl10.13a*	308.7	406.1
10	630	39	*bnl17.02*	319.1	417.7
10	631	40	*tip5*	325.7	424.2
10	632	41	*umc1993*	351.0	452.2
10	633	42	*ufg15*	369.6	471.4
10	634	43	*bnl7.49a(hmd)*	411.0	511.6
10	635	44	*bnlg1677*	420.6	528.0
10	636	45	*mmp181*	433.6	547.7
10	637	46	*npi254b*	445.3	556.3
10	638	47	*bnlg1450*	462.5	577.3
10	639	48	*php20568a*	479.5	599.0
10	640	49	*umc2021*	490.3	611.9
10	641	50	*umc2126*	496.6	622.6
10	642	51	*asg19b*	504.0	637.4
10	643	52	*csu48*	522.8	651.5

[a] The marker number given in sequential order across all markers on all chromosomes
[b] The marker number given in sequential order on individual chromosomes.
[c] The position of the markers along a chromosome using the 94 subset of IBM RILs.
[d] The position of the markers along a chromosome using the 274 subset of IBM RILs.

Appendix 2: List of maize inbred lines phenotyped each field season

1. Subset of 90 inbred lines from the maize diversity panel for association mapping in 2004.

38-11 A441-5 A554 A6 A619 A632 B104 B14A B37 B68 B73 B84 B97 C103 CI187-2 CM105 CM174 CML247 CML258 CML261 CML277 CML281 CML333 CML61 CML91 CMV3 D940Y EP1 F2 F2834T F44 F7 GT112 H95 H99 HP301 I137TN I29 IA2132 IDS28 Il101 Il14H Il677A K55 Ki11 Ki21 Ki3 Ki43 Ki44 Ki2007 Ky21 M162W M37W Mo17 Mo24W MS153 N192 N28Ht NC250 NC258 NC260 NC296 NC298 NC300 NC320 NC338 NC348 NC350 NC354 ND246 Oh43 Oh7B P39 Pa91 SA24 SC213R SC55 Sg18 T232 T8 Tx601 Tzi10 Tzi18 Tzi8 U267Y Va26 W153R W182B W64A Wf9

2. Subset of 91 inbred lines from the maize diversity panel for association mapping in 2005.

38-11 A441-5 A554 A6 A619 A632 B104 B14A B37 B68 B73 B84 B97 C103 CI187-2 CM105 CM174 CML247 CML258 CML261 CML277 CML333 CML61 CML91 CMV3 D940Y EP1 F2 F2834T F44 F7 GT112 H95 H99 HP301 Hi27 I137TN I29 IA2132 IDS28 Il101 Il14H Il677A K55 Ki11 Ki21 Ki3 Ki43 Ki44 Ki2007 Ky21 M162W M37W Mo17 Mo24W MS153 N192 N28Ht NC250 NC258 NC260 NC296 NC298 NC300 NC304 NC320 NC338 NC348 NC350 NC354 ND246 Oh43 Oh7B P39 Pa91 SA24 SC213R SC55 Sg18 T232 T8 Tx601 Tzi10 Tzi18 Tzi8 U267Y Va26 W153R W182B W64A Wf9

3. Subset of 260 inbred lines from the maize diversity panel for association mapping in 2008.

33-16 38-11 4226 4722 811 A188 A214N A239 A441-5 A554 A556 A6 A619 A632 A634 A635 A641 A654 A659 A661 A679 A680 A682 Ab28A B10 B103 B104 B105 B109 B14A B164 B2 B37 B46 B52 B57 B64 B68 B73 B73Htrhm B75 B76 B77 B79 B84 B96 B97 C123 C49A CH701-30 CH9 CI187-2 CI21E CI28A CI31A CI44 CI64 CI66 CI90C CM105 CM174 CM37 CM7 CML103 CML108 CML154Q CML157Q CML218 CML220 CML228 CML238 CML247 CML258 CML261 CML277 CML287 CML311 CML314 CML321 CML322 CML323 CML328 CML333 CML38 CML52 CML9 CML91 CML92 CMV3 CO106 CO109 CO125 CO255 D940Y DE1 DE2 DE811 E2558W EP1 F2 F2834T F44 F6 GA209 GT112 H100 H105W H49 H84 H91 H95 H99 Hi27 HP301 HY I137TN I205 I29 IA2132 IDS28 IDS69 IDS91 Il101 Il14H Il677A K148 K4 K55 K64 Ki11 Ki21 Ki3 Ki43 Ky21 Ky226 Ky228 L317 L578 M14 M162W M37W Mo17 Mo18W Mo1W Mo24W Mo45 Mo46 Mo47 MoG MS1334 MS153 MS71 Mt42 N192 N28Ht N6 NC222 NC230 NC232 NC236 NC250 NC258 NC260 NC262 NC264 NC268 NC290A NC292 NC294 NC296 NC296A NC298 NC300 NC302 NC304 NC306 NC308 NC310 NC312 NC314 NC316 NC318 NC320 NC322 NC326 NC328 NC33 NC330 NC332 NC334 NC336 NC338 NC342 NC344 NC348 NC350 NC352 NC354 NC356 NC358 NC360 NC362 NC364 NC366 NC368 NC370 NC372 ND246 Oh40B Oh43 Oh43E Oh603 Oh7B OS420 P39 Pa762 Pa875 Pa880 Pa91 R109B R168 R177 R229 R4 SA24 SC213R SC357 SC55 SD40 SD44 Sg1533 Sg18 T232 T234 T8 Tzi10 Tzi11 Tzi16 Tzi18 Tzi25 Tzi8 Tzi9 Tx601 U267Y Va102 Va14 Va17 Va26 Va35 Va59 Va85 Va99 VaW6 W153R W182B W22 W401 W64A Wf9 Yu796NS

APPENDIX 3. Sequence polymorphisms in the fifth exon of *d3* for 275 lines from the maize association panel.

		Position in the gene											
Line	Synonym	2888	2893	2894	2898	2900	2905	2907	2909	2910	2912	2916	2918
811		.	-	.	T	T	G	T	-	G	----	T	CATTCAT
33-16	3316	----	G	---CGG	.	.	T	.	.	T	.	.	.
38-11	3811	----	G	---CGG	G	C	T	A	A	T	GCGG	A	CATTCAT
4226		----	G	---CGG	G	C	T	A	A	T	GCGG	A	CATTCAT
4722		----	G	---CGG	G	C	T	A	A	T	GCGG	A	CATTCAT
A188		----	G	---CGG	G	C	T	A	A	T	GCGG	A	CATTCAT
A214N		----	G	---CGG	G	C	T	A	A	T	GCGG	A	CATTCAT
A239		----	G	---CGG	G	C	T	A	A	T	GCGG	A	CATTCAT
A272		----	G	---CGG	G	C	T	A	A	T	GCGG	A	CATTCAT
A441-5	A4415	----	G	---CGG	G	C	T	A	A	T	GCGG	A	CATTCAT
A554		----	G	---CGG	G	C	T	A	A	T	GCGG	A	CATTCAT
A556		----	G	---CGG	G	C	T	A	A	T	GCGG	A	CATTCAT
A6		----	G	---CGG	G	C	T	A	A	T	GCGG	A	CATTCAT
A619		----	G	---CGG	G	C	T	A	A	T	GCGG	A	CATTCAT
A632		----	G	---CGG	G	C	T	A	A	T	GCGG	A	CATTCAT
A634		----	G	---CGG	G	C	T	A	A	T	GCGG	A	CATTCAT
A635		----	G	---CGG	G	C	T	A	A	T	GCGG	A	CATTCAT
A641		----	G	---CGG	G	C	T	A	A	T	GCGG	A	CATTCAT
A654		----	G	---CGG	G	C	T	A	A	T	GCGG	A	CATTCAT
A659		----	G	---CGG	G	C	T	A	A	T	GCGG	A	CATTCAT
A661		----	G	---CGG	G	C	T	A	A	T	GCGG	A	CATTCAT
A679		----	G	---CGG	G	C	T	A	A	T	GCGG	A	CATTCAT
A680		----	G	---CGG	G	C	T	A	A	T	GCGG	A	CATTCAT
A682		----	G	---CGG	G	C	T	A	A	T	GCGG	A	CATTCAT
Ab28A	AB28A	----	G	---CGG	G	C	T	A	A	T	GCGG	A	CATTCAT
B10		----	G	---CGG	G	C	T	A	A	T	GCGG	A	CATTCAT
B103		----	G	---CGG	G	C	T	A	A	T	GCGG	A	CATTCAT
B104		----	G	---CGG	G	C	T	A	A	T	GCGG	A	CATTCAT
B105		----	G	---CGG	G	C	T	A	A	T	GCGG	A	CATTCAT
B109		----	G	---CGG	G	C	T	A	A	T	GCGG	A	CATTCAT
B14A		----	G	---CGG	G	C	T	A	A	T	GCGG	A	CATTCAT
B164		----	G	---CGG	G	C	T	A	A	T	GCGG	A	CATTCAT
B2		----	G	---CGG	G	C	T	A	A	T	GCGG	A	CATTCAT
B37		----	G	---CGG	G	C	T	A	A	T	GCGG	A	CATTCAT
B46		----	G	---CGG	G	C	T	A	A	T	GCGG	A	CATTCAT

B52		TGCT	G	TTGCTG	T	T	T	.	A	T	GCGG	A	-------
B57		----	G	---CGG	G	C	T	A	A	T	GCGG	A	CATTCAT
B64		----	G	TTGCTG	T	-	.	T	.	-	.	A	CATTCAT
B68		----	G	---CGG	G	C	T	A	A	T	GCGG	A	CATTCAT
B73		----	G	---CGG	G	C	T	A	A	T	GCGG	A	CATTCAT
B73Htrhm	B73HTRHM	----	G	---CGG	G	C	T	A	A	T	GCGG	A	CATTCAT
B75		----	G	---CGG	G	C	T	A	A	T	GCGG	A	CATTCAT
B76		----	G	---CGG	G	C	T	A	A	T	GCGG	A	CATTCAT
B77		----	G	---CGG	G	.	T	.	A	T	GCGG	A	CATTCAT
B79		----	G	---CGG	G	C	T	A	A	T	GCGG	A	CATTCAT
B84		----	G	---CGG	G	C	T	A	A	T	GCGG	A	CATTCAT
B96		----	G	---CGG	G	C	T	A	A	T	GCGG	A	CATTCAT
B97		----	G	---CGG	G	C	T	A	A	T	GCGG	A	CATTCAT
C103		----	G	---CGG	G	C	T	A	A	T	GCGG	A	CATTCAT
C123		----	G	---CGG	G	C	T	A	A	T	GCGG	A	CATTCAT
C49A		----	G	---CGG	G	C	T	A	A	T	GCGG	A	CATTCAT
CH701-30	CH70130	----	G	---CGG	G	C	T	A	A	T	GCGG	A	CATTCAT
CH9		----	G	---CGG	G	C	T	A	A	T	GCGG	A	CATTCAT
CI187-2	CI1872	----	G	---CGG	G	C	T	A	A	T	GCGG	A	CATTCAT
CI21E		----	G	---CGG	G	C	T	A	A	T	GCGG	A	CATTCAT
CI28A		----	G	---CGG	G	C	T	A	A	T	GCGG	A	CATTCAT
CI31A		----	G	---CGG	G	C	T	A	A	T	GCGG	A	CATTCAT
CI3A		.	.	.	.	.	.	.	.	.	.	.	.
CI44		----	G	---CGG	G	C	T	A	A	T	GCGG	A	CATTCAT
CI64		----	G	---CGG	G	C	T	A	A	T	GCGG	A	CATTCAT
CI66		----	G	---CGG	G	C	T	A	A	T	GCGG	A	CATTCAT
CI90C		----	G	---CGG	G	C	T	A	A	T	GCGG	A	CATTCAT
CM105		----	G	---CGG	G	C	T	A	A	T	GCGG	A	CATTCAT
CM174		----	G	---CGG	G	C	T	A	A	T	GCGG	A	CATTCAT
CM37		----	G	---CGG	G	C	T	A	A	T	GCGG	A	CATTCAT
CM7		----	G	---CGG	G	C	T	A	A	T	GCGG	A	CATTCAT
CML10		----	G	---CGG	G	C	T	A	A	T	GCGG	A	CATTCAT
CML103		----	G	---CGG	G	C	T	A	A	T	GCGG	A	CATTCAT
CML108		----	G	---CGG	G	C	T	A	A	T	GCGG	A	CATTCAT
CML154Q		.	.	.	.	.	.	.	.	.	.	.	.
CML157Q		----	G	---CGG	G	C	T	A	A	T	GCGG	A	CATTCAT
CML158Q		----	G	---CGG	G	C	T	A	A	T	GCGG	A	CATTCAT
CML218		----	G	---CGG	G	C	T	A	A	T	GCGG	A	CATTCAT
CML220		----	G	---CGG	G	C	T	A	A	T	GCGG	A	CATTCAT
CML228		----	G	---CGG	G	C	T	A	A	T	GCGG	A	CATTCAT
CML238		----	G	---CGG	G	C	T	A	A	T	GCGG	A	CATTCAT
CML247		----	G	---CGG	G	C	T	A	A	T	GCGG	A	CATTCAT

CML254		----	G	---CGG	G	C	T	A	A	T	GCGG	A	CATTCAT
CML258		----	G	---CGG	G	C	T	A	A	T	GCGG	A	CATTCAT
CML261		----	G	---CGG	G	C	T	A	A	T	GCGG	A	CATTCAT
CML277		----	G	---CGG	G	C	T	A	A	T	GCGG	A	CATTCAT
CML281		----	G	---CGG	G	C	T	A	A	T	GCGG	A	CATTCAT
CML287		----	G	---CGG	G	C	T	A	A	T	GCGG	A	CATTCAT
CML311		----	G	---CGG	G	C	T	A	A	T	GCGG	A	CATTCAT
CML314		----	G	---CGG	G	C	T	A	A	T	GCGG	A	CATTCAT
CML321		----	G	---CGG	G	C	T	A	A	T	GCGG	A	CATTCAT
CML322		----	G	---CGG	G	C	T	A	A	T	GCGG	A	CATTCAT
CML323		----	G	---CGG	G	C	T	A	A	T	GCGG	A	CATTCAT
CML328		----	G	---CGG	G	C	T	A	A	T	GCGG	A	CATTCAT
CML331		----	G	---CGG	G	C	T	A	A	T	GCGG	A	CATTCAT
CML333		----	G	---CGG	G	C	T	A	A	T	GCGG	A	CATTCAT
CML38		----	G	---CGG	G	C	T	A	A	T	GCGG	A	CATTCAT
CML5		----	G	---CGG	G	C	T	A	A	T	GCGG	A	CATTCAT
CML52		----	G	---CGG	G	C	T	A	A	T	GCGG	A	CATTCAT
CML9		----	G	---CGG	G	C	T	A	A	T	GCGG	A	CATTCAT
CML91		----	G	---CGG	G	C	T	A	A	T	GCGG	A	CATTCAT
CML92		----	G	---CGG	G	C	T	A	A	T	GCGG	A	CATTCAT
CMV3		----	G	---CGG	G	C	T	A	A	T	GCGG	A	CATTCAT
CO106		----	G	---CGG	G	C	T	A	A	T	GCGG	A	CATTCAT
CO109		----	G	---CGG	G	C	T	A	A	T	GCGG	A	CATTCAT
CO125		----	G	---CGG	G	C	T	A	A	T	GCGG	A	CATTCAT
CO255		----	G	---CGG	G	C	T	A	A	T	GCGG	A	CATTCAT
D940Y		----	G	---CGG	G	C	T	A	A	T	GCGG	A	CATTCAT
DE1		----	G	---CGG	G	C	T	A	A	T	GCGG	A	CATTCAT
DE2		----	G	---CGG	G	C	T	A	A	T	GCGG	A	CATTCAT
DE811		----	G	---CGG	G	C	T	A	A	T	GCGG	A	CATTCAT
E2558W		----	G	---CGG	G	C	T	A	A	T	GCGG	A	CATTCAT
EP1		----	G	---CGG	G	C	T	A	A	T	GCGG	A	CATTCAT
F2		----	G	---CGG	G	C	T	A	A	T	GCGG	A	CATTCAT
F2834T		----	G	---CGG	G	C	T	A	A	T	GCGG	A	CATTCAT
F44		----	G	---CGG	G	C	T	A	A	T	GCGG	A	CATTCAT
F6		----	G	---CGG	G	C	T	A	A	T	GCGG	A	CATTCAT
F7		----	G	---CGG	G	C	T	A	A	T	GCGG	A	CATTCAT
GA209		----	G	---CGG	G	C	T	A	A	T	GCGG	A	CATTCAT
GT112		----	G	---CGG	G	C	T	A	A	T	GCGG	A	CATTCAT
H100		----	G	.	.	.	T	.	A	T	GCGG	.	.
H105w	H105W	----	C	TTGCTG	T	T	G	T	-	G	----	T	CATTCAT
H49		----	G	---CGG	G	C	T	A	A	T	GCGG	A	CATTCAT
H84		----	C	TTGCTG	T	T	G	T	-	G	----	T	CATTCAT

H91		----	C	TTGCTG	T	T	G	T	-	G	----	T	CATTCAT
H95		----	C	TTGCTG	T	T	G	T	-	G	----	T	CATTCAT
H99		.	-	.	T	T	G	T	-	G	----	T	CATTCAT
Hi27	HI27	----	C	TTGCTG	T	T	G	T	-	G	----	T	CATTCAT
HP301		----	G	---CGG	G	C	T	A	A	T	GCGG	A	CATTCAT
Hy	HY	----	C	TTGCTG	T	T	G	T	-	G	----	T	CATTCAT
I137TN		----	C	TTGCTG	T	T	G	T	-	G	----	T	CATTCAT
I205		----	G	---CGG	G	C	T	A	A	T	GCGG	A	CATTCAT
I29		----	C	TTGCTG	T	T	G	T	-	G	----	T	CATTCAT
IA2132		----	C	TTGCTG	T	T	G	T	-	G	----	T	CATTCAT
IDS28		----	G	---CGG	G	C	T	A	A	T	GCGG	A	CATTCAT
IDS69		----	G	---CGG	G	C	T	A	A	T	GCGG	A	CATTCAT
IDS91		----	G	---CGG	G	C	T	A	A	T	GCGG	A	CATTCAT
Il101	IL101	----	G	---CGG	G	C	T	A	A	T	GCGG	A	CATTCAT
Il677a	IL677A	----	C	TTGCTG	T	T	G	T	-	G	----	T	CATTCAT
K148		----	G	---CGG	G	C	T	A	A	T	GCGG	A	CATTCAT
K4		----	C	TTGCTG	T	T	G	T	-	G	----	T	CATTCAT
K55		----	G	---CGG	G	C	T	A	A	T	GCGG	A	CATTCAT
K64		----	G	---CGG	G	C	T	A	A	T	GCGG	A	CATTCAT
Ki11	KI11	----	G	---CGG	G	C	T	A	A	T	GCGG	A	CATTCAT
Ki2007	KI2007	----	C	TTGCTG	T	T	G	T	-	G	----	T	CATTCAT
Ki21	KI21	----	C	TTGCTG	T	T	G	T	-	G	----	T	CATTCAT
Ki3	KI3	----	C	TTGCTG	T	T	G	T	-	G	----	T	CATTCAT
Ki43	KI43	----	C	TTGCTG	T	T	G	T	-	G	----	T	CATTCAT
Ki44	KI44	TGCT	G	-TGCTG	G	C	T	A	-	T	GCGG	A	-------
Ky21	KY21	----	G	---CGG	G	C	T	A	A	T	GCGG	A	CATTCAT
Ky226	KY226	TGCT	G	-TGCTG	G	C	T	A	-	T	GCGG	A	-------
Ky228	KY228	----	G	---CGG	G	C	T	A	A	T	GCGG	A	CATTCAT
L317		----	G	---CGG	G	C	T	A	A	T	GCGG	A	CATTCAT
L578		----	G	---CGG	G	C	T	A	A	T	GCGG	A	CATTCAT
M14		----	G	---CGG	G	C	T	A	A	T	GCGG	A	CATTCAT
M162W		----	G	---CGG	G	C	T	A	A	T	GCGG	A	CATTCAT
M37W		TGCT	G	-TGCTG	G	C	T	A	-	T	GCGG	A	-------
Mo17	MO17	TGCT	G	-TGCTG	G	C	T	A	-	T	GCGG	A	-------
Mo18W	MO18W	TGCT	G	-TGCTG	G	C	T	A	-	T	GCGG	A	-------
Mo1W	MO1W	TGCT	G	-TGCTG	G	C	T	A	-	T	GCGG	A	-------
Mo24W	MO24W	----	G	---CGG	G	C	T	A	A	T	GCGG	A	CATTCAT
Mo45	MO45	TGCT	G	-TGCTG	G	C	T	A	-	T	GCGG	A	-------
Mo46	MO46	TGCT	G	-TGCTG	G	C	T	A	-	T	GCGG	A	-------
Mo47	MO47	TGCT	G	-TGCTG	G	C	T	A	-	T	GCGG	A	-------
MoG	MOG	----	G	---CGG	G	C	T	A	A	T	GCGG	A	CATTCAT
MS1334		TGCT	G	-TGCTG	G	C	T	A	-	T	GCGG	A	-------

MS153		----	G	---CGG	G	C	T	A	A	T	GCGG	A	CATTCAT
MS71		TGCT	G	-TGCTG	G	C	T	A	-	T	GCGG	A	-------
Mt42	MT42	----	G	---CGG	G	C	T	A	A	T	GCGG	A	CATTCAT
N192		TGCT	G	-TGCTG	G	C	T	A	-	T	GCGG	A	-------
N28Ht	N28HT	TGCT	G	-TGCTG	G	C	T	A	-	T	GCGG	A	-------
N6		TGCT	G	-TGCTG	G	C	T	A	-	T	GCGG	A	-------
NC222		TGCT	G	-TGCTG	G	C	T	A	-	T	GCGG	A	-------
NC230		----	G	---CGG	G	C	T	A	A	T	GCGG	A	CATTCAT
NC232		TGCT	G	-TGCTG	G	C	T	A	-	T	GCGG	A	-------
NC236		TGCT	G	-TGCTG	G	C	T	A	-	T	GCGG	A	-------
NC250		TGCT	G	-TGCTG	G	C	T	A	-	T	GCGG	A	-------
NC258		TGCT	G	-TGCTG	G	C	T	A	-	T	GCGG	A	-------
NC260		TGCT	G	-TGCTG	G	C	T	A	-	T	GCGG	A	-------
NC262		TGCT	G	-TGCTG	G	C	T	A	-	T	GCGG	A	-------
NC264		TGCT	G	-TGCTG	G	C	T	A	-	T	GCGG	A	-------
NC268		----	G	---CGG	G	C	T	A	A	T	GCGG	A	CATTCAT
NC290A		TGCT	G	-TGCTG	G	C	T	A	-	T	GCGG	A	-------
NC292		TGCT	G	-TGCTG	G	C	T	A	-	T	GCGG	A	-------
NC294		TGCT	G	-TGCTG	G	C	T	A	-	T	GCGG	A	-------
NC296		----	G	---CGG	G	C	T	A	A	T	GCGG	A	CATTCAT
NC296A		----	G	---CGG	G	C	T	A	A	T	GCGG	A	CATTCAT
NC298		----	G	---CGG	G	C	T	A	A	T	GCGG	A	CATTCAT
NC300		TGCT	G	-TGCTG	G	C	T	A	-	T	GCGG	A	-------
NC302		TGCT	G	-TGCTG	G	C	T	A	-	T	GCGG	A	-------
NC304		TGCT	G	-TGCTG	G	C	T	A	-	T	GCGG	A	-------
NC306		----	G	---CGG	G	C	T	A	A	T	GCGG	A	CATTCAT
NC308		TGCT	G	-TGCTG	G	C	T	A	-	T	GCGG	A	-------
NC310		TGCT	G	-TGCTG	G	C	T	A	-	T	GCGG	A	-------
NC312		----	G	---CGG	G	C	T	A	A	T	GCGG	A	CATTCAT
NC314		----	G	---CGG	G	C	T	A	A	T	GCGG	A	CATTCAT
NC316		.	.	.	.	.	.	.	.	.	.	.	.
NC318		TGCT	G	-TGCTG	G	C	T	A	-	T	GCGG	A	-------
NC320		TGCT	G	-TGCTG	G	C	T	A	-	T	GCGG	A	-------
NC322		TGCT	G	-TGCTG	G	C	T	A	-	T	GCGG	A	-------
NC326		----	G	---CGG	G	C	T	A	A	T	GCGG	A	CATTCAT
NC328		TGCT	G	-TGCTG	G	C	T	A	-	T	GCGG	A	-------
NC33		TGCT	G	-TGCTG	G	C	T	A	-	T	GCGG	A	-------
NC330		TGCT	G	-TGCTG	G	C	T	A	-	T	GCGG	A	-------
NC332		TGCT	G	-TGCTG	G	C	T	A	-	T	GCGG	A	-------
NC334		TGCT	G	-TGCTG	G	C	T	A	-	T	GCGG	A	-------
NC336		----	G	---CGG	G	C	T	A	A	T	GCGG	A	CATTCAT
NC338		----	G	---CGG	G	C	T	A	A	T	GCGG	A	CATTCAT

NC342		TGCT	G	-TGCTG	G	C	T	A	-	T	GCGG	A	-------
NC344		----	G	---CGG	G	C	T	A	A	T	GCGG	A	CATTCAT
NC346		----	G	---CGG	G	C	T	A	A	T	GCGG	A	CATTCAT
NC348		TGCT	G	-TGCTG	G	C	T	A	-	T	GCGG	A	-------
NC350		----	G	---CGG	G	C	T	A	A	T	GCGG	A	CATTCAT
NC352		----	G	---CGG	G	C	T	A	A	T	GCGG	A	CATTCAT
NC354		TGCT	G	-TGCTG	G	C	T	A	-	T	GCGG	A	-------
NC356		----	G	---CGG	G	C	T	A	A	T	GCGG	A	CATTCAT
NC358		----	G	---CGG	G	C	T	A	A	T	GCGG	A	CATTCAT
NC360		TGCT	G	-TGCTG	G	C	T	A	-	T	GCGG	A	-------
NC362		TGCT	G	-TGCTG	G	C	T	A	-	T	GCGG	A	-------
NC364		.	.	.	.	.	.	.	.	.	.	.	.
NC366		----	G	---CGG	G	C	T	A	A	T	GCGG	A	CATTCAT
NC368		TGCT	G	-TGCTG	G	C	T	A	-	T	GCGG	A	-------
NC370		TGCT	G	-TGCTG	G	C	T	A	-	T	GCGG	A	-------
NC372		----	G	---CGG	G	C	T	A	A	T	GCGG	A	CATTCAT
ND246		----	G	---CGG	G	.	T	A	A	T	GCGG	A	CATTCAT
Oh40B	OH40B	TGCT	G	-TGCTG	G	C	T	A	-	T	GCGG	A	-------
Oh43	OH43	TGCT	G	-TGCTG	G	C	T	A	-	T	GCGG	A	-------
Oh43E	OH43E	TGCT	G	-TGCTG	G	C	T	A	-	T	GCGG	A	-------
Oh603	OH603	----	G	---CGG	G	C	T	A	A	T	GCGG	A	CATTCAT
Oh7B	OH7B	----	G	---CGG	G	C	T	A	A	T	GCGG	A	CATTCAT
OS420		TGCT	G	-TGCTG	G	C	T	A	-	T	GCGG	A	-------
P39		----	G	---CGG	G	C	T	A	A	T	GCGG	A	CATTCAT
Pa762	PA762	TGCT	G	-TGCTG	G	C	T	A	-	T	GCGG	A	-------
Pa875	PA875	.	.	.	.	.	.	.	.	.	.	.	.
Pa880	PA880	TGCT	G	-TGCTG	G	C	T	A	-	T	GCGG	A	-------
Pa91	PA91	TGCT	G	-TGCTG	G	C	T	A	-	T	GCGG	A	-------
Q6199		TGCT	G	-TGCTG	G	C	T	A	-	T	GCGG	A	-------
R109B		TGCT	G	-TGCTG	G	C	T	A	-	T	GCGG	A	-------
R168		----	G	---CGG	G	C	T	A	A	T	GCGG	A	CATTCAT
R177		TGCT	G	-TGCTG	G	C	T	A	-	T	GCGG	A	-------
R229		----	G	---CGG	G	C	T	A	A	T	GCGG	A	CATTCAT
R4		TGCT	G	-TGCTG	G	C	T	A	-	T	GCGG	A	-------
SA24		----	G	---CGG	G	C	T	A	A	T	GCGG	A	CATTCAT
SC213R		TGCT	G	-TGCTG	G	C	T	A	-	T	GCGG	A	-------
SC357		TGCT	G	-TGCTG	G	C	T	A	-	T	GCGG	A	-------
SC55		----	G	---CGG	G	C	T	A	A	T	GCGG	A	CATTCAT
SD40		TGCT	G	-TGCTG	G	C	T	A	-	T	GCGG	A	-------
SD44		TGCT	G	-TGCTG	G	C	T	A	-	T	GCGG	A	-------
Sg1533	SG1533	----	G	---CGG	G	C	T	A	A	T	GCGG	A	CATTCAT
Sg18	SG18	----	G	---CGG	G	C	T	A	A	T	GCGG	A	CATTCAT

T232		TGCT	G	-TGCTG	G	C	T	A	-	T	GCGG	A	-------
T234		----	G	---CGG	G	C	T	A	A	T	GCGG	A	CATTCAT
T8		TGCT	G	-TGCTG	G	C	T	A	-	T	GCGG	A	-------
Tx601	TX601	TGCT	G	-TGCTG	G	C	T	A	-	T	GCGG	A	-------
Tzi10	TZI10	.	-	.	T	T	G	T	-	G	----	T	CATTCAT
Tzi11	TZI11	TGCT	G	-TGCTG	G	C	T	A	-	T	GCGG	A	-------
Tzi16	TZI16	TGCT	G	-TGCTG	G	C	T	A	-	T	GCGG	A	-------
Tzi18	TZI18	TGCT	G	-TGCTG	G	C	T	A	-	T	GCGG	A	-------
Tzi25	TZI25	TGCT	G	-TGCTG	G	C	T	A	-	T	GCGG	A	-------
Tzi8	TZI8	----	G	---CGG	G	C	T	A	A	T	GCGG	.	CATTCAT
Tzi9	TZI9	----	G	---CGG	G	C	T	A	A	T	GCGG	A	CATTCAT
U267Y		TGCT	G	-TGCTG	G	C	T	A	-	T	GCGG	A	-------
Va102	VA102	TGCT	G	-TGCTG	G	C	T	A	-	T	GCGG	A	-------
Va14	VA14	TGCT	G	-TGCTG	G	C	T	A	-	T	GCGG	A	-------
Va17	VA17	TGCT	G	-TGCTG	G	C	T	A	-	T	GCGG	A	-------
Va26	VA26	TGCT	G	-TGCTG	G	C	T	A	-	T	GCGG	A	-------
Va35	VA35	TGCT	G	-TGCTG	G	C	T	A	-	T	GCGG	A	-------
Va59	VA59	TGCT	G	-TGCTG	G	C	T	A	-	T	GCGG	A	-------
Va85	VA85	----	G	---CGG	G	C	T	A	A	T	GCGG	A	CATTCAT
Va99	VA99	----	G	---CGG	G	C	T	A	A	T	GCGG	A	CATTCAT
VaW6	VAW6	TGCT	G	-TGCTG	G	C	T	A	-	T	GCGG	A	-------
W117Ht	W117HT	----	G	-TGCTG	G	C	T	A	-	T	GCGG	A	CATTCAT
W153R		----	G	---CGG	G	C	T	A	A	T	GCGG	A	CATTCAT
W182B		----	G	-TGCTG	G	C	T	A	-	T	GCGG	A	CATTCAT
W22		----	G	-TGCTG	G	.	T	A	-	T	GCGG	A	-------
W401		----	G	-TGCTG	G	C	T	A	-	T	GCGG	A	CATTCAT
W64A		TGCT	G	-TGCTG	G	C	T	A	-	T	GCGG	A	-------
WD		----	G	---CGG	.	.	T	A	-	T	GCGG	.	.
Wf9	WF9	.	.	.	T	.	T	A	-	T	GCGG	A	.
Yu796_NS		----	G	---CGG	G	C	T	A	-	T	GCGG	A	CATTCAT

APPENDIX 4. Sequence polymorphisms in the promoter region of *D8* in 266 lines from the maize association panel.

			Position in gene					
Line	Synonym	Group	677	680	695	699	702	710
811		.	C	T	G	T	GTG-AAA	---
33-16	3316	NSS	C	T	G	T	GTG-AAA	---
38-11	3811	NSS	C	T	.	T	.	.
4226		NSS	C	T	G	T	GTG-AAA	---
4722		NSS	C	T	G	T	GTG-AAA	---
A188		NSS	C	T	G	T	GTG-AAA	---
A214N		MXD	C	T	G	T	GTG-AAA	---
A239		NSS	C	T	G	T	GTG-AAA	---
A272		TS	C	T	G	T	GTG-AAA	---
A441-5	A4415	MXD	C	T	G	T	GTG-AAA	---
A554		NSS	C	T	G	T	GTG-AAA	---
A556		NSS	C	T	G	T	GTG-AAA	---
A6		TS	C	T	G	T	GTG-AAA	---
A619		NSS	G	C	G	C	-------	CCT
A632		SS	C	T	G	T	GTG-AAA	---
A634		SS	C	T	G	T	GTG-AAA	---
A635		SS	C	T	G	T	GTG-AAA	---
A641		MXD	C	T	G	T	GTG-AAA	---
A654		NSS	C	T	G	T	GTG-AAA	---
A659		NSS	C	T	G	T	GTG-AAA	---
A661		NSS	C	T	G	T	GTG-AAA	---
A679		SS	C	T	G	T	GTG-AAA	---
A680		SS	C	T	G	T	GTG-AAA	---
A682		NSS	C	T	G	T	GTG-AAA	---
Ab28A	AB28A	MXD	C	T	G	T	GTG-AAA	---
B10		MXD	C	T	G	T	GTG-AAA	---
B103		NSS	C	T	G	T	GTG-AAA	---
B104		MXD	C	T	G	T	GTG-AAA	---
B105		MXD	C	T	G	T	GTG-AAA	---
B109		SS	C	T	G	T	GTG-AAA	---
B14A		SS	C	T	G	T	GTG-AAA	---
B164		MXD	C	T	G	T	GTG-AAA	---
B2		NSS	C	T	G	T	GTG-AAA	---
B37		SS	C	T	G	T	GTG-AAA	---
B46		MXD	C	T	G	T	GTG-AAA	---

B52		NSS	C	T	G	T	GTG-AAA	---
B57		NSS	C	T	G	T	GTG-AAA	---
B64		SS	C	T	G	T	GTG-AAA	---
B68		SS	C	T	G	T	GTG-AAA	---
B73		SS	C	T	G	T	GTG-AAA	---
B73Htrhm	B73HTRHM	SS	C	T	G	T	GTG-AAA	---
B75		NSS	C	T	G	T	GTG-AAA	---
B76		SS	C	T	G	T	GTG-AAA	---
B77		NSS	C	T	G	T	GTG-AAA	---
B79		MXD	C	T	G	T	GTG-AAA	---
B84		SS	C	T	G	T	GTG-AAA	---
B96		TS	C	T	G	T	GTG-AAA	---
B97		NSS	C	T	G	T	GTG-AAA	---
C103		NSS	.	.	.	.	.	.
C123		NSS	C	T	G	T	GTG-AAA	---
C49A		NSS	C	T	G	T	GTG-AAA	---
CH701-30	CH70130	NSS	C	T	G	T	GTG-AAA	---
CH9		NSS	C	T	G	T	GTG-AAA	---
CI187-2	CI1872	NSS	C	T	G	T	GTG-AAA	---
CI28A		MXD	C	T	G	T	GTG-AAA	---
CI31A		NSS	C	T	G	T	GTG-AAA	---
CI3A		NSS	C	T	G	T	GTG-AAA	---
CI44		NSS	C	C	C	T	GTG-AAA	---
CI64		NSS	C	T	G	T	GTG-AAA	---
CI66		NSS	C	T	G	T	GTG-AAA	---
CM105		SS	G	C	G	C	-------	CCT
CM174		SS	G	C	G	C	-------	CCT
CM37		NSS	C	T	G	T	GTG-AAA	---
CM7		NSS	G	C	G	C	-------	CCT
CML10		TS	C	T	G	T	GTG-AAA	---
CML103		TS	G	C	G	C	-------	CCT
CML108		TS	C	T	G	T	GTG-AAA	---
CML154Q		TS	C	T	G	T	GTG-AAA	---
CML157Q		TS	G	C	G	C	-------	CCT
CML158Q		TS	C	T	G	T	GTG-AAA	---
CML218		MXD	C	T	G	T	GTG-AAA	---
CML220		TS	C	T	G	T	GTG-AAA	---
CML228		TS	C	C	C	T	GTG-AAA	---
CML238		TS	C	T	G	T	GTG-AAA	---
CML247		TS	C	T	G	T	GTG-AAA	---
CML254		TS	C	T	G	T	GTG-AAA	---
CML258		TS	C	C	C	T	GTG-AAA	---

CML261		TS	G	C	G	C	-------	CCT
CML277		TS	C	T	G	T	GTG-AAA	---
CML281		TS	C	T	G	T	GTG-AAA	---
CML287		TS	C	T	G	T	GTG-AAA	---
CML311		TS	C	T	G	T	GTG-AAA	---
CML314		TS	C	C	C	T	GTG-AAA	---
CML321		TS	C	C	C	T	GTG-AAA	---
CML322		TS	C	T	G	T	GTG-AAA	---
CML323		MXD	C	T	G	T	GTG-AAA	---
CML328		MXD	C	T	G	T	GTG-AAA	---
CML333		TS	C	T	G	T	GTG-AAA	---
CML38		TS	C	C	C	T	GTG-AAA	---
CML5		TS	C	T	G	T	GTG-AAA	---
CML52		TS	C	T	G	T	GTG-AAA	---
CML9		TS	G	C	G	C	-------	CCT
CML91		MXD	C	T	G	T	GTG-AAA	---
CML92		MXD	C	T	G	T	GTG-AAA	---
CMV3		NSS	G	C	G	C	-------	CCT
CO106		NSS	C	T	G	T	GTG-AAA	---
CO109		NSS	G	C	G	C	-------	CCT
CO125		NSS	C	T	G	T	GTG-AAA	---
CO255		MXD	C	T	G	T	GTG-AAA	---
D940Y		MXD	C	T	G	T	GTG-AAA	---
DE1		NSS	C	T	G	T	GTG-AAA	---
DE2		NSS	C	T	G	T	GTG-AAA	---
DE811		MXD	C	T	G	T	GTG-AAA	---
E2558W		NSS	C	T	G	T	GTG-AAA	---
EP1		MXD	C	T	G	T	GTG-AAA	---
F2		MXD	C	T	G	T	GTG-AAA	---
F2834T		MXD	G	C	G	C	-------	CCT
F44		MXD	C	T	G	T	GTG-AAA	---
F6		MXD	C	T	G	T	GTG-AAA	---
F7		MXD	G	C	G	C	-------	CCT
GA209		NSS	C	T	G	T	GTG-AAA	---
GT112		NSS	C	T	G	T	GTG-AAA	---
H100		SS	C	T	G	T	GTG-AAA	---
H105w	H105W	MXD	C	T	G	T	GTG-AAA	---
H49		NSS	C	T	G	T	GTG-AAA	---
H84		MXD	C	T	G	T	GTG-AAA	---
H91		SS	C	T	G	T	GTG-AAA	---
H95		NSS	G	C	G	C	-------	CCT
H99		NSS	C	C	C	T	GTG-AAA	---

Hi27	HI27	MXD	C	T	G	T	GTG-AAA	---
Hy	HY	NSS	C	T	G	T	GTG-AAA	---
I137TN		MXD	C	C	C	T	GTG-AAA	---
I205		MXD	C	T	G	T	GTG-AAA	---
I29		popcorn	G	C	G	C	-------	CCT
IA2132		Sweet	C	T	G	T	GTG-AAA	---
IDS28		popcorn	C	T	G	T	GTG-AAA	---
IDS69		popcorn	C	T	G	T	GTG-AAA	---
Il677a	IL677A	Sweet	C	T	G	T	GTG-AAA	---
K148		NSS	C	T	G	T	GTG-AAA	---
K55		NSS	C	T	G	T	GTG-AAA	---
K64		NSS	C	T	G	T	GTG-AAA	---
Ki11	KI11	TS	C	T	G	T	GTG-AAA	---
Ki21	KI21	TS	C	C	C	T	GTG-AAA	---
Ki3	KI3	MXD	C	T	G	T	GTG-AAA	---
Ki43	KI43	TS	.	.	.	.	.	.
Ki44	KI44	TS	C	T	G	T	GTG-AAA	---
K4		NSS	C	T	G	T	GTG-AAA	---
Ky21	KY21	NSS	C	T	G	T	GTG-AAA	---
Ky226	KY226	MXD	C	T	G	T	GTG-AAA	---
Ky228	KY228	MXD	C	T	G	T	GTG-AAA	---
L317		NSS	C	T	G	T	GTG-AAA	---
L578		MXD	C	C	C	T	GTG-AAA	---
M14		NSS	C	T	G	T	GTG-AAA	---
M162W		NSS	C	T	G	T	GTG-AAA	---
M37W		MXD	C	T	G	T	GTG-AAA	---
Mo17	MO17	NSS	.	.	C	T	GTG-AAA	---
Mo18W	MO18W	MXD	C	T	G	T	GTG-AAA	---
Mo24W	MO24W	NSS	C	T	G	T	GTG-AAA	---
Mo45	MO45	MXD	C	T	G	T	GTG-AAA	---
Mo46	MO46	NSS	C	C	C	T	GTG-AAA	---
Mo47	MO47	MXD	C	T	G	T	GTG-AAA	---
MoG	MOG	NSS	G	C	G	C	-------	CCT
MS1334		NSS	C	?	G	T	GTG-AAA	---
MS153		NSS	G	C	G	C	-------	CCT
MS71		NSS	C	T	G	T	GTG-AAA	---
MT42		MXD	C	T	G	T	GTG-AAA	---
N192		SS	C	T	G	C	-------	CCT
N28Ht	N28HT	MXD	C	T	G	T	GTG-AAA	---
N6		NSS	C	T	G	T	GTG-AAA	---
NC222		NSS	C	T	G	T	GTG-AAA	---
NC230		NSS	C	T	G	T	GTG-AAA	---

NC232	NSS	C	C	C	T	GTG-AAA	---
NC236	NSS	C	T	G	T	GTG-AAA	---
NC250	SS	C	T	G	T	GTG-AAA	---
NC258	NSS	C	T	G	T	GTG-AAA	---
NC260	NSS	C	C	C	T	GTG-AAA	---
NC262	NSS	C	T	G	T	GTG-AAA	---
NC264	TS	C	T	G	T	GTG-AAA	---
NC268	SS	C	T	G	T	GTG-AAA	---
NC290A	NSS	C	T	G	T	GTG-AAA	---
NC292	SS	C	T	G	T	GTG-AAA	---
NC294	SS	C	T	G	T	GTG-AAA	---
NC296	TS	C	T	G	T	GTG-AAA	---
NC296A	TS	C	T	G	T	GTG-AAA	---
NC298	TS	C	T	G	T	GTG-AAA	---
NC300	TS	C	T	G	T	GTG-AAA	---
NC302	TS	C	T	G	T	GTG-AAA	---
NC304	TS	G	C	G	C	-------	CCT
NC306	SS	C	T	G	T	GTG-AAA	---
NC308	SS	C	T	G	T	GTG-AAA	---
NC310	SS	C	T	G	T	GTG-AAA	---
NC312	SS	C	T	G	T	GTG-AAA	---
NC314	SS	C	T	G	T	GTG-AAA	---
NC316	.	C	T	G	T	GTG-AAA	---
NC318	TS	C	T	G	T	GTG-AAA	---
NC320	TS	C	T	G	T	GTG-AAA	---
NC322	SS	C	T	G	T	GTG-AAA	---
NC326	SS	C	T	G	T	GTG-AAA	---
NC328	SS	C	T	G	T	GTG-AAA	---
NC33	NSS	C	T	G	T	GTG-AAA	---
NC330	SS	C	T	G	T	GTG-AAA	---
NC332	TS	C	T	G	T	GTG-AAA	---
NC334	TS	C	T	G	T	GTG-AAA	---
NC336	TS	C	T	G	T	GTG-AAA	---
NC338	TS	C	T	G	T	GTG-AAA	---
NC342	NSS	C	C	C	T	GTG-AAA	---
NC344	NSS	C	T	G	T	GTG-AAA	---
NC348	TS	C	T	G	T	GTG-AAA	---
NC350	TS	C	T	G	T	GTG-AAA	---
NC352	TS	C	T	G	T	GTG-AAA	---
NC354	TS	C	C	C	T	GTG-AAA	---
NC356	TS	C	T	G	T	GTG-AAA	---
NC358	TS	C	T	G	T	GTG-AAA	---

NC360		MXD	C	C	C	T	GTG-AAA	---
NC362		MXD	C	T	G	T	GTG-AAA	---
NC364		MXD	C	T	G	T	GTG-AAA	---
NC366		MXD	C	T	G	T	GTG-AAA	---
NC368		SS	C	T	G	T	GTG-AAA	---
NC370		TS	C	T	G	T	GTG-AAA	---
NC372		SS	C	T	G	T	GTG-AAA	---
ND246		MXD	G	C	G	C	-------	CCT
Oh40B	OH40B	NSS	G	C	G	C	-------	CCT
Oh43	OH43	NSS	G	C	G	C	-------	CCT
Oh43E	OH43E	NSS	G	C	G	C	-------	CCT
Oh603	OH603	MXD	C	T	G	T	GTG-AAA	---
Oh7B	OH7B	NSS	.	.	.	.	.	.
OS420		NSS	C	T	G	T	GTG-AAA	---
P39		Sweet	G	C	G	C	-------	CCT
Pa762	PA762	NSS	G	C	G	C	-------	CCT
Pa875	PA875	NSS	C	C	C	T	.	---
Pa880	PA880	NSS	C	C	C	T	GTG-AAA	---
Pa91	PA91	NSS	C	C	C	T	GTG-AAA	---
Q6199		TS	C	C	C	T	GTG-AAA	---
R109B		NSS	C	T	G	T	GTG-AAA	---
R168		NSS	C	T	G	T	GTG-AAA	---
R177		NSS	G	C	G	C	-------	CCT
R229		SS	C	T	G	T	GTG-AAA	---
R4		NSS	C	T	G	T	GTG-AAA	---
SA24		popcorn	C	T	G	T	GTG-AAA	---
SC213R		MXD	C	C	C	T	GTG-AAA	---
SC357		MXD	C	T	G	T	GTG-AAA	---
SC55		MXD	C	T	G	T	GTG-AAA	---
SD40		MXD	C	T	G	T	GTG-AAA	---
SD44		NSS	C	C	C	T	GTG-AAA	---
Sg1533	SG1533	popcorn	C	T	G	T	GTG-AAA	---
Sg18	SG18	popcorn	C	T	G	T	GTG-AAA	---
T232		MXD	C	T	G	T	GTG-AAA	---
T234		NSS	G	C	G	C	-------	CCT
T8		NSS	G	C	G	C	-------	CCT
Tx601	TX601	TS	C	C	C	T	GTG-AAA	---
Tzi10	TZI10	TS	C	T	G	T	GTG-AAA	---
Tzi11	TZI11	TS	C	T	G	T	GTG-AAA	---
Tzi16	TZI16	MXD	C	T	G	T	GTG-AAA	---
Tzi18	TZI18	TS	C	T	G	T	GTG-AAA	---
Tzi25	TZI25	MXD	C	T	G	T	GTG-AAA	---

Tzi8	TZI8	TS	C	T	G	T	GTG-AAA	---
Tzi9	TZI9	TS	C	T	G	T	GTG-AAA	---
U267Y		MXD	C	C	C	T	GTG-AAA	---
Va102	VA102	NSS	C	T	G	T	GTG-AAA	---
Va14	VA14	NSS	C	C	C	T	GTG-AAA	---
Va17	VA17	NSS	C	C	C	T	GTG-AAA	---
Va26	VA26	NSS	G	C	G	C	-------	CCT
Va35	VA35	NSS	G	C	G	C	-------	CCT
Va59	VA59	NSS	C	T	G	T	GTG-AAA	---
Va85	VA85	NSS	C	T	G	T	GTG-AAA	---
Va99	VA99	NSS	C	C	C	T	GTG-AAA	---
VaW6	VAW6	MXD	C	C	C	T	GTG-AAA	---
W117Ht	W117HT	MXD	C	T	G	T	GTG-AAA	---
W153R		NSS	C	T	G	T	GTG-AAA	---
W182B		NSS	.	C	G	.	-------	CCT
W22		NSS	C	T	G	T	GTG-AAA	---
W401		NSS	C	T	G	T	GTG-AAA	---
W64A		NSS	C	C	C	T	GTG-AAA	---
WD		NSS	C	T	G	T	GTG-AAA	---
Wf9	WF9	NSS	C	C	C	T	GTG-AAA	---
Yu796_NS	YU796NS	MXD	C	T	G	T	GTG-AAA	---

APPENDIX 5. *phytochromeB2* sequence polymorphisms in 241 lines from the maize association panel.

			Position in gene											
Line	Synonym	Group	22	115	117	145	162	187	264	276	281	317	318	349
811		.	A	-	A-	A	T	T	T-	-	A	T	G	GT
33-11	3311	NSS	A	-	--	A	T	T	T-	-	A	T	G	GT
4722		NSS	A	-	A-	A	T	T	T-	-	A	T	G	GT
A188		NSS	A	-	--	A	T	T	T-	-	A	T	G	GT
A239		NSS	A	-	A-	A	T	T	T-	-	A	T	G	GT
A272		TS	A	-	A-	A	T	T	T-	-	A	T	G	GT
A441-5	A4415	MXD	G	T	A-	C	-	G	T-	-	A	C	G	GT
A554		NSS	A	-	--	A	T	T	T-	-	A	T	G	GT
A556		NSS	A	-	--	A	T	T	T-	-	A	T	G	GT
A6		TS	A	-	A-	A	T	T	T-	-	A	T	G	GT
A619		NSS	G	T	A-	C	-	G	T-	-	A	C	G	GT
A632		SS	G	T	A-	C	-	G	T-	-	A	C	G	GT
A634		SS	A	-	A-	A	T	T	T-	-	A	T	G	GT
A635		SS	A	-	A-	A	T	T	T-	-	A	T	G	GT
A641		MXD	A	-	A-	A	T	T	T-	-	A	T	G	GT
A654		NSS	A	-	A-	A	T	T	T-	-	A	T	G	GT
A659		NSS	A	-	A-	A	T	T	T-	-	A	T	G	GT
A661		NSS	A	-	A-	A	T	T	T-	-	A	T	G	GT
A679		SS	G	T	A-	C	-	G	T-	-	A	C	G	GT
A680		SS	G	T	A-	C	-	G	T-	-	A	C	G	GT
A682		NSS	A	-	A-	A	T	T	T-	-	A	T	G	GT
Ab28A	AB28A	MXD	A	-	A-	A	T	T	T-	-	A	T	G	GT
B10		MXD	A	-	A-	A	T	T	T-	-	A	T	G	GT
B103		NSS	A	-	A-	A	T	T	T-	-	A	T	G	GT
B104		MXD	G	T	A-	C	-	G	T-	-	A	C	G	GT
B105		MXD	A	-	A-	A	T	T	T-	-	A	T	G	GT
B109		SS	G	T	A-	C	-	G	T-	-	A	C	G	GT
B14A		SS	G	T	A-	C	-	G	T-	-	A	C	G	GT
B164		MXD	A	-	--	A	T	T	T-	-	A	T	G	GT
B2		NSS	A	-	--	A	T	T	T-	-	A	T	G	GT
B37		SS	G	T	A-	C	-	G	T-	-	A	C	G	GT
B46		MXD	A	-	A-	A	T	T	T-	-	A	T	G	GT
B52		NSS	A	-	A-	A	T	T	T-	-	A	T	G	GT

B57		NSS	A	-	A-	A	T	T	T-	-	A	T	G	GT
B64		SS	.	.	.	.	T	?	T-	-	A	?	G	GT
B68		SS	G	T	A-	C	-	G	T-	-	A	C	G	GT
B73		SS	G	T	A-	C	-	G	T-	-	A	C	G	GT
B73Htrhm	B73HTRHM	SS	G	T	A-	C	-	G	T-	-	A	C	G	GT
B75		NSS	A	-	A-	A	T	T	T-	-	A	T	G	GT
B76		SS	G	T	A-	C	-	G	T-	-	A	C	G	GT
B77		NSS	A	-	A-	A	T	T	T-	-	A	T	G	GT
B79		MXD	A	-	A-	A	T	T	T-	-	A	T	G	GT
B84		SS	G	T	A-	C	-	G	T-	-	A	C	G	GT
B96		TS	A	-	A-	A	T	T	T-	-	A	T	G	GT
B97		NSS	A	-	--	A	T	T	T-	-	A	T	G	GT
C49A		NSS	A	-	A-	A	T	T	T-	-	A	T	G	GT
CH9		NSS	A	-	--	A	T	T	T-	-	A	T	G	GT
CI21E		NSS	A	-	A-	A	T	T	T-	-	A	T	G	GT
CI28A		MXD	A	-	--	A	T	T	T-	-	A	T	G	GT
CI31A		NSS	G	-	--	C	T	G	TT	-	A	T	G	GT
CI3A		NSS	A	-	A-	A	T	T	T-	-	A	T	G	GT
CI44		NSS	A	-	A-	A	T	T	T-	-	A	T	G	GT
CI64		NSS	A	-	A-	A	T	T	T-	-	A	T	G	GT
CI66		NSS	A	-	--	A	T	T	T-	-	A	T	G	GT
CI90C		MXD	A	-	A-	A	T	T	T-	-	A	T	G	GT
CM105		SS	G	T	A-	C	-	G	T-	-	A	C	G	GT
CM174		SS	G	T	A-	C	-	G	T-	-	A	C	G	GT
CM7		NSS	A	-	--	A	T	T	T-	-	A	T	G	GT
CML10		TS	G	T	A-	C	-	G	T-	-	A	C	G	GT
CML108		TS	G	-	--	C	T	G	TT	-	A	T	G	GT
CML157Q		TS	A	-	A-	A	T	T	T-	-	A	T	G	GT
CML158Q		TS	A	-	A-	A	T	T	T-	-	A	T	G	GT
CML218		MXD	A	-	A-	A	T	T	T-	-	A	T	G	GT
CML220		TS	A	-	A-	A	T	T	T-	-	A	T	G	GT
CML228		TS	A	-	A-	A	T	T	T-	-	A	T	G	GT
CML238		TS	A	-	A-	A	T	T	T-	-	A	T	G	GT
CML247		TS	A	-	A-	A	T	T	T-	-	A	T	G	GT
CML254		TS	.	-	A-	A	T	T	T-	-	A	T	G	GT
CML258		TS	G	T	A-	C	-	G	T-	-	A	C	G	GT
CML261		TS	A	-	A-	A	T	T	T-	-	A	T	G	GT
CML277		TS	A	-	AA	A	A	.	--	T	A	C	A	?
CML281		TS	G	T	A-	C	-	G	T-	-	A	C	G	GT
CML287		TS	G	T	A-	C	-	G	T-	-	A	C	G	GT
CML311		TS	A	-	A-	A	T	T	T-	-	A	T	G	GT

CML314		TS	A	-	A-	A	T	T	T-	-	A	T	G	GT
CML321		TS	A	-	A-	A	T	T	T-	-	A	T	G	GT
CML322		TS	A	-	A-	A	T	T	T-	-	A	T	G	GT
CML323		MXD	A	-	--	A	T	T	T-	-	A	T	G	GT
CML328		MXD	A	-	A-	A	T	T	T-	-	A	T	G	GT
CML333		TS	G	T	A-	C	-	G	T-	-	A	C	G	GT
CML38		TS	A	-	A-	A	T	T	T-	-	A	T	G	GT
CML5		TS	A	-	A-	A	T	T	T-	-	A	T	G	GT
CML9		TS	A	-	AA	A	A	.	--	T	-	C	A	--
CML91		MXD	A	-	A-	A	T	T	T-	-	A	T	G	GT
CML92		MXD	A	-	A-	A	T	T	T-	-	A	T	G	GT
CMV3		NSS	G	T	A-	C	-	G	T-	-	A	C	G	GT
CO106		NSS	A	-	A-	A	T	T	T-	-	A	T	G	GT
CO109		NSS	A	-	A-	A	T	T	T-	-	A	T	G	GT
CO125		NSS	A	-	A-	A	T	T	T-	-	A	T	G	GT
CO255		MXD	A	-	A-	A	T	T	T-	-	A	T	G	GT
D940Y		MXD	A	-	A-	A	T	T	T-	-	A	T	G	GT
DE1		NSS	A	-	A-	A	T	T	T-	-	A	T	G	GT
DE2		NSS	A	-	A-	A	T	T	T-	-	A	T	G	GT
DE811		MXD	A	-	A-	A	T	T	T-	-	A	T	G	GT
E2558W		NSS	A	-	A-	A	T	T	T-	-	A	T	G	GT
EP1		MXD	G	T	A-	C	-	G	T-	-	A	C	G	GT
F2		MXD	G	T	A-	C	-	G	T-	-	A	C	G	GT
F2834T		MXD	A	-	A-	A	T	T	T-	-	A	T	G	GT
F44		MXD	A	-	A-	A	T	T	T-	-	A	T	G	GT
F6		MXD	A	-	A-	A	T	T	T-	-	A	T	G	GT
F7		MXD	G	T	A-	C	-	G	T-	-	A	C	G	GT
GA209		NSS	A	-	A-	A	T	T	T-	-	A	T	G	GT
GT112		NSS	G	T	A-	C	-	G	T-	-	A	C	G	GT
H100		SS	A	-	A-	A	T	T	T-	-	A	T	G	GT
H105w	H105W	MXD	A	-	A-	A	T	T	T-	-	A	T	G	GT
H49		NSS	A	-	A-	A	T	T	T-	-	A	T	G	GT
H84		MXD	G	T	A-	C	-	G	T-	-	A	C	G	GT
H91		SS	A	-	A-	A	T	T	T-	-	A	T	G	GT
H95		NSS	G	-	A-	A	T	T	T-	-	A	T	G	GT
H99		NSS	G	T	A-	C	-	G	T-	-	A	C	G	GT
Hi27	HI27	MXD	A	-	A-	A	T	T	T-	-	A	T	G	GT
Hy	HY	NSS	A	-	A-	A	T	T	T-	-	A	T	G	GT
I137TN		MXD	G	T	A-	C	-	G	T-	-	A	C	G	GT
I205		MXD	A	-	--	A	T	T	T-	-	A	T	G	GT
IDS28		Popcorn	G	T	A-	C	-	G	T-	-	A	C	G	GT
IDS69		Popcorn	A	-	A-	A	T	T	T-	-	A	T	G	GT

IDS91		Popcorn	A	-	A-	A	T	T	T-	-	A	T	G	GT
Il101	IL101	Sweet	G	T	A-	C	-	G	T-	-	A	C	G	GT
Il14H	IL14H	Sweet	G	T	A-	C	-	G	T-	-	A	C	G	GT
K148		NSS	A	-	A-	A	T	T	T-	-	A	T	G	GT
K4		NSS	A	-	A-	A	T	T	T-	-	A	T	G	GT
K55		NSS	A	-	A-	A	T	T	T-	-	A	T	G	GT
K64		NSS	A	-	A-	A	T	T	T-	-	A	T	G	GT
Ki11	KI11	TS	A	-	A-	A	T	T	T-	-	A	T	G	GT
Ki2007	KI2007	TS	G	T	A-	C	-	G	T-	-	A	C	G	GT
Ki21	KI21	TS	A	-	A-	A	T	T	T-	-	A	T	G	GT
Ki3	KI3	MXD	G	T	A-	C	-	G	T-	-	A	C	G	GT
Ki43	KI43	TS	A	-	A-	A	T	T	T-	-	A	T	G	GT
Ki44	KI44	TS	G	T	A-	C	T	G	T-	-	A	C	G	GT
Ky21	KY21	NSS	G	T	A-	C	-	G	T-	-	A	C	G	GT
Ky226	KY226	MXD	A	-	A-	A	T	T	T-	-	A	T	G	GT
Ky228	KY228	MXD	A	-	A-	A	T	T	T-	-	A	T	G	GT
L317		NSS	A	-	A-	A	T	T	T-	-	A	T	G	GT
L578		MXD	A	-	A-	A	T	T	T-	-	A	T	G	GT
M14		NSS	A	-	A-	A	T	T	T-	-	A	T	G	GT
M162W		NSS	A	-	A-	A	T	T	T-	-	A	T	G	GT
Mo18W	MO18W	MXD	A	-	A-	A	T	T	T-	-	A	T	G	GT
Mo1W	MO1W	NSS	A	-	A-	A	T	T	T-	-	A	T	G	GT
Mo24W	MO24W	MXD	G	T	A-	C	-	G	T-	-	A	C	G	GT
Mo44	MO44	.	A	-	A-	A	T	T	T-	-	A	T	G	GT
Mo45	MO45	MXD	A	-	A-	A	T	T	T-	-	A	T	G	GT
Mo46	MO46	NSS	A	-	A-	A	T	T	T-	-	A	T	G	GT
Mo47	MO47	MXD	A	-	A-	A	T	T	T-	-	A	T	G	GT
MoG	MOG	NSS	A	-	A-	A	T	T	T-	-	A	T	G	GT
MS1334		NSS	A	-	--	A	T	T	T-	-	A	T	G	GT
MS153		NSS	G	T	A-	C	-	G	T-	-	A	C	G	GT
MS71		NSS	A	-	A-	A	T	T	T-	-	A	T	G	GT
Mt42	MT42	MXD	A	-	A-	A	T	T	T-	-	A	T	G	GT
N28Ht	N28HT	MXD	G	T	A-	C	.	G	T-	-	A	C	G	GT
N6		NSS	G	T	A-	C	-	G	T-	-	A	C	G	GT
NC222		NSS	A	-	A-	A	T	T	T-	-	A	T	G	GT
NC230		NSS	A	-	A-	A	T	T	T-	-	A	T	G	GT
NC232		NSS	A	-	A-	A	T	T	T-	-	A	T	G	GT
NC236		NSS	A	-	A-	A	T	T	T-	-	A	T	G	GT
NC250		SS	G	T	A-	C	-	G	T-	-	A	C	G	GT
NC258		NSS	G	T	A-	C	-	G	T-	-	A	C	G	GT
NC260		NSS	G	T	A-	C	-	G	T-	-	A	C	G	GT
NC262		NSS	G	T	A-	C	-	G	T-	-	A	C	G	GT

NC264		TS	G	T	A-	C	-	G	T-	-	A	C	G	GT
NC290A		NSS	G	T	A-	C	-	G	T-	-	A	C	G	GT
NC292		SS	G	T	A-	C	-	G	T-	-	A	C	G	GT
NC294		SS	G	T	A-	C	-	G	T-	-	A	C	G	GT
NC296		TS	G	T	A-	C	-	G	T-	-	A	C	G	GT
NC296A		TS	G	T	A-	C	-	G	T-	-	A	C	G	GT
NC298		TS	G	T	A-	C	-	G	T-	-	A	C	G	GT
NC300		TS	G	T	A-	C	-	G	T-	-	A	C	G	GT
NC302		TS	A	-	A-	A	T	T	T-	-	A	T	G	GT
NC304		TS	G	T	A-	C	-	G	T-	-	A	C	G	GT
NC306		SS	G	T	A-	C	-	G	T-	-	A	C	G	GT
NC308		SS	G	T	A-	C	-	G	T-	-	A	C	G	GT
NC310		SS	G	T	A-	C	-	G	T-	-	A	C	G	GT
NC312		SS	G	T	A-	C	-	G	T-	-	A	C	G	GT
NC314		SS	G	T	A-	C	-	G	T-	-	A	C	G	GT
NC316		.	A	-	AA	A	A	.	--	T	-	C	A	--
NC318		TS	G	T	A-	C	-	G	T-	-	A	C	G	GT
NC320		TS	G	T	A-	C	-	G	T-	-	A	C	G	GT
NC322		SS	G	T	A-	C	-	G	T-	-	A	C	G	GT
NC326		SS	G	T	A-	C	-	G	T-	-	A	C	G	GT
NC328		SS	G	T	A-	C	-	G	T-	-	A	C	G	GT
NC33		NSS	G	T	A-	C	-	G	T-	-	A	C	G	GT
NC330		SS	G	T	A-	C	-	G	T-	-	A	C	G	GT
NC332		TS	G	T	A-	C	-	G	T-	-	A	C	G	GT
NC334		TS	G	T	A-	C	-	G	T-	-	A	C	G	GT
NC336		TS	G	T	A-	C	-	G	T-	-	A	C	G	GT
NC338		TS	G	T	A-	C	-	G	T-	-	A	C	G	GT
NC342		NSS	A	-	AA	A	A	.	--	T	-	C	A	--
NC344		NSS	G	T	A-	C	-	G	T-	-	A	C	G	GT
NC348		TS	G	T	A-	C	-	G	T-	-	A	C	G	GT
NC350		TS	G	T	A-	C	-	G	T-	-	A	C	G	GT
NC352		TS	G	T	A-	C	-	G	T-	-	A	C	G	GT
NC354		TS	G	T	A-	C	-	G	T-	-	A	C	G	GT
NC356		TS	G	T	A-	C	-	G	T-	-	A	C	G	GT
NC358		TS	G	T	A-	C	-	G	T-	-	A	C	G	GT
NC360		MXD	G	T	A-	C	-	G	T-	-	A	C	G	GT
NC364		MXD	A	-	A-	A	T	T	T-	-	A	T	G	GT
NC368		SS	A	-	AA	A	A	.	--	T	-	C	A	--
NC370		TS	A	-	A-	A	T	T	T-	-	A	T	G	GT
NC372		SS	G	T	A-	C	-	G	T-	-	A	C	G	GT
Oh40B	OH40B	NSS	A	-	A-	A	T	T	T-	-	A	T	G	GT
Oh43	OH43	NSS	G	T	A-	C	-	G	T-	-	A	C	G	GT

Oh43E	OH43E	NSS	G	T	A-	C	-	G	T-	-	A	C	G	GT
Oh603	OH603	MXD	A	-	A-	A	T	T	T-	-	A	T	G	GT
Oh7B	OH7B	NSS	G	T	A-	C	-	G	T-	-	A	C	G	GT
OS420		NSS	G	T	A-	C	-	G	T-	-	A	C	G	GT
P39		Sweet	G	T	A-	C	-	G	T-	-	A	C	G	GT
Pa880	PA880	NSS	G	T	A-	C	-	G	T-	-	A	C	G	GT
Pa91	PA91	NSS	G	T	A-	C	-	G	T-	-	A	C	G	GT
R109B		NSS	G	T	A-	C	-	G	T-	-	A	C	G	GT
R168		NSS	G	T	A-	C	-	G	T-	-	A	C	G	GT
R229		SS	G	T	A-	C	-	G	T-	-	A	C	G	GT
SA24		Popcorn	G	T	A-	C	-	G	T-	-	A	C	G	GT
SC213R		MXD	G	T	A-	C	-	G	T-	-	A	C	G	GT
SC357		MXD	.	-	A-	A	T	T	T-	-	A	T	G	GT
SC55		MXD	G	T	A-	C	-	G	T-	-	A	C	G	GT
SD40		MXD	G	T	A-	C	-	G	T-	-	A	C	G	GT
Sg1533	SG1533	Popcorn	G	T	A-	C	-	G	T-	-	A	C	G	GT
Sg18	SG18	Popcorn	G	T	A-	C	-	G	T-	-	A	C	G	GT
T232		MXD	G	T	A-	C	T	G	T-	-	A	C	G	GT
T234		NSS	A	-	A-	A	T	T	T-	-	A	T	G	GT
T8		NSS	G	T	A-	C	-	G	T-	-	A	C	G	GT
Tx601	TX601	TS	G	T	A-	C	-	G	T-	-	A	C	G	GT
Tzi10	TZI10	TS	G	T	A-	C	-	G	T-	-	A	C	G	GT
Tzi11	TZI11	TS	G	T	A-	C	-	G	T-	-	A	C	G	GT
Tzi18	TZI18	TS	G	T	A-	C	-	G	T-	-	A	C	G	GT
Tzi25	TZI25	MXD	G	T	A-	C	-	G	T-	-	A	C	G	GT
Tzi8	TZI8	TS	G	T	A-	C	-	G	T-	-	A	C	G	GT
Tzi9	TZI9	TS	G	T	A-	C	-	G	T-	-	A	C	G	GT
Va14	VA14	NSS	A	-	--	A	T	T	T-	-	A	T	G	GT
Va17	VA17	NSS	G	T	A-	C	-	G	T-	-	A	C	G	GT
Va59	VA59	NSS	A	-	--	A	T	T	T-	-	A	T	G	GT
Va85	VA85	NSS	G	T	A-	C	-	G	T-	-	A	C	G	GT
Va99	VA99	NSS	.	T	A-	C	-	G	T-	-	A	C	G	GT
VaW6	VAW6	MXD	A	-	A-	A	T	T	T-	-	A	T	G	GT
W153R		NSS	A	-	A-	A	T	T	T-	-	A	T	G	GT
W182B		NSS	A	-	A-	A	T	T	T-	-	A	T	G	GT
W22		NSS	A	-	--	A	T	T	T-	-	A	T	G	GT
W401		NSS	A	-	--	A	T	T	T-	-	A	T	G	GT
W64A		NSS	A	-	--	A	T	T	T-	-	A	T	G	GT
WD		NSS	A	-	A-	A	T	T	T-	-	A	T	G	GT
Wf9	WF9	NSS	G	T	A-	C	-	G	T-	-	A	C	G	GT
Yu96_NS	YU96NS	MXD	A	-	A-	A	T	.	T-	-	A	T	G	GT

VITA

Michael J. Gerau was born in Columbia, Missouri on June 11th, 1980. He graduated from David H. Hickman High School in May of 1998. Michael performed research on root development under different soil moisture levels as an undergraduate in Dr. Georgia Davis' lab while pursuing a double major in Chemistry and Microbiology at the University of Missouri-Columbia.

After graduation in December of 2004 Michael enrolled in the Graduate School at the University of Missouri-Columbia in the Division of Plant Sciences. Michael continued to research maize root development in graduate school. Upon attaining his PhD he plans to pursue a career focused on crop improvement using molecular breeding approaches.